Table of Contents

Instrumentation and Chemicals

^{1}H NMR (600 MHz), ^{11}B NMR (192 MHz), ^{13}C NMR (151 MHz), ^{19}F NMR (564 MHz), ^{29}Si NMR (119 MHz), ^{31}P NMR (243 MHz), and ^{119}Sn NMR (224 MHz) spectra were recorded on a JEOL ECZ-600 spectrometer. Chemical shifts in ^{1}H NMR spectra were recorded in delta (δ) units, parts per million (ppm) relative to residual $CHCl_3$ (δ = 7.26 ppm) or tetramethylsilane (δ = 0.00 ppm). Chemical shifts in ^{13}C NMR spectra were recorded in delta (δ) units, parts per million (ppm) relative to $CDCl_3$ (δ = 77.16 ppm). For ^{11}B, ^{19}F, ^{29}Si, and ^{31}P NMR spectra, $BF_3{\cdot}OEt_2$ (^{11}B: δ = 0.00 ppm), and fluorobenzene (^{19}F: δ = –113.50 ppm) were used as an external standard, respectively. For ^{29}Si, ^{31}P, and ^{119}Sn NMR spectra, tetramethylsilane (^{29}Si: δ = 0.00 ppm), H_3PO_4 (^{31}P: δ = 0.00 ppm), and tetramethylstannane (^{119}Sn: δ = 0.00 ppm) were used as an internal standard, respectively. The following abbreviations are used for spin multiplicity: s = singlet, d = doublet, t = triplet, q = quartet, m = multiplet, br = broad. High resolution mass spectra (HRMS) were obtained on a Bruker micrOTOF II-KR spectrometer in Atmospheric Pressure Chemical Ionization (APCI) method using "LC/MS tuning mix, for APCI, low concentration" (Agilent Technologies, Inc.) as the internal standard.

All non-aqueous reactions were carried out under an inert atmosphere of N_2 gas in oven-dried glassware unless otherwise noted. Dehydrated THF, Et_2O, and DME was purchased from Kanto Chemical Co., Inc. and stored under a nitrogen atmosphere. Dehydrated 1,4-dioxane and acetone were purchased from FUJIFILM Wako Pure Chemical Corporation and stored under an atmosphere of nitrogen. Trimethyl borate, triisopropyl borate, methoxyboronic acid pinacol ester (MeOBpin), ethoxyboronic acid pinacol ester (EtOBpin), isopropoxyboronic acid pinacol ester (*i*PrOBpin), and benzaldehyde were purchased from commercial suppliers and distilled prior to use. Unless otherwise noted, materials obtained from commercial suppliers were used without further purification. Analytical thin layer chromatography (TLC) was performed on Merck precoated analytical plates, 0.25-mm thick, silica gel 60 F_{254}. Preparative flash chromatography was performed using Silica Gel (Wakosil® C-300 purchased from FUJIFILM Wako Pure Chemical Corporation, or Silica Gel 60N, spherical neutral, particle size 100-210 μm, purchased from Kanto Chemical Co., Inc.). Preparative recycling gel permeation chromatography (GPC) was performed on a JAI LC-9260 II NEXT system using $CHCl_3$ as the eluent. Melting points were determined on a Stanford Research Systems MPA100 melting point apparatus.

Stainless steel (SUS304) T-shaped micromixers with an inner diameter of 250, 500, and 1000 μm and stainless steel anchor-shaped micromixer with an inner diameter of 250 μm were manufactured by Sanko Seiki Co., Inc. Stainless steel (SUS316) microtube reactors with inner

diameters of 250, 500, and 1000 μm were purchased from GL Sciences and were cut into appropriate lengths. The micromixers and microtube reactors were connected with stainless steel fittings (GL Sciences, 1/16 OUW). The flow microreactor system was immersed in a cooling bath to control reaction temperature. The solutions were continuously introduced to the flow microreactor system using Harvard model PHD ULTRA.

Preparation of Reagents and Substrates

Preparation of lithium and sodium naphthalenide

Lithium naphthalenide (LiNp) was prepared according to the literature procedure with some modification.[1] Lithium (0.278 g, 40.0 mmol) and naphthalene (5.64 g, 44.0 mmol) were mixed in anhydrous THF (0.40 M). The mixture was stirred for room temperature until the solution became dark green and lithium was completely consumed (ca. 2 h). Sodium naphthalenide (NaNp) was also prepared (stirred for ca. 4 h) according to the same procedure.

Preparation of lithium and potassium 4,4'-di-*tert*-butylbiphenylide

Lithium 4,4'-di-*tert*-butylbiphenylide (LiDTBB) was prepared according to the literature procedure with some modification.[1] Lithium (0.278 g, 40.0 mmol) and 4,4'-di-*tert*-butylbiphenyl (13.9 g, 52.0 mmol) were mixed in anhydrous THF (0.40 M). The mixture was stirred at 0 °C until the solution became dark blue and lithium was completely consumed (ca. 3-5 h).

Preparation of 4,4'-di-*tert*-butylbiphenyl

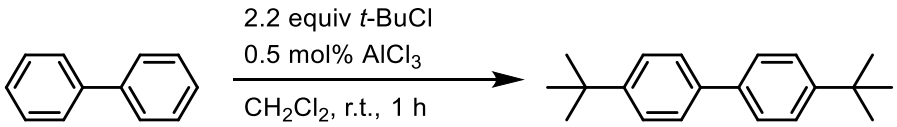

An oven-dried 1000-mL flask was charged with biphenyl (54.0 g, 350 mmol), *tert*-butyl chloride (84.9 mL, 770 mmol, 2.2 equiv), and CH_2Cl_2 (300 mL). $AlCl_3$ (0.233 g, 1.75 mmol, 0.5 mol%) was slowly added portionwise to the flask until gas evolution ceased (ca. 1 h). The reaction mixture was quenched with MeOH and the resulting solution was washed twice with H_2O and then with saturated aqueous $NaHCO_3$. The organic layer was dried over Na_2SO_4 and concentrated under reduced pressure. The solid was washed with *i*PrOH and dried under vacuum to give 4,4'-di-*tert*-butylbiphenyl (52.1 g, 196 mmol, 56%) as a white solid.

^{1}H NMR ($CDCl_3$): δ 7.53 (d, J = 8.1 Hz, 4H), 7.45 (d, J = 8.1 Hz, 4H), 1.36 (s, 18H).

^{13}C NMR ($CDCl_3$): δ 150.0, 138.3, 126.8, 125.8, 34.7, 31.5.

HRMS (APCI-MS, positive): m/z = 266.2029. Calcd. for $C_{20}H_{26}$: 266.2029 $[M]^+$.

Melting point: 126.7–127.7 °C

The resonances in the ^{1}H and ^{13}C NMR spectra were consistent with the report values.[2]

Preparation of 1b, 1c, 1e, 1f, 1h, and 1i

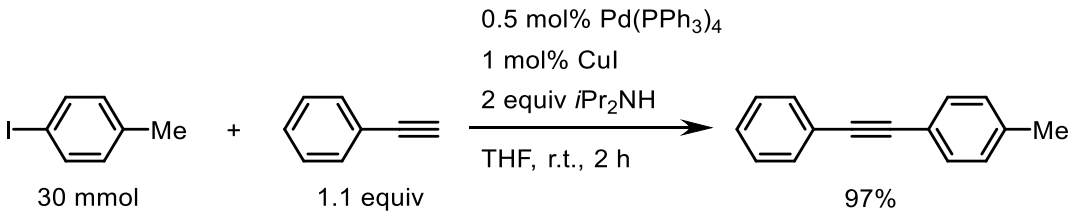

The synthesis of phenyl *p*-tolyl acetylene (**1b**) is representative. An oven-dried 100-mL flask was charged under a nitrogen atmosphere with $Pd(PPh_3)_4$ (0.173 g, 0.150 mmol, 0.5 mol%), CuI (57.0 mg, 0.300 mmol, 1 mol%) and THF (5 mL). A mixture of ethynylbenzene (3.62 mL, 33.0 mmol, 1.1 equiv), 4-iodotoluene (6.54 g, 30.0 mmol), diisopropylamine (8.43 mL, 60.0 mmol, 2 equiv), and THF (50 mL) was added to the flask slowly. After the resulting mixture was stirred at room temperature for 2 h, the crude mixture was passed through pads of silica gel and alumina with EtOAc as an eluent. The combined organic layer was washed with aqueous 10% HCl and then twice with brine. The organic layer was dried over Na_2SO_4 and concentrated under reduced pressure. The residue was purified by column chromatography on silica gel (hexane) to give **1b** (5.61 g, 29.2 mmol, 97%) as a white solid.

^{1}H NMR ($CDCl_3$): δ 7.53–7.51 (m, 2H), 7.43 (d, J = 6.9 Hz, 2H), 7.36–7.30 (m, 3H), 7.16 (d, J = 6.9 Hz, 2H), 2.37 (s, 3H).

^{13}C NMR ($CDCl_3$): δ 138.5, 131.7, 131.6, 129.3, 128.4, 128.2, 123.6, 120.3, 89.7, 88.9, 21.7.

HRMS (APCI-MS, positive): *m/z* = 192.0931. Calcd. for $C_{15}H_{12}$: 192.0934 $[M]^+$.

Melting point: 70.9–71.7 °C

The resonances in the ^{1}H and ^{13}C NMR spectra were consistent with the report values.[3]

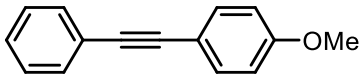

Obtained in 94% yield (20.0 mmol scale) using 4-iodoanisole, 1 mol% $Pd(PPh_3)_4$, 2 mol% CuI, and 1 equivalent ethynylbenzene. The residue was purified by column chromatography on silica gel (hexane/AcOEt = 40/1) to give **1c** (3.91 g, 18.8 mmol) as a white solid.

^{1}H NMR ($CDCl_3$): δ 7.52–7.46 (m, 4H), 7.35–7.30 (m, 3H), 7.16 (d, J = 9.0 Hz, 2H), 3.83 (s, 3H).

^{13}C NMR ($CDCl_3$): δ 159.7, 133.2, 131.6, 128.4, 128.1, 123.7, 115.5, 114.1, 89.5, 88.2, 55.4.

HRMS (APCI-MS, positive): *m/z* = 208.0883. Calcd. for $C_{15}H_{12}O$: 208.0883 $[M]^+$.

Melting point: 57.6–59.7 °C

All the resonances in ^{1}H and ^{13}C spectra ($CDCl_3$) were consistent with the reported values.[3]

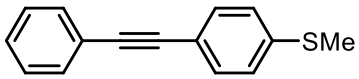

Obtained in 84% yield using 4-bromothioanisole. The reaction mixture was refluxed for 2 h. The residue was purified by column chromatography on silica gel (hexane) to give **1e** (5.63 g, 25.1 mmol) as a white solid.

^{1}H NMR ($CDCl_3$): δ 7.52 (dd, J = 7.5, 2.1 Hz, 2H), 7.44 (d, J = 8.1 Hz, 2H), 7.36–7.31 (m, 3H), 7.21 (d, J = 8.1 Hz, 2H), 2.50 (s, 3H).

^{13}C NMR ($CDCl_3$): δ 139.4, 132.0, 131.7, 128.5, 128.3, 126.0, 123.4, 119.7, 89.6, 89.3, 15.5.

HRMS (APCI-MS, positive): *m/z* = 224.0656. Calcd. for $C_{15}H_{12}S$: 224.0654 $[M]^+$.

Melting point: 90.1–91.7 °C

All the resonances in ^{1}H and ^{13}C spectra ($CDCl_3$) were consistent with the reported values.[4]

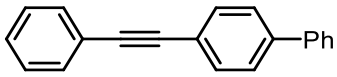

Obtained in 66% yield using 4-bromobiphenyl, 1 mol% $Pd(PPh_3)_4$, and 2 mol% CuI. The mixture was refluxed for 2 h. The residue was purified by column chromatography on silica gel (hexane) to give **1f** (5.00 g, 19.7 mmol) as a pale yellow solid.

^{1}H NMR ($CDCl_3$): δ 7.62–7.31 (m, 8H), 7.46 (t, J = 7.5 Hz, 2H), 7.38–7.33 (m, 4H).

^{13}C NMR ($CDCl_3$): δ 141.1, 140.4, 132.2, 131.7, 129.0, 128.5, 128.4, 127.8, 127.1, 123.4, 122.3 (one aromatic carbon signal could not be located due to overlapping). 90.2, 89.4.

HRMS (APCI-MS, positive): *m/z* = 254.1090. Calcd. for $C_{20}H_{14}$: 254.1090 $[M]^+$.

Melting point: 160.1–162.2 °C

All the resonances in ^{1}H and ^{13}C spectra ($CDCl_3$) were consistent with the reported values.[5]

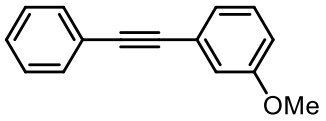

Obtained in 72% yield using 3-iodoanisole. The residue was purified by column chromatography on silica gel (hexane) and recrystallized from MeOH to give **1h** (4.53 g, 21.7 mmol) as a white solid.

^{1}H NMR ($CDCl_3$): δ 7.54 (dd, J = 7.2, 1.8 Hz, 2H), 7.37–7.32 (m, 3H), 7.25 (t, J = 8.1 Hz, 1H, overllaping with residual $CHCl_3$), 7.13 (d, J = 7.2 Hz, 1H), 7.07 (m, 1H), 6.90 (dd, J = 8.1, 1.2 Hz, 1H), 3.83 (s, 3H).

^{13}C NMR ($CDCl_3$): δ 159.5, 131.8, 129.6, 128.50, 128.46, 124.4, 124.3, 123.3, 116.5, 115.1, 89.4, 89.3, 55.4.

HRMS (APCI-MS, positive): *m/z* = 208.0880. Calcd. for $C_{15}H_{12}O$: 208.0883 $[M]^+$.

Melting point: 78.3–79.1 °C

All the resonances in ^1H and ^{13}C spectra ($CDCl_3$) were consistent with the reported values.[4]

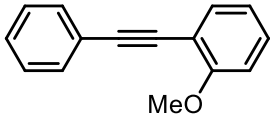

Obtained in 99% yield using 2-iodoanisole. The residue was purified by column chromatography on silica gel (hexane) to give **1i** (6.21 g, 29.8 mmol) as a pale yellow oil.

^1H NMR ($CDCl_3$): δ 7.57–7.56 (m, 2H), 7.50–7.49 (m, 1H), 7.40–7.29 (m, 4H), 6.94 (t, J = 7.8 Hz, 1H), 6.90 (d, J = 7.8 Hz, 1H), 3.91 (s, 3H).

^{13}C NMR ($CDCl_3$): δ 160.7, 133.7, 131.8, 129.9, 128.4, 128.2, 123.7, 120.6, 112.6, 110.9, 93.6, 85.9, 56.0.

HRMS (APCI-MS, positive): *m/z* = 208.0882. Calcd. for $C_{15}H_{12}O$: 208.0883 $[M]^+$.

All the resonances in ^1H and ^{13}C spectra ($CDCl_3$) were consistent with the reported values.[3]

Preparation of (*R,E*)-(−)-*N*-(4-Methoxybenzylidene)-*tert*-butanesulfinamide

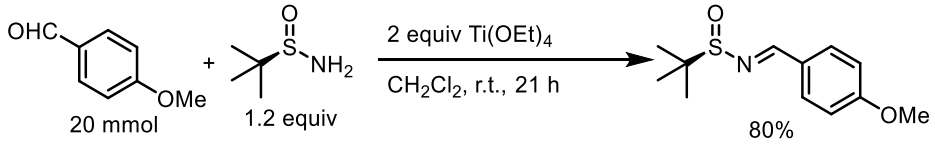

An oven-dried 100-mL flask was charged under a nitrogen atmosphere with 4-methoxybenzaldehyde (2.72 g, 20.0 mmol), (*R*)-(+)-*tert*-butyl sulfinimide (2.91 g, 24.0 mmol, 1.2 equiv), and CH_2Cl_2 (40 mL). $Ti(OEt)_4$ (9.12 g, 40.0 mmol) was added to the flask slowly. After the mixture was stirred for 21 h at room temperature, aqueous saturated $NaHCO_3$ was added. The resulting suspension was filtered through a Celite® pad and extracted three times with CH_2Cl_2. The combined organic layer was dried over Na_2SO_4 and concentrated under reduced pressure. The residue was purified by column chromatography on silica gel (hexane/AcOEt = 5/1) to give (*R,E*)-(−)-*N*-(4-methoxybenzylidene)-*tert*-butanesulfinamide (4.01 g, 15.9 mmol, 80%) as a white solid.

^1H NMR ($CDCl_3$): δ 8.51 (s, 1H), 7.81 (d, J = 9.0 Hz, 2H), 6.98 (d, J = 9.0 Hz, 2H), 3.88 (s, 3H), 1.25 (s, 9H).

^{13}C NMR ($CDCl_3$): δ 163.1, 161.9, 131.4, 127.4, 114.4, 57.7, 55.6, 22.7.

HRMS (APCI-MS, positive): *m/z* = 240.1057. Calcd. for $C_{12}H_{18}NO_2S$: 240.1053 $[M+H]^+$.

Melting point: 93.5–94.2 °C

All the resonances in ^{1}H and ^{13}C spectra ($CDCl_3$) were consistent with the reported values.[6]

Preparation of *N*,*N*-diethyl-2-(4-iodophenoxy)ethanamine

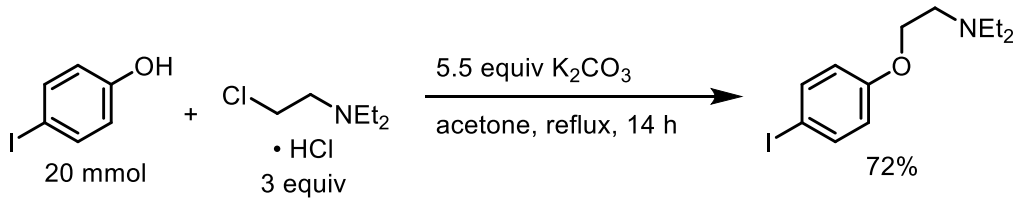

An oven-dried 1000-mL flask was charged with 4-iodophenol (4.40 g, 20.0 mmol), 2-(diethylamino)ethyl chloride hydrochloride (10.3 g, 60.0 mmol, 3 equiv), potassium carbonate (15.2 g, 110 mmol, 5.5 equiv), and acetone (500 mL) under a nitrogen atmosphere. After the mixture was refluxed for 14 h, the resulting mixture was cooled to room temperature, and H_2O (200 mL) was added. The resulting solution was concentrated under reduced pressure, and extracted three times with CH_2Cl_2. The combined organic layer was dried over Na_2SO_4 and concentrated under reduced pressure. The residue was purified by column chromatography on silica gel (hexane/AcOEt = 1/1) to give *N*,*N*-diethyl-2-(4-iodophenoxy)ethanamine (4.56 g, 14.3 mmol, 74%) as a colorless oil.

^{1}H NMR ($CDCl_3$): δ 7.54 (d, J = 9.0 Hz, 2H), 6.86 (d, J = 9.0 Hz, 2H), 4.02 (t, J = 5.4 Hz, 2H), 2.87 (brt, 2H), 2.64 (brq, 4H), 1.07 (t, J = 7.8 Hz, 6H).

^{13}C NMR ($CDCl_3$): δ 158.8, 138.2, 117.0, 82.8, 66.8, 51.7, 47.9, 12.0.

HRMS (APCI-MS, positive): *m/z* =320.0507. Calcd. for $C_{12}H_{19}INO$: 320.0506 $[M+H]^+$.

Screening Conditions

Screening of alkoxyborane electrophile

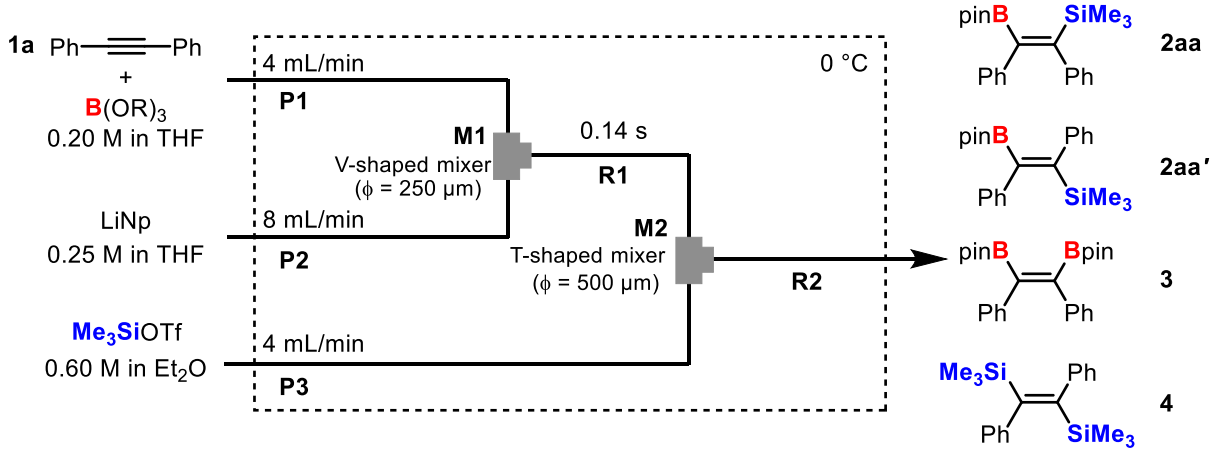

A flow microreactor system consisting of an anchor-shaped micromixer (**M1**), a T-shaped micromixer (**M2**), two microtube reactors (**R1**, **R2**), and three pre-cooling units (**P1**, **P2**, and

P3, inner diameter ϕ = 1000 μm, length L = 100 cm) was used. The flow microreactor system was immersed in a cooling bath (0 °C). A solution of diphenylacetylene (**1a**) containing alkoxyborane electrophile (0.20 M in THF, flow rate: 4 mL/min), and a solution of LiNp (0.25 M in THF, flow rate: 8 mL/min) were introduced to **M1** (ϕ = 250 μm) using syringe pumps, and the mixed solution was passed through **R1** (L = 3.5 cm, ϕ = 1000 μm). A solution of trimethylsilyl trifluoromethanesulfonate (0.60 M in Et_2O, flow rate: 4 mL/min) was then introduced to **M2** (ϕ = 500 μm) using a syringe pump, and the resulting solution was passed through **R2** (L = 200 cm, ϕ = 1000 μm). After a steady state was reached, the product solution was collected into a vial with saturated aqueous NH_4Cl for 15 s. The resulting biphasic solution was extracted three times with AcOEt. The combined organic layer was dried over Na_2SO_4 and concentrated under reduced pressure. The yields were determined by NMR analysis. The results are summarized in Table S1.

Table S1. Screening of alkoxyborane electrophile.

entry	$B(OR)_3$	NMR Yield (%)				
		1a	**2aa**	**2aa′**	**3**	**4**
1[a]	$B(OMe)_3$	0	15	1	0	9
2	MeOBpin	0	60	1	trace	5
3	EtOBpin	0	**72**	1	trace	4
4	*i*PrOBpin	0	68	1	0	3
5[a]	$B(O\textit{i}Pr)_3$	0	12	3	0	22
6[a]	$B(OSiMe_3)_3$	7	4	4	trace	22
7[a,b]	$B_3O_3(OMe)_3$	0	1	5	trace	10

[a] The resulting solution was treated with pinacol (1.5 equiv)

[b] 0.33 equiv of $B_3O_3(OMe)_3$

Temperature screening

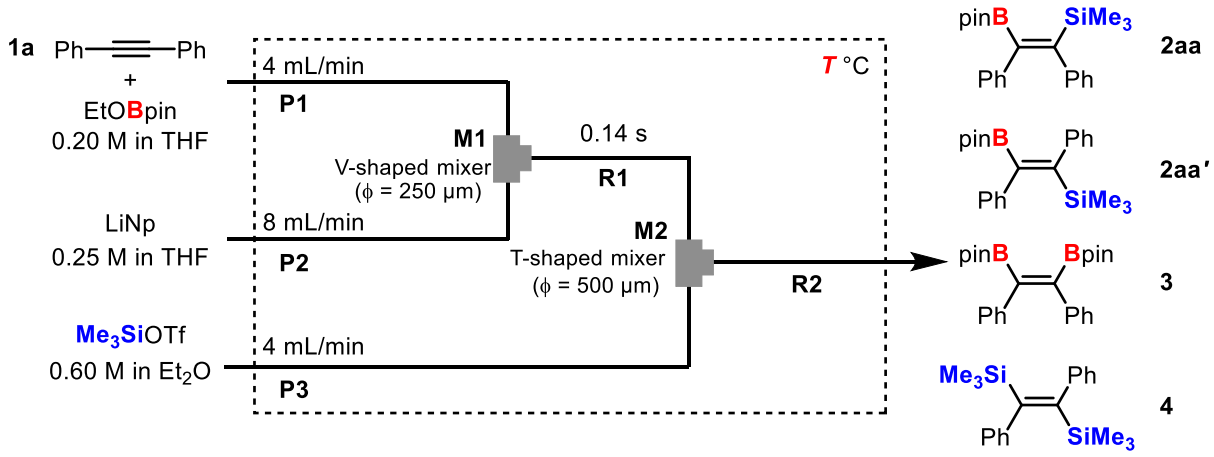

A flow microreactor system consisting of an anchor-shaped micromixer (**M1**), a T-shaped micromixer (**M2**), two microtube reactors (**R1**, **R2**), and three pre-cooling units (**P1**, **P2**, and **P3**, inner diameter ϕ = 1000 μm, length L = 100 cm) was used. The flow microreactor system was immersed in a cooling bath (T °C). A solution of diphenylacetylene (**1a**) containing EtOBpin (0.20 M in THF, flow rate: 4 mL/min), and a solution of LiNp (0.25 M in THF, flow rate: 8 mL/min) were introduced to **M1** (ϕ = 250 μm) using syringe pumps, and the mixed solution was passed through **R1** (L = 3.5 cm, ϕ = 1000 μm). A solution of trimethylsilyl trifluoromethanesulfonate (0.60 M in Et_2O, flow rate: 4 mL/min) was introduced to **M2** (ϕ = 500 μm) using a syringe pump, and the resulting solution was passed through **R2** (L = 200 cm, ϕ = 1000 μm). After a steady state was reached, the product solution was collected into a vial with saturated aqueous NH_4Cl for 15 s. The resulting biphasic solution was extracted three times with AcOEt. The combined organic layer was dried over Na_2SO_4 and concentrated under reduced pressure. The yields were determined by NMR analysis. The results are summarized in Table S2.

Table S2. Temperature screening.

entry	*T* (°C)	NMR Yield (%) 1a	2aa	2aa′	3	4
1	20	0	64	3	7	2
2	0	0	72	1	trace	4
3	–20	0	**84**	0	trace	3
4	–40	0	64	0	0	2
5	–60	0	66	1	0	10
6	–78	7	29	1	0	38

Residence time screening

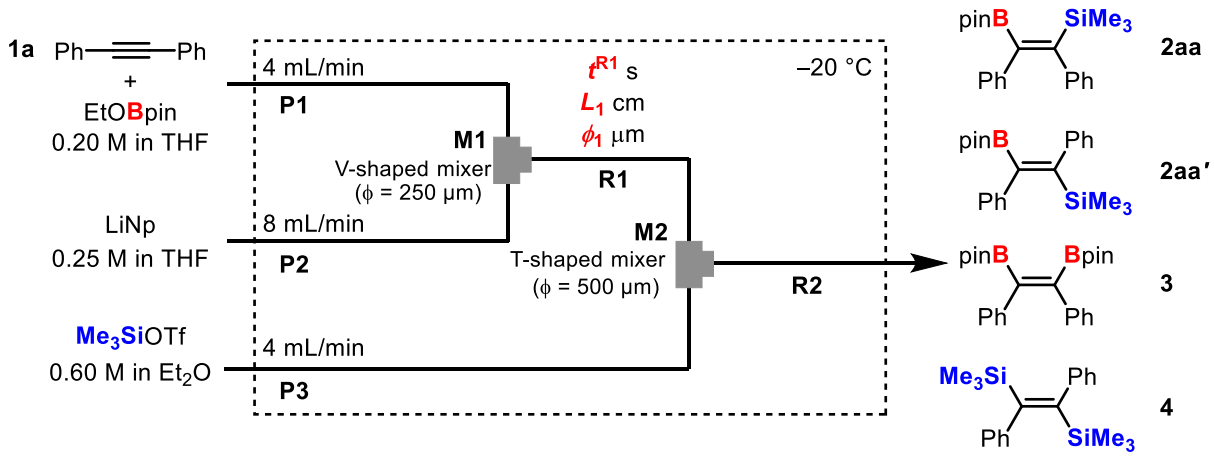

A flow microreactor system consisting of an anchor-shaped micromixer (**M1**), a T-shaped micromixer (**M2**), two microtube reactors (**R1**, **R2**), and three pre-cooling units (**P1**, **P2**, and **P3**, inner diameter ϕ = 1000 μm, length L = 100 cm) was used. The flow microreactor system was immersed in a cooling bath (–20 °C). A solution of diphenylacetylene (**1a**) containing EtOBpin (0.20 M in THF, flow rate: 4 mL/min), and a solution of LiNp (0.25 M in THF, flow rate: 8 mL/min) were introduced to **M1** (ϕ = 250 μm) using syringe pumps, and the mixed solution was passed through **R1** (L_1 cm, ϕ_1 μm). A solution of trimethylsilyl trifluoromethanesulfonate (0.60 M in Et_2O, flow rate: 4 mL/min) was introduced to **M2** (ϕ = 500 μm) using a syringe pump, and the resulting solution was passed through **R2** (L = 200 cm, ϕ = 1000 μm). After a steady state was reached, the product solution was collected into a vial with saturated aqueous NH_4Cl for 15 s. The resulting biphasic solution was extracted three times with AcOEt. The combined organic layer was dried over Na_2SO_4 and concentrated under

reduced pressure. The yields were determined by NMR analysis. The results are summarized in Table S3.

Table S3. Residence time screening.

entry	L_1 (cm)	t^{R1} (s)	ϕ_1 (μm)	NMR Yield (%) 1a	2aa	2aa′	3	4
1	3.5	0.0086	250	0	74	0	trace	5
2	3.5	0.034	500	0	77	0	trace	4
3	3.5	0.14	1000	0	**84**	0	trace	3
4	6	0.24	1000	0	79	0	trace	2
5	12.5	0.49	1000	0	78	0	trace	2
6	25	0.98	1000	0	76	0	2	3
7	50	1.96	1000	0	75	0	1	2
8	100	3.93	1000	0	76	0	trace	2
9	200	7.86	1000	0	73	0	trace	2
10	1000	39.3	1000	0	66	0	1	1

Effect of flow rate

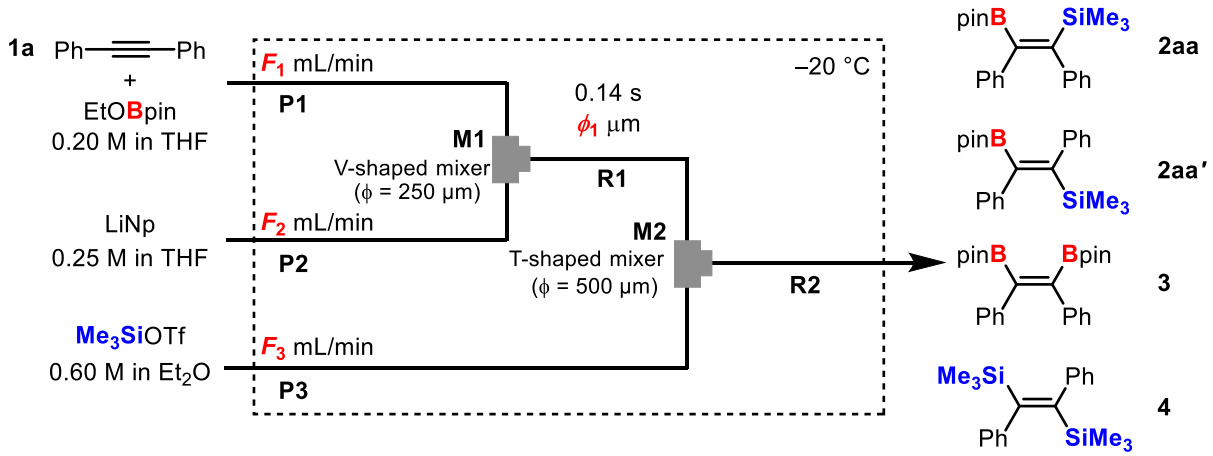

A flow microreactor system consisting of an anchor-shaped micromixer (**M1**), a T-shaped micromixer (**M2**), two microtube reactors (**R1**, **R2**), and three pre-cooling units (**P1**, **P2**, and **P3**, inner diameter ϕ = 1000 μm, length L = 100 cm) was used. The flow microreactor system was immersed in a cooling bath (–20 °C). A solution of diphenylacetylene (**1a**) containing EtOBpin (0.20 M in THF, flow rate: F_1 mL/min), and a solution of LiNp (0.25 M in THF, flow rate: F_2 mL/min) were introduced to **M1** (ϕ = 250 μm) using syringe pumps, and the mixed solution was passed through **R1** (L = 3.5 cm, ϕ_1 μm). A solution of trimethylsilyl trifluoromethanesulfonate (0.60 M in Et_2O, flow rate: F_3 mL/min) was introduced to **M2** (ϕ =

500 μm) using a syringe pump, and the resulting solution was passed through **R2** (L = 200 cm, ϕ = 1000 μm). After a steady state was reached, the product solution was collected into a vial with saturated aqueous NH_4Cl for 15 s. The resulting biphasic solution was extracted three times with AcOEt. The combined organic layer was dried over Na_2SO_4 and concentrated under reduced pressure. The yields were determined by NMR analysis. The results are summarized in Table S4.

Table S4. Effect of flow rate.

entry	F_1 (mL/min)	F_2 (mL/min)	F_3 (mL/min)	ϕ_1 (μm)	NMR Yield (%) 1a	2aa	2aa′	3	4
1	4	8	4	1000	0	**84**	0	trace	3
2	1	2	1	500	35	34	0	1	4
3	0.25	0.5	0.25	250	42	14	0	2	2

Effect of the mixer M1

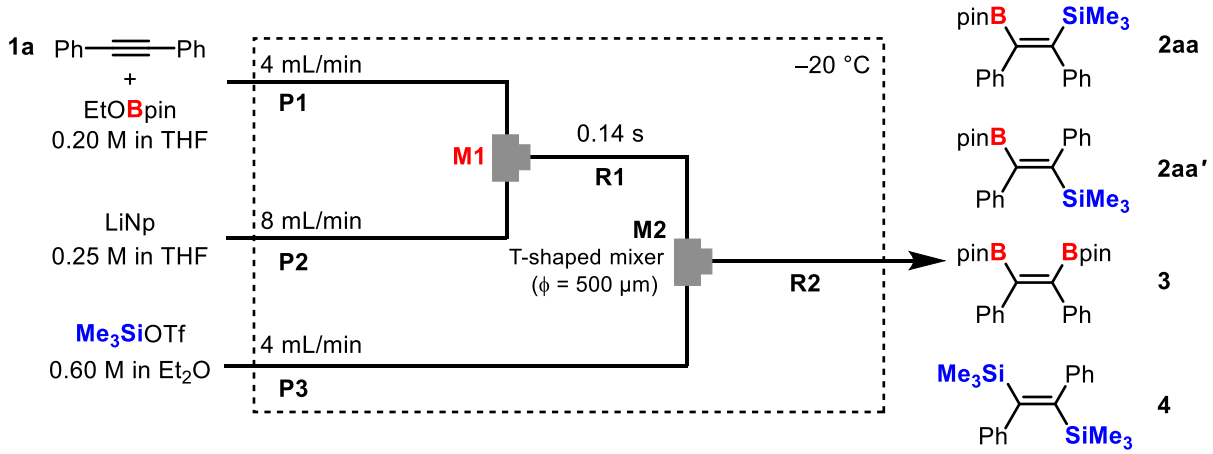

A flow microreactor system consisting of a micromixer (**M1**), a T-shaped micromixer (**M2**), two microtube reactors (**R1**, **R2**), and three pre-cooling units (**P1**, **P2**, and **P3**, inner diameter ϕ = 1000 μm, length L = 100 cm) was used. The flow microreactor system was immersed in a cooling bath (–20 °C). A solution of diphenylacetylene (**1a**) containing EtOBpin (0.20 M in THF, flow rate: 4 mL/min), and a solution of LiNp (0.25 M in THF, flow rate: 8 mL/min) were introduced to **M1** using syringe pumps, and the mixed solution was passed through **R1** (L = 3.5 cm, ϕ = 1000 μm). A solution of trimethylsilyl trifluoromethanesulfonate (0.60 M in Et_2O, flow rate: 4 mL/min) was introduced to **M2** (ϕ = 500 μm) using a syringe pump, and the resulting solution was passed through **R2** (L = 200 cm, ϕ = 1000 μm). After a steady state was reached, the product solution was collected into a vial with saturated aqueous NH_4Cl for 15 s. The resulting biphasic solution was extracted three times with AcOEt. The combined organic layer

was dried over Na_2SO_4 and concentrated under reduced pressure. The yields were determined by NMR analysis. The results are summarized in Table S5.

Table S5. Effect of the mixer **M1**.

entry	mixer **M1** (type, internal diameter)	NMR Yield (%)				
		1a	**2aa**	**2aa'**	**3**	**4**
1	V-shaped, 250 μm	0	**84**	0	trace	3
2	T-shaped, 250 μm	0	75	trace	0	2
3	T-shaped, 500 μm	15	50	0	trace	9
4	T-shaped, 1000 μm	30	28	0	0	23

Reductive borylsilylation of diphenylacetylene using batch reactors

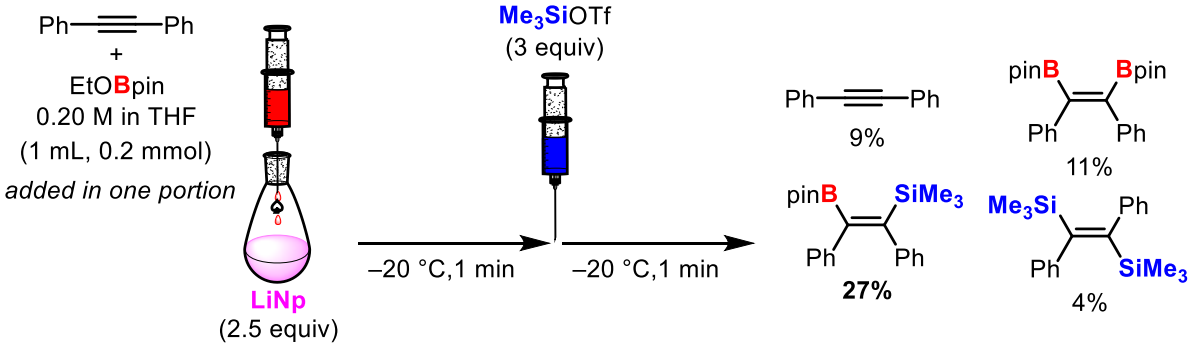

An oven-dried Schlenk tube was charged under a nitrogen atmosphere with LiNp (0.25 M in THF, 2.0 mL, 2.5 equiv). A solution of diphenylacetylene and EtOBpin (0.20 M in THF, 1.0 mL, 0.20 mmol) was added in one portion. After the resulting mixture was stirred for 1 min at –20 °C, Me_3SiOTf (0.60 M in Et_2O, 1.0 mL, 3 equiv) was added to the flask. After the resulting mixture was stirred for 1 min at –20 °C, the solution was treated with saturated aqueous NH_4Cl. The resulting biphasic solution was extracted three times with AcOEt. The combined organic layer was dried over Na_2SO_4 and concentrated under reduced pressure. Yields were determined by NMR analysis.

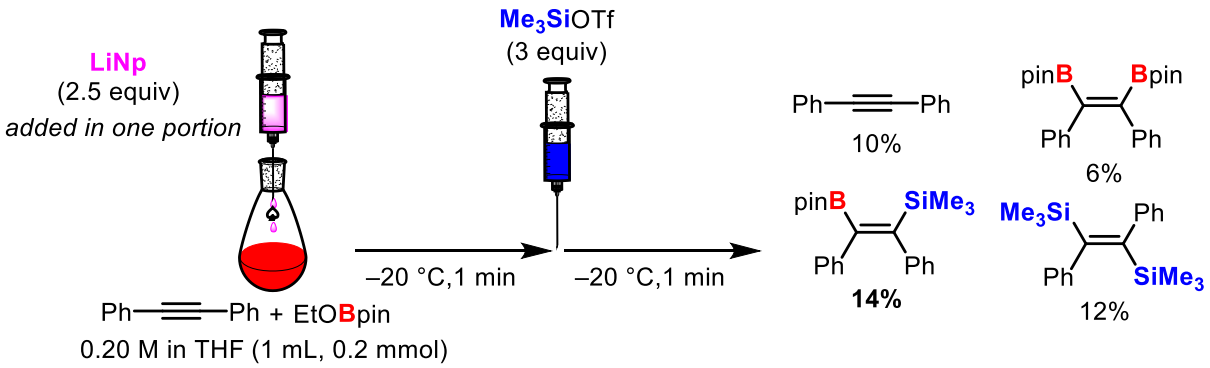

An oven-dried Schlenk tube was charged under a nitrogen atmosphere with a solution of diphenylacetylene and EtOBpin (0.20 M in THF, 1.0 mL, 0.20 mmol). LiNp (0.25 M in THF, 2.0 mL, 2.5 equiv) was added in one portion. After the resulting mixture was stirred for 1 min at –20 °C, Me_3SiOTf (0.60 M in Et_2O, 1.0 mL, 3 equiv) was added to the flask. After the resulting mixture was stirred for 1 min at –20 °C, the solution was treated with saturated aqueous NH_4Cl. The resulting biphasic solution was extracted three times with AcOEt. The combined organic layer was dried over Na_2SO_4 and concentrated under reduced pressure. Yields were determined by NMR analysis.

Reaction of unsymmetrical alkyne 1b

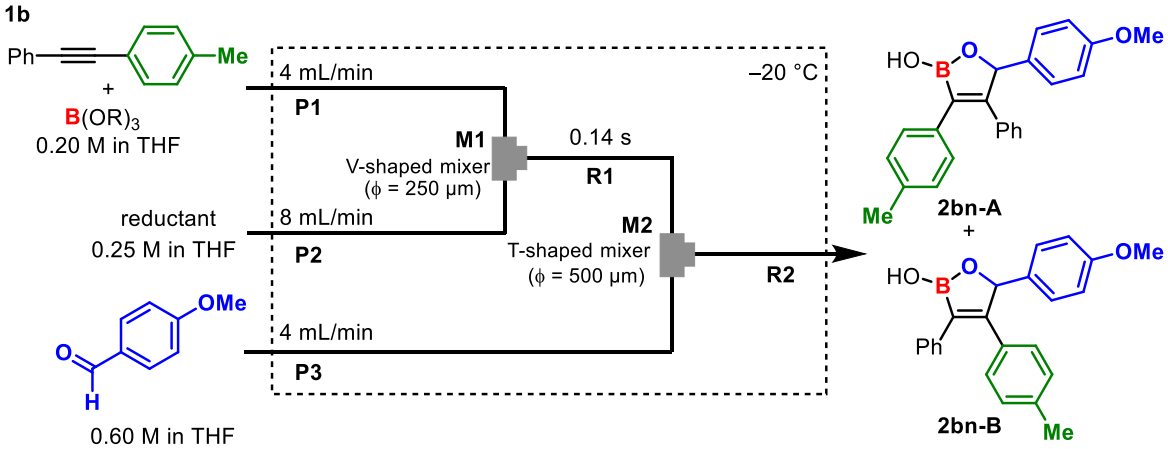

A flow microreactor system consisting of an anchor-shaped micromixer (**M1**), a T-shaped micromixer (**M2**), two microtube reactors (**R1**, **R2**), and three pre-cooling units (**P1**, **P2**, and **P3**, inner diameter ϕ = 1000 μm, length L = 100 cm)) was used. The flow microreactor system was immersed in a cooling bath (–20 °C). A solution of **1b** containing alkoxyborane electrophile (0.20 M in THF, flow rate: 4 mL/min), and a solution of reductant (0.25 M in THF, flow rate: 8 mL/min) were introduced to **M1** (ϕ = 250 μm) using syringe pumps, and the mixed solution was passed through **R1** (L = 3.5 cm, ϕ = 1000 μm). A solution of 4-methoxybenzaldehyde (0.60 M in THF, flow rate: 4 mL/min) was introduced to **M2** (ϕ = 500 μm) using a syringe pump, and

the resulting solution was passed through **R2** (L = 200 cm, ϕ = 1000 μm). After a steady state was reached, the product solution was collected into a vial with aqueous 10% HCl for 15 s. The resulting biphasic solution was extracted three times with AcOEt. The combined organic layer was dried over Na_2SO_4 and concentrated under reduced pressure. The yields were determined by NMR analysis. The results are summarized in Table S6.

Table S6. Reaction of unsymmetrical alkyne **1b**.

entry	B(OR)$_3$	reductant	NMR Yield (%)		
			2bn-A	**2bn-B**	**ratio of A/B**
1	MeOBpin	LiNp	35	20	63/37
2	EtOBpin	LiNp	44	26	63/37
3	*i*PrOBpin	LiNp	36	10	64/36
4	MeOBpin	NaNp	45	9	83/17
5	EtOBpin	NaNp	52	9	85/15
6	*i*PrOBpin	NaNp	**60**	**6**	**92/8**

Experimental Procedures and Compound Characterization

Synthesis of 2aa-2al

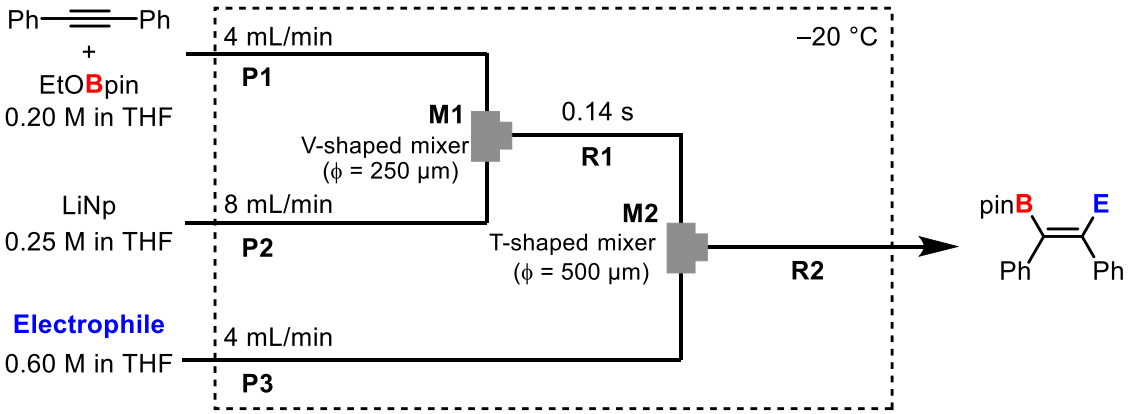

A flow microreactor system consisting of an anchor-shaped micromixer (**M1**), a T-shaped micromixer (**M2**), two microtube reactors (**R1**, **R2**), and three pre-cooling units (**P1**, **P2**, and **P3**, inner diameter ϕ = 1000 μm, length L = 100 cm)) was used. The flow microreactor system was immersed in a cooling bath (–20 °C). A solution of diphenylacetylene (**1a**) containing EtOBpin (0.20 M in THF, flow rate: 4 mL/min), and a solution of LiNp (0.25 M in THF, flow rate: 8 mL/min) were introduced to **M1** (ϕ = 250 μm) using syringe pumps, and the mixed solution was passed through **R1** (L = 3.5 cm, ϕ = 1000 μm). A solution of electrophile (0.60 M

in THF, flow rate: 4 mL/min) was introduced to **M2** (ϕ = 500 μm) using a syringe pump, and the resulting solution was passed through **R2** (L = 200 cm, ϕ = 1000 μm). After a steady state was reached, the product solution was collected into a vial with saturated aqueous NH_4Cl for 15 s. The resulting biphasic solution was extracted three times with AcOEt. The combined organic layer was dried over Na_2SO_4 and concentrated under reduced pressure.

(*E*)-(1,2-Diphenyl-2-(4,4,5,5-tetramethyl-1,3,2-dioxaborolan-2-yl)vinyl)trimethylsilane (2aa):

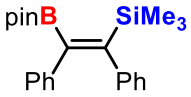

Obtained in 81% yield using trimethylsilyl trifluoromethanesulfonate (0.60 M in Et_2O). The residue was purified by column chromatography on silica gel (hexane/AcOEt = 50/1) and GPC to give **2aa** (61.2 mg, 0.162 mmol, *syn*:*anti* >99:1) as a white solid.

^{1}H NMR ($CDCl_3$): δ 7.05–7.00 (m, 4H), 6.94–6.92 (m, 4H), 6.73 (dd, J = 8.4, 1.5 Hz, 2H), 1.28 (s, 12H), 0.16 (s, 9H).

^{13}C NMR ($CDCl_3$): δ 157.1, 114.7, 142.7, 129.0, 128.3, 127.35, 127.26, 125.4, 124.7, 84.1, 25.3, 0.54 (The carbon bearing a boron atom was hardly observed due to the quadrupolar relaxation mechanism of ^{11}B nucleus).

^{11}B NMR ($CDCl_3$): δ 30.3 (br).

^{29}Si NMR ($CDCl_3$): δ –5.03.

HRMS (APCI–MS, positive): *m/z* = 378.2189. Calcd. for $C_{23}H_{31}BO_2Si$: 378.2185 $[M]^+$.

Melting point: 101.4–105.2 °C

All the resonances in ^{1}H and ^{13}C spectra ($CDCl_3$) were consistent with the reported values.[7]

(*Z*)-2-(1,2-Diphenylvinyl)-4,4,5,5-tetramethyl-1,3,2-dioxaborolane (2ab):

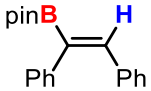

Obtained in 79% yield using MeOH. The residue was purified by column chromatography on silica gel (hexane/AcOEt = 50/1) to give **2ab** (48.5 mg, 0.158 mmol, *syn*:*anti* >99:1) as a white solid.

^{1}H NMR ($CDCl_3$): δ 7.36 (s, 1H), 7.26 (t, J = 7.5 Hz, 2H), 7.22–7.16 (m, 3H), 7.12–7.10 (m, 3H), 7.06–7.04 (m, 2H), 1.31 (s, 12H).

^{13}C NMR ($CDCl_3$): δ 143.3, 140.6, 137.1, 130.1, 129.0, 128.4, 128.0, 127.7, 126.4, 83.9, 24.9 (The carbon bearing a boron atom was hardly observed due to the quadrupolar relaxation mechanism of ^{11}B nucleus).

^{11}B NMR ($CDCl_3$): δ 30.4 (br).

HRMS (APCI-MS, positive): *m/z* = 306.1785. Calcd. for $C_{20}H_{23}BO_2$: 306.1789 $[M]^+$.

Melting point: 82.9–86.8 °C

All the resonances in ^{1}H and ^{13}C spectra ($CDCl_3$) were consistent with the reported values.[8]

(*Z*)-2-(1,2-Diphenylvinyl-2-*d*)-4,4,5,5-tetramethyl-1,3,2-dioxaborolane (2ac):

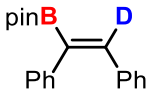

Obtained in 77% yield (97%D) using MeOD. The residue was purified by column chromatography on silica gel (hexane/AcOEt = 50/1) to give **2ac** (47.3 mg, 0.154 mmol, *syn*:*anti* >99:1) as a white solid.

^{1}H NMR ($CDCl_3$): δ 7.36 (s, 0.03H), 7.28–7.25 (m, 2H), 7.22–7.16 (m, 3H), 7.12–7.04 (m, 5H), 1.31 (s, 12H).

^{13}C NMR ($CDCl_3$): δ 142.9 (t, *J* = 23.4 Hz), 140.6, 137.0, 130.1, 129.0, 128.4, 128.0, 127.7, 126.4, 83.9, 24.9 (The carbon bearing a boron atom was hardly observed due to the quadrupolar relaxation mechanism of ^{11}B nucleus).

^{11}B NMR ($CDCl_3$): δ 32.7 (br).

HRMS (APCI-MS, positive): *m/z* = 308.1927. Calcd. for $C_{20}H_{23}DBO_2$: 308.1930 $[M+H]^+$.

Melting point: 81.5–85.4 °C

Deuterium incorporation expected at δ 7.36. The level of deuterium incorporation was determined as 97% (^{1}H NMR).

(*E*)-Tributyl(1,2-diphenyl-2-(4,4,5,5-tetramethyl-1,3,2-dioxaborolan-2-yl)vinyl)stannane (2ad):

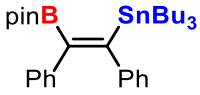

Obtained in 79% yield using Bu_3SnBr. The residue was purified by column chromatography on silica gel (hexane/CH_2Cl_2 = 5/1) to give **2ad** (94.3 mg, 0.158 mmol, *syn*:*anti* = 96:4) as a colorless oil.

^{1}H NMR ($CDCl_3$): δ 7.03–7.00 (m, 4H), 6.94 (t, J = 8.1 Hz, 1H), 6.88–6.86 (m, 3H), 6.62–6.61 (dd, J = 8.1, 1.2 Hz, 2H), 1.43–1.34 (m, 6H), 1.29 (s, 12H), 1.27–1.21 (m, 6H), 0.96 (s, 0.04×12H, *anti* isomer), 0.94–0.75 (m, 15H).

^{13}C NMR ($CDCl_3$): δ 169.8, 147.3, 142.9, 129.7, 127.4, 127.0, 126.9, 125.0, 124.2, 84.0, 29.3 (t, J = 10.2 Hz), 27.7 (t, J = 29.7 Hz), 24.9, 13.9, 13.1 (The carbon bearing a boron atom was hardly observed due to the quadrupolar relaxation mechanism of ^{11}B nucleus).

^{11}B NMR ($CDCl_3$): δ 29.8 (br).

^{119}Sn NMR ($CDCl_3$): δ –51.4.

HRMS (APCI-MS, positive): *m/z* = 597.2928. Calcd. for $C_{32}H_{50}BO_2{}^{119}Sn$: 597.2932 $[M+H]^+$.

All the resonances in ^{1}H and ^{13}C spectra ($CDCl_3$) were consistent with the reported values.[8]

(*Z*)-2-(1,2-Diphenylprop-1-en-1-yl)-4,4,5,5-tetramethyl-1,3,2-dioxaborolane (2ae):

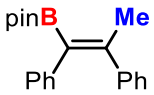

Obtained in 88% yield using MeOTf (0.60 M in Et_2O). The residue was purified by column chromatography on silica gel (hexane/AcOEt = 50/1) to give **2ae** (56.5 mg, 0.176 mmol, *syn*:*anti* >99:1) as a white solid.

^{1}H NMR ($CDCl_3$): δ 7.14–7.04 (m, 5H), 7.00–6.98 (m, 3H), 6.91 (d, J = 6.6 Hz, 2H), 2.36 (s, 3H), 1.33 (s, 12H).

^{13}C NMR ($CDCl_3$): δ 149.2, 143.8, 141.9, 129.8, 128.7, 127.8, 127.6, 126.4, 125.3, 83.8, 25.1, 24.9 (The carbon bearing a boron atom was hardly observed due to the quadrupolar relaxation mechanism of ^{11}B nucleus).

^{11}B NMR ($CDCl_3$): δ 30.9 (br).

HRMS (APCI-MS, positive): *m/z* = 320.1947. Calcd. for $C_{21}H_{25}BO_2$: 320.1946 $[M]^+$.

Melting point: 107.7–110.2 °C

All the resonances in ^{1}H and ^{13}C spectra ($CDCl_3$) were consistent with the reported values.[10]

(*E*)-2-(2-Fluoro-1,2-diphenylvinyl)-4,4,5,5-tetramethyl-1,3,2-dioxaborolane (2af):

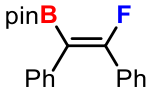

Obtained in 57% yield using NFSI. The residue was purified by column chromatography on silica gel (hexane/AcOEt = 50/1) to give **2af** (36.7 mg, 0.113 mmol, *syn*:*anti* >99:1) as a white solid. The stereochemistry of the product was confirmed by X-ray crystallography.

^{1}H NMR ($CDCl_3$): δ 7.24–7.12 (m, 10H), 1.33 (s, 12H).

^{13}C NMR ($CDCl_3$): δ 164.0 (d, J = 254 Hz), 137.4 (d, J = 14.5 Hz), 132.4 (d, J = 30.4 Hz), 129.8 (d, J = 2.9 Hz), 129.4, 128.9 (d, J = 5.9 Hz), 128.5, 127.9, 126.6, 84.0, 24.8 (The carbon bearing a boron atom was hardly observed due to the quadrupolar relaxation mechanism of ^{11}B nucleus).

^{11}B NMR ($CDCl_3$): δ 30.2 (br).

^{19}F NMR ($CDCl_3$): δ –83.9.

HRMS (APCI-MS, positive): *m/z* = 324.1697. Calcd. for $C_{20}H_{22}BFO_2$: 324.1695 $[M]^+$.

Melting point: 76.1 °C (decomp.)

(*E*)-2-(2-Chloro-1,2-diphenylvinyl)-4,4,5,5-tetramethyl-1,3,2-dioxaborolane (2ag):

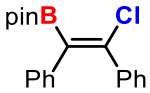

Obtained in 84% yield using hexachloroethane. The residue was purified by column chromatography on silica gel (hexane/AcOEt = 50/1) to give **2ag** (56.9 mg, 0.167 mmol, *syn*:*anti* >99:1) as a white solid. The stereochemistry of the product was confirmed by X-ray crystallography.

^{1}H NMR ($CDCl_3$): δ 7.22 (d, J = 7.5 Hz, 2H), 7.17–7.09 (m, 6H), 7.01 (d, J = 7.5 Hz, 2H), 1.36 (s, 12H).

^{13}C NMR ($CDCl_3$): δ 138.7, 138.6, 138.4, 129.7, 128.9, 128.5, 128.4, 128.0, 126.8, 84.6, 24.8 (The carbon bearing a boron atom was hardly observed due to the quadrupolar relaxation mechanism of ^{11}B nucleus).

^{11}B NMR ($CDCl_3$): δ 29.9 (br).

HRMS (APCI-MS, positive): *m/z* = 340.1401. Calcd. for $C_{20}H_{22}B^{35}ClO_2$: 340.1399 $[M]^+$.

Melting point: 101.8–107.9 °C

(*E*)-2-(2-Bromo-1,2-diphenylvinyl)-4,4,5,5-tetramethyl-1,3,2-dioxaborolane (2ah):

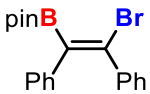

Obtained in 63% yield using tetrabromomethane. The residue was purified by column chromatography on silica gel (hexane/AcOEt = 50/1) to give **2ah** (56.9 mg, 0.167 mmol, *syn*:*anti* >99:1) as a pale yellow solid. The stereochemistry of the product was confirmed by X-ray crystallography.

^{1}H NMR ($CDCl_3$): δ 7.21–7.19 (m, 2H), 7.15–7.09 (m, 6H), 7.01 (d, J = 6.0 Hz, 2H), 1.37 (s, 12H).

^{13}C NMR ($CDCl_3$): δ 140.1, 139.4, 129.8, 129.3, 128.7, 128.3, 128.0, 126.8 (one aromatic carbon signal could not be located due to overlapping), 84.7, 24.8 (The carbon bearing a boron atom was hardly observed due to the quadrupolar relaxation mechanism of ^{11}B nucleus).

^{11}B NMR ($CDCl_3$): δ 29.8 (br).

HRMS (APCI-MS, positive): *m/z* = 384.0893. Calcd. for $C_{20}H_{22}B^{79}BrO_2$: 384.0893 $[M]^+$.

Melting point: 120.3–123.7 °C

(*E*)-1,2,3-Triphenyl-3-(4,4,5,5-tetramethyl-1,3,2-dioxaborolan-2-yl)prop-2-en-1-one (2ai):

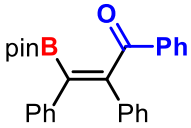

Obtained in 47% yield using benzonitrile. The reaction was quenched by aqueous 10% HCl instead of saturated aqueous NH_4Cl. The residue was purified by column chromatography on silica gel (hexane/AcOEt = 10/1) to give **2ai** (38.9 mg, 0.0948 mmol, *syn*:*anti* >99:1) as a yellow solid. The stereochemistry of the product was confirmed by NOE.

^{1}H NMR ($CDCl_3$): δ 7.61 (d, *J* = 7.0 Hz, 2H), 7.49 (t, *J* = 7.0 Hz, 1H), 7.28–7.17 (m, 10H), 7.00 (d, *J* = 7.0 Hz, 2H), 1.32 (s, 12H).

^{13}C NMR ($CDCl_3$): δ 198.8, 142.8, 138.5, 135.9, 134.1, 133.9, 131.4, 130.3, 129.1, 128.7, 128.4, 128.2, 127.84, 127.80, 82.3, 25.7 (The carbon bearing a boron atom was hardly observed due to the quadrupolar relaxation mechanism of ^{11}B nucleus).

^{11}B NMR ($CDCl_3$): δ 20.0 (br).

HRMS (APCI-MS, positive): *m/z* = 411.2135. Calcd. for $C_{27}H_{28}BO_3$: 411.2131 $[M+H]^+$.

Melting point: 148.9–152.4 °C

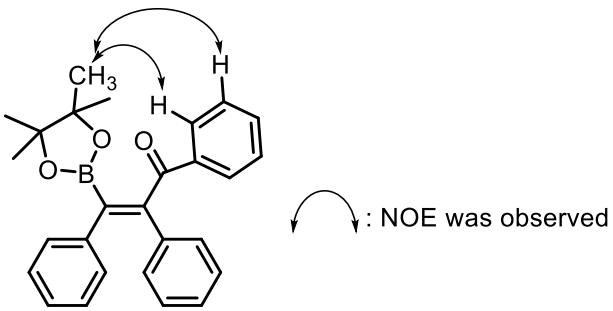

(*E*)-*N*,2,3-Triphenyl-3-(4,4,5,5-tetramethyl-1,3,2-dioxaborolan-2-yl)acrylamide (2aj):

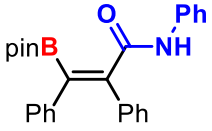

Obtained in 70% yield using phenyl isocyanate. The residue was purified by column chromatography on silica gel (hexane/AcOEt = 5/1 to 3/1) to give **2aj** (59.6 mg, 0.140 mmol, *syn*:*anti* >99:1) as a white solid. The stereochemistry of the product was confirmed by NOE.

^{1}H NMR ($CDCl_3$): δ 7.61 (s, 1H), 7.49 (d, J = 7.8 Hz, 2H), 7.41–7.31 (m, 7H), 7.23–7.16 (m, 6H), 1.30 (s, 12H).

^{13}C NMR ($CDCl_3$): δ 172.1, 171.1 (br), 137.7, 135.5, 133.3, 132.6, 130.0. 129.7, 129.3, 128.79, 128.76, 127.9, 127.7, 126.6, 121.2, 81.2, 25.9.

^{11}B NMR ($CDCl_3$): δ 16.0 (br).

HRMS (APCI-MS, positive): *m/z* = 426.2236. Calcd. for $C_{27}H_{29}BNO_3$: 426.2240 $[M+H]^+$.

Melting point: 169.7–175.7 °C

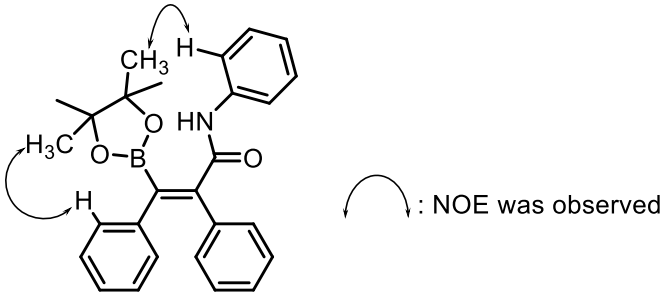

(*E*)-(1,2-Diphenyl-2-(4,4,5,5-tetramethyl-1,3,2-dioxaborolan-2-yl)vinyl)diphenylphosphine oxide (2ak):

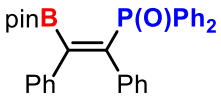

Obtained in 66% yield using diphenylphosphinic chloride. The residue was purified by column chromatography on silica gel (hexane/AcOEt = 3/1) to give **2ak** (66.8 mg, 0.132 mmol, *syn*:*anti* >99:1) as a white solid. The stereochemistry of the product was confirmed by NOE.

^{1}H NMR ($CDCl_3$): δ 7.73–7.60 (m, 4H), 7.61 (t, J = 7.5 Hz, 2H), 7.50–7.47 (m, 4H), 7.26 (d, J = 7.5 Hz, 2H), 7.14–7.03 (m, 6H), 6.70 (d, J = 7.5 Hz, 2H), 1.18 (s, 12H).

^{13}C NMR ($CDCl_3$): δ 140.0 (d, J = 21.7 Hz), 134.8 (d, J = 17.4 Hz), 133.3 (d, J = 2.9 Hz), 132.7 (d, J = 11.5 Hz), 130.3 (d, J = 92.6 Hz), 129.6 (d, J = 4.4 Hz), 129.1 (d, J = 13.0 Hz), 128.4, 128.2, 127.39, 127.35, 127.0 (d, J = 104.2 Hz), 126.5, 80.6. 26.0 (The carbon bearing a boron atom was hardly observed due to the quadrupolar relaxation mechanism of ^{11}B nucleus).

^{11}B NMR ($CDCl_3$): δ 13.2 (br).

^{31}P NMR ($CDCl_3$): δ 46.0.

HRMS (APCI-MS, positive): *m/z* = 507.2255. Calcd. for $C_{32}H_{32}BO_3P$: 507.2260 $[M+H]^+$.

Melting point: 183.1–187.4 °C

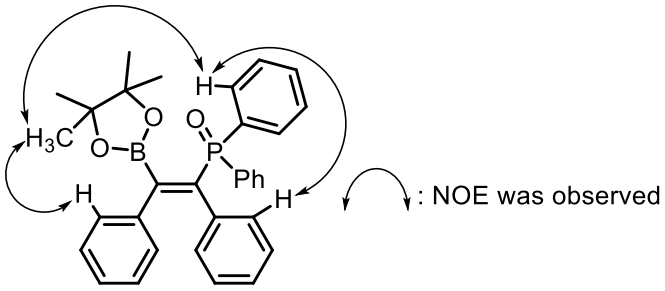

(*E*)-4,4,5,5-tetramethyl-2-(2-methylthio-1,2-diphenylvinyl)-1,3,2-dioxaborolane (2al):

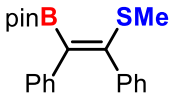

Obtained in 79% yield from dimethyl disulfide. The residue was purified by column chromatography on silica gel (hexane/AcOEt = 20/1) to give **2al** (55.4 mg, 0.157 mmol, 79%, *syn*:*anti* = >99:1) as a white solid. The stereochemistry of the product was confirmed by NOE.

^{1}H NMR ($CDCl_3$): δ 7.23–7.15 (m, 5H), 7.09–6.99 (m, 5H), 1.94 (s, 3H), 1.38 (s, 12H).

^{13}C NMR ($CDCl_3$): δ 145.1, 140.0, 137.7, 130.3, 129.2, 128.1, 128.0. 127.5, 126.1, 84.1, 24.8, 16.1 (the signal of the carbon at the ipso position of the boron atom was not observed).

^{11}B NMR ($CDCl_3$): δ 29.9 (br).

HRMS (APCI-MS, positive): *m/z* = 352.1669. Calcd. for $C_{21}H_{25}BO_2S$: 352.1667 $[M]^+$.

Melting point: 71.2 °C (decomp.)

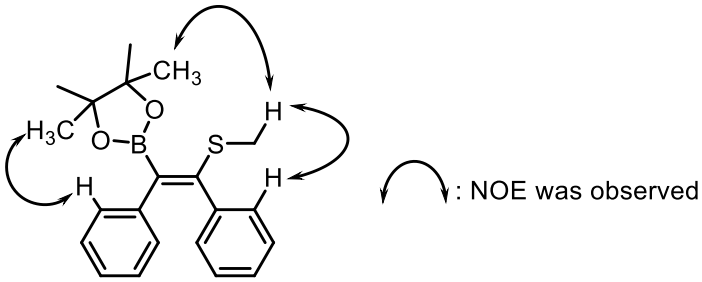

(*E*)-2-(1,2-diphenyl-2-(*p*-tolylthio)vinyl)-4,4,5,5-tetramethyl-1,3,2-dioxaborolane (2am):

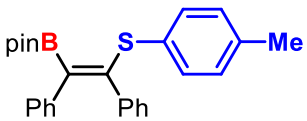

Obtained in 80% yield from di-*p*-tolyl disulfide. The residue was purified by column chromatography on silica gel (hexane/AcOEt = 40/1) to give **2am** (68.7 mg, 0.160 mmol, 80%, *syn*:*anti* = >99:1) as a white solid. The stereochemistry of the product was confirmed by NOE.

^{1}H NMR ($CDCl_3$): δ 7.22 (d, J = 8.4 Hz, 2H), 7.17–7.06 (m, 7H), 7.00–6.99 (m, 3H), 6.93 (d, J = 8.4 Hz, 2H), 2.20 (s, 3H), 1.36 (s, 12H).

^{13}C NMR ($CDCl_3$): δ 142.6, 139.8, 138.3, 136.7, 131.3, 130.8, 130.5. 129.4, 129.2, 128.1, 127.7. 127.3, 126.5, 84.3, 24.8, 16.1 (the signal of the carbon at the ipso position of the boron atom was not observed).

^{11}B NMR ($CDCl_3$): δ 30.3 (br).

HRMS (APCI-MS, positive): *m/z* = 428.1980. Calcd. for $C_{27}H_{29}BO_2S$: 428.1981 $[M]^+$.

Melting point: 103.2–106.6 °C

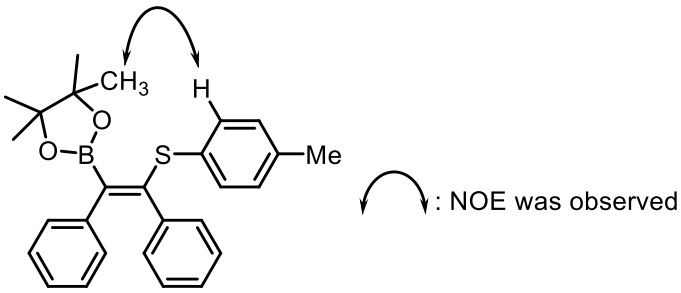

(*E*)-2-(1,2-diphenyl-2-(phenylselanyl)vinyl)-4,4,5,5-tetramethyl-1,3,2-dioxaborolane (2an):

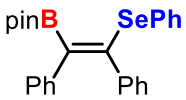

Obtained in 71% yield from diphenyl diselenide. The residue was purified by column chromatography on silica gel (hexane/AcOEt = 40/1) to give **2an** (65.4 mg, 0.142 mmol, 71%, *syn*:*anti* = >99:1) as a white solid. The stereochemistry of the product was confirmed by X-ray crystallography.

^{1}H NMR ($CDCl_3$): δ 7.41–7.40 (m, 2H), 7.11–7.06 (m, 10H), 6.98–6.96 (m, 3H), 1.37 (s, 12H).

^{13}C NMR ($CDCl_3$): δ 142.1 (br), 140.6, 140.3, 140.1, 133.4, 130.4, 130.2. 129.1, 128.7, 128.1, 127.5. 127.1, 127.0, 126.5, 84.4, 24.9.

^{11}B NMR ($CDCl_3$): δ 29.6 (br).

HRMS (APCI-MS, positive): *m/z* = 462.1270. Calcd. for $C_{26}H_{27}BO_2{}^{80}Se$: 462.1270 $[M]^+$.

Melting point: 112.5–115.1 °C

(*E*)-4,4,5,5-Tetramethyl-2-(2-(perfluorophenyl)-1,2-diphenylvinyl)-1,3,2-dioxaborolane (2ao):

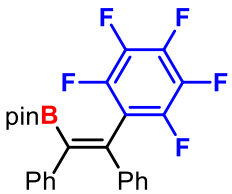

Obtained in 78% yield using hexafluorobenzene. NaNp was used insead of LiNp. The residue was purified by column chromatography on silica gel (hexane/CH_2Cl_2 = 10/1) to give **2ao** (74.0 mg, 0.157 mmol, *syn*:*anti* >99:1) as a white solid. The stereochemistry of the product was confirmed by X-ray crystallography.

^{1}H NMR ($CDCl_3$): δ 7.16–7.05 (m, 8H), 6.97–6.96 (m, 2H), 1.14 (s, 12H).

^{13}C NMR ($CDCl_3$): δ 144.6 (dm, J = 250.1 Hz), 140.6 (dm, J = 251.9 Hz), 140.1, 139.6, 137.8, 137.5 (dm, J = 251.7 Hz), 129.7, 129.6, 128.1, 128.0, 127.6, 126.7, 118.9–118.6 (m), 84.0, 24.5 (The carbon bearing a boron atom was hardly observed due to the quadrupolar relaxation mechanism of ^{11}B nucleus).

^{11}B NMR ($CDCl_3$): δ 30.1 (br).

^{19}F NMR ($CDCl_3$): δ –141.4 (dd, J = 21.9, 7.6 Hz, 2F), –157.1 (t, J = 21.9 Hz, 1F), –163.9 (td, J = 21.9, 7.6 Hz, 2F).

HRMS (APCI-MS, positive): *m/z* = 472.1633. Calcd. for $C_{26}H_{22}BF_5O_2$: 472.1632 $[M]^+$.

Melting point: 112.5–115.1 °C

Synthesis of 2ap-2av

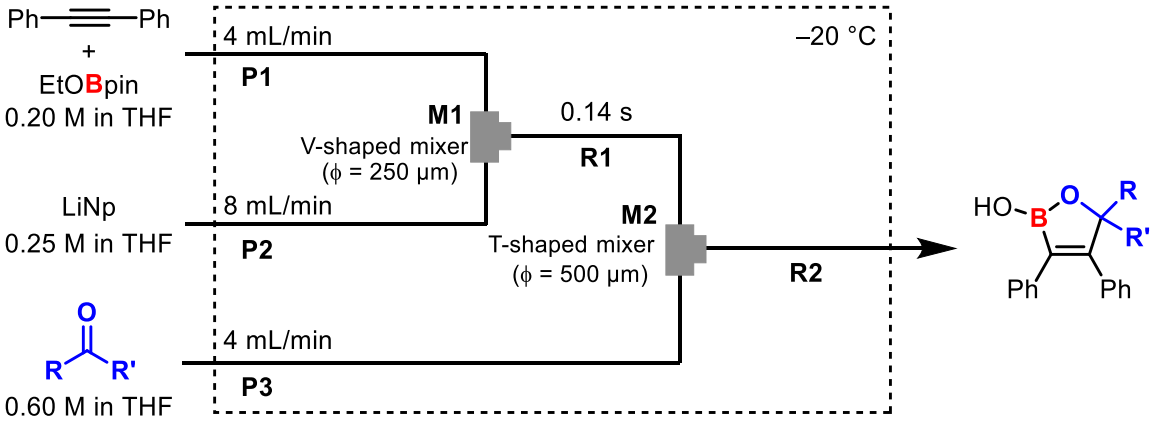

A flow microreactor system consisting of an anchor-shaped micromixer (**M1**), a T-shaped micromixer (**M2**), two microtube reactors (**R1**, **R2**), and three pre-cooling units (**P1**, **P2**, and **P3**, inner diameter ϕ = 1000 μm, length L = 100 cm) was used. The flow microreactor system was immersed in a cooling bath (–20 °C). A solution of diphenylacetylene (**1a**) containing EtOBpin (0.20 M in THF, flow rate: 4 mL/min), and a solution of LiNp (0.25 M in THF, flow rate: 8 mL/min) were introduced to **M1** (ϕ = 250 μm) using syringe pumps, and the mixed solution was passed through **R1** (L = 3.5 cm, ϕ = 1000 μm). A solution of carbonyl compound (0.60 M in THF, flow rate: 4 mL/min) was introduced to **M2** (ϕ = 500 μm) using a syringe pump, and the resulting solution was passed through **R2** (L = 200 cm, ϕ = 1000 μm). After a steady state was reached, the product solution was collected into a vial with aqueous 10% HCl.

The resulting biphasic solution was extracted three times with AcOEt. The combined organic layer was dried over Na_2SO_4 and concentrated under reduced pressure.

2,5-Dihydro-2-hydroxy-3,4,5-triphenyl-1,2-oxaborole (2ap):

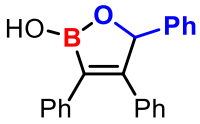

Obtained in 86% yield using benzaldehyde. The residue was purified by column chromatography on silica gel (hexane/AcOEt = 10/1) to give **2ap** (53.4 mg, 0.171 mmol) as a white solid.

^{1}H NMR ($CDCl_3$): δ 7.27–7.24 (m, 9H), 7.20–7.13 (m, 4H), 6.98 (dd, J = 8.1, 1.5 Hz, 2H), 6.01 (s, 1H), 4.69 (br, 1H).

^{13}C NMR ($CDCl_3$): δ 163.2, 138.2, 136.2, 135.2, 128.8, 128.7, 128.54, 128.52, 128.4, 128.2, 127.4, 127.0 (one aromatic carbon signal could not be located due to overlapping), 86.3 (The carbon bearing a boron atom was hardly observed due to the quadrupolar relaxation mechanism of ^{11}B nucleus).

^{11}B NMR ($CDCl_3$): δ 32.4 (br).

HRMS (APCI-MS, positive): *m/z* = 312.1322. Calcd. for $C_{21}H_{17}BO_2$: 312.1320 $[M]^+$.

Melting point: 156.8 °C (decomp.)

2,5-Dihydro-2-hydroxy-3,4-diphenyl-5-(4-methoxyphenyl)-1,2-oxaborole (2aq):

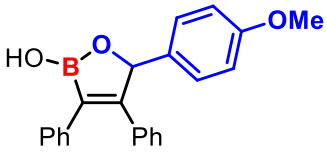

Obtained in 86% yield using 4-methoxybenzaldehyde. The residue was purified by column chromatography on silica gel (hexane/AcOEt = 5/1) to give **2aq** (59.1 mg, 0.173 mmol) as a white solid.

^{1}H NMR ($CDCl_3$): δ 7.27–7.23 (m, 4H), 7.20–7.14 (m, 6H), 6.99 (dd, J = 8.0, 2.0 Hz, 2H), 6.80 (d, J = 8.0 Hz, 2H), 5.97 (s, 1H), 4.73 (br, 1H), 3.75 (s, 3H).

^{13}C NMR ($CDCl_3$): δ 163.0, 159.7, 136.3, 135.4, 130.4, 128.82, 128.76, 128.53, 128.50, 128.4, 128.1, 126.9, 114.1, 85.8, 55.3 (The carbon bearing a boron atom was hardly observed due to the quadrupolar relaxation mechanism of ^{11}B nucleus).

^{11}B NMR ($CDCl_3$): δ 32.6 (br).

HRMS (APCI-MS, positive): *m/z* = 342.1430. Calcd. for $C_{22}H_{19}BO_3$: 342.1426 $[M]^+$.

Melting point: 121.4 °C (decomp.)

2,5-Dihydro-2-hydroxy-3,4-diphenyl-5-(4-fluorophenyl)-1,2-oxaborole (2ar):

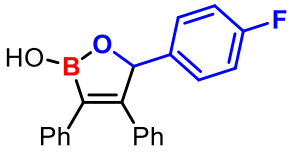

Obtained in 89% yield using 4-fluorobenzaldehyde. The residue was purified by column chromatography on silica gel (hexane/AcOEt = 10/1 to 5/1) to give **2ar** (58.7 mg, 0.178 mmol) as a white solid.

^{1}H NMR ($CDCl_3$): δ 7.27–7.15 (m, 10H), 6.98–6.93 (m, 4H), 6.00 (s, 1H), 4.75 (br, 1H).

^{13}C NMR ($CDCl_3$): δ 162.9, 162.7 (d, J = 246 Hz), 136.0, 135.1, 134.1 (d, J = 3.0 Hz), 129.1 (d, J = 8.6 Hz), 128.8, 128.54, 128.51, 128.4, 128.3, 127.1, 115.6 (d, J = 21.7 Hz), 85.5 (The carbon bearing a boron atom was hardly observed due to the quadrupolar relaxation mechanism of ^{11}B nucleus).

^{11}B NMR ($CDCl_3$): δ 32.7 (br).

^{19}F NMR ($CDCl_3$): δ –114.0.

HRMS (APCI-MS, positive): m/z = 330.1226. Calcd. for $C_{21}H_{16}BFO_2$: 330.1226 $[M]^+$.

Melting point: 136.7–141.4 °C

Methyl 4-(2-hydroxy-3,4-diphenyl-2,5-dihydro-1,2-oxaborol-5-yl)benzoate (2as):

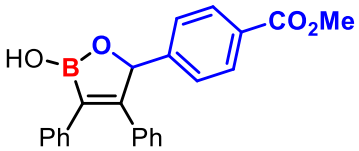

Obtained in 74% yield using methyl 4-formylbenzoate. The residue was purified by column chromatography on silica gel (hexane/AcOEt = 5/1) to give **2as** (55.0 mg, 0.149 mmol) as a white solid.

^{1}H NMR ($CDCl_3$): δ 7.92 (d, J = 8.4 Hz, 2H), 7.29–7.14 (m, 10H), 6.96–6.95 (m, 2H), 6.05 (s, 1H), 4.84 (br, 1H), 3.87 (s, 3H).

^{13}C NMR ($CDCl_3$): δ 167.0, 162.8, 143.3, 135.8, 134.9, 130.1, 129.9, 128.8, 128.52, 128.48, 128.4, 128.3, 127.2, 127.1, 85.6, 52.3 (The carbon bearing a boron atom was hardly observed due to the quadrupolar relaxation mechanism of ^{11}B nucleus).

^{11}B NMR ($CDCl_3$): δ 33.0 (br).

HRMS (APCI-MS, positive): m/z = 370.1378. Calcd. for $C_{23}H_{19}BO_4$: 370.1375 $[M]^+$.

Melting point: 106.4–110.0 °C

2,5-Dihydro-2-hydroxy-3,4,5,5-tetraphenyl-1,2-oxaborole (2at):

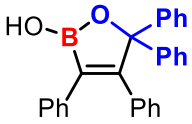

Obtained in 66% yield using benzophenone. The residue was purified by column chromatography on silica gel (hexane/AcOEt = 10/1) to give **2at** (50.9 mg, 0.131 mmol) as a white solid.

^{1}H NMR ($CDCl_3$): δ 7.33–7.29 (m, 11H), 7.18–7.17 (m, 5H), 7.08 (t, J = 7.8 Hz, 2H), 6.69 (d, J = 7.8 Hz, 2H), 4.68 (br, 1H).

^{13}C NMR ($CDCl_3$): δ 166.8, 141.2, 136.5, 136.1, 129.7, 129.1, 128.3, 128.2, 128.13, 128.06, 128.0, 126.9 (one aromatic carbon signal could not be located due to overlapping), 93.1 (The carbon bearing a boron atom was hardly observed due to the quadrupolar relaxation mechanism of ^{11}B nucleus).

^{11}B NMR ($CDCl_3$): δ 32.8 (br).

HRMS (APCI-MS, positive): m/z = 388.1631. Calcd. for $C_{27}H_{21}BO_2$: 388.1634 $[M]^+$.

Melting point: 100.9 °C (decomp.)

2,5-Dihydro-2-hydroxy-5,5-dimethyl-3,4-diphenyl-1,2-oxaborole (2au):

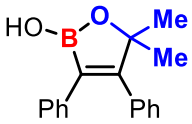

Obtained in 42% yield using acetone. The residue was purified by column chromatography on silica gel (hexane/AcOEt = 10/1) to give **2au** (22.1 mg, 0.0837 mmol) as a white solid.

^{1}H NMR ($CDCl_3$): δ 7.35–7.29 (m, 3H), 7.16–7.08 (m, 7H), 4.81 (br, 1H), 1.44 (s, 6H).

^{13}C NMR ($CDCl_3$): δ 169.7, 137.2, 136.2, 128.8, 128.7, 128.4, 128.2, 127.8, 126.7, 86.5, 27.0 (The carbon bearing a boron atom was hardly observed due to the quadrupolar relaxation mechanism of ^{11}B nucleus).

^{11}B NMR ($CDCl_3$): δ 34.1 (br).

HRMS (APCI-MS, positive): m/z = 264.1317. Calcd. for $C_{17}H_{17}BO_2$: 264.1319 $[M]^+$.

Melting point: 115.4 °C (decomp.)

7,8-Diphenyl-5-oxa-6-boraspiro[3.4]oct-7-en-6-ol (2av):

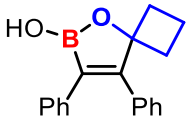

Obtained in 75% yield using cyclobutanone. The residue was purified by column chromatography on silica gel (hexane/AcOEt = 10/1) to give **2av** (41.6 mg, 0.151 mmol) as a white solid.

^{1}H NMR ($CDCl_3$): δ 7.40–7.43 (m, 3H), 7.25–7.24 (m, 2H), 7.16–7.09 (m, 5H), 4.88 (br, 1H), 2.51–2.44 (m, 4H), 1.84–1.77 (m, 1H), 1.89–1.11 (m, 1H).

^{13}C NMR ($CDCl_3$): δ 165.3, 136.9, 136.1, 128.85, 128.77, 128.4, 128.2, 127.8, 126.7, 89.0, 32.6, 13.3 (The carbon bearing a boron atom was hardly observed due to the quadrupolar relaxation mechanism of ^{11}B nucleus).

^{11}B NMR ($CDCl_3$): δ 31.9 (br).

HRMS (APCI-MS, positive): *m/z* = 277.1397. Calcd. for $C_{18}H_{18}BO_2$: 277.1398 $[M+H]^+$.

Melting point: 108.9 °C (decomp.)

Synthesis of 2aw

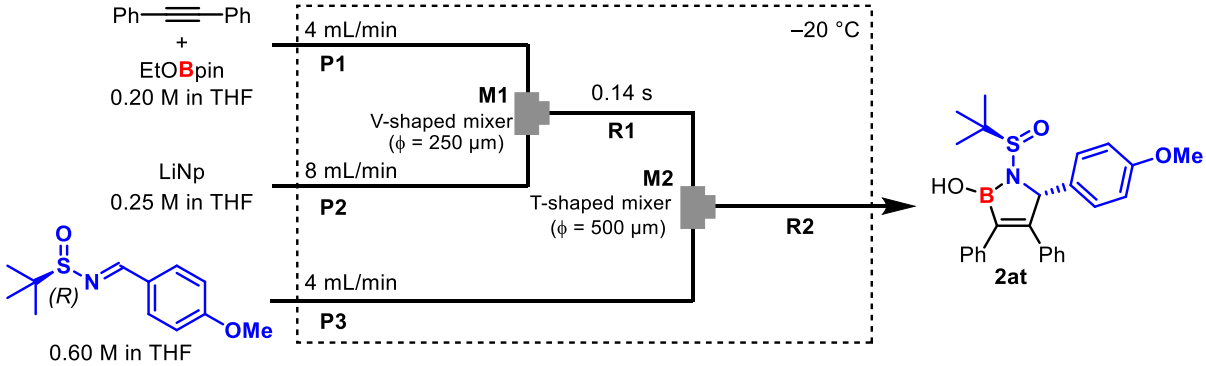

A flow microreactor system consisting of an anchor-shaped micromixer (**M1**), a T-shaped micromixer (**M2**), two microtube reactors (**R1**, **R2**), and three pre-cooling units (**P1**, **P2**, and **P3**, inner diameter ϕ = 1000 μm, length L = 100 cm) was used. The flow microreactor system was immersed in a cooling bath (–20 °C). A solution of diphenylacetylene (**1a**) containing EtOBpin (0.20 M in THF, flow rate: 4 mL/min), and a solution of LiNp (0.25 M in THF, flow rate: 8 mL/min) were introduced to **M1** (ϕ = 250 μm) using syringe pumps, and the mixed solution was passed through **R1** (L = 3.5 cm, ϕ = 1000 μm). A solution of (*R,E*)-(−)-*N*-(4-methoxybenzylidene)-*tert*-butanesulfinamide (0.60 M in THF, flow rate: 4 mL/min) was introduced to **M2** (ϕ = 500 μm) using a syringe pump, and the resulting solution was passed through **R2** (L = 200 cm, ϕ = 1000 μm). After a steady state was reached, the product solution was collected into a vial with saturated aqueous NH_4Cl for 15 s. The resulting biphasic solution

was extracted three times with AcOEt. The combined organic layer was dried over Na_2SO_4 and concentrated under reduced pressure. The residue was purified by column chromatography on silica gel (toluene/AcOEt = 10/1) to give **2aw** (34.9 mg, 0.0784 mmol, 39%) as a white solid. Obtained **2aw** was as a single diastereomer, but single crystals for X-ray crystallography to confirm the stereochemistry could not be grown.

^{1}H NMR (acetone-d_6): δ 7.22–7.07 (m, 13H), 6.74 (td, J = 9.0, 2.4 Hz, 2H), 5.95 (s, 1H), 3.68 (s, 3H), 1.03 (s, 9H).

^{13}C NMR (acetone-d_6): δ 161.5, 160.1, 137.9, 136.9, 132.0, 130.6, 130.0, 129.9, 128.7, 128.4, 127.2, 114.4 (one aromatic carbon signal could not be located due to overlapping), 71.1, 59.2, 55.3, 23.2 (The carbon bearing a boron atom was hardly observed due to the quadrupolar relaxation mechanism of ^{11}B nucleus).

^{11}B NMR ($CDCl_3$): δ 34.7 (br).

HRMS (APCI-MS, positive): m/z = 446.1957. Calcd. for $C_{26}H_{29}BNO_3S$: 446.1960 $[M+H]^+$.

Melting point: 115.5 °C (decomp.)

Synthesis of 2bn-2kn

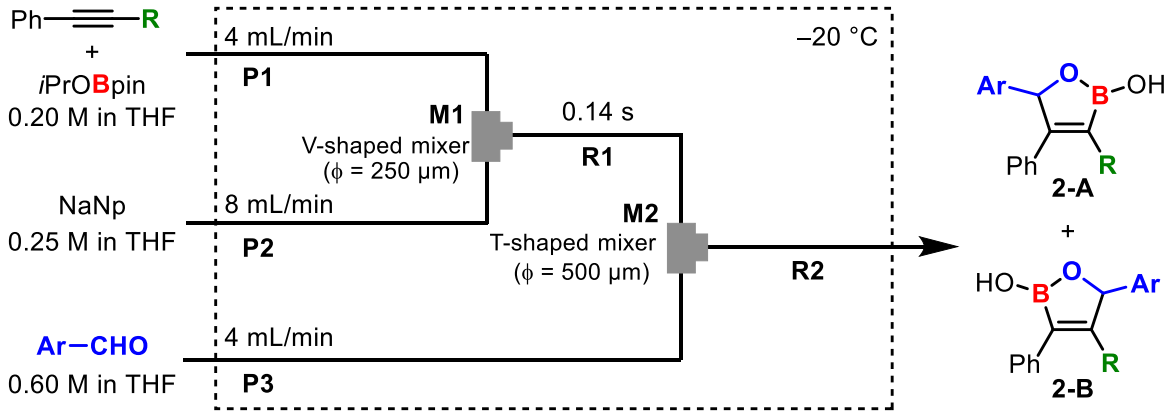

A flow microreactor system consisting of an anchor-shaped micromixer (**M1**), a T-shaped micromixer (**M2**), two microtube reactors (**R1**, **R2**), and three pre-cooling units (**P1**, **P2**, and **P3**, inner diameter ϕ = 1000 μm, length L = 100 cm) was used. The flow microreactor system was immersed in a cooling bath (–20 °C). A solution of substrate containing *i*PrOBpin (0.20 M in THF, flow rate: 4 mL/min), and a solution of NaNp (0.25 M in THF, flow rate: 8 mL/min) were introduced to **M1** (ϕ = 250 μm) using syringe pumps, and the mixed solution was passed through **R1** (L = 3.5 cm, ϕ = 1000 μm). A solution of aldehyde (0.60 M in THF, flow rate: 4 mL/min) was introduced to **M2** (ϕ = 500 μm) using a syringe pump, and the resulting solution was passed through **R2** (L = 200 cm, ϕ = 1000 μm). After a steady state was reached, the product solution was collected into a vial with aqueous 10% HCl. The resulting biphasic

solution was extracted three times with AcOEt. The combined organic layer was dried over Na_2SO_4 and concentrated under reduced pressure.

2,5-Dihydro-2-hydroxy-3-(4-methyl)phenyl-4-phenyl-5-(4-methoxy)phenyl-1,2-oxaborole (2bn-A) and 2,5-dihydro-2-hydroxy-3-phenyl-4-(4-methyl)phenyl-5-(4-methoxy)phenyl-1,2-oxaborole (2bn-B)

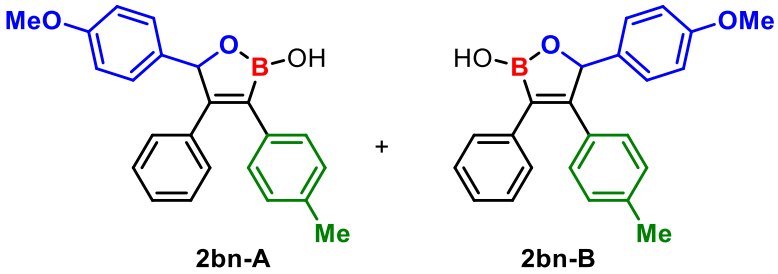

2bn-A **2bn-B**

Obtained in 67% yield from **2b** and 4-methoxybenzaldehyde. The residue was purified by column chromatography on silica gel (hexane/AcOEt = 5/1) to give **2bn-A** and **2bn-B** (48.0 mg, 0.135 mmol, **2bn-A**:**2bn-B** = 91:9) as a white solid. The stereochemistry of the products was confirmed by NOE.

^{1}H NMR ($CDCl_3$):

For **2bn-A**: δ 7.19–7.15 (m, 7H), 7.05 (d, J = 7.8 Hz, 2H), 7.00–6.99 (m, 2H), 6.79 (d, J = 7.8 Hz, 2H), 5.96 (s, 1H), 4.83 (br, 1H), 3.75 (s, 3H), 2.30 (s, 3H).

For **2bn-B**: δ 7.28–7.24 (m, 2H, overlapping with residual $CHCl_3$), 7.19–7.15 (m, 5H), 6.94 (d, J = 7.8 Hz, 2H), 6.89 (d, J = 7.8 Hz, 2H), 6.80–6.79 (m, 2H), 5.97 (s, 1H), 4.83 (br, 1H), 3.75 (s, 3H), 2.24 (s, 3H).

^{13}C NMR ($CDCl_3$):

For **2bn-A**: δ 162.0, 159.6, 136.6, 135.6, 133.2, 132.4 (br), 130.4, 129.2, 128.8, 128.7, 128.5, 128.4, 128.0, 114.0, 85.8, 55.3, 21.3.

For **2bn-B**: δ 162.7, 159.6, 138.0, 136.5, 132.4 (br), 132.2, 130.5, 129.1, 129.0, 128.85, 128.76, 128.4, 126.8, 114.0, 85.7, 55.3, 21.4.

^{11}B NMR ($CDCl_3$): δ 33.0 (br).

HRMS (APCI-MS, positive): m/z = 356.1578. Calcd. for $C_{23}H_{21}BO_3$: 356.1582 $[M]^+$.

Melting point: 105.2 °C (decomp.)

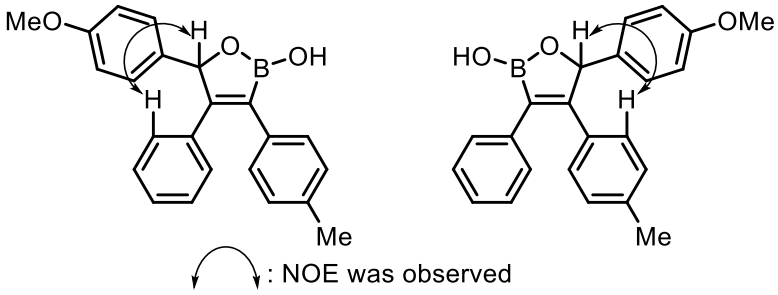

2,5-Dihydro-2-hydroxy-3-phenyl-4,5-di(4-methoxy)phenyl-1,2-oxaborole (2cn-A):

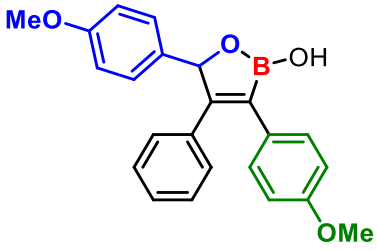

Obtained in 76% yield from **2c** and 4-methoxybenzaldehyde. The residue was purified by column chromatography on silica gel (hexane/AcOEt = 5/1) to give **2cn-A** (56.8 mg, 0.153 mmol) as a pale yellow solid. The stereochemistry of the product was confirmed by X-ray crystallography.

^{1}H NMR ($CDCl_3$): δ 7.23 (d, J = 7.2 Hz, 2H), 7.17–7.16 (m, 5H), 7.00 (dd, J = 7.2, 2.4 Hz, 2H), 6.80–6.78 (m, 4H), 5.93 (s, 1H), 4.53 (br, 1H), 3.78 (s, 3H), 3.76 (s, 3H).

^{13}C NMR ($CDCl_3$): δ 161.4, 159.6, 158.6, 135.8, 130.4, 130.1, 128.7, 128.6, 128.5, 128.4, 128.0, 114.0, 113.9, 85.9, 55.31, 55.29 (The carbon bearing a boron atom was hardly observed due to the quadrupolar relaxation mechanism of ^{11}B nucleus).

^{11}B NMR ($CDCl_3$): δ 32.8 (br).

HRMS (APCI-MS, positive): m/z = 372.1528. Calcd. for $C_{23}H_{21}BO_4$: 372.1531 $[M]^+$.

Melting point: 116.9 °C (decomp.)

2,5-Dihydro-2-hydroxy-3-(4-methoxyphenyl)-4-phenyl-5-(4-fluorophenyl)-1,2-oxaborole (2co-A):

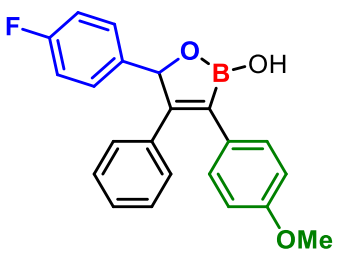

Obtained in 61% yield from **2c** and 4-fluorobenzaldehyde. The product solution was collected for 375 s (5.00 mmol scale). The residue was purified by column chromatography on

silica gel (hexane/AcOEt = 5/1) to give **2co-A** (1.10 g, 3.06 mmol) as a white solid. The stereochemistry of the product was confirmed by NOE.

^{1}H NMR ($CDCl_3$): δ 7.23–7.17 (m, 7H), 6.99–6.93 (m, 4H), 6.78 (d, J = 9.0 Hz, 2H), 5.96 (s, 1H), 4.72 (br, 1H), 3.78 (s, 3H).

^{13}C NMR ($CDCl_3$): δ 162.7 (d, J = 247 Hz), 161.3, 158.7, 135.5, 134.2 (d, J = 2.9 Hz), 130.1, 129.1 (d, J = 8.6 Hz), 128.6, 128.4, 128.3, 128.2, 115.6 (d, J = 21.7 Hz), 113.9, 85.5, 55.3 (The carbon bearing a boron atom was hardly observed due to the quadrupolar relaxation mechanism of ^{11}B nucleus).

^{11}B NMR ($CDCl_3$): δ 32.9 (br).

^{19}F NMR ($CDCl_3$): δ –114.1.

HRMS (APCI-MS, positive): *m/z* = 360.1327. Calcd. for $C_{22}H_{18}BFO_3$: 360.1331 $[M]^+$.

Melting point: 151.9–156.4 °C

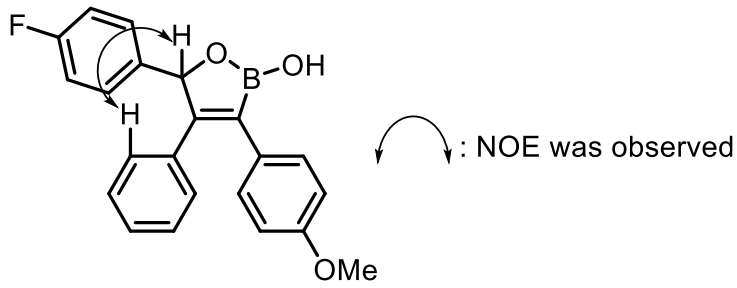

2,5-Dihydro-2-hydroxy-3-phenyl-4-(4-trimethylsilyl)phenyl-5-(4-methoxy)phenyl-1,2-oxaborole (2dn-B):

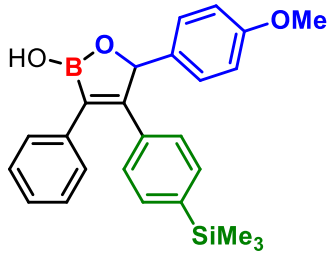

Obtained in 79% yield from **2d** and 4-methoxybenzaldehyde. The residue was purified by column chromatography on silica gel (hexane/AcOEt = 5/1) to give **2dn-B** (65.1 mg, 0.157 mmol) as a white solid. The stereochemistry of the product was confirmed by NOE.

^{1}H NMR ($CDCl_3$): δ 7.28–7.25 (m, 6H), 7.22–7.19 (m, 3H), 6.97 (d, J = 8.4 Hz, 2H), 6.82 (d, J = 8.4 Hz, 2H), 5.98 (s, 1H), 4.74 (br, 1H), 3.77 (s, 3H), 0.19 (s, 9H).

^{13}C NMR ($CDCl_3$): δ 162.5, 159.7, 140.6, 136.5, 135.4, 133.3, 130.5, 128.9, 128.8, 128.5, 127.7, 126.9, 114.1, 85.7, 55.3, –1.07 (The carbon bearing a boron atom was hardly observed due to the quadrupolar relaxation mechanism of ^{11}B nucleus).

^{11}B NMR ($CDCl_3$): δ 32.6 (br).

^{29}Si NMR ($CDCl_3$): δ –4.12.

HRMS (APCI-MS, positive): *m/z* = 414.1822. Calcd. for $C_{25}H_{27}BO_3Si$: 414.1822 $[M]^+$.

Melting point: 171.1–174.1 °C

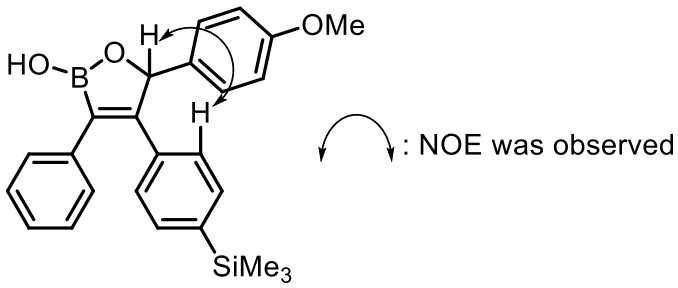

2,5-Dihydro-2-hydroxy-3-phenyl-4-(4-methylsulfanyl)phenyl-5-(4-methoxy)phenyl-1,2-oxaborole (2en-B):

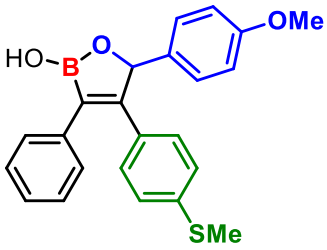

Obtained in 60% yield from **2e** and 4-methoxybenzldehyde. The residue was purified by column chromatography on silica gel (hexane/AcOEt = 5/1) to give **2en-B** (46.5 mg, 0.120 mmol) as a white solid. The stereochemistry of the product was confirmed by NOE.

^{1}H NMR (acetone-d_6): δ 7.85 (s, 1H), 7.30 (d, J = 7.2 Hz, 2H), 7.25–7.21 (m, 4H), 7.18 (t, J = 7.2 Hz, 1H), 7.05–7.02 (m, 4H), 6.82–6.80 (m, 2H), 6.07 (s, 1H), 3.72 (s, 3H), 2.41 (s, 3H).

^{13}C NMR (acetone-d_6): δ 163.2, 160.4, 139.6, 138.0, 134.4 (br), 132.9, 132.3, 129.9, 129.7, 129.5, 128.9, 127.3, 126.1, 114.5, 85.6, 55.4, 14.8.

^{11}B NMR ($CDCl_3$): δ 32.6 (br).

HRMS (APCI-MS, positive): *m/z* = 388.1307. Calcd. for $C_{23}H_{21}BO_3S$: 388.1303 $[M]^+$.

Melting point: 123.5 °C (decomp.)

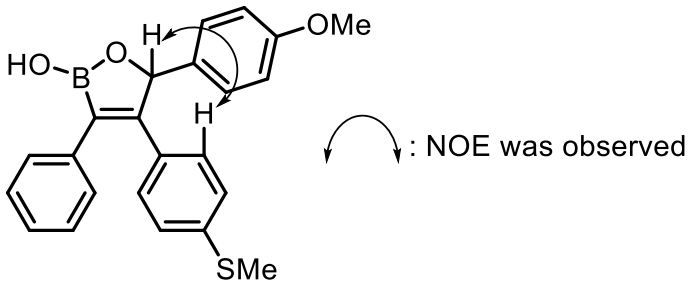

2,5-Dihydro-2-hydroxy-3-phenyl-4-(4-trimethylsilyl)phenyl-5-(4-methoxy)phenyl-1,2-oxaborole (2fn-B):

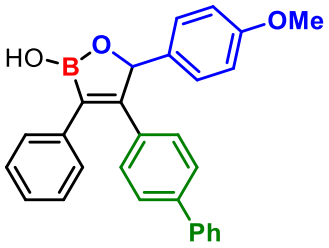

Obtained in 73% yield from **2f** and 4-methoxybenzaldehyde. The residue was purified by column chromatography on silica gel (hexane/AcOEt = 5/1) to give **2fn-B** (60.8 mg, 0.145 mmol) as a white solid. The stereochemistry of the product was confirmed by NOE.

^{1}H NMR (acetone-d_6): δ 7.92 (s, 1H), 7.59 (d, J = 6.6 Hz, 2H), 7.49–7.47 (m, 2H), 7.42–7.39 (m, 2H), 7.35–7.31 (m, 3H), 7.27–7.23 (m, 4H), 7.21–7.18 (m, 3H), 6.83–6.81 (m, 2H), 6.14 (s, 1H), 3.71 (s, 3H).

^{13}C NMR (acetone-d_6): δ 163.4, 160.5, 141.0, 140.9, 138.0, 135.7 (br), 134.4, 132.3, 130.0, 129.81, 129.76, 129.6, 129.0, 128.4, 127.5, 127.4, 114.6 (one aromatic carbon signal could not be located due to overlapping), 85.7, 55.4.

^{11}B NMR ($CDCl_3$): δ 32.6 (br).

HRMS (APCI-MS, positive): m/z = 418.1740. Calcd. for $C_{28}H_{23}BO_3$: 418.1740 $[M]^+$.

Melting point: 134.1 °C (decomp.)

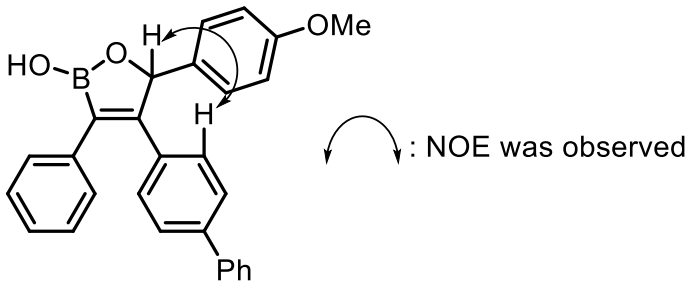

2,5-Dihydro-2-hydroxy-3-phenyl-4-(4-phenylethynyl)phenyl-5-(4-methoxy)phenyl-1,2-oxaborole (2gn-B):

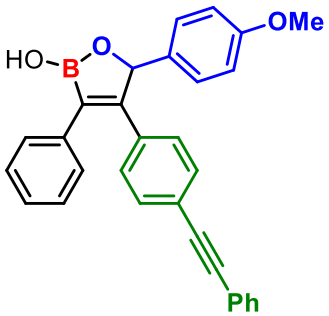

Obtained in 58% yield. A solution of **2g** containing *i*PrOBpin (0.080 M in THF, flow rate: 6.67 mL/min), and a solution of NaNp (0.25 M in THF, flow rate: 5.33 mL/min) were introduced to **M1** (ϕ = 250 μm) using syringe pumps. A solution of 4-methoxybenzaldehyde (0.60 M in THF, flow rate: 2.67 mL/min) was introduced to **M2**. After a steady state was reached, the product solution was collected for 22.5 s. The residue was purified by column chromatography on silica gel (hexane/AcOEt = 5/1) to give **2gn-B** (51.3 mg, 0.116 mmol) as a white solid. The stereochemistry of the product was confirmed by X-ray crystallography.

^{1}H NMR (acetone-d_6): δ 7.99 (s, 1H), 7.52–7.50 (m, 2H), 7.39–7.31 (m, 7H), 7.27–7.19 (m, 5H), 7.14 (d, J = 8.4 Hz, 2H), 6.83–6.81 (m, 2H), 6.12 (s, 1H), 3.72 (s, 3H).

^{13}C NMR (acetone-d_6): δ 163.1, 160.5, 137.6, 137.0, 134.8 (br), 132.3, 132.1, 131.9, 129.8, 129.7, 129.5, 129.4, 129.0, 127.5, 123.9, 123.3, 114.5 (one aromatic carbon signal could not be located due to overlapping), 90.8, 89.8, 85.6, 55.4.

^{11}B NMR ($CDCl_3$): δ 32.7 (br).

HRMS (APCI-MS, positive): *m/z* = 442.1744. Calcd. for $C_{30}H_{23}BO_3$: 442.1740 $[M]^+$.

Melting point: 121.6 °C (decomp.)

2,5-Dihydro-2-hydroxy-3-(3-methoxy)phenyl-4-phenyl-5-(4-methoxy)phenyl-1,2-oxaborole (2hn-A) and 2,5-dihydro-2-hydroxy-3-phenyl-4-(3-methoxy)phenyl-5-(4-methoxy)phenyl-1,2-oxaborole (2hn-B)

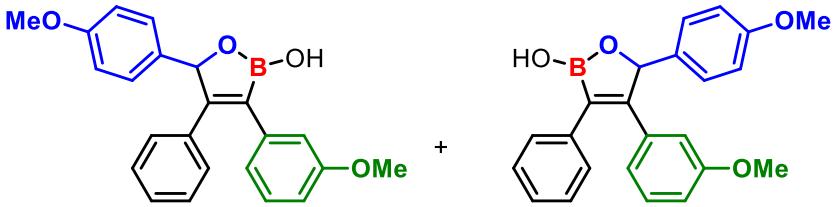

2hn-A **2hn-B**

Obtained in 90% yield from **2h** and 4-methoxybenzaldehyde. The residue was purified by column chromatography on silica gel (hexane/AcOEt = 5/1) to give **2hn-A** and **2hn-B** (56.0 mg, 0.157 mmol, **2hn-A**:**2hn-B** = 28:72) as a pale yellow solid. The stereochemistry of the products was confirmed by NOE.

^{1}H NMR (acetone-d_6):

For **2hn-A**: δ 7.90 (s, 1H), 7.31–7.07 (m, 8H), 6.89 (d, J = 7.2 Hz, 1H), 6.84–6.80 (m, 3H), 6.74–6.71 (m, 1H), 6.05 (s, 1H), 3.72 (s, 3H), 3.61 (s, 3H).

For **2hn-B**: δ 7.88 (s, 1H), 7.31–7.07 (m, 8H), 6.84–6.80 (m, 2H), 6.74–6.71 (m, 1H), 6.66 (d, J = 7.2 Hz, 1H), 6.632–6.625 (m, 1H), 6.06 (s, 1H), 3.73 (s, 3H), 3.58 (s, 3H).

^{13}C NMR (acetone-d_6):

For **2hn-A**: δ 164.2, 160.3, 160.2, 138.9, 136.8, 134.0 (br), 131.9, 129.7, 129.3, 129.2, 128.9, 128.5, 122.1, 114.9, 114.4, 113.0, 85.7, 55.3, 55.0.

For **2hn-B**: δ 163.6, 160.3, 160.2, 137.81, 137.79, 134.0 (br), 132.0, 130.0, 129.6, 129.4, 128.8, 127.2, 121.5, 114.7, 114.4, 114.1, 85.6, 55.3, 55.1.

^{11}B NMR ($CDCl_3$): δ 32.9 (br).

HRMS (APCI-MS, positive): *m/z* = 372.1530. Calcd. for $C_{23}H_{21}BO_4$: 372.1531 $[M]^+$.

Melting point: 70.3 °C (decomp.)

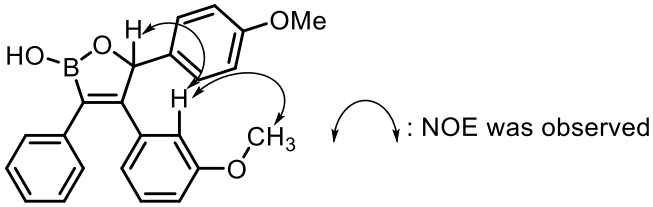

2,5-Dihydro-2-hydroxy-3-phenyl-4-(2-methoxy)phenyl-(4-methoxy)phenyl-1,2-oxaborole (2in-B):

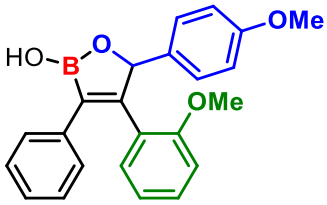

Obtained in 51% yield from **2i** and 4-methoxybenzaldehyde. The residue was purified by column chromatography on silica gel (hexane/AcOEt = 5/1) to give **2in-B** (37.7 mg, 0.101 mmol) as a white solid. The stereochemistry of the product was confirmed by NOE.

^{1}H NMR (acetone-d_6): δ 7.86 (s, 1H), 7.28 (d, J = 7.8 Hz, 2H), 7.18–7.09 (m, 6H), 6.94 (d, J = 7.8 Hz, 1H), 6.77–6.66 (m, 4H), 6.11 (s, 1H), 3.702 (s, 3H), 3.696 (s, 3H).

^{13}C NMR (acetone-d_6): δ 162.9, 160.2, 157.6, 138.1, 132.2, 131.1, 130.1, 129.4, 129.0, 128.6, 127.1, 126.0, 121.1, 114.2, 112.0, 85.5, 55.7, 55.4 (The carbon bearing a boron atom was hardly observed due to the quadrupolar relaxation mechanism of ^{11}B nucleus).

^{11}B NMR ($CDCl_3$): δ 32.9 (br).

HRMS (APCI-MS, positive): *m/z* = 372.1530. Calcd. for $C_{23}H_{21}BO_4$: 372.1531 $[M]^+$.

Melting point: 55.5 °C (decomp.)

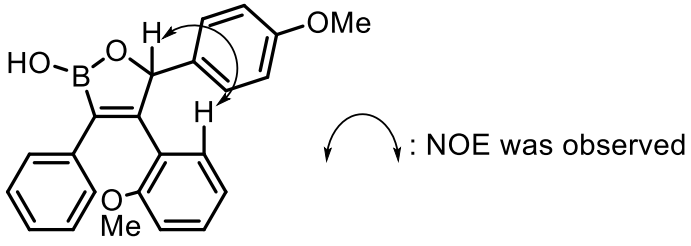

2,5-Dihydro-2-hydroxy-3-methyl-4-phenyl-5-(4-methoxy)phenyl-1,2-oxaborole (2jn-A):

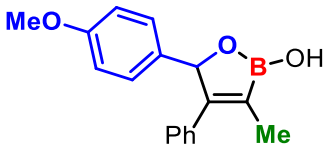

Obtained in 52% yield from **2j** and 4-methoxybenzaldehyde. LiDTBB was used instead of NaNp. The residue was purified by column chromatography on silica gel (hexane/AcOEt = 5/1) to give **2jn-A** (29.0 mg, 0.104 mmol) as a white solid. The stereochemistry of the products were confirmed by NOE.

^{1}H NMR (acetone-d_6): δ 7.63 (s, 1H), 7.31–7.20 (m, 5H), 7.13 (d, J = 9.0 Hz, 2H), 6.76 (d, J = 9.0 Hz, 2H), 5.979 (s, 0.5H, isomer 1), 5.975 (s, 0.5H, isomer 2), 3.70 (s, 3H), 1.903 (s, 1.5H, isomer 1), 1.901 (s, 1.5 H, isomer 2).

^{13}C NMR (acetone-d_6): δ 163.3, 160.3, 136.7, 132.9, 129.4, 129.2, 129.1, 128.4, 114.4, 85.4, 55.4, 12.5. (The carbon bearing a boron atom was hardly observed due to the quadrupolar relaxation mechanism of ^{11}B nucleus).

^{11}B NMR ($CDCl_3$): δ 32.8 (br).

HRMS (APCI-MS, positive): *m/z* = 280.1269. Calcd. for $C_{23}H_{21}BO_4$: 280.1268 $[M]^+$.

Melting point: 61.4 °C (decomp.)

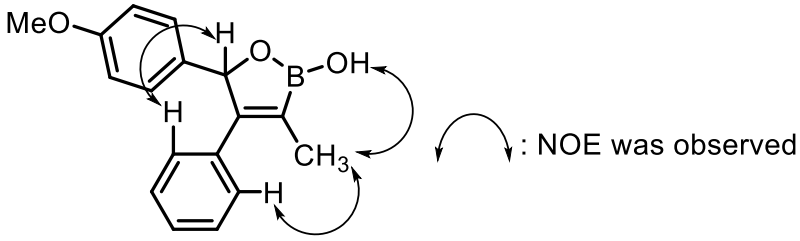

Synthesis of Zuclomifene (5)

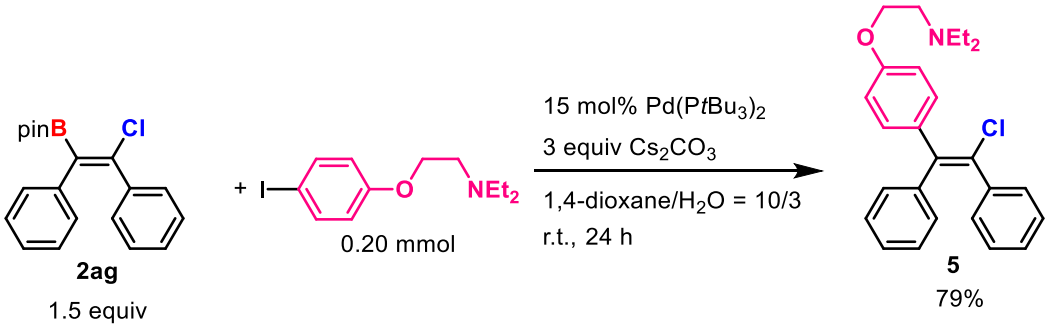

Compound **2ag** (0.102 g, 0.300 mmol, 1.5 equiv), *N*,*N*-diethyl-2-(4-iodophenoxy)ethan-1-amine (63.8 mg, 0.200 mmol), Cs_2CO_3 (0.195 g, 0.600 mmol, 3 equiv), Pd(P*t*Bu$_3$)$_2$ (15.3 mg, 0.0300 mmol, 15 mol%), 1,4-dioxane (0.2 mL), and H_2O (0.03 mL) were added to a Schlenk flask. The mixture was degassed with N_2 three times. The reaction mixture was heated at room

temperature for 24 h. After the reaction mixture was cooled to room temperature, the reaction was quenched with brine and the resulting biphasic solution was extracted three times with AcOEt. The combined organic layer was dried over Na_2SO_4 and concentrated under reduced pressure. The residue was purified by column chromatography on silica gel (hexane/AcOEt/NEt_3 = 50/50/1) to give **5** (64.4 mg, 0.159 mmol, 79%) as a white solid.

^{1}H NMR ($CDCl_3$): δ 7.31–7.28 (m, 4H), 7.17–7.16 (m, 3H), 7.09–7.08 (m, 3H), 6.95 (dd, 7.2, 2.4 Hz, 2H), 6.90 (d, J = 8.4 Hz, 2H), 4.19 (t, J = 5.7 Hz, 2H), 3.03 (t, J = 5.7 Hz, 2H), 2.80 (q, J = 7.2 Hz, 4H), 1.17 (t, J = 7.2 Hz, 6H).

^{13}C NMR ($CDCl_3$): δ 157.9, 141.4, 139.9, 139.7, 134.7, 131.4, 130.8, 130.1, 129.4, 128.00, 127.96, 127.1, 114.1 (one aromatic carbon signal could not be located due to overlapping), 65.6, 51.5, 47.8, 11.2.

HRMS (APCI-MS, positive): m/z = 406.1928. Calcd. for $C_{26}H_{29}{}^{35}ClNO$: 406.1932 $[M+H]^+$.

Melting point: 46.4–49.0 °C

Synthesis of (*E*)-(4-(1-chloro-2-phenyl-2-(4,4,5,5-tetramethyl-1,3,2-dioxaborolan-2-yl)vinyl)phenyl)trimethylsilane (2eg)

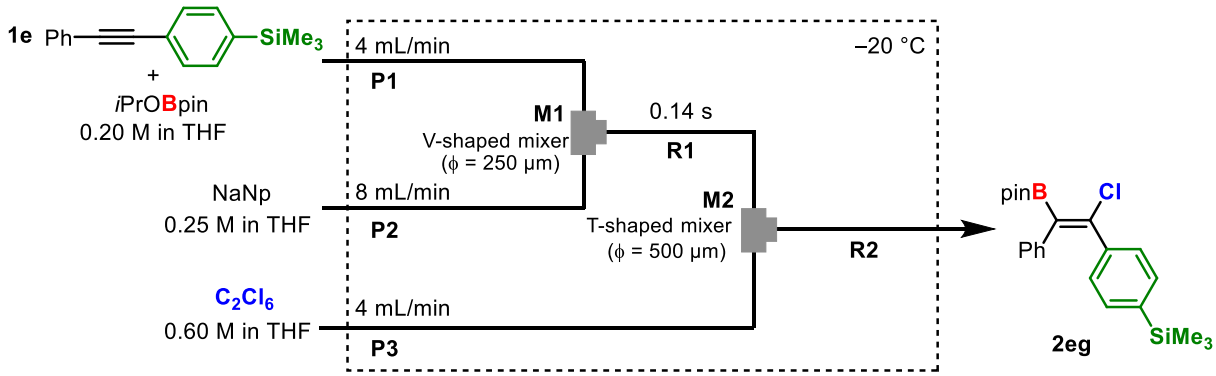

A flow microreactor system consisting of an anchor-shaped micromixer (**M1**), a T-shaped micromixer (**M2**), two microtube reactors (**R1**, **R2**), and three pre-cooling units (**P1**, **P2**, and **P3**, inner diameter ϕ = 1000 μm, length L = 100 cm)) was used. The flow microreactor system was immersed in a cooling bath (–20 °C). A solution of **1e** containing *i*PrOBpin (0.20 M in THF, flow rate: 4 mL/min), and a solution of NaNp (0.25 M in THF, flow rate: 8 mL/min) were introduced to **M1** (ϕ = 250 μm) using syringe pumps, and the mixed solution was passed through **R1** (L = 3.5 cm, ϕ = 1000 μm). A solution of electrophile (0.60 M in THF, flow rate: 4 mL/min) was introduced to **M2** (ϕ = 500 μm) using a syringe pump, and the resulting solution was passed through **R2** (L = 200 cm, ϕ = 1000 μm). After a steady state was reached, the product solution was collected into a flask with saturated aqueous NH_4Cl for 375 s. The

resulting biphasic solution was extracted three times with AcOEt. The combined organic layer was dried over Na_2SO_4 and concentrated under reduced pressure. The residue was purified by column chromatography on silica gel (hexane/AcOEt = 50/1) and recrystallized from MeOH to give **2eg** (1.45 g, 3.51 mmol, 70%) as a white solid.

^{1}H NMR ($CDCl_3$): δ 7.31 (d, J = 8.4 Hz, 2H), 7.19 (d, J = 8.4 Hz, 2H), 7.15–7.10 (m, 3H), 7.03 (dd, J = 8.4, 1.2 Hz, 2H), 1.36 (s, 12H), 0.21 (s, 9H). The stereochemistry of the products was confirmed by NOE.

^{13}C NMR ($CDCl_3$): δ 141.2, 138.7, 138.6, 138.5, 133.0, 128.9, 128.8, 128.4, 126.8, 84.6, 24.8, –1.09 (The carbon bearing a boron atom was hardly observed due to the quadrupolar relaxation mechanism of ^{11}B nucleus).

^{11}B NMR ($CDCl_3$): δ 29.9 (br).

^{29}Si NMR ($CDCl_3$): δ –4.00.

HRMS (APCI-MS, positive): m/z = 412.1794. Calcd. for $C_{23}H_{30}B^{35}ClO_2Si$: 412.1796 $[M]^+$.

Melting point: 129.9–130.3 °C

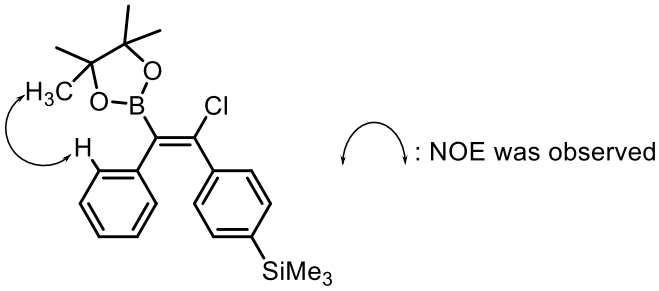

Procedure for Suzuki-Miyaura cross coupling of compound 2eg

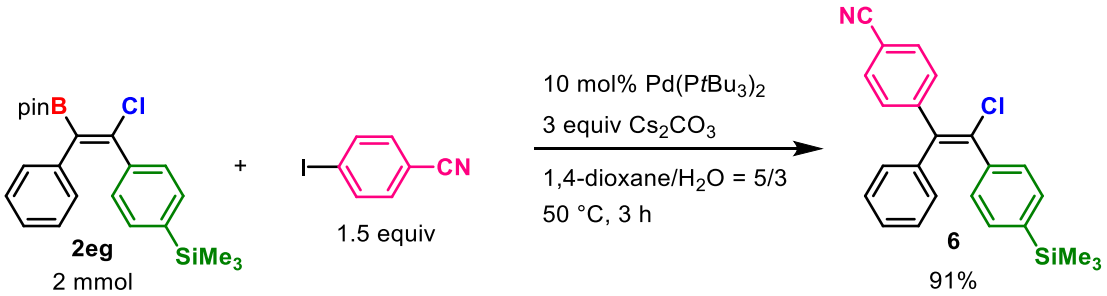

Compound **2eg** (0.826 g, 2.00 mmol), 4-iodobenzonitrile (0.687 g, 3.00 mmol, 1.5 equiv), Cs_2CO_3 (1.96 g, 6.00 mmol, 3 equiv), Pd(P*t*Bu$_3$)$_2$ (0.102 g, 0.200 mmol, 10 mol%), 1,4-dioxane (2.0 mL), and H_2O (1.2 mL) were added to a Schlenk flask. The mixture was de-gassed with N_2 three times. The reaction mixture was heated at 50 °C for 3 h. After the reaction mixture was cooled to room temperature, the reaction was quenched with saturated aqueous NH_4Cl and the resulting biphasic solution was extracted three times with AcOEt. The combined organic layer was dried over Na_2SO_4 and concentrated under reduced pressure. The residue was purified by

column chromatography on silica gel (hexane/toluene = 5/1 to 3/1) to give **6** (0.705 g, 1.82 mmol, 91%) as a white solid.

^{1}H NMR ($CDCl_3$): δ 7.66 (d, J = 8.4 Hz, 2H), 7.49 (d, J = 8.4 Hz, 2H), 7.34 (d, J = 8.4 Hz, 2H), 7.27 (d, J = 8.4 Hz, 2H), 7.17–7.12 (m, 3H), 6.93 (dd, J = 8.4, 1.8 Hz, 2H), 0.23 (s, 9H).

^{13}C NMR ($CDCl_3$): δ 146.8, 141.6, 140.1, 138.9, 138.7, 133.1, 132.2, 132.1, 130.9, 130.6, 129.1, 128.4, 127.7, 119.0, 111.3, –1.10.

^{29}Si NMR ($CDCl_3$): δ –3.85.

HRMS (APCI-MS, positive): m/z = 387.1206. Calcd. for $C_{24}H_{22}{}^{35}ClNSi$: 387.1205 $[M]^+$.

Melting point: 139.7–142.6 °C

Procedure for Suzuki-Miyaura cross coupling of compound 6

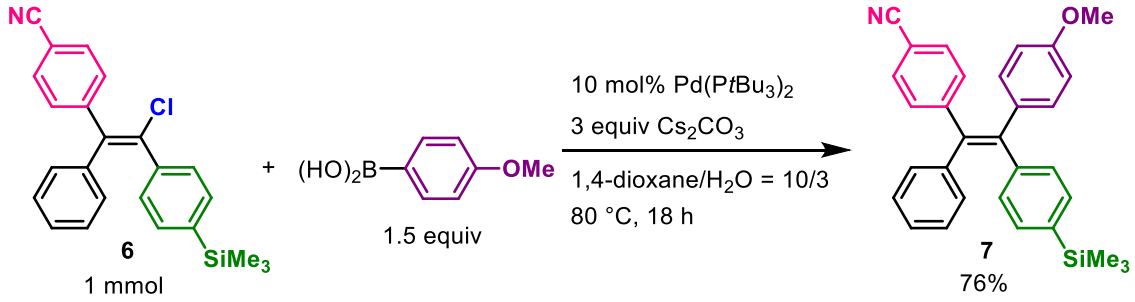

Compound **6** (0.388 g, 1.00 mmol), 4-methoxyphenylboronic acid (0.228 g, 1.50 mmol, 1.5 equiv), Cs_2CO_3 (0.978 g, 3.00 mmol, 3 equiv), $Pd(PtBu_3)_2$ (51.1 mg, 0.100 mmol, 10 mol%), 1,4-dioxane (2.0 mL), and H_2O (0.6 mL) were added to a Schlenk flask. The mixture was degassed with N_2 three times. The reaction mixture was heated at 80 °C for 18 h. After the reaction mixture was cooled to room temperature, the reaction was quenched with saturated aqueous NH_4Cl and the resulting biphasic solution was extracted three times with AcOEt. The combined organic layer was dried over Na_2SO_4 and concentrated under reduced pressure. The residue was purified by column chromatography on silica gel (hexane/toluene = 1/1) to give **7** (0.348 g, 0.758 mmol, 76%) as a white solid.

^{1}H NMR ($CDCl_3$): δ 7.38 (d, J = 8.0 Hz, 2H), 7.24 (d, J = 7.0 Hz, 2H), 7.13–7.11 (m, 5H), 6.97 (d, J = 7.0 Hz, 4H), 6.90 (d, J = 8.0 Hz, 2H), 6.66 (d, J = 8.0 Hz, 2H), 3.76 (s, 3H), 0.20 (s, 9H)

^{13}C NMR ($CDCl_3$): δ 158.8, 149.5, 143.4, 143.1, 143.0, 139.2, 138.4, 135.3, 132.8, 132.1, 131.7, 131.4, 130.5, 128.1, 126.9, 119.3, 113.5, 109.7 (one aromatic carbon signal could not be located due to overlapping), 55.3, –1.00.

^{29}Si NMR ($CDCl_3$): δ –4.37.

HRMS (APCI-MS, positive): m/z = 459.2018. Calcd. for $C_{31}H_{29}NOSi$: 459.2013 $[M]^+$.

Melting point: 185.4–187.1 °C

Procedure for Suzuki-Miyaura cross coupling of compound 2co-A

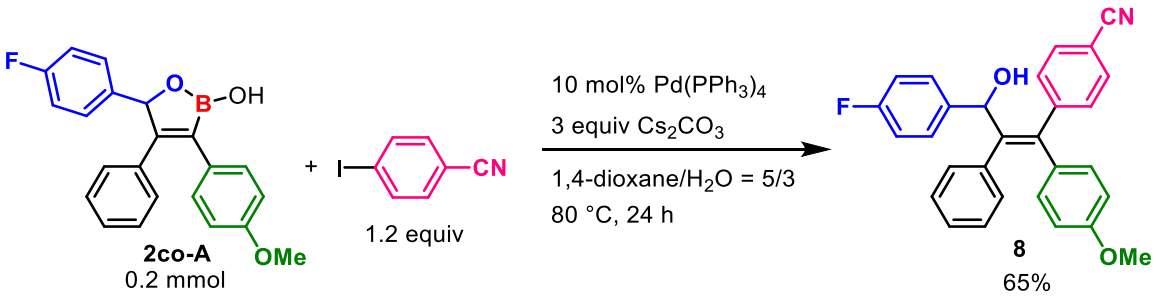

Compound **2co-A** (72.0 mg, 0.200 mmol), 4-iodobenzonitrile (55.0 mg, 0.300 mmol, 1.2 equiv), Cs_2CO_3 (0.195 g, 0.600 mmol, 3 equiv), $Pd(PPh_3)_4$ (23.1 mg, 0.0200 mmol, 10 mol%), 1,4-dioxane (1.0 mL), and H_2O (0.6 mL) were added to a Schlenk flask. The mixture was de-gassed with N_2 three times. The reaction was heated at 80 °C for 24 h. After the reaction mixture was cooled to room temperature, the reaction was quenched with saturated aqueous NH_4Cl and the resulting biphasic solution was extracted three times with AcOEt. The combined organic layer was dried over Na_2SO_4 and concentrated under reduced pressure. The residue was purified by column chromatography on silica gel (toluene/hexane = 1/0 to 1/1) to give **8** (56.8 mg, 0.130 mmol, 65%) as a white solid.

^{1}H NMR ($CDCl_3$): δ 7.71 (d, J = 8.1 Hz, 2H), 7.54 (d, J = 8.1 Hz, 2H), 7.17–7.07 (m, 5H), 6.98 (t, J = 8.1 Hz, 2H), 6.82 (d, J = 8.1 Hz, 2H), 6.78 (d, J = 8.1 Hz, 2H), 6.56 (d, J = 8.1 Hz, 2H), 5.74 (s, 1H), 3.68 (s, 3H), 1.93 (br, 1H).

^{13}C NMR ($CDCl_3$): δ 162.1 (d, J = 246 Hz), 158.4, 147.2, 141.2, 140.9, 138.0 (d, J = 2.9 Hz), 136.9, 133.1, 132.5, 131.6, 131.1, 130.6, 127.9, 127.6 (d, J = 8.8 Hz), 127.4, 118.8, 115.2 (d, J = 21.7 Hz), 113.3, 111.3, 73.3, 55.1.

^{19}F NMR ($CDCl_3$): δ –115.7.

HRMS (APCI-MS, positive): m/z = 435.1629. Calcd. for $C_{29}H_{22}FNO_2$: 435.1629 $[M]^+$.

Melting point: 62.1 °C (decomp.)

Procedure for synthesis of compound 9

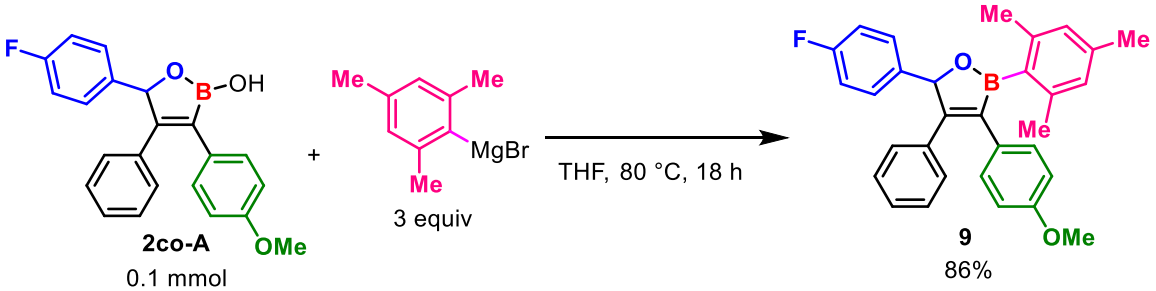

Compound **2co-A** (36.0 mg, 0.100 mmol) and THF (0.5 mL) were added to a Schlenk flask. The mixture was de-gassed with N_2 three times. Mesitylmagnesium bromide (0.96 M in THF,

0.31 mL, 3 equiv) was added to the mixture and heated at 80 °C for 18 h. After the reaction mixture was cooled to room temperature, the reaction was quenched with saturated aqueous NH_4Cl and the resulting biphasic solution was extracted three times with AcOEt. The combined organic layer was dried over Na_2SO_4 and concentrated under reduced pressure. The residue was purified by column chromatography on silica gel (hexane/AcOEt = 20/1) to give **9** (39.8 mg, 0.0861 mmol, 86%) as a white solid.

^{1}H NMR ($CDCl_3$): δ 7.28 (dd, J = 9.0, 5.4 Hz, 2H), 7.19–7.16 (m, 3H), 7.07–7.05 (dd, J = 6.3, 3.3 Hz, 2H), 6.98–6.92 (m, 4H), 6.78 (s, 2H), 6.63 (d, J = 9.0 Hz, 2H), 6.36 (s, 1H), 3.71 (s, 3H), 2.27 (s, 3H), 2.20 (s, 6H).

^{13}C NMR ($CDCl_3$): δ 163.2, 162.7 (d, J = 247 Hz), 158.4, 141.0 (br), 140.0, 138.4, 135.2, 133.9 (d, J = 2.9 Hz), 133.0 (br), 129.8, 129.4 (d, J = 7.1 Hz), 129.2, 128.7, 128.5, 128.2, 127.4, 115.6 (d, J = 21.7 Hz), 113.7, 91.6, 55.1, 22.3, 21.4.

^{11}B NMR ($CDCl_3$): δ 50.4.

^{19}F NMR ($CDCl_3$): δ –114.0.

HRMS (APCI-MS, positive): *m/z* = 462.2169. Calcd. for $C_{31}H_{28}BFO_2$: 462.2166 $[M]^+$.

Melting point: 145.0 °C (decomp.)

Procedure for synthesis of I'

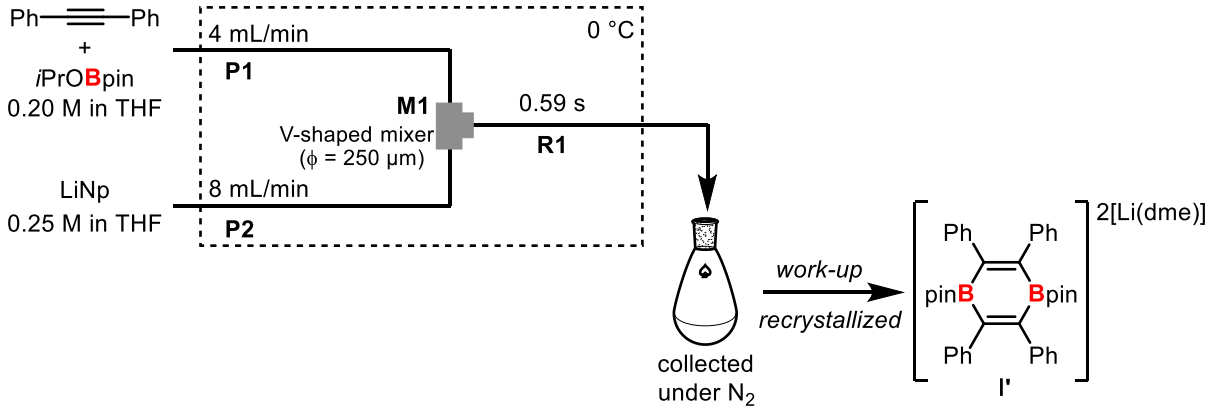

A flow microreactor system consisting of an anchor-shaped micromixer (**M1**) and two pre-cooling units (**P1** and **P2**, inner diameter ϕ = 1000 μm, length L = 100 cm) was used. The flow microreactor system was immersed in a cooling bath (0 °C). A solution of diphenylacetylene (**1a**) containing *i*PrOBpin (0.20 M in THF, flow rate: 4 mL/min), and a solution of LiNp (0.25 M in THF, flow rate: 8 mL/min) were introduced to **M1** (ϕ = 250 μm) using syringe pumps, and the mixed solution was passed through **R1** (L = 15 cm, ϕ = 1000 μm). After a steady state was reached, the product solution was collected into a Schlenk tube for 480 s (6.4 mmol scale) under N_2. The collected solution was dried under vacuum to remove THF. The dark brown

residue was dissolved in DME (30 mL) and centrifuged to remove insoluble materials. The brown supernatant was collected into another Schlenk tube and concentrated to ca. 5 mL. The solution was layered with hexane (10 mL) and stored at –20 °C to afford colorless crystals along with a brown oil. The structure of **I'** was unambiguously determined by X-ray crystallography with the obtained colorless crystal (See Figure S6).

X-ray Crystallography

Crystallographic data of **2af**, **2ag**, **2ah**, **2an**, **2ao, 2cn**, **2gn**, and **I'** are summarized in Tables S7, S8, and S9. Suitable crystals for X-ray analysis were placed on the end of a micro-mount coated with NVH oil. The X-ray intensity data collection was carried out on a Rigaku R-AXIS RAPID with an image plate detector at –150 °C or a Rigaku XTALAB P200 with a photon-counting detector at –180 °C using Cu-Kα radiation (λ = 1.5418 Å). Equivalent reflections were merged and the collected images were processed by a Rigaku RAPID AUTO or CrysAlisPro program. The initial structures were determined by SHELXS.[11] The further structure determination was performed by Fourier transform method and refined by least squares method on SHELXL.[12] All reflections were used during refinement with the exception of some abnormal reflections. Non-hydrogen atoms with the exception of the OH groups were refined anisotropically and hydrogen atoms were refined using riding models. The thermal ellipsoids of the disorders were fixed by SHELXL restraints. For **2af**, three crystallographically independent, but chemically equivalent molecules are present in the asymmetric unit. For **2ag**, the pinacolato group was disordered over two positions. For **2ao** and **2cn**, two crystallographically independent, but chemically equivalent molecules are present in the asymmetric unit. For **2gn**, the aryl and OMe groups were disordered over two positions. For **2gn** and **I'**, one site occupied by hexane was identified in the asymmetric unit. This site was considerably disordered and treated by SQUEEZE as a diffuse contribution.[13] In the resulting void space, contributions of 57 e^- per unit cell for **2gn** and 32 e^- per unit cell for **I'** were found and taken to represent 0.25 hexane for **2gn** and 0.5 hexane for **I'** in the asymmetric unit. These results were checked by the IUCR's CheckCIF routine. Alerts shown in the CheckCIF output are related to the disordered groups.

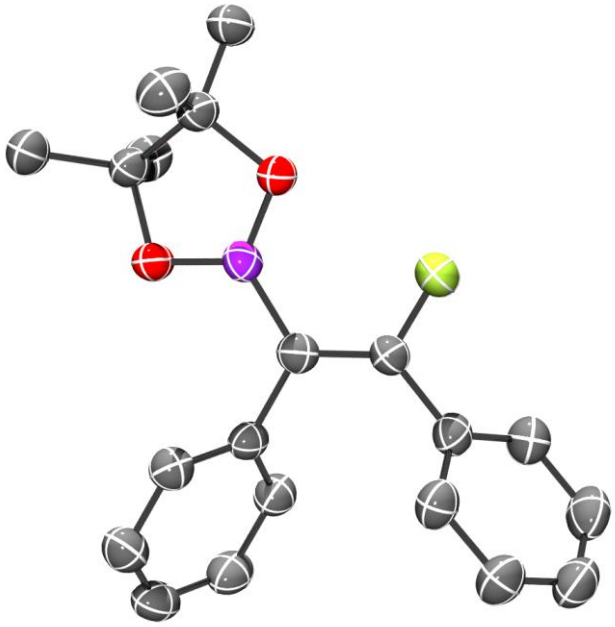

Figure S1. Molecular structures of **2af** with thermal ellipsoids at 50% probability.

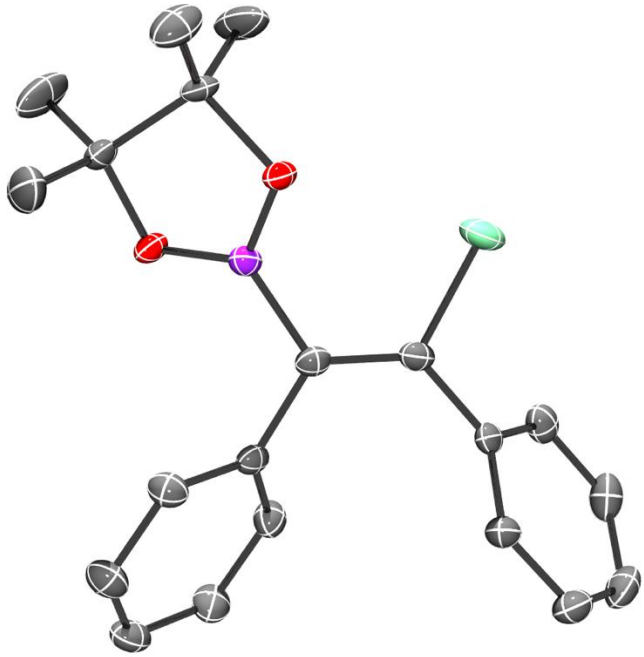

Figure S2. Molecular structures of **2ag** with thermal ellipsoids at 50% probability.

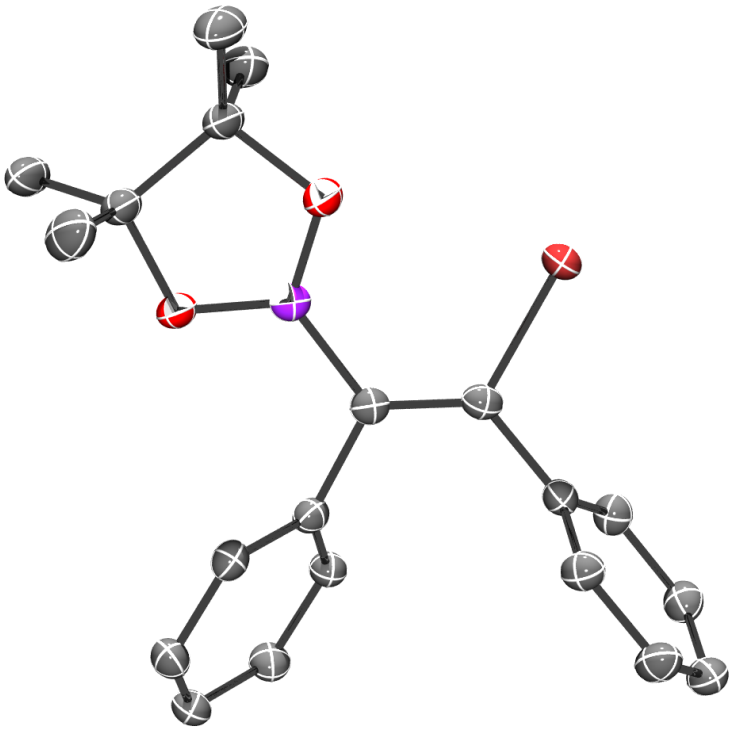

Figure S3. Molecular structure of **2ah** with thermal ellipsoids at 50% probability.

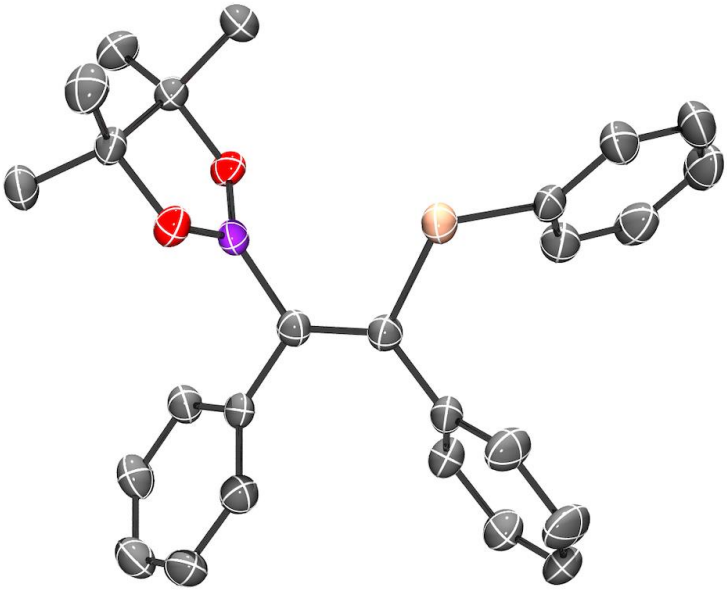

Figure S4. Molecular structure of **2an** with thermal ellipsoids at 50% probability.

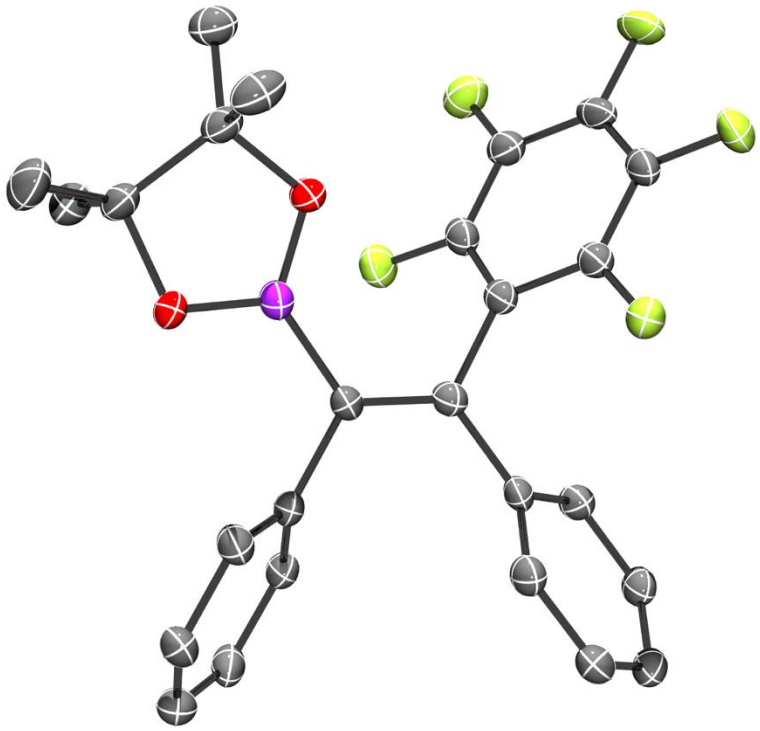

Figure S5. Molecular structure of **2ao** with thermal ellipsoids at 50% probability.

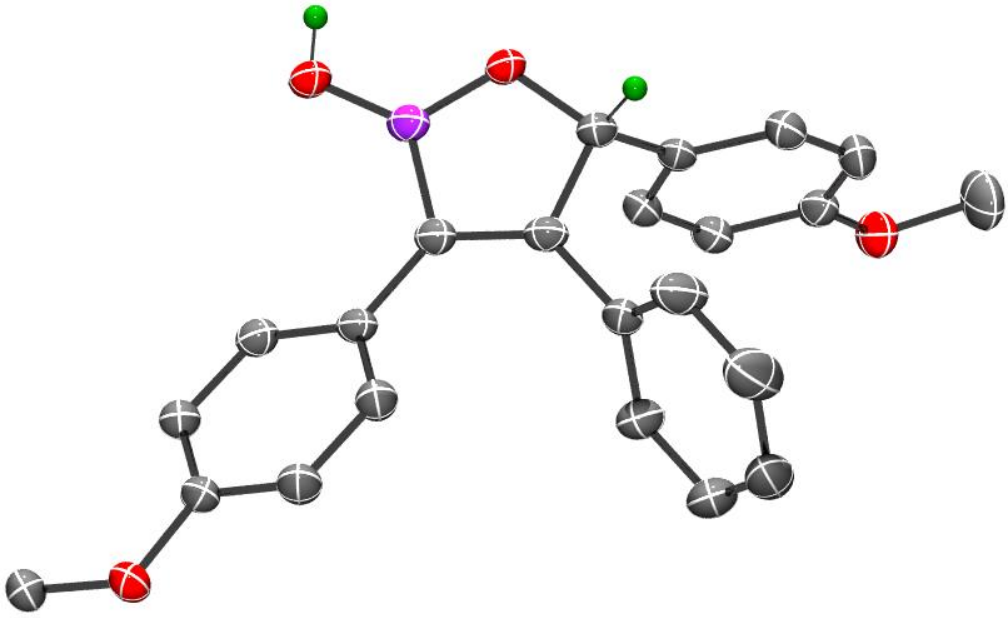

Figure S6. Molecular structure of **2cn** with thermal ellipsoids at 50% probability.

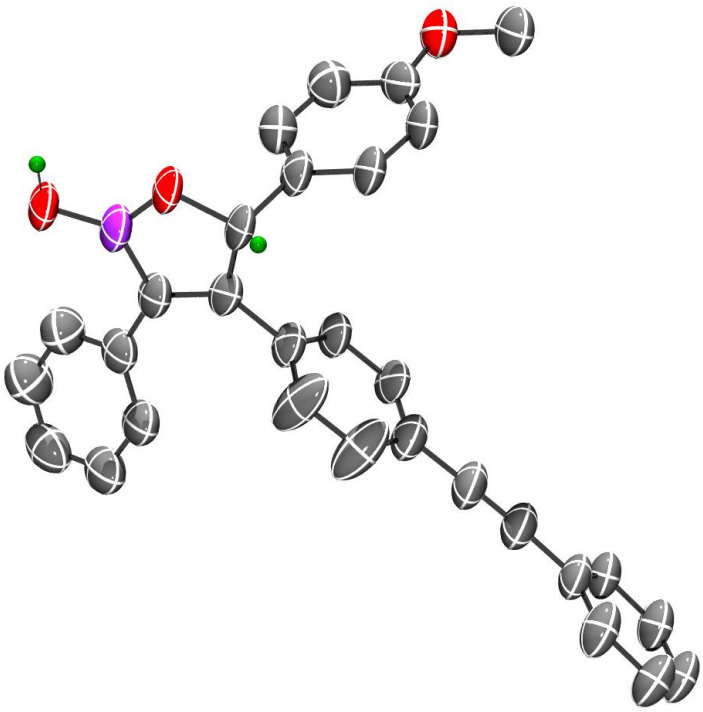

Figure S7. Molecular structure of **2gn** with thermal ellipsoids at 50% probability.

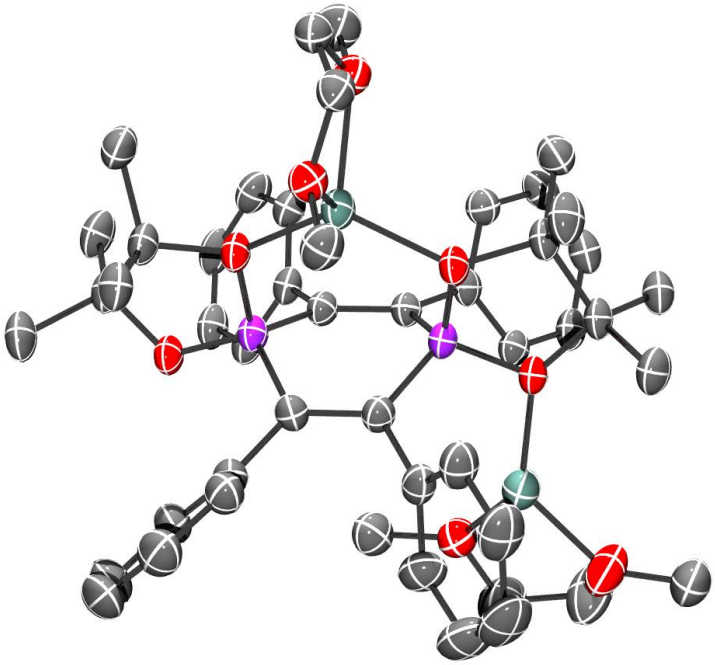

Figure S8. Molecular structure of **I'** with thermal ellipsoids at 50% probability.

Table S7. Summary of structure determinations of **2af**, **2ag**, and **2ah**.

Compound	**2af**	**2ag**	**2ah**
Formula	$C_{20}H_{22}B_1O_2F_1$	$C_{20}H_{22}B_1O_2Cl_1$	$C_{20}H_{22}B_1O_2Br_1$
Formula weight	342.18	340.63	385.09
Temperature / °C	–180	–180	–180
λ (Å)	1.54184	1.54184	1.54184
Crystal size / mm^3	0.10×0.05×0.01	0.10×0.08×0.05	0.21×0.15×0.15
Crystal system	*Monoclinic*	*Monoclinic*	*Orthorhombic*
Space group	*C*2/*c*	$P2_1$	*Pbca*
a / Å	41.2828(12)	6.26170(10)	11.9552(2)
b / Å	6.2666(3)	15.7051(2)	18.7102(2)
c / Å	41.4397(12)	9.8095(3)	16.5240(2)
α / °	90	90	90
β / °	99.943(3)	108.606(2)	90
γ / °	90	90	90
V / $Å^3$	10559.5(6)	914.25(4)	3696.16(9)
Z	24	2	8
μ mm^{-1}	0.673	1.904	3.087
$D_{calcd.}$ / $g \cdot cm^{-3}$	1.224	1.237	1.384
F(000)	4128	360	1584
Refl./restr./param.	10362/0/661	2954/1/255	3722/0/221
Completeness	0.994	0.986	0.999
GOF	1.048	1.075	1.066
R_1 ($I > 2\sigma(I)$)	0.0569	0.0329	0.0330
wR_2 ($I > 2\sigma(I)$)	0.1588	0.0839	0.0845
R_1 (all data)	0.0875	0.0329	0.0389
wR_2 (all data)	0.1892	0.0839	0.0875
Largest diff. peak and hole /$e \cdot Å^{-3}$	0.206, –0.548	0.180, –0.390	0.374, –0.557
CCDC number	2247528	2224345	2224346

Table S8. Summary of structure determination of **2an**, **2ao**, and **2cn**

Compound	**2an**	**2ao**	**2cn**
Formula	$C_{26}H_{27}B_1O_2Se_1$	$C_{26}H_{22}B_1O_2F_5$	$C_{23}H_{21}B_1O_4$
Formula weight	461.24	472.24	372.21
Temperature / °C	–180	–180	–180
λ (Å)	1.54184	1.54184	1.54184
Crystal size / mm^3	0.18×0.12×0.10	0.08×0.02×0.02	0.12×0.08×0.03
Crystal system	*Triclinic*	*Monoclinic*	*Triclinic*
Space group	*P*-1	$P2_1/c$	*P*-1
a / Å	6.31960(10)	6.1879(3)	5.8273(2)
b / Å	11.4873(2)	41.6439(14)	16.1848(5)
c / Å	16.8309(3)	17.8690(6)	21.7687(6)
α / °	105.1137(18)	90	105.759(3)
β / °	98.1147(17)	97.366(4)	94.920(2)
γ / °	97.0743(17)	90	98.517(2)
V / $Å^3$	4566.6(3)	4566.6(3)	1936.93(11)
Z	2	8	4
μ mm^{-1}	2.346	0.962	0.690
$D_{calcd.}$ / $g \cdot cm^{-3}$	1.331	1.374	1.276
F(000)	476	1952	784
Refl./restr./param.	4555/0/275	8960/0/621	7514/0/517
Completeness	0.982	0.991	0.977
GOF	1.091	1.025	1.022
R_1 ($I > 2\sigma(I)$)	0.0257	0.0733	0.0481
wR_2 ($I > 2\sigma(I)$)	0.0686	0.1890	0.1157
R_1 (all data)	0.0266	0.1104	0.0688
wR_2 (all data)	0.0690	0.2179	0.1269
Largest diff. peak and hole / $e \cdot Å^{-3}$	0.216, –0.432	0.372, –0.389	0.396, –0.290
CCDC number	2247529	2224348	2224347

Table S9. Summary of structure determination of **2gn** and **I'**

Compound	**2gn**	**I'**
Formula	$C_{31.5}H_{26.5}B_1O_3$	$C_{51}H_{71}B_2O_8Li_2$
Formula weight	463.84	847.57
Temperature / °C	–180	–150
λ (Å)	1.54184	1.54187
Crystal size / mm^3	0.10×0.02×0.02	0.23×0.20×0.10
Crystal system	*Monoclinic*	*Triclinic*
Space group	$P2_1/c$	$P\bar{1}$
a / Å	19.1422(9)	10.5397(3)
b / Å	5.4943(4)	12.5200(3)
c / Å	24.2513(11)	20.9594(5)
α / °	90	78.167(6)
β / °	92.804(4)	81.725(6)
γ / °	90	65.527(5)
V / $Å^3$	2547.5(2)	2458.36(15)
Z	4	2
μ mm^{-1}	0.597	0.582
$D_{calcd.}$ / $g \cdot cm^{-3}$	1.209	1.145
F(000)	978	914
Refl./restr./param.	5060/67/367	8833/0/553
Completeness	0.995	0.983
GOF	1.047	1.065
R_1 ($I > 2\sigma(I)$)	0.0689	0.0631
wR_2 ($I > 2\sigma(I)$)	0.1857	0.1684
R_1 (all data)	0.1176	0.0692
wR_2 (all data)	0.2191	0.1749
Largest diff. peak and hole / $e \cdot Å^{-3}$	0.259, –0.280	0.486, –0.288
CCDC number	2224349	2224350

References

1. Nagaki, A., Yamashita, H., Hirose, K., Tsuchihashi, Y. & Yoshida, J. Alkyllithium Compounds Bearing Electrophilic Functional Groups: A Flash Chemistry Approach. *Angew. Chem. Int. Ed.* **58**, 4027–4030 (2019).
2. Rathore, R. & Burns, C. L. A Practical One-Pot Synthesis of Soluble Hexa-*peri*-hexabenzocoronene and Isolation of Its Cation-Radical Salt. *J. Org. Chem.* **68**, 4071–4074 (2003).
3. Sakai, N., Annaka, K. & Konakahara, T. Palladium-Catalyzed Coupling Reaction of Terminal Alkynes with Aryl Iodides in the Presence of Indium Tribromide and Its Application to a One-Pot Synthesis of 2-Phenylindole. *Org. Lett.* **6**, 1527–1530 (2004).
4. Wang, S., Wang, M., Wang, L., Wang, B., Li, P. & Yang, J. CuI-catalyzed Suzuki coupling reaction of organoboronic acids with alkynyl bromides. *Tetrahedron* **67**, 4800–4806 (2011).
5. Li, P., Wang, L. & Li, H. Application of recoverable nanosized palladium(0) catalyst in Sonogashira reaction. *Tetrahedron* **61**, 8633–8640 (2005).
6. Chelouan, A., Recio, R., Alcudia, A., Khiar, N. & Fernández, I. DMAP-Catalyzed Sulfinylation of Diacetone-D-Glucose: Improved Method for the Synthesis of Enantiopure *tert*-Butyl Sulfoxides and *tert*-Butanesulfinamides. *Eur. J. Org. Chem.* 6935–6944 (2014).
7. Lawson, J. R., Fasano, V., Cid, J., Vitorica-Yrezabal, I. & Ingleson, M. J. The Carboboration of Me_3Si-Substituted Alkynes and Allenes with Boranes and Borocations. *Dalton Trans.* **45**, 6060–6070 (2016).
8. Lee, H. J., Yonekura, Y., Kim, N., Yoshida, J. & Kim, H. Regioselective Synthesis of alpha-Functional Stilbenes via Precise Control of Rapid Cis-Trans Isomerization in Flow. *Org. Lett.* **23**, 2904–2910 (2021).
9. Takemono, Y., Yoshida, H. & Takaki, K. Copper-Catalyzed Three-Compnent Borylstannylation of Alkynes. *Chem. Eur. J.* **18**, 14841−14844 (2012).
10. Alfaro, R., Parra, A., Alemán, J., García-Ruano, J. L. & Tortosa, M. Copper(I)-Catalyzed Formal Carboboration of Alkynes: Synthesis of Tri- and Tetrasubstituted Vinylboronates. *J. Am. Chem. Soc.* **134**, 15165–15168 (2012).
11. Sheldrick, G. M. A short history of *SHELX*. *Acta Crystallogr.* **A64**, 112–122 (2008).
12. Sheldrick, G. M. Crystal structure refinement with *SHELXL*. *Acta Crystallogr.* **C71**, 3–8 (2015).
13. Spek, A. L. PLATON SQUEEZE: a tool for the calculation of the disordered solvent contribution to the calculated structure factors. *Acta Cryst.* **C71**, 9–18 (2015).

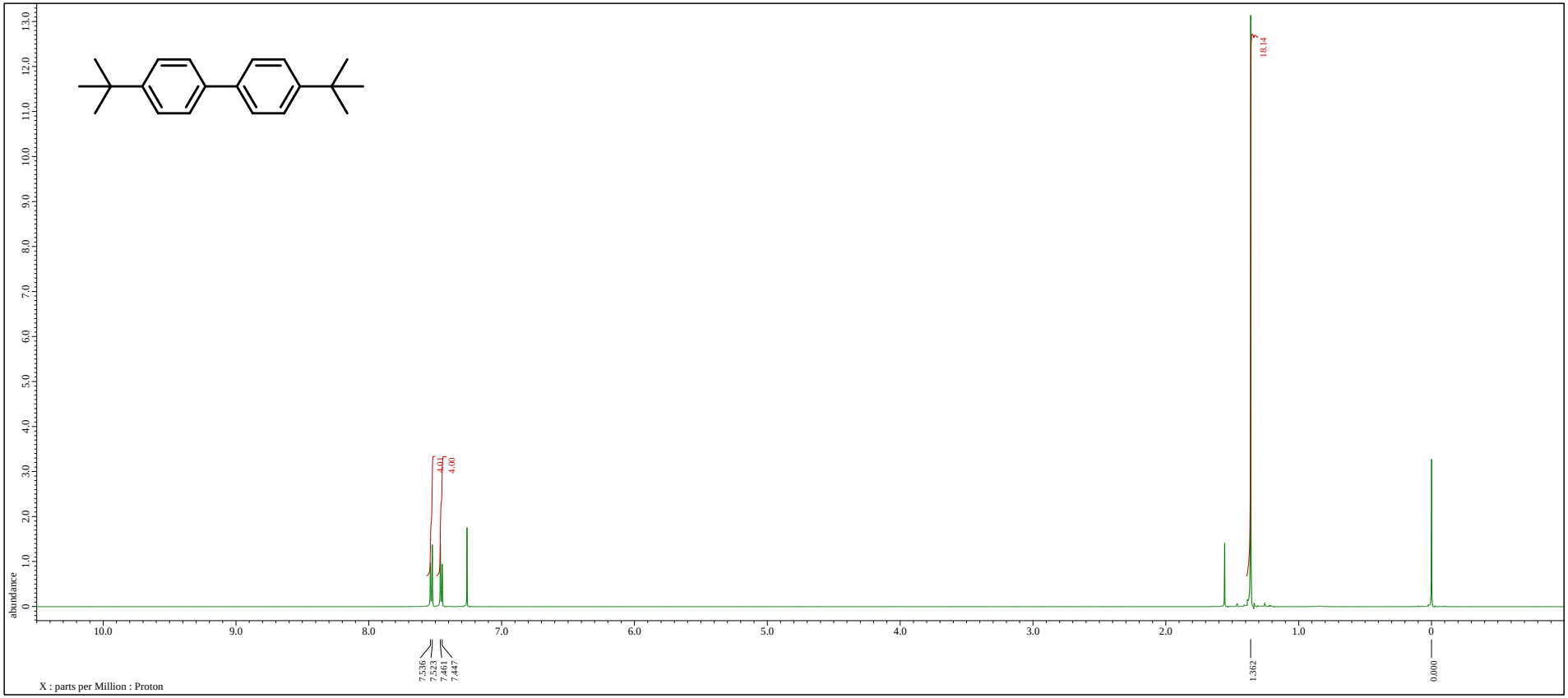

Figure S9. ^{1}H NMR (600 MHz, $CDCl_3$) spectrum of 4,4'-di-*tert*-butylbiphenyl.

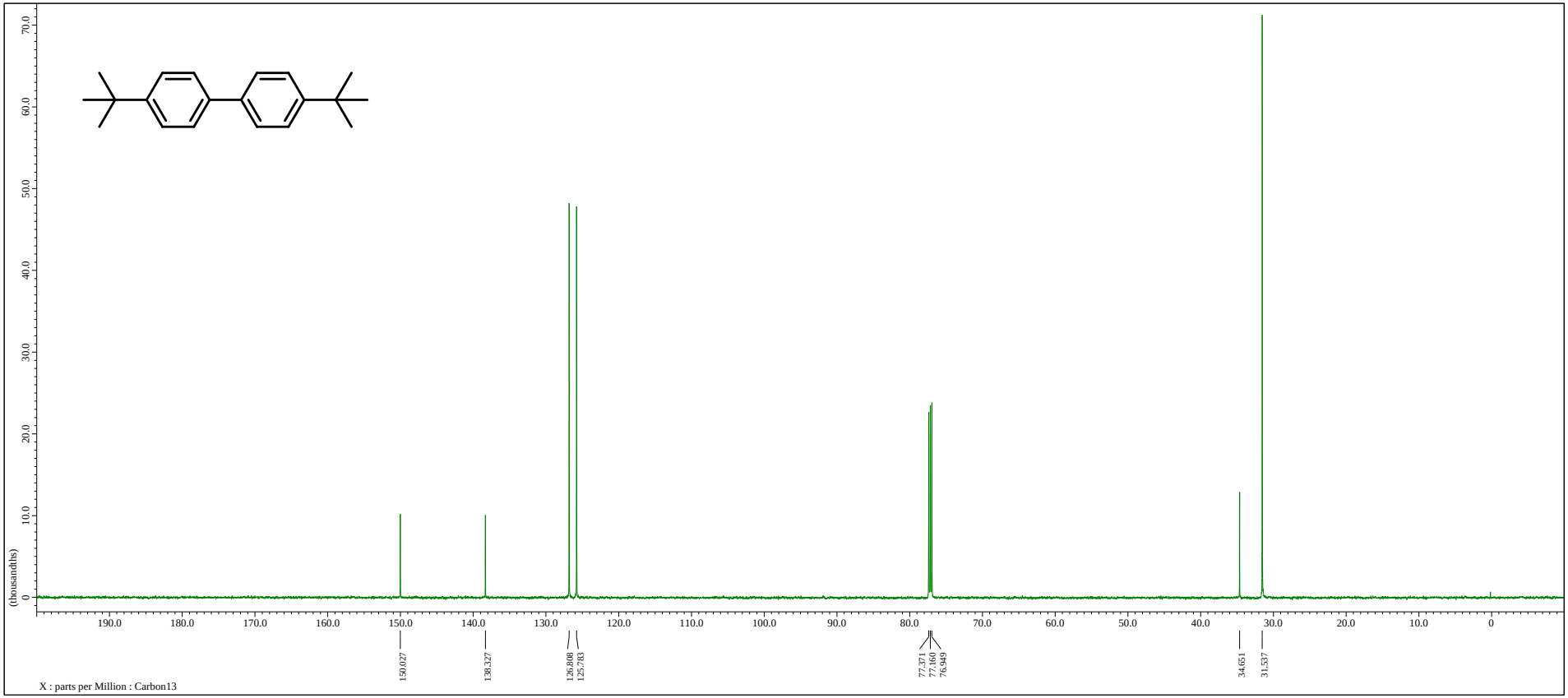

Figure S10. ^{13}C NMR (151 MHz, $CDCl_3$) spectrum of 4,4'-di-*tert*-butylbiphenyl.

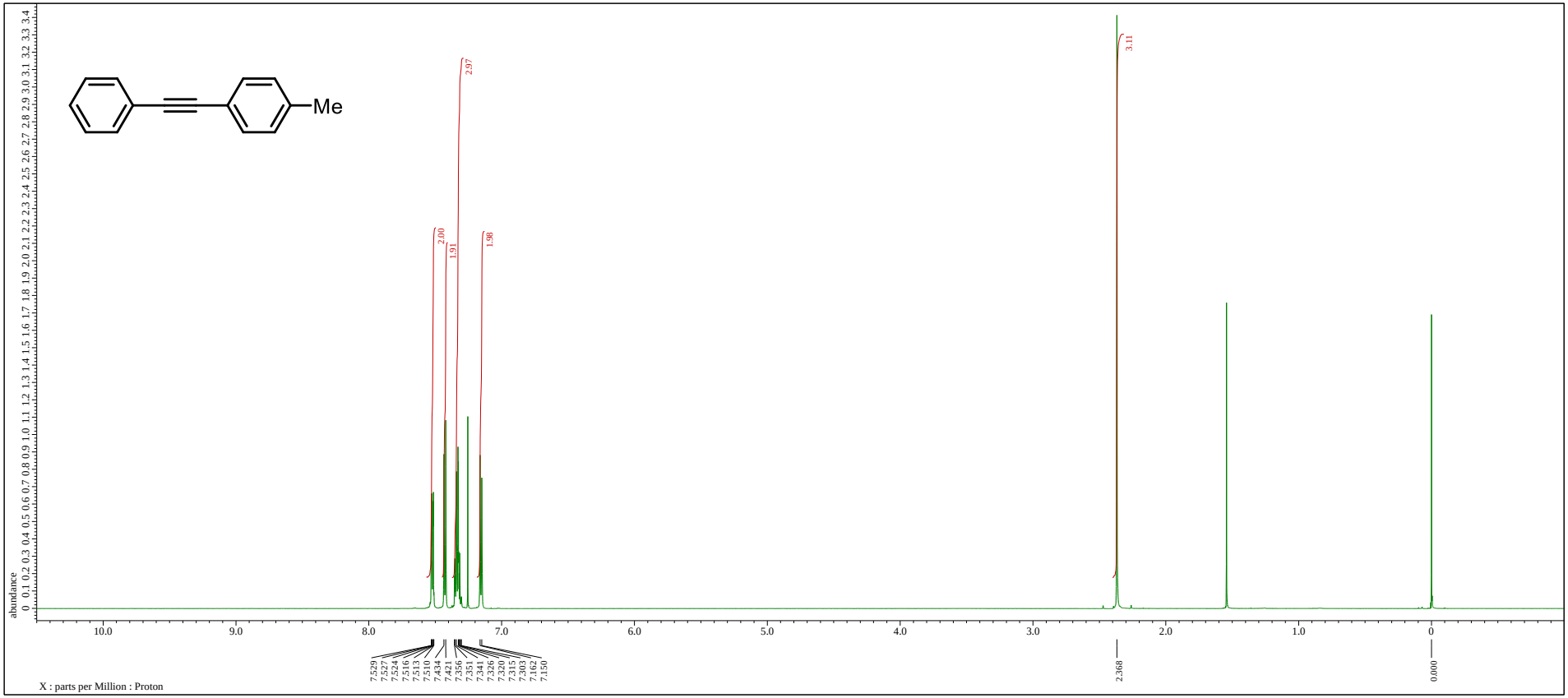

Figure S11. ^{1}H NMR (600 MHz, $CDCl_3$) spectrum of **1b**.

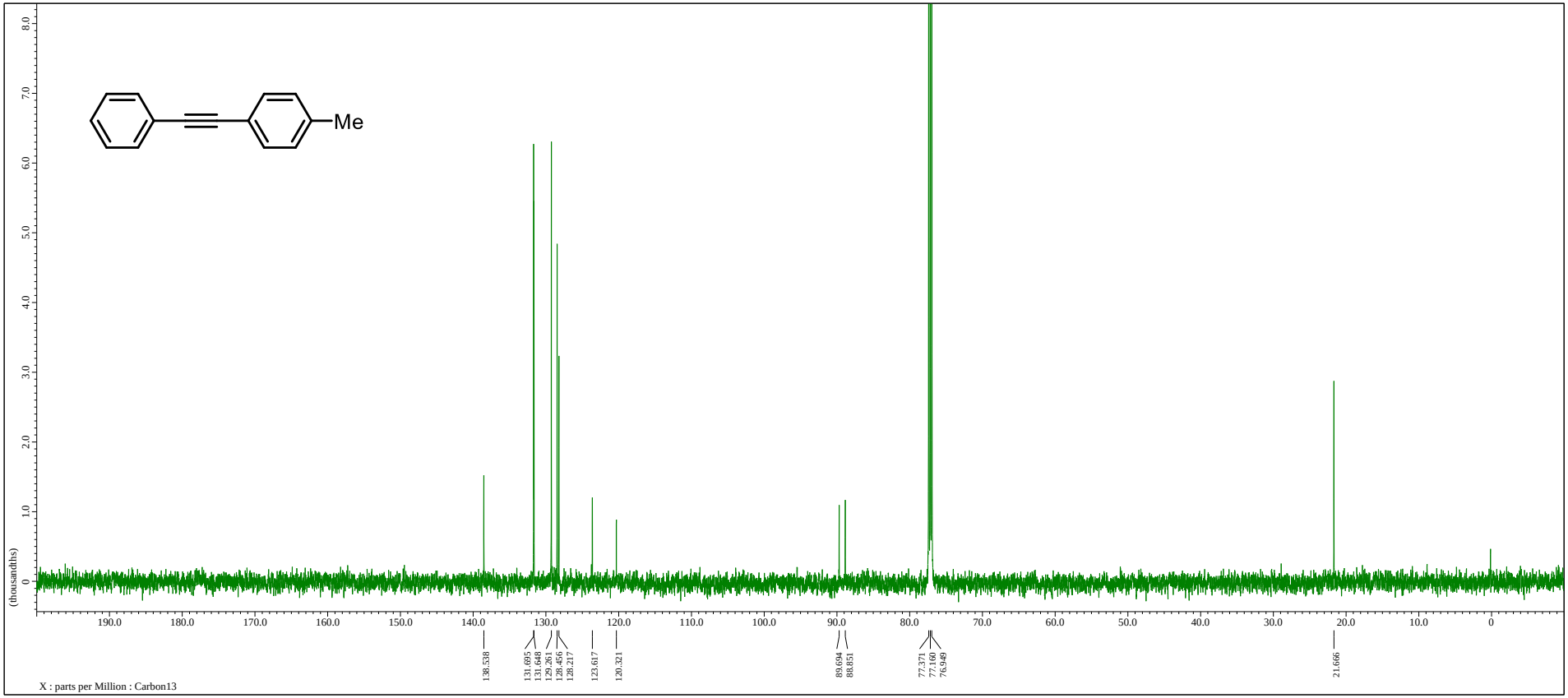

Figure S12. ^{13}C NMR (151 MHz, $CDCl_3$) spectrum of **1b**.

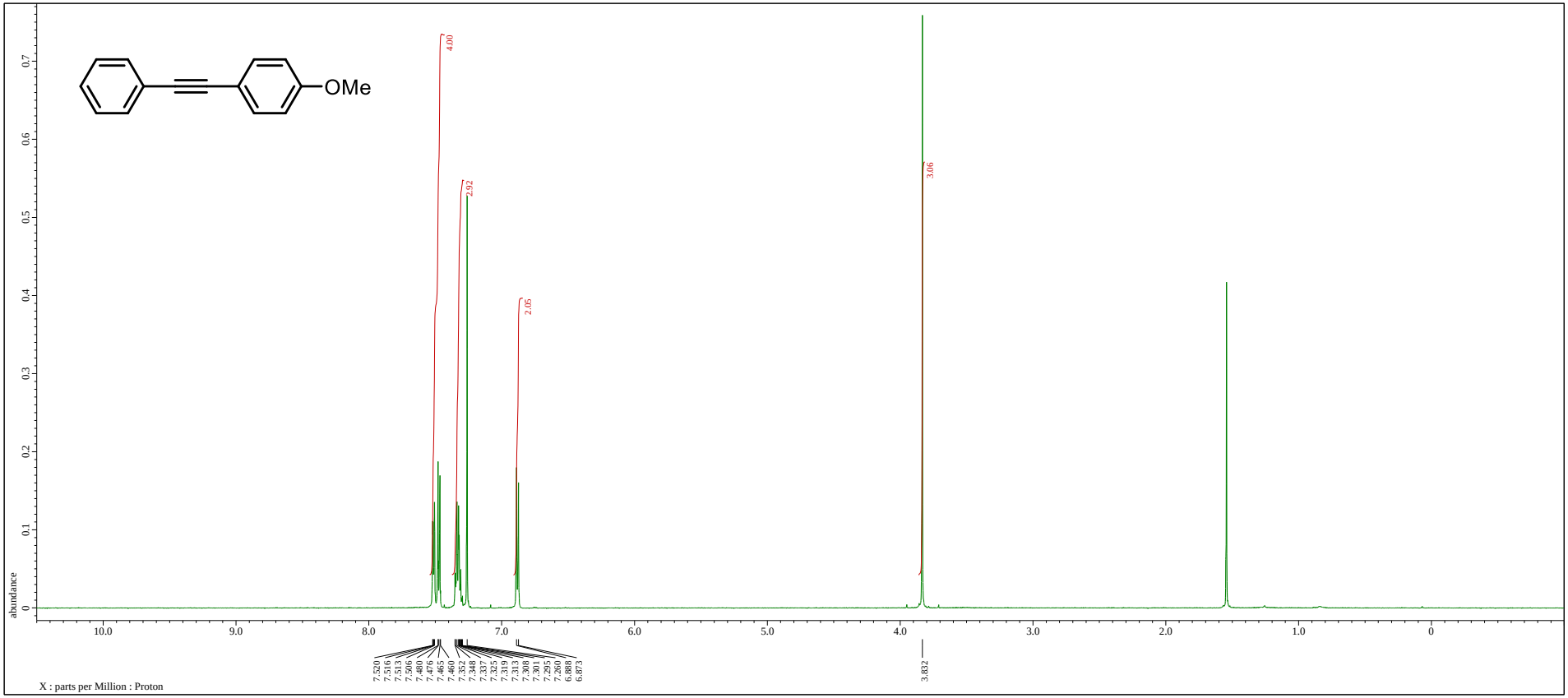

Figure S13. ^{1}H NMR (600 MHz, $CDCl_3$) spectrum of **1c**.

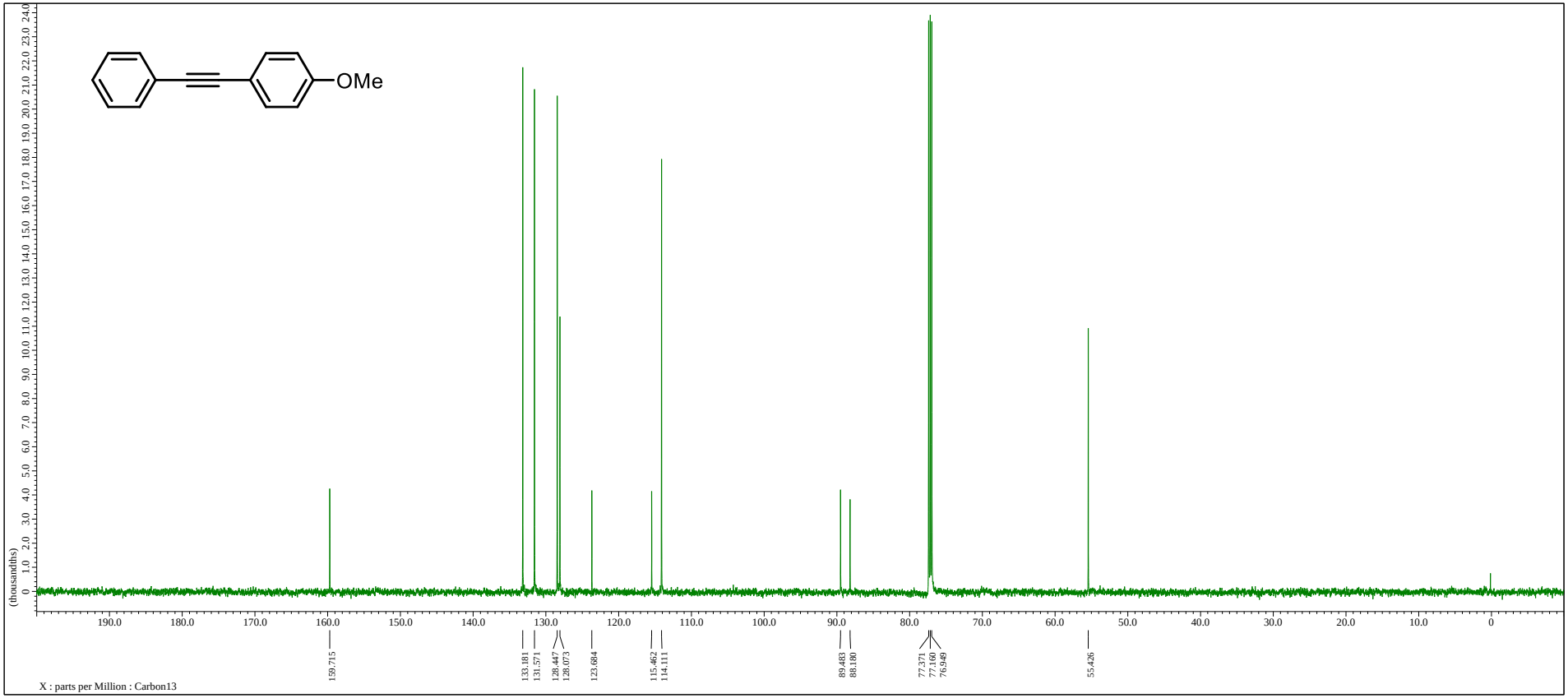

Figure S14. ^{13}C NMR (151 MHz, $CDCl_3$) spectrum of **1c**.

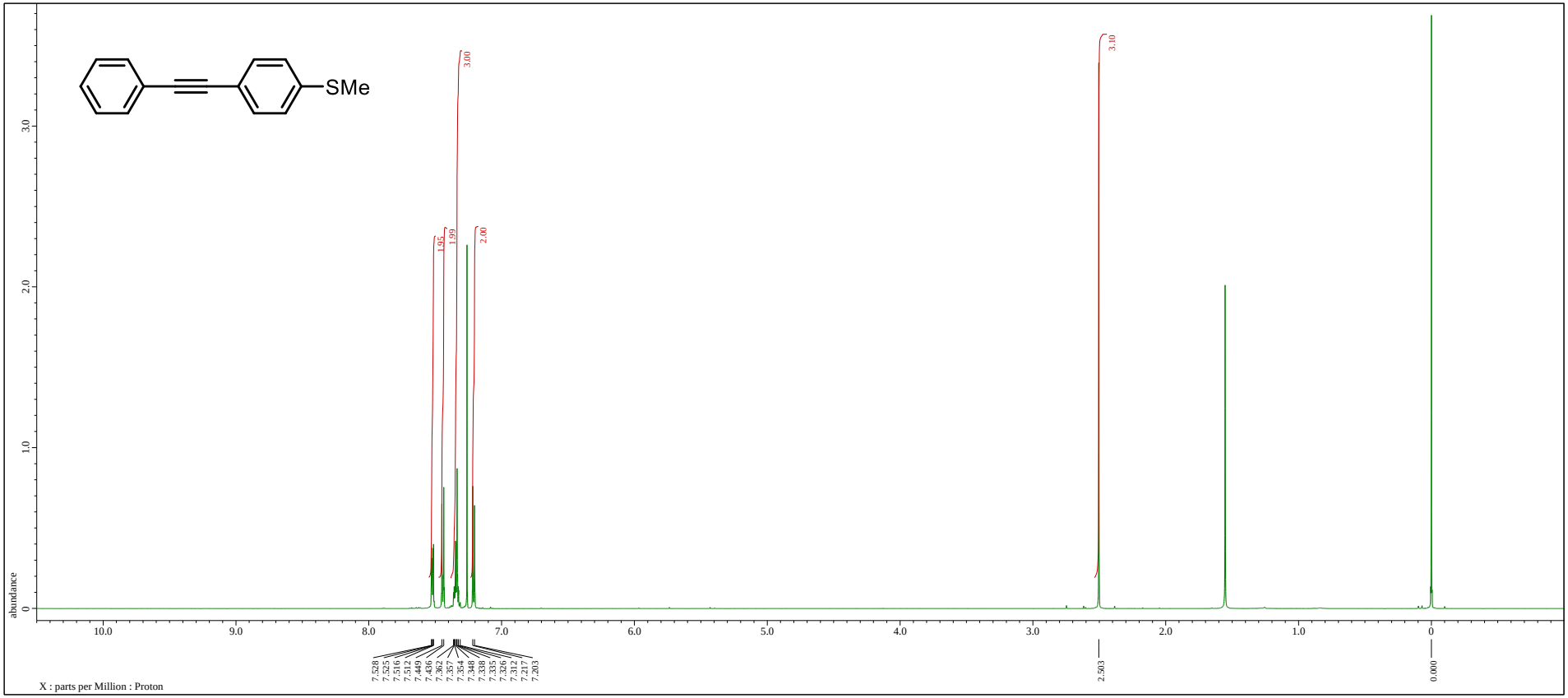

Figure S15. ^{1}H NMR (600 MHz, $CDCl_3$) spectrum of **1e**.

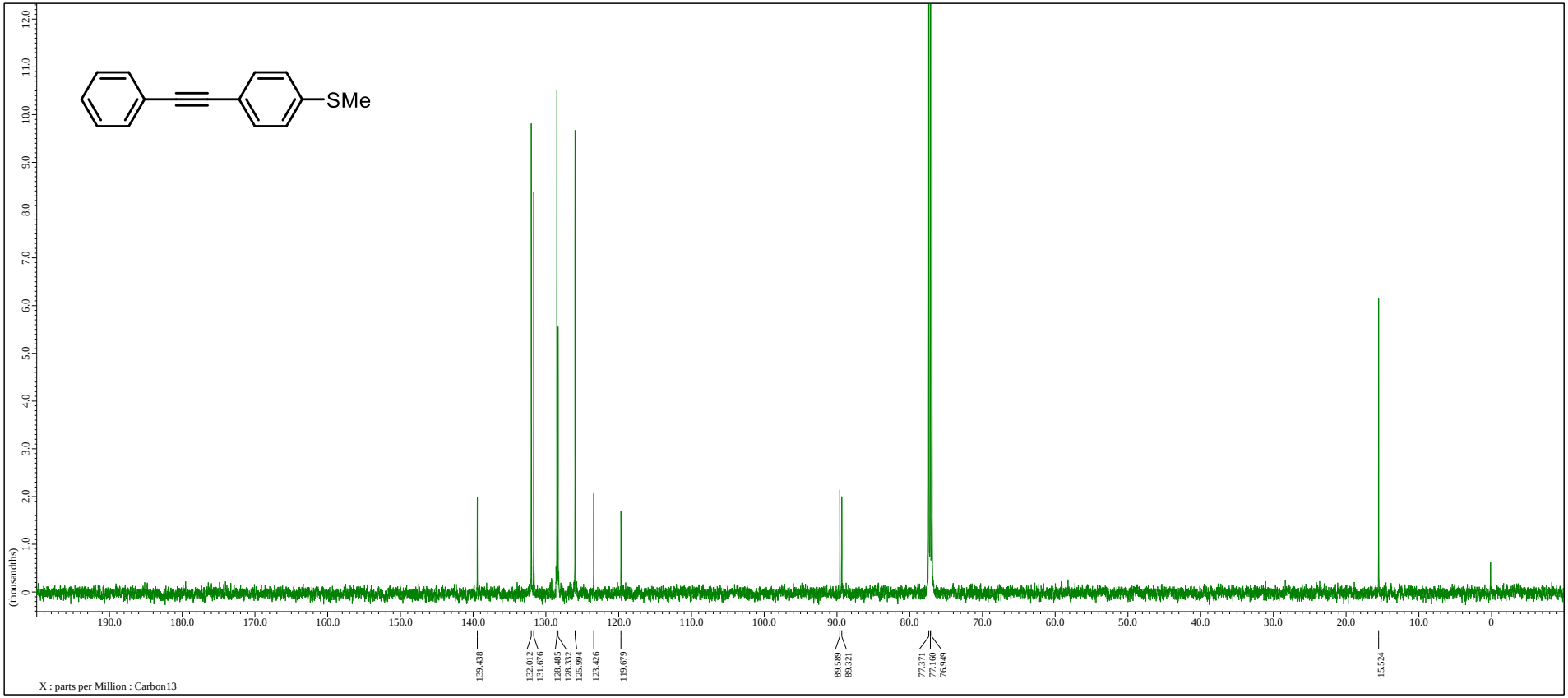

Figure S16. ^{13}C NMR (151 MHz, $CDCl_3$) spectrum of **1e**.

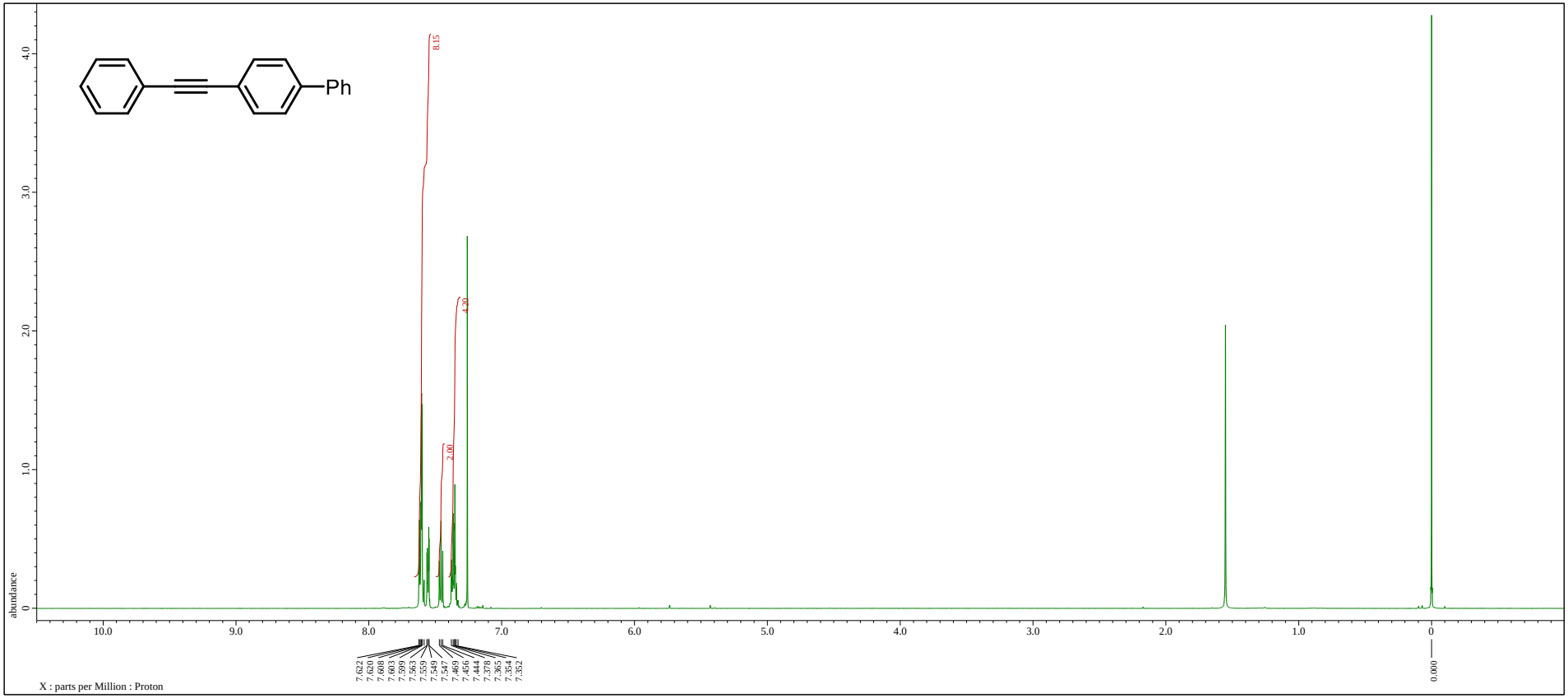

Figure S17. ^{1}H NMR (600 MHz, $CDCl_3$) spectrum of **1f**.

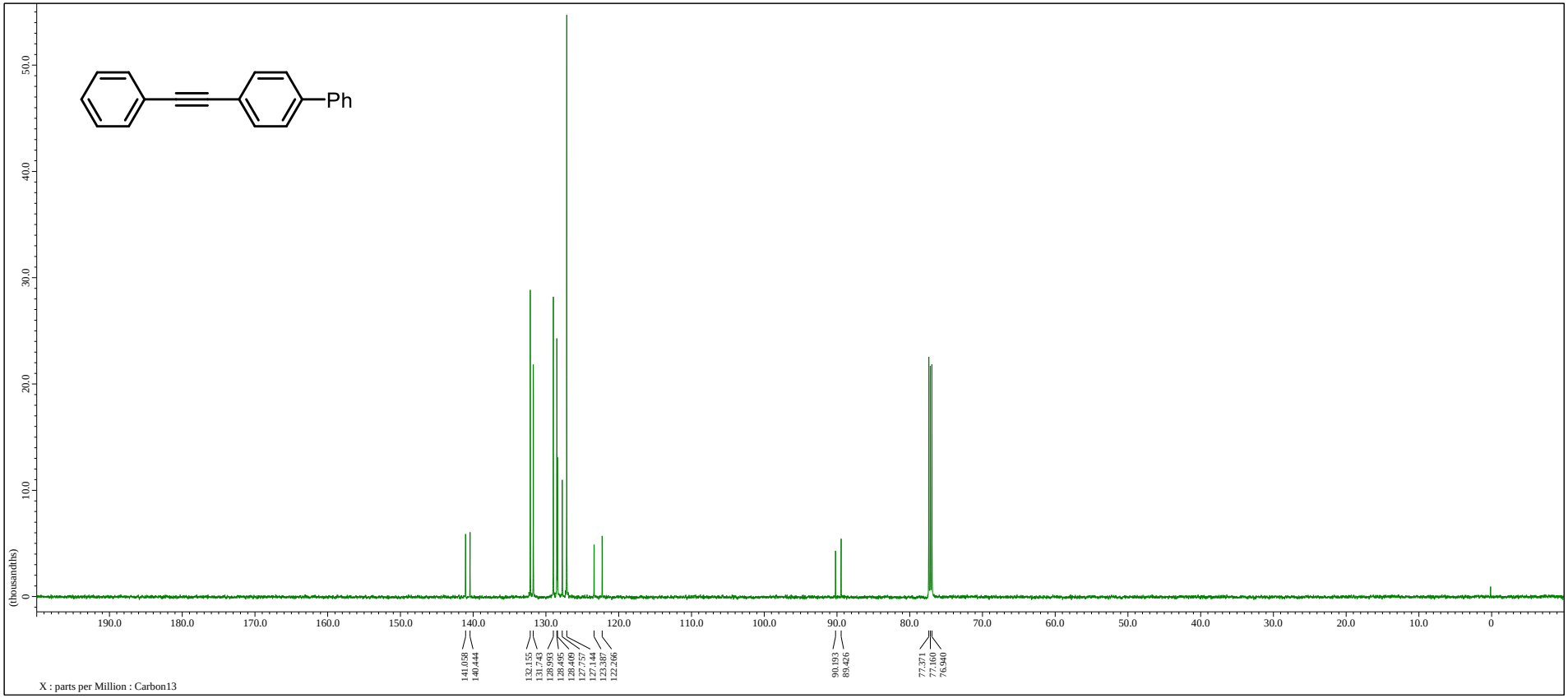

Figure S18. ^{13}C NMR (151 MHz, $CDCl_3$) spectrum of **1f**.

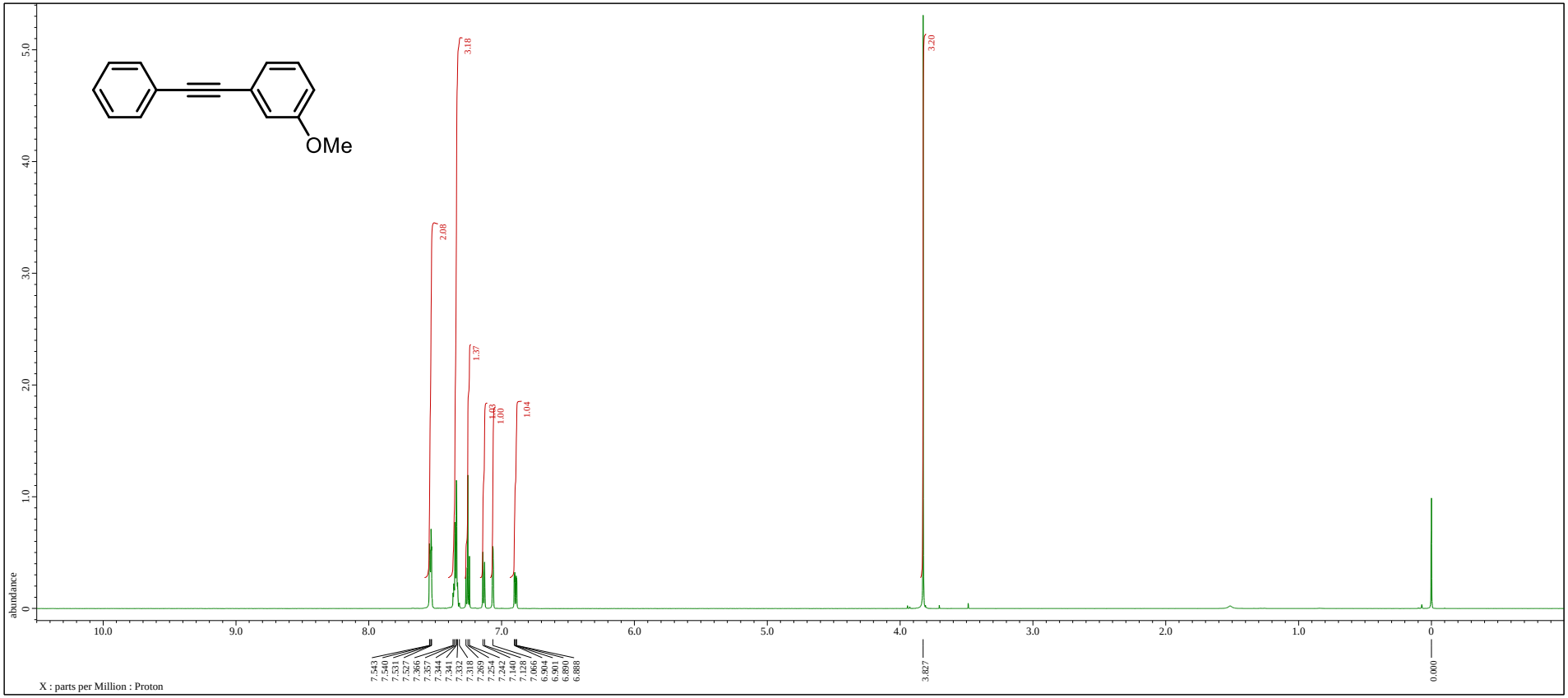

Figure S19. ^{1}H NMR (600 MHz, $CDCl_3$) spectrum of **1h**.

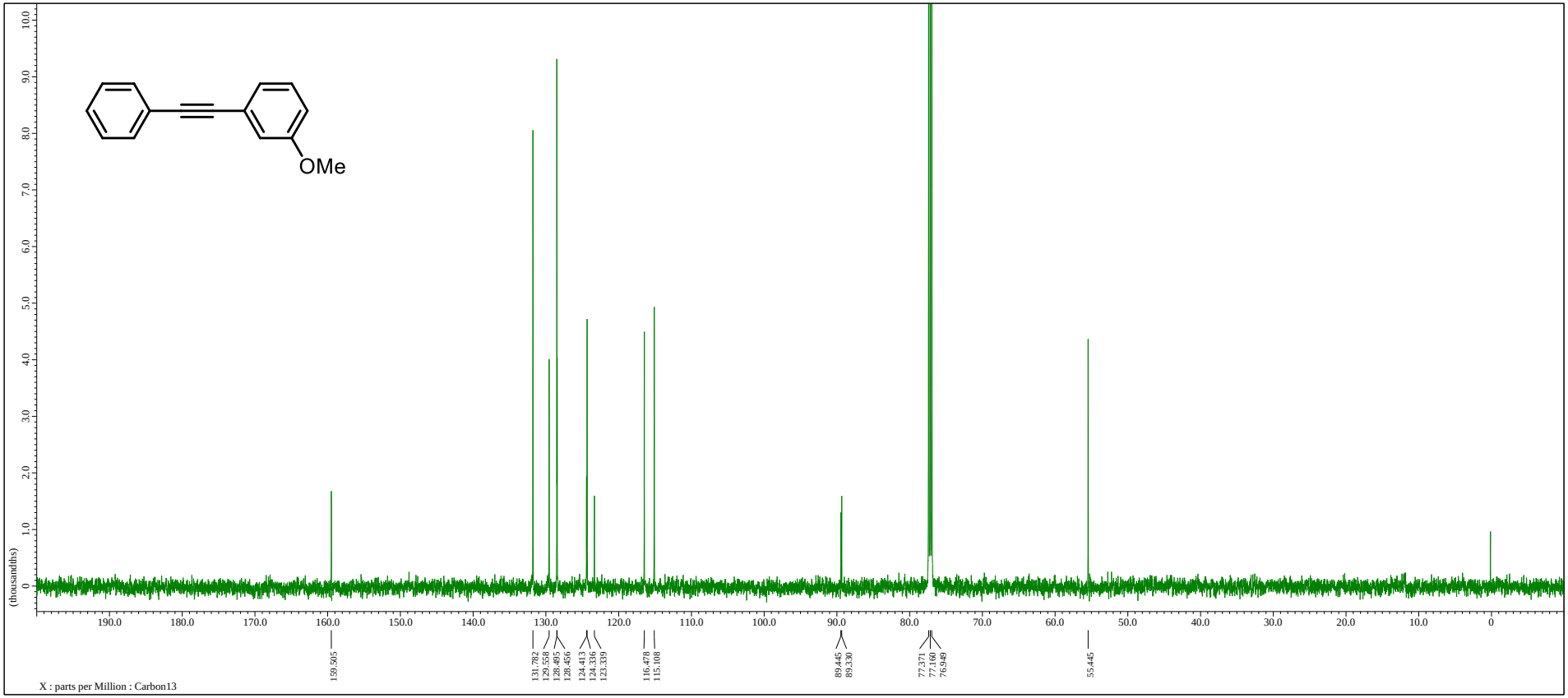

Figure S20. ^{13}C NMR (151 MHz, $CDCl_3$) spectrum of **1h**.

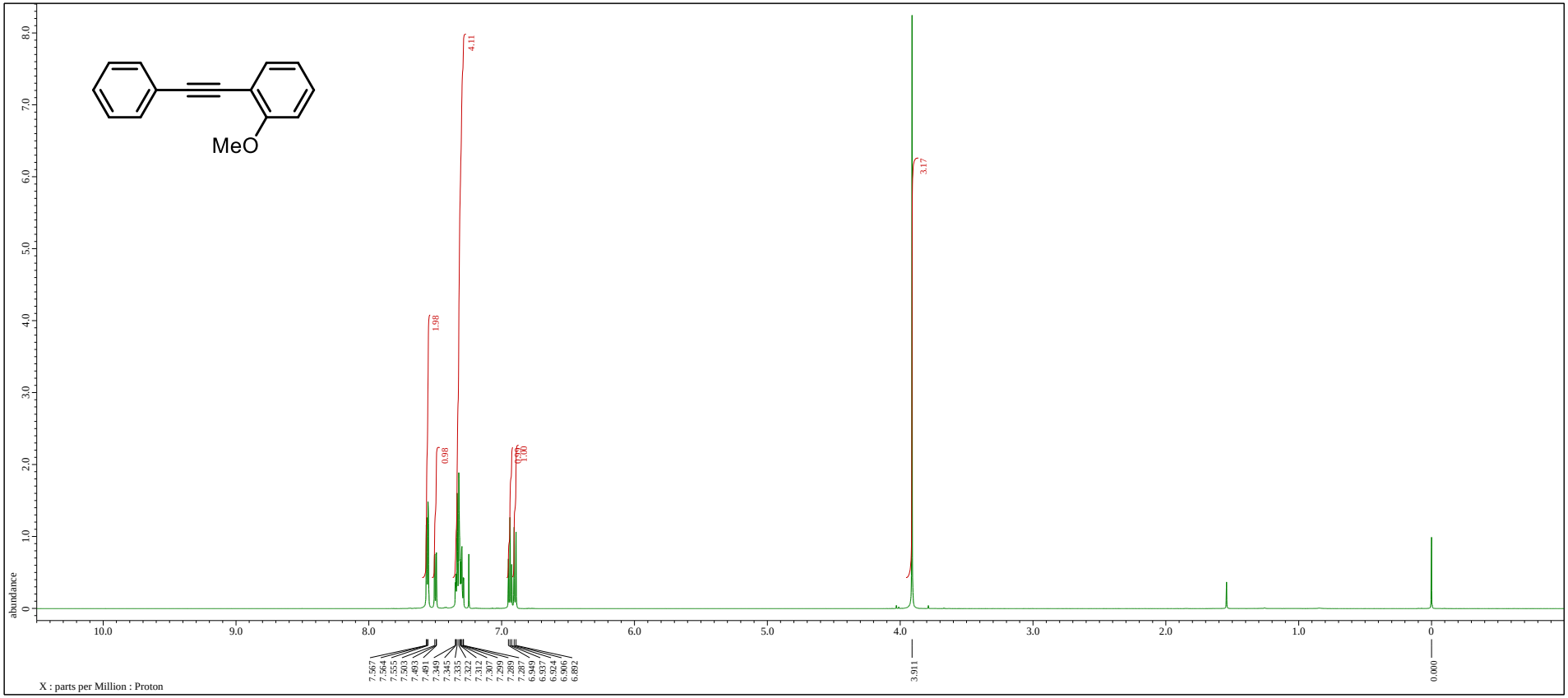

Figure S21. ^{1}H NMR (600 MHz, $CDCl_3$) spectrum of **1i**.

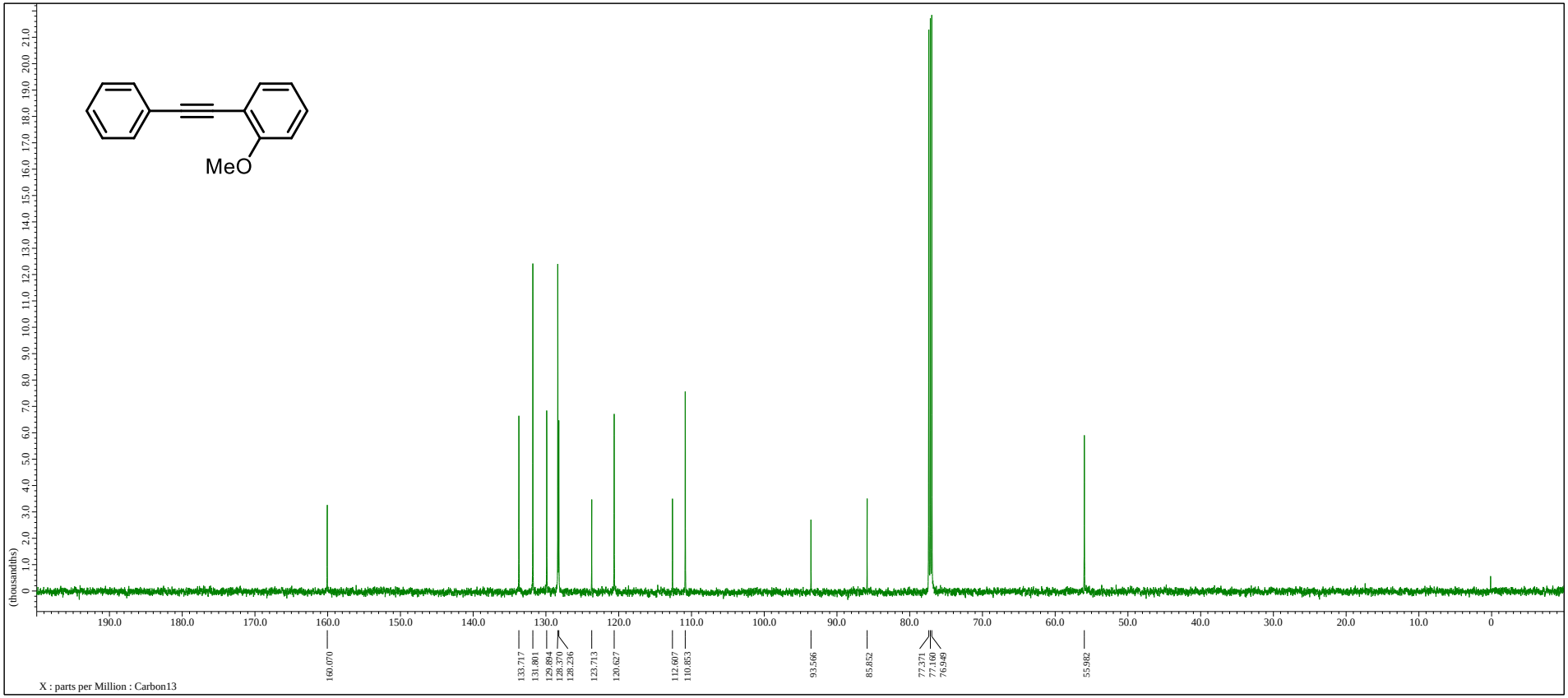

Figure S22. ^{13}C NMR (151 MHz, $CDCl_3$) spectrum of **1i**.

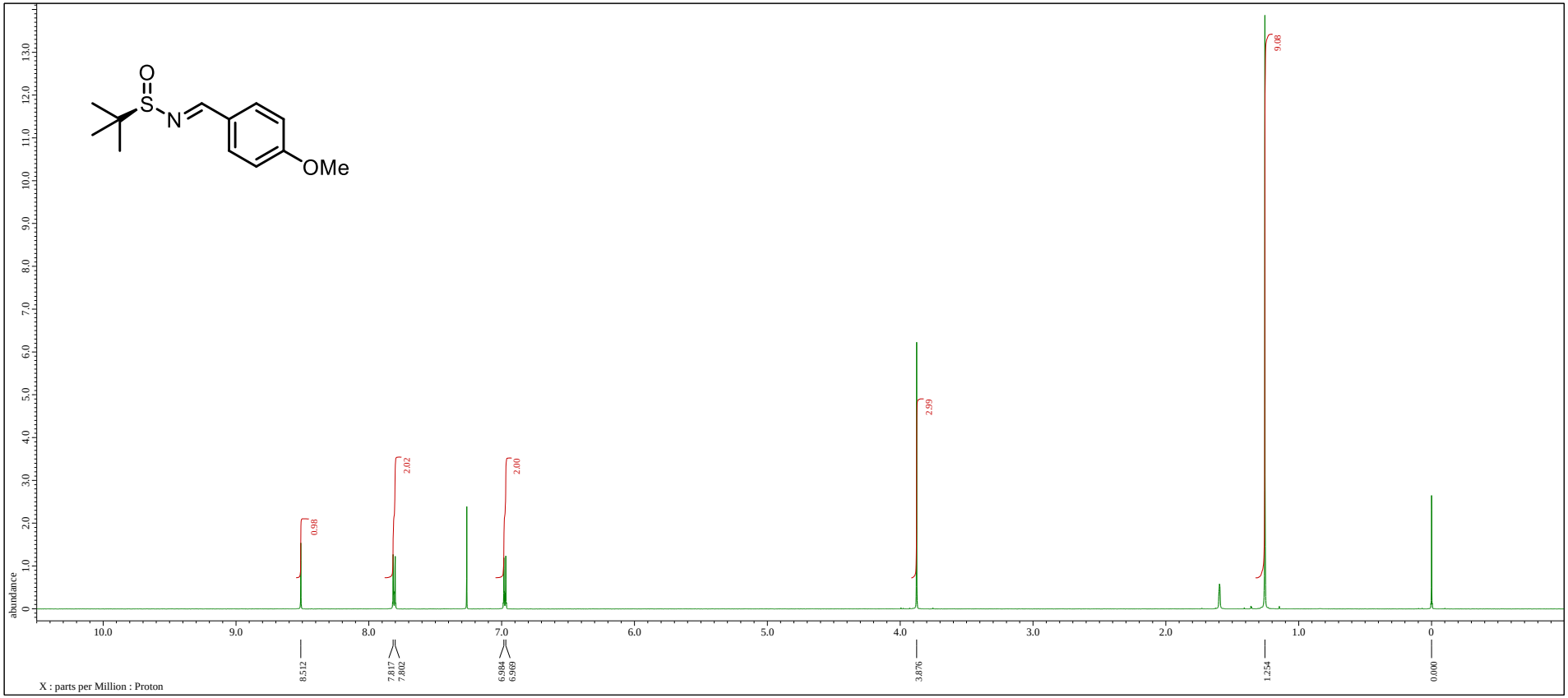

Figure S23. ^{1}H NMR (600 MHz, $CDCl_3$) spectrum of (*R,E*)-(−)-*N*-(4-Methoxybenzylidene)-*tert*-butanesulfinamide.

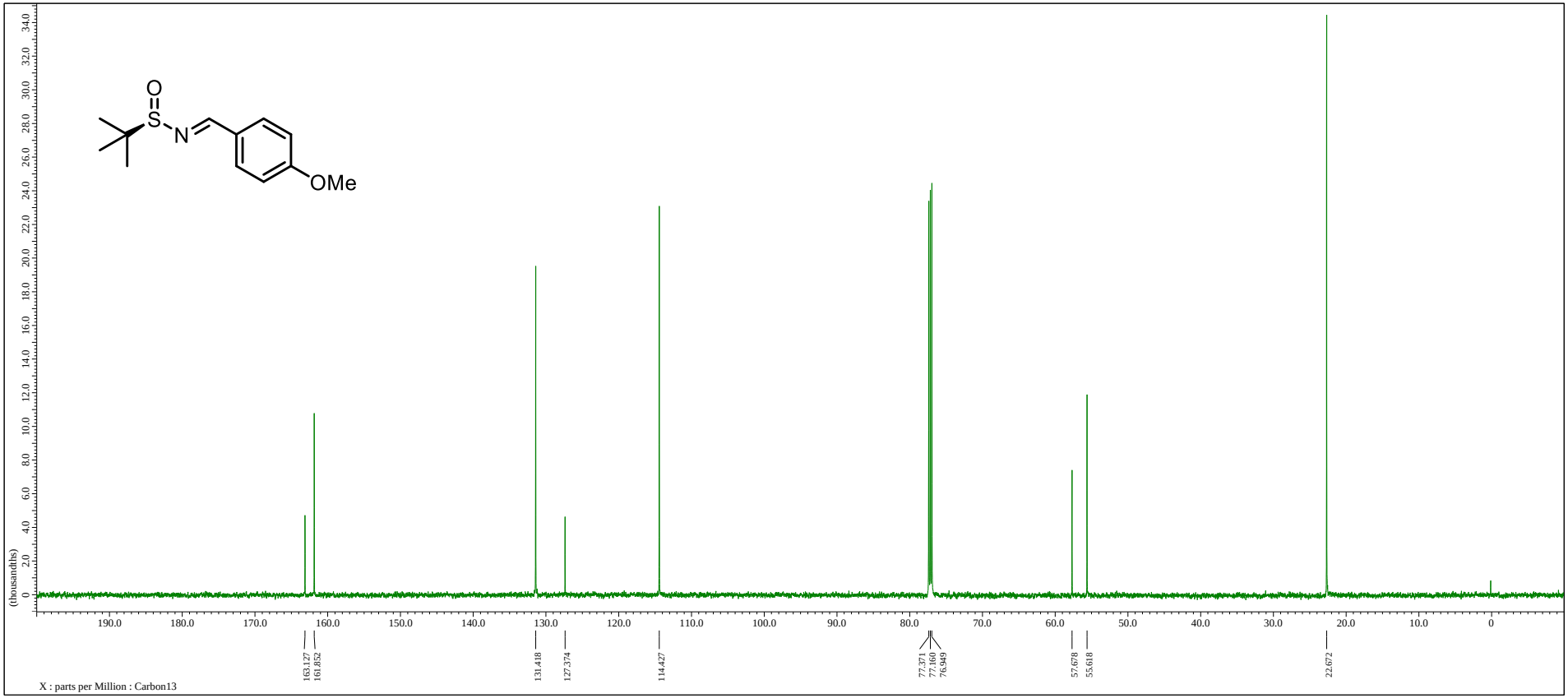

Figure S24. ^{13}C NMR (151 MHz, $CDCl_3$) spectrum of (*R,E*)-(−)-*N*-(4-Methoxybenzylidene)-*tert*-butanesulfinamide.

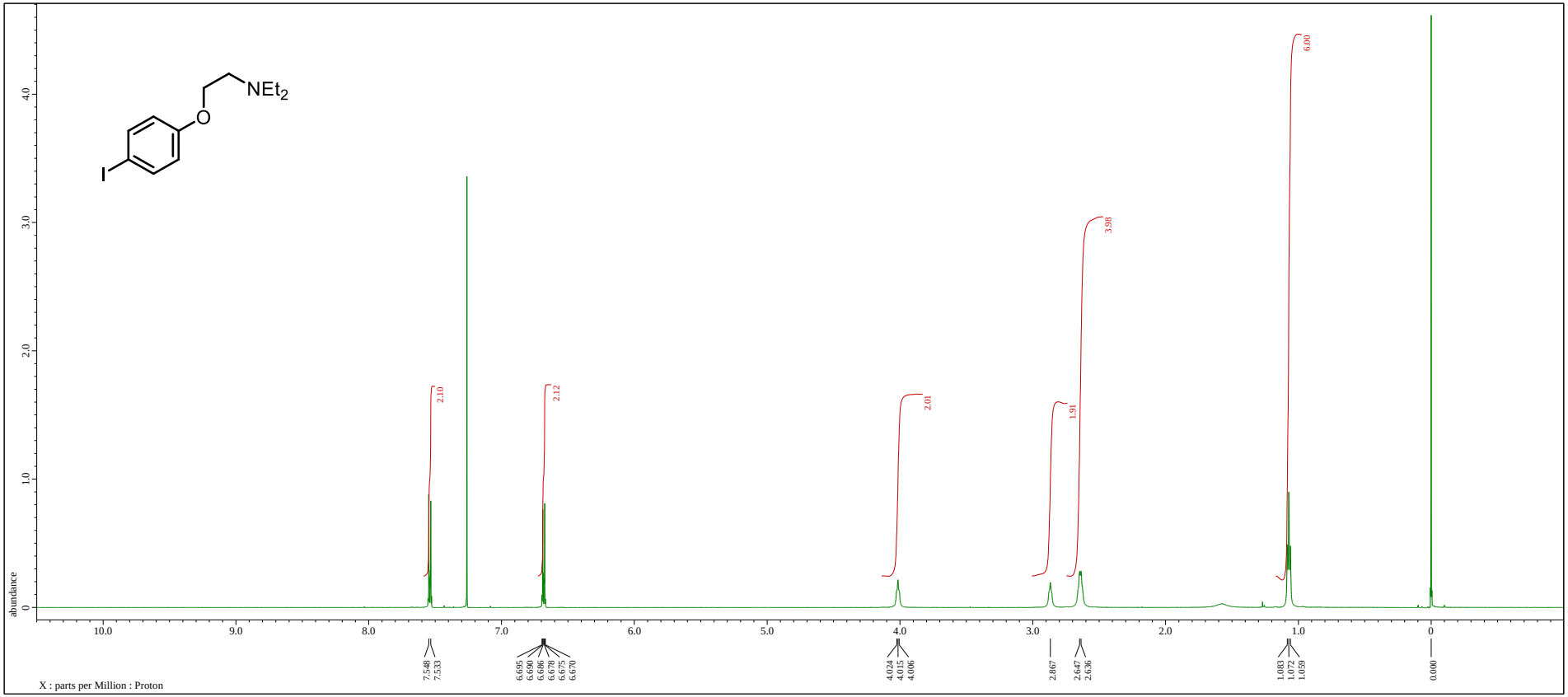

Figure S25. ^{1}H NMR (600 MHz, $CDCl_3$) spectrum of *N*,*N*-diethyl-2-(4-iodophenoxy)ethanamine.

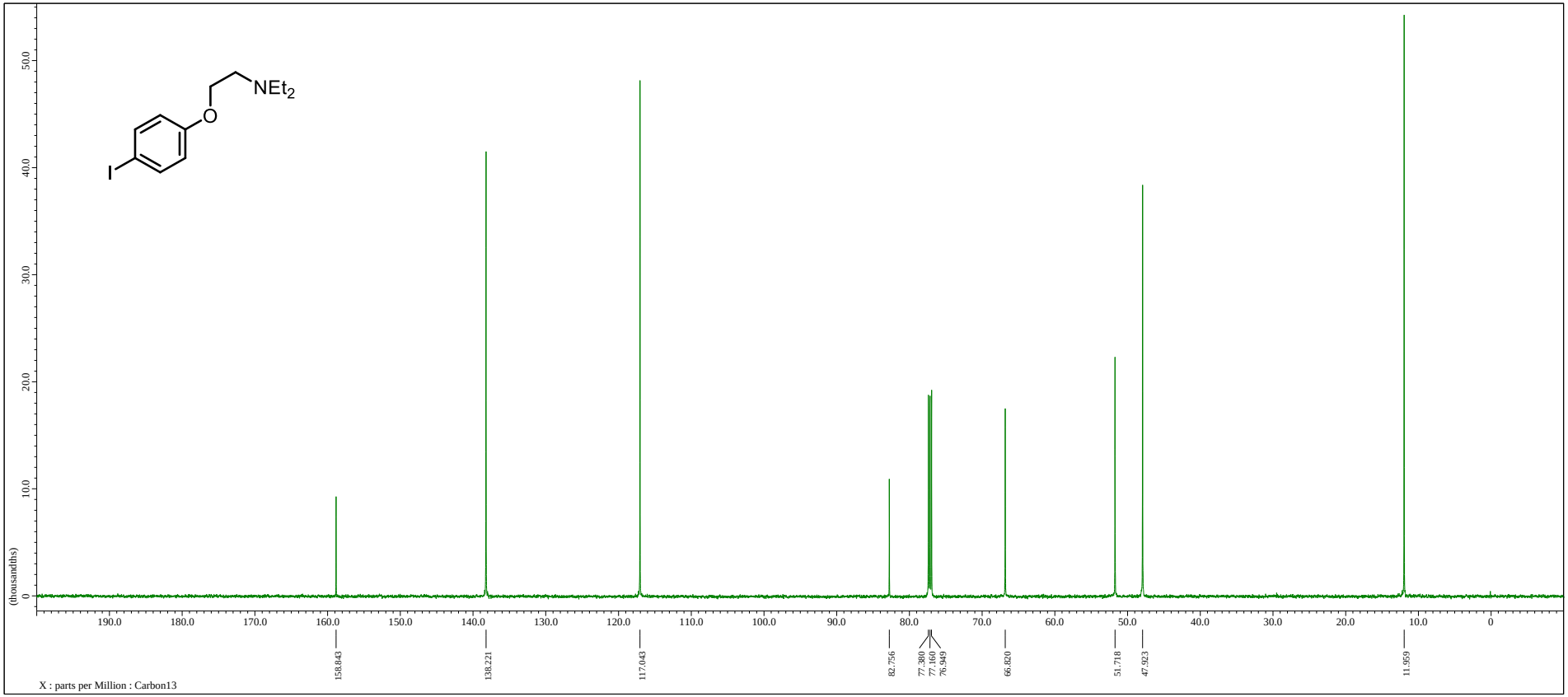

Figure S26. ^{13}C NMR (151 MHz, $CDCl_3$) spectrum of *N*,*N*-diethyl-2-(4-iodophenoxy)ethanamine.

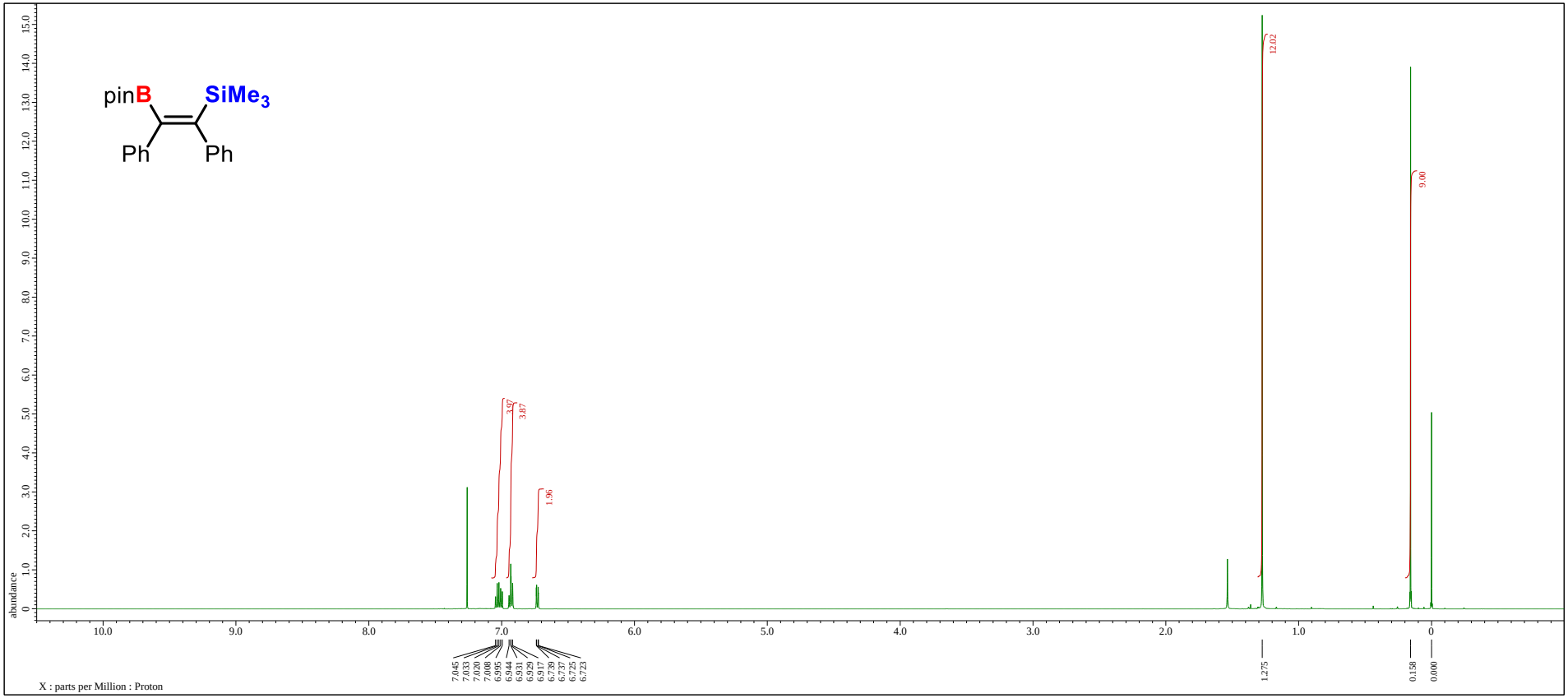

Figure S27. ^{1}H NMR (600 MHz, $CDCl_3$) spectrum of **2aa**.

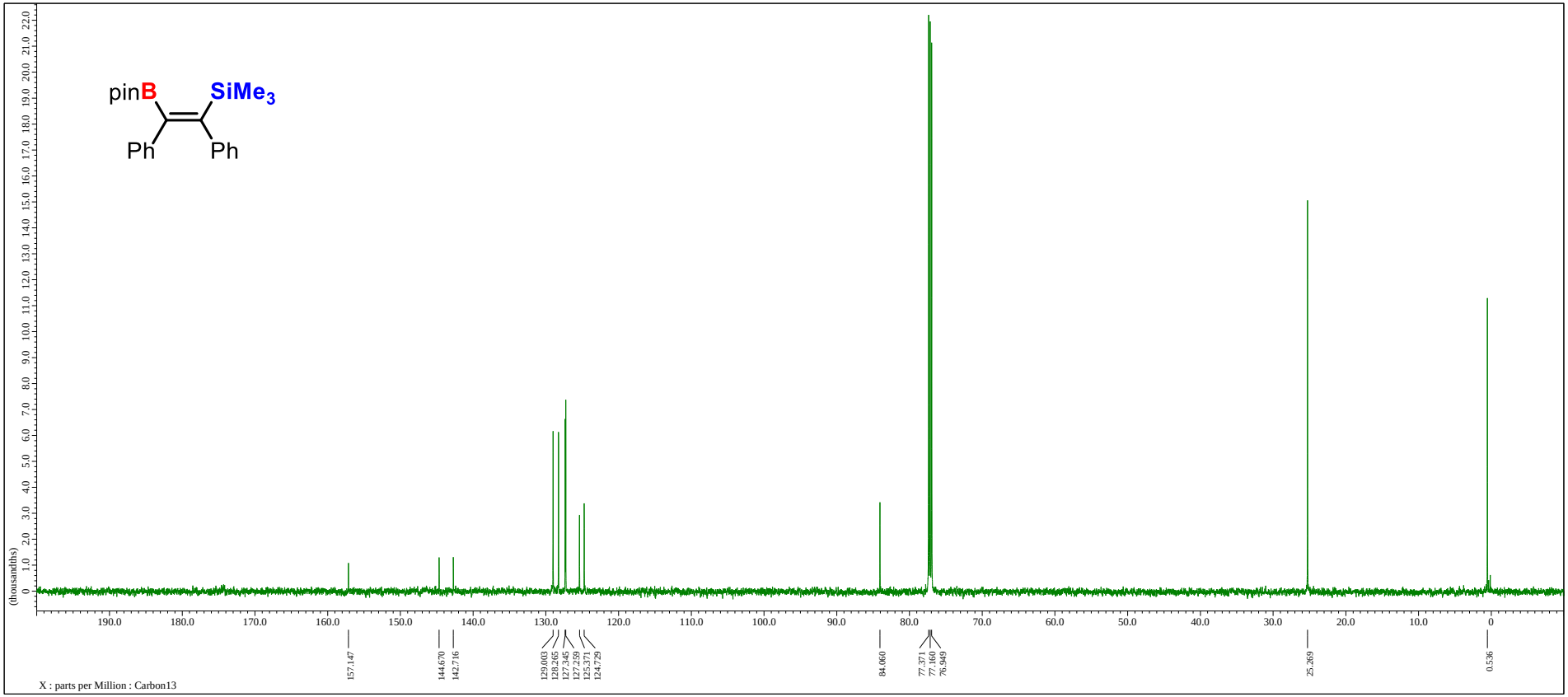

Figure S28. ^{13}C NMR (151 MHz, $CDCl_3$) spectrum of **2aa**.

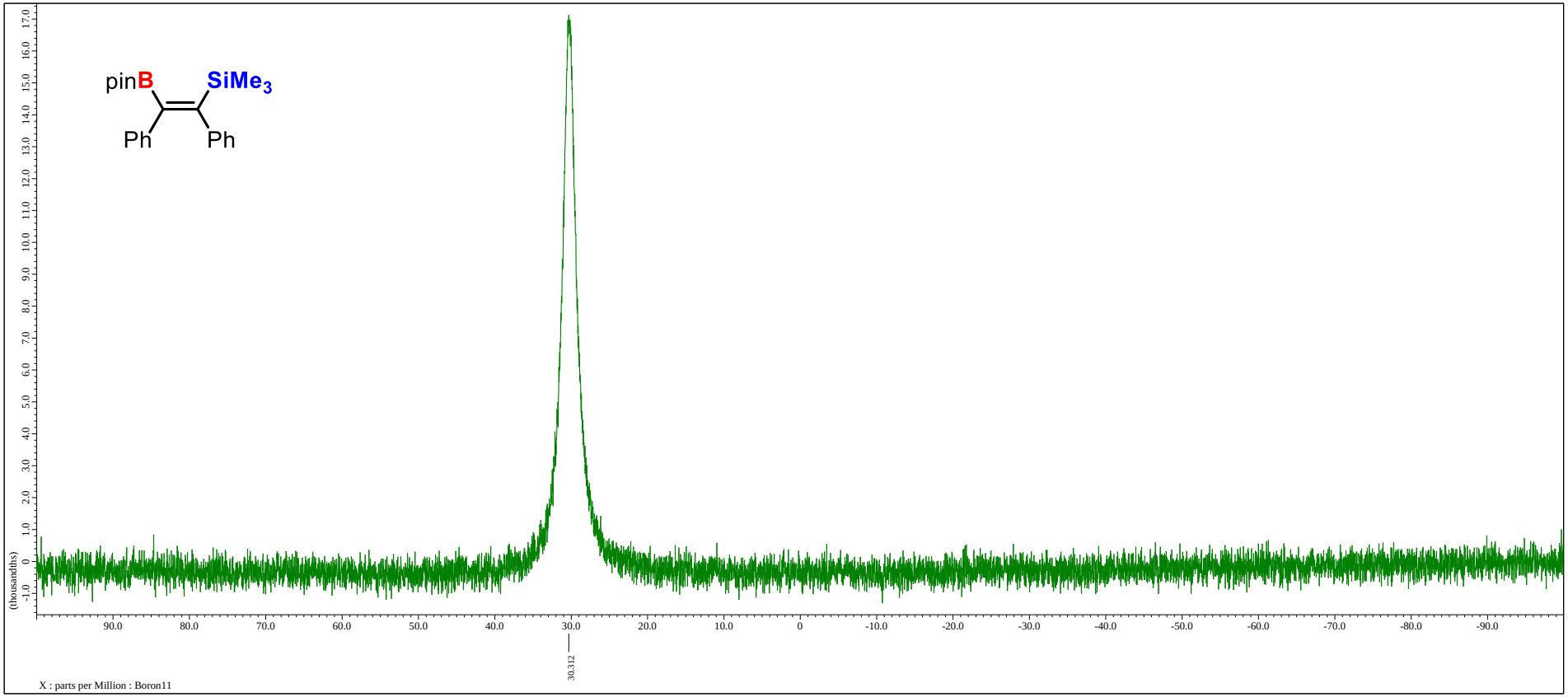

Figure S29. ^{11}B NMR (192 MHz, $CDCl_3$) spectrum of **2aa**.

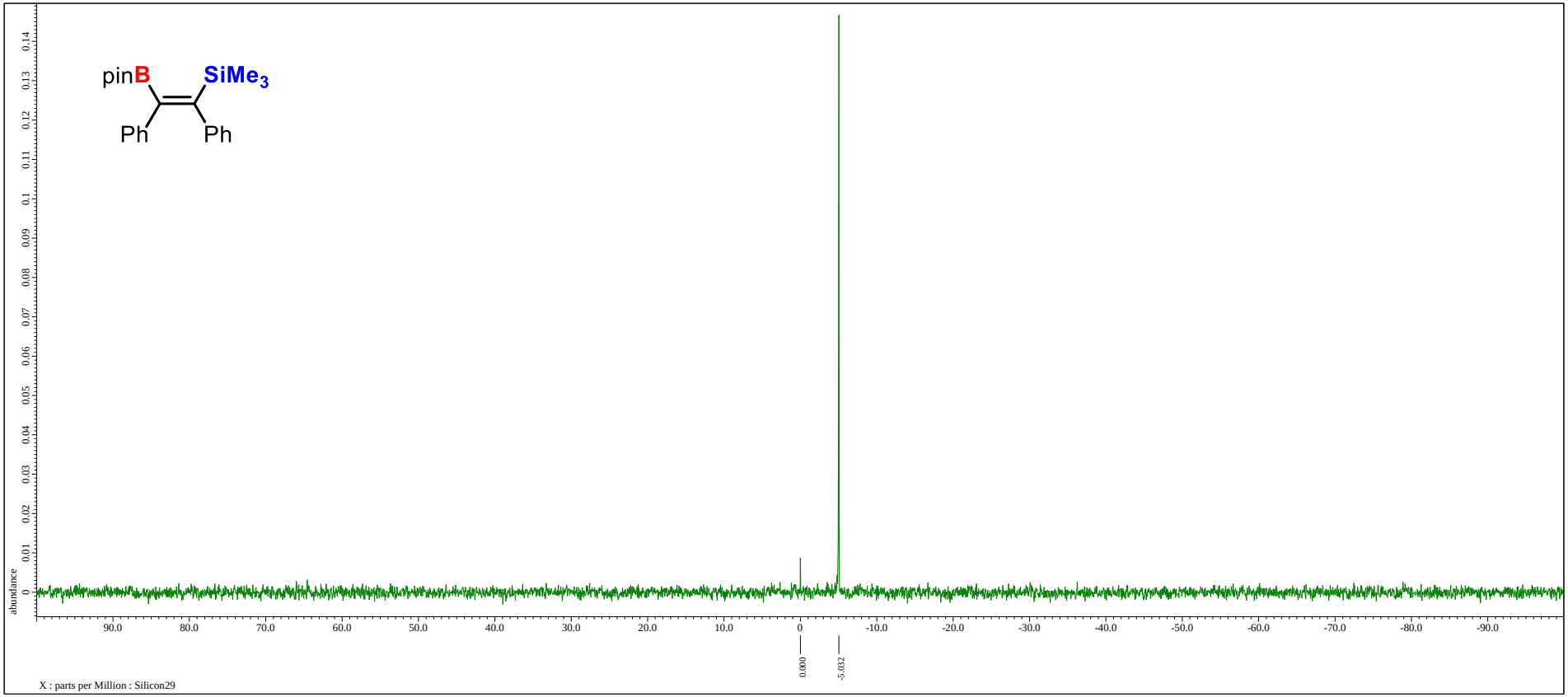

Figure S30. ^{29}Si NMR (119 MHz, $CDCl_3$) spectrum of **2aa**.

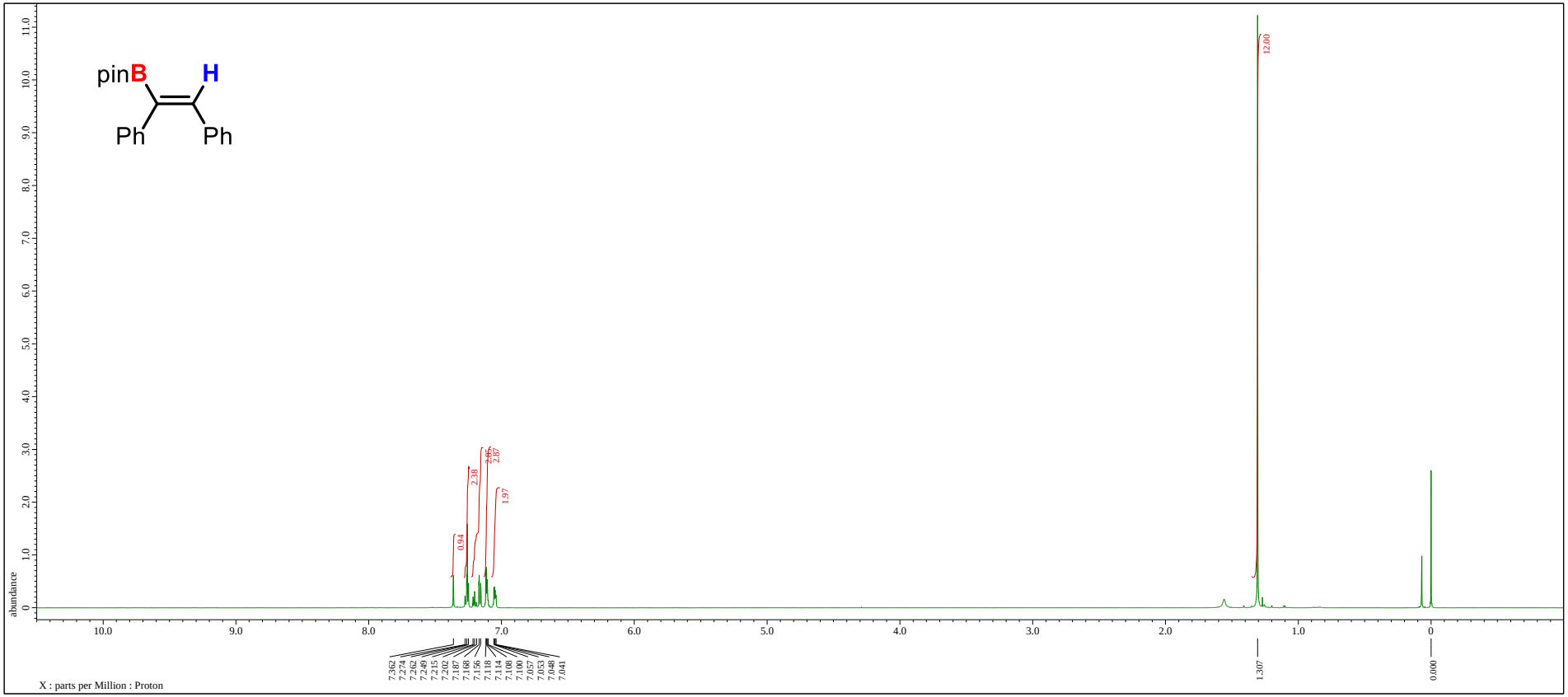

Figure S31. ^{1}H NMR (600 MHz, $CDCl_3$) spectrum of **2ab**.

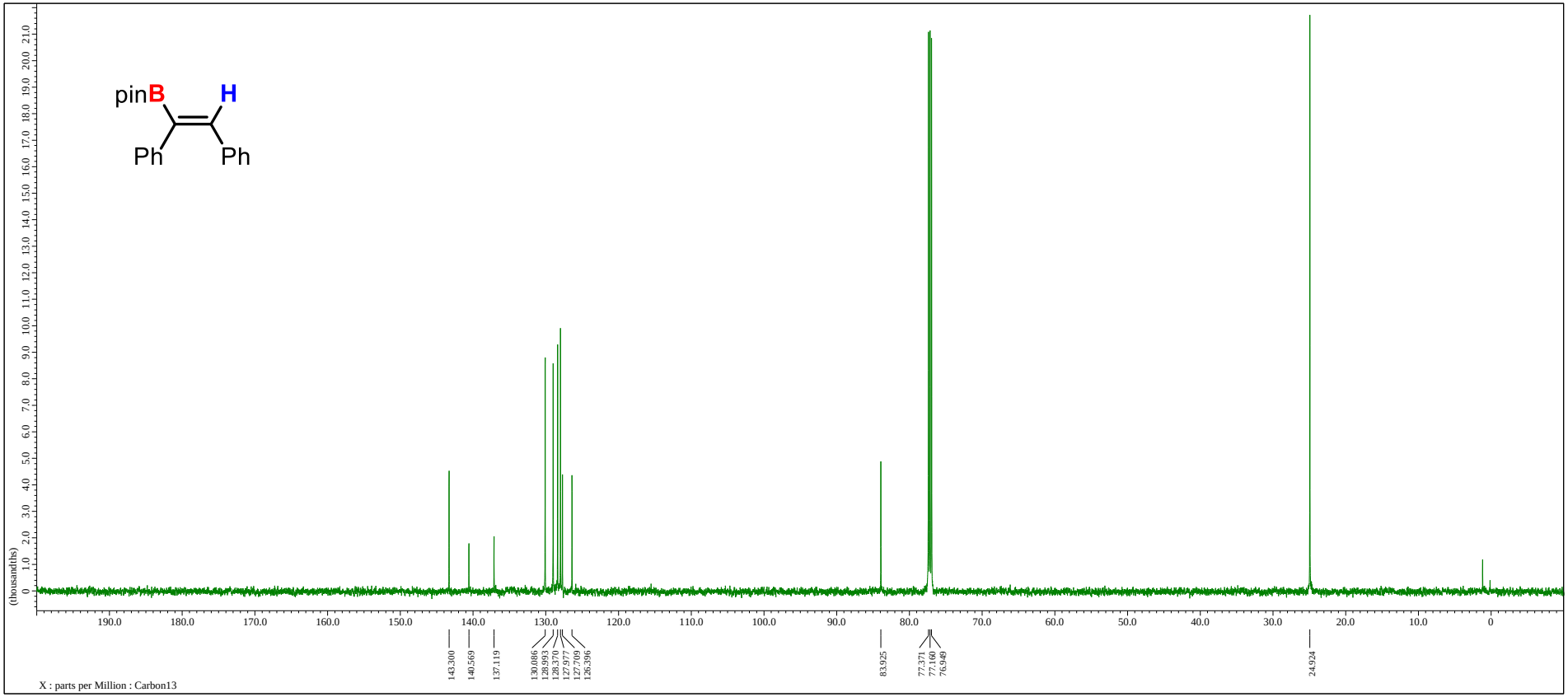

Figure S32. ^{13}C NMR (151 MHz, $CDCl_3$) spectrum of **2ab**.

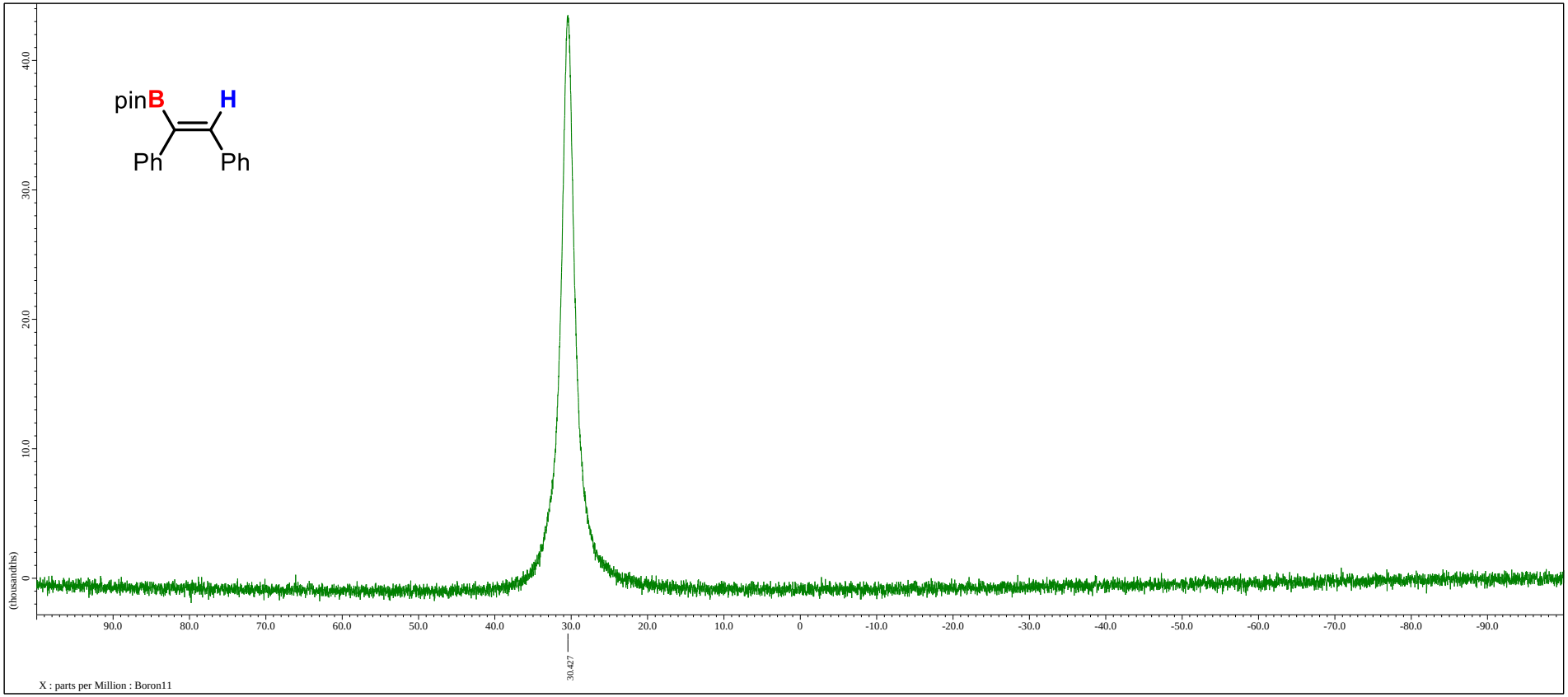

Figure S33. ^{11}B NMR (192 MHz, $CDCl_3$) spectrum of **2ab**.

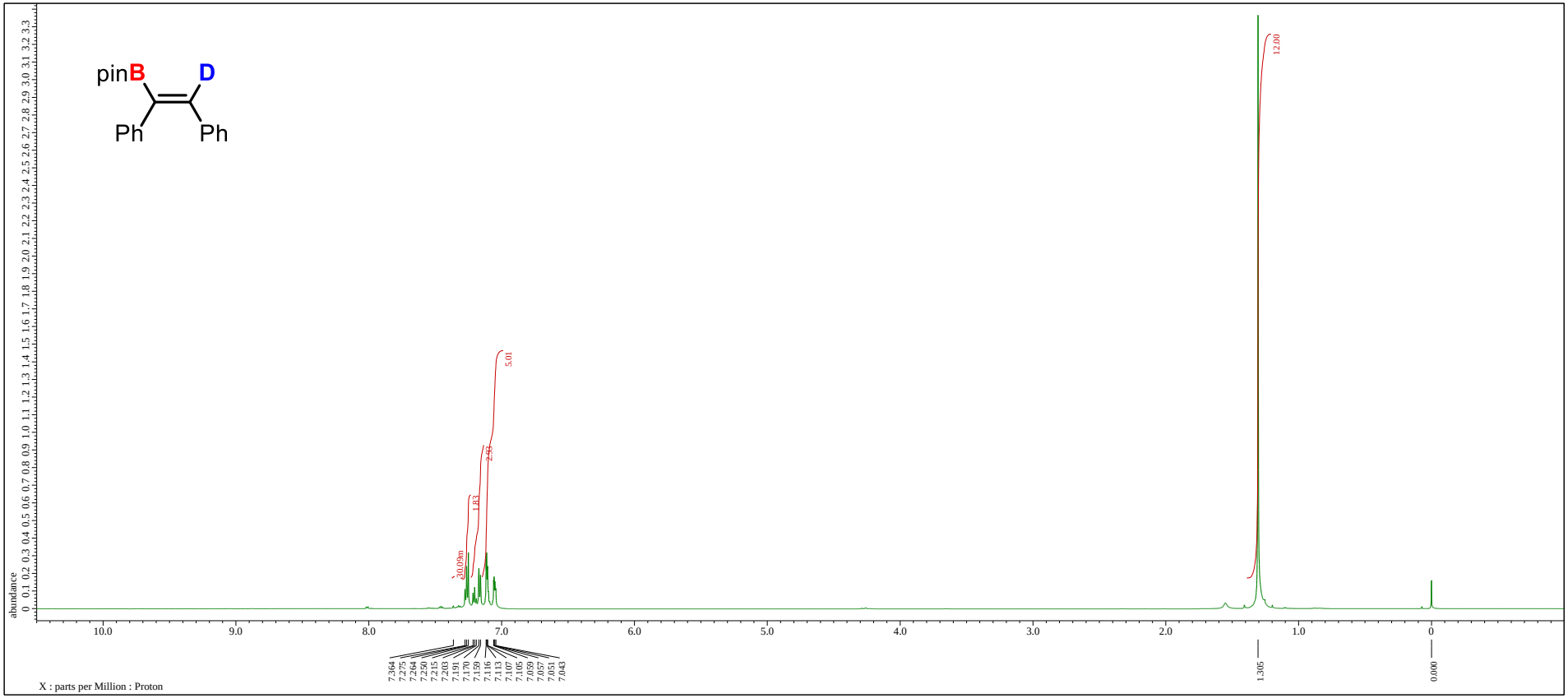

Figure S34. ^{1}H NMR (600 MHz, $CDCl_3$) spectrum of **2ac**.

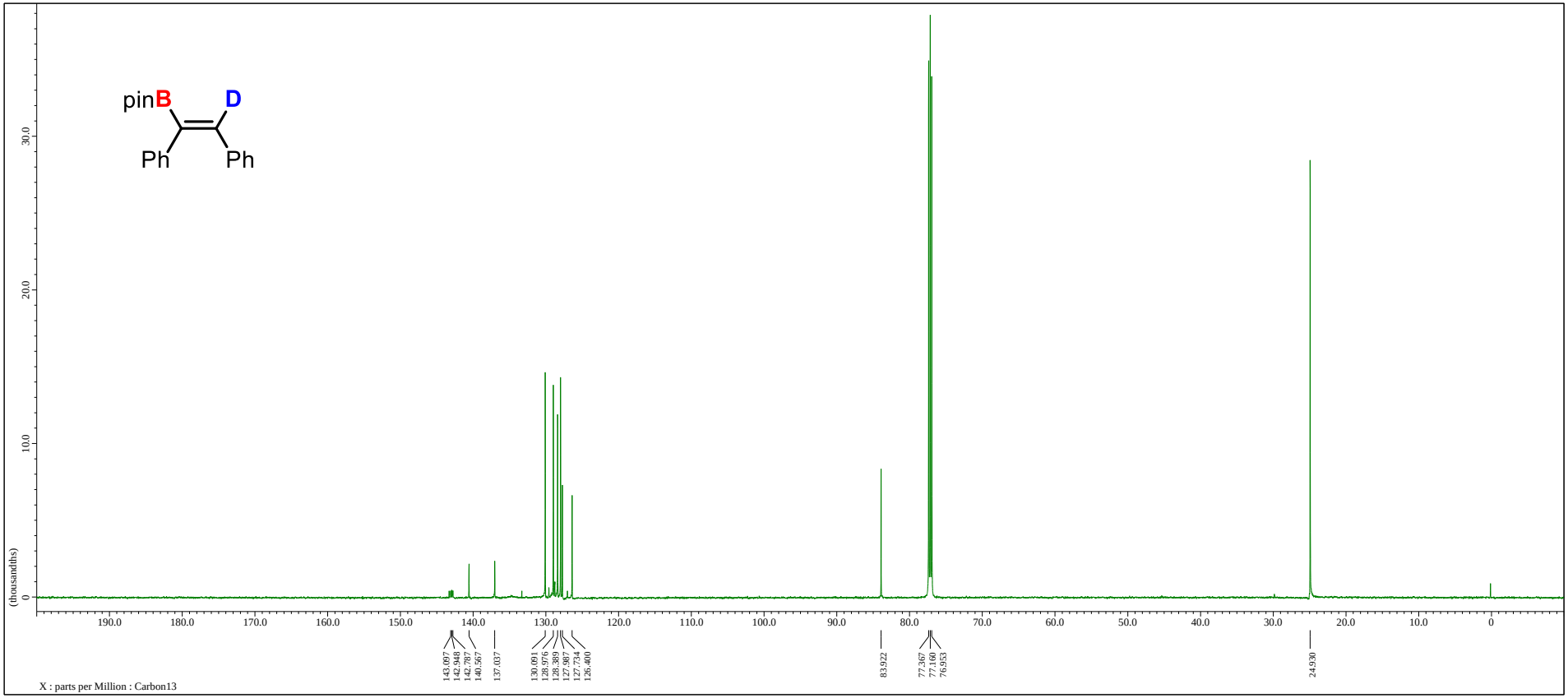

Figure S35. ^{13}C NMR (151 MHz, $CDCl_3$) spectrum of **2ac**.

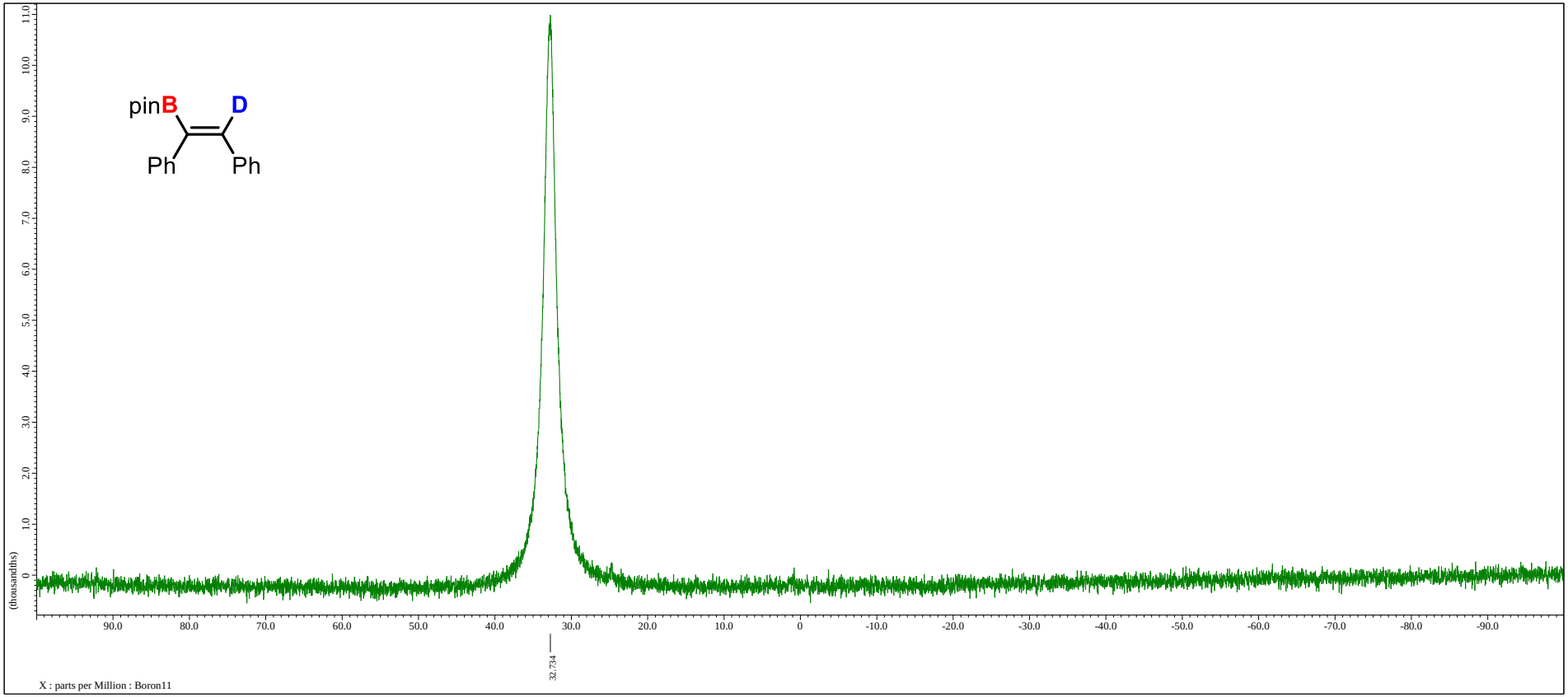

Figure S36. ^{11}B NMR (192 MHz, $CDCl_3$) spectrum of **2ac**.

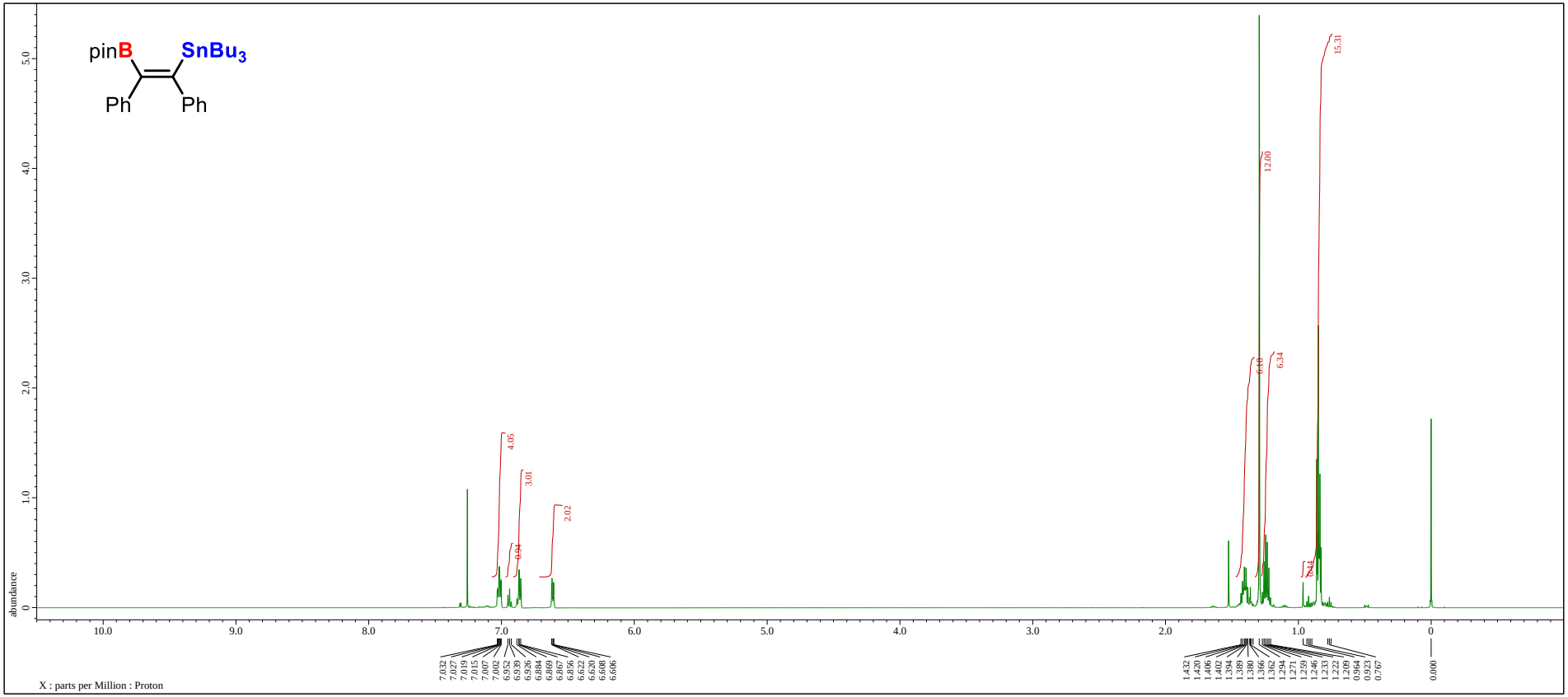

Figure S37. ^{1}H NMR (600 MHz, $CDCl_3$) spectrum of **2ad**.

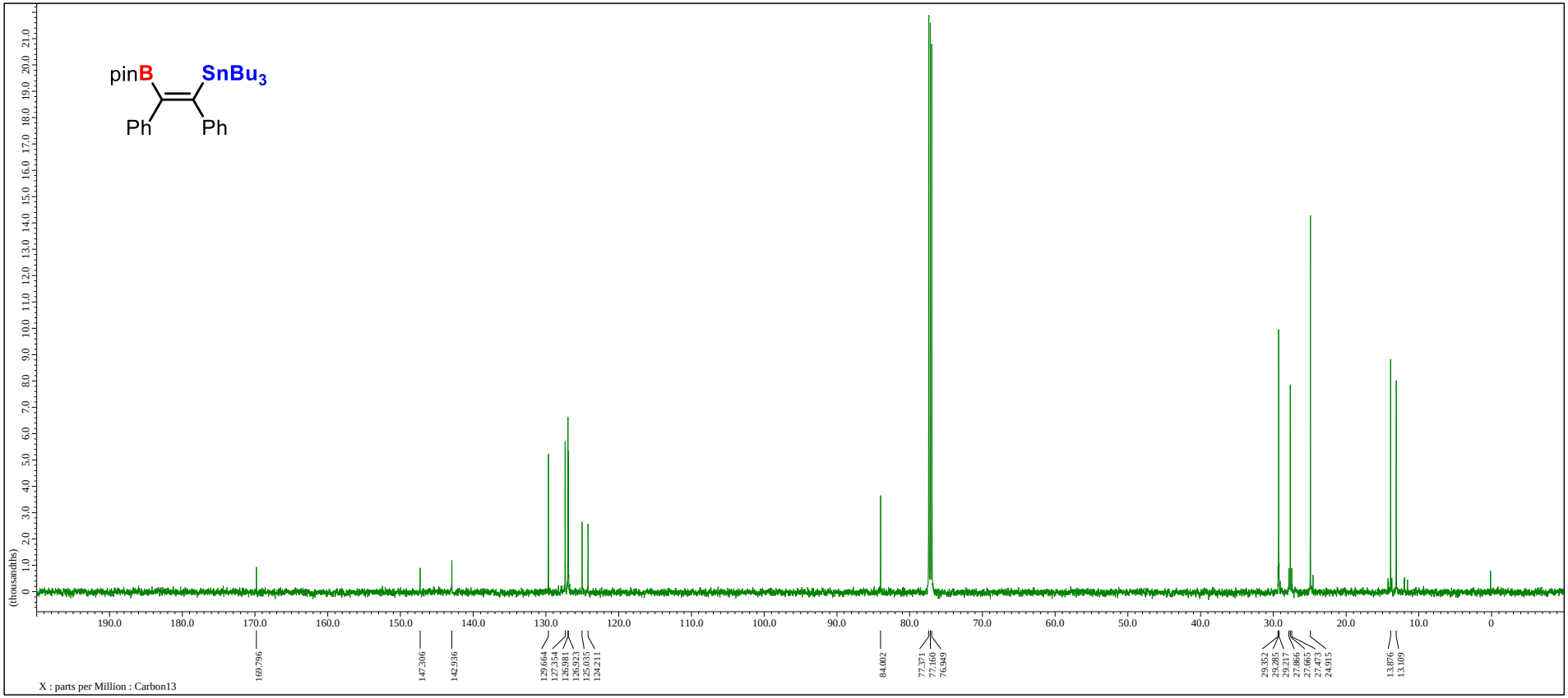

Figure S38. ^{13}C NMR (151 MHz, $CDCl_3$) spectrum of **2ad**.

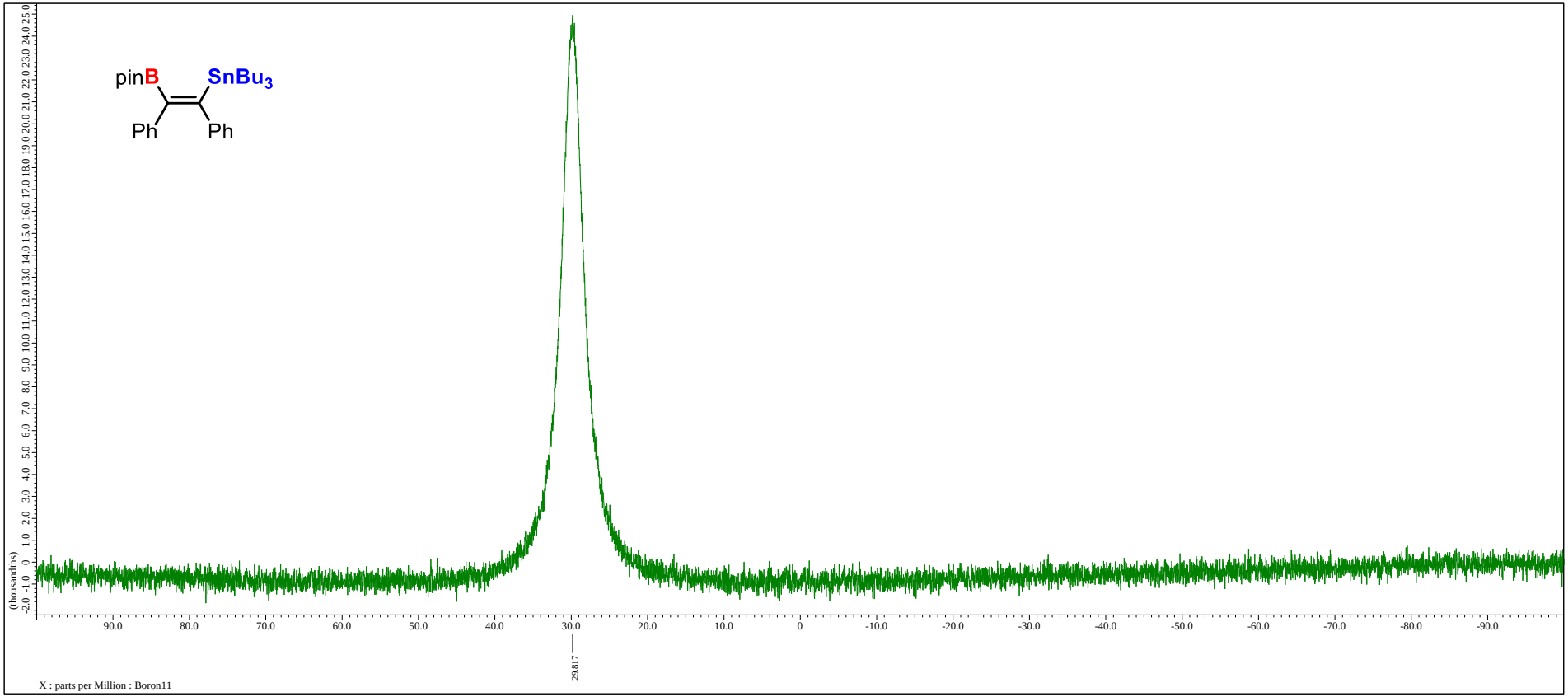

Figure S39. ^{11}B NMR (243 MHz, $CDCl_3$) spectrum of **2ad**.

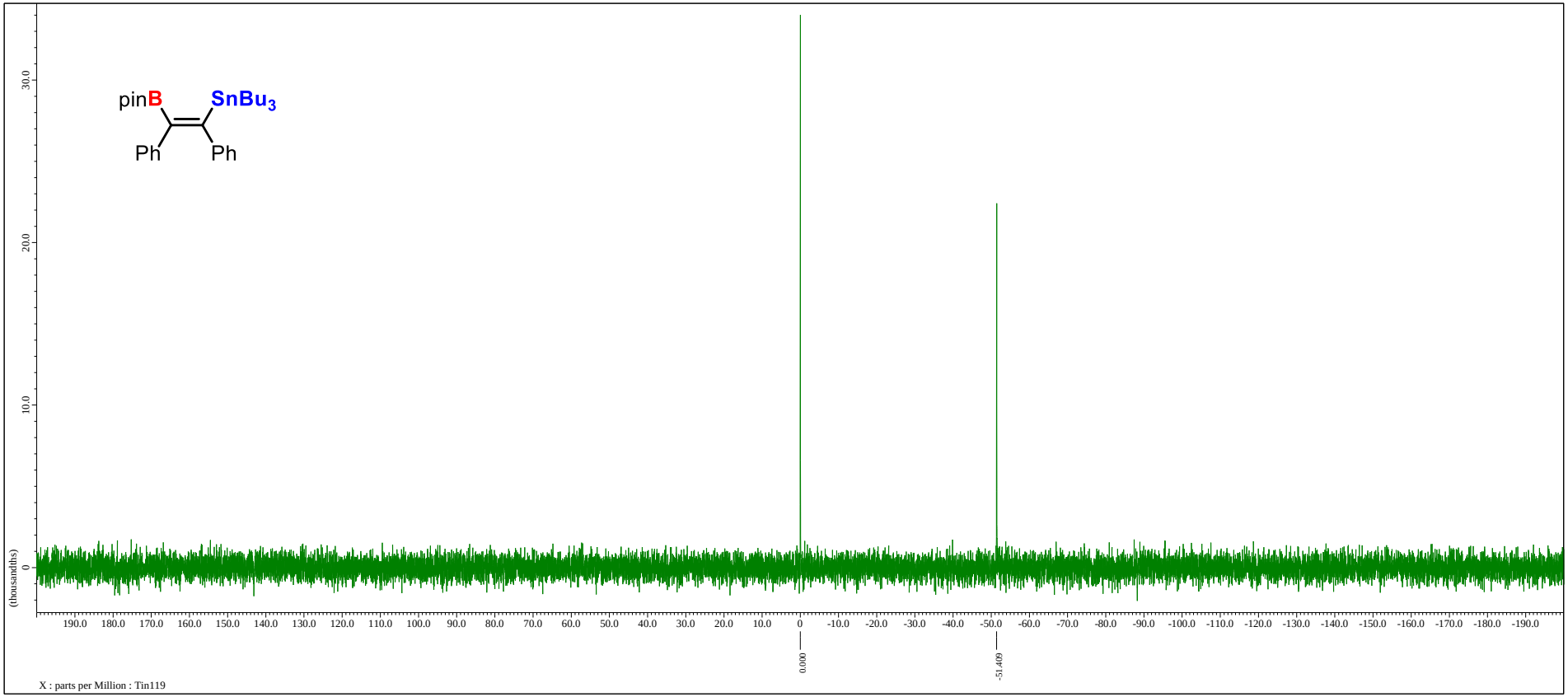

Figure S40. ^{119}Sn NMR (224 MHz, $CDCl_3$) spectrum of **2ad**.

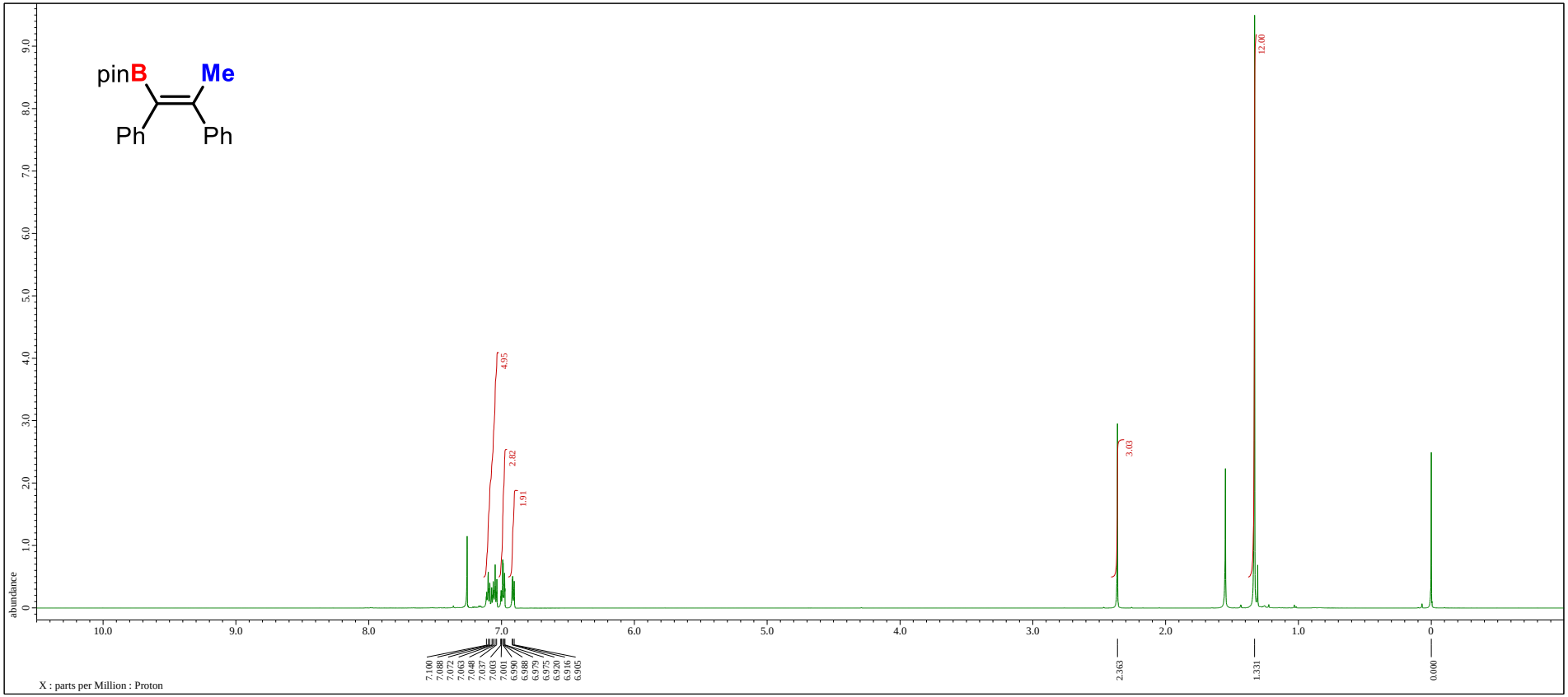

Figure S41. ^{1}H NMR (600 MHz, $CDCl_3$) spectrum of **2ae**.

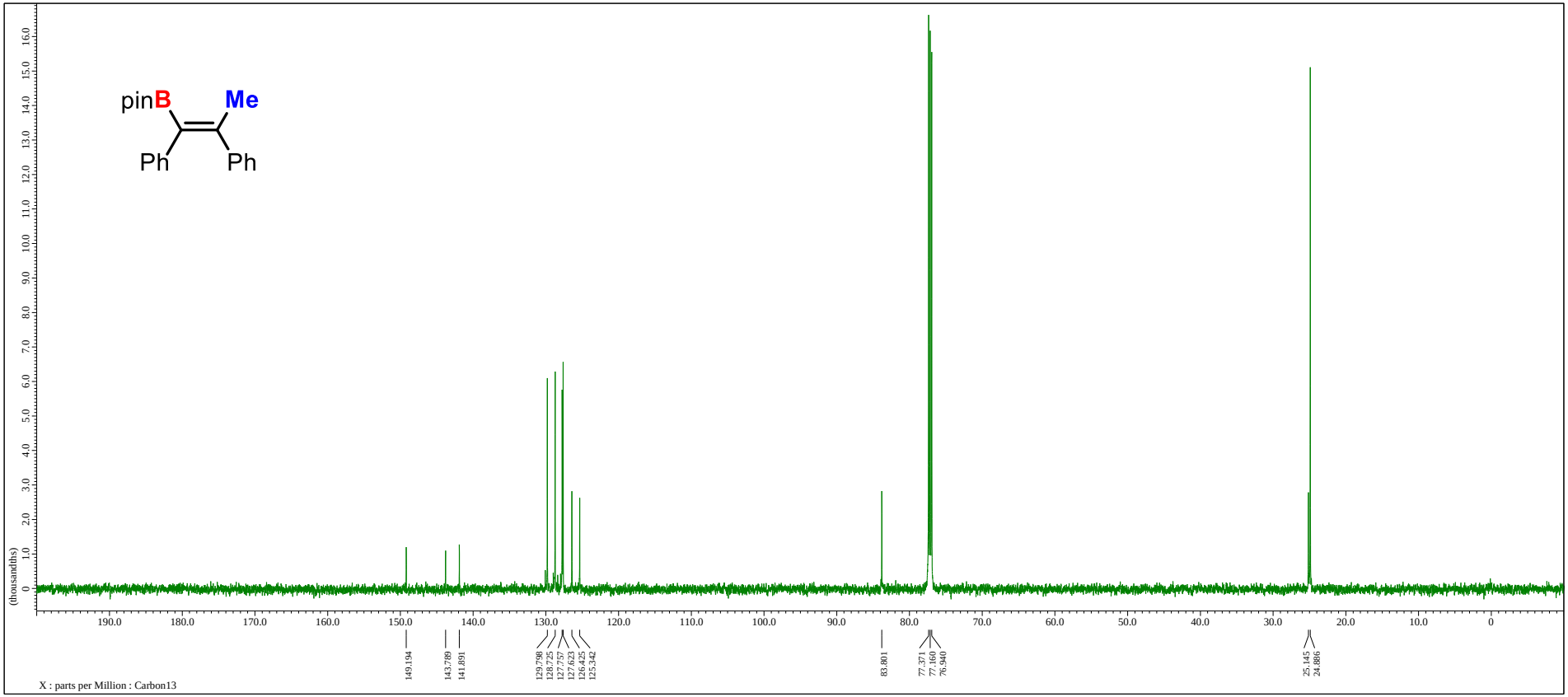

Figure S42. ^{13}C NMR (151 MHz, $CDCl_3$) spectrum of **2ae**.

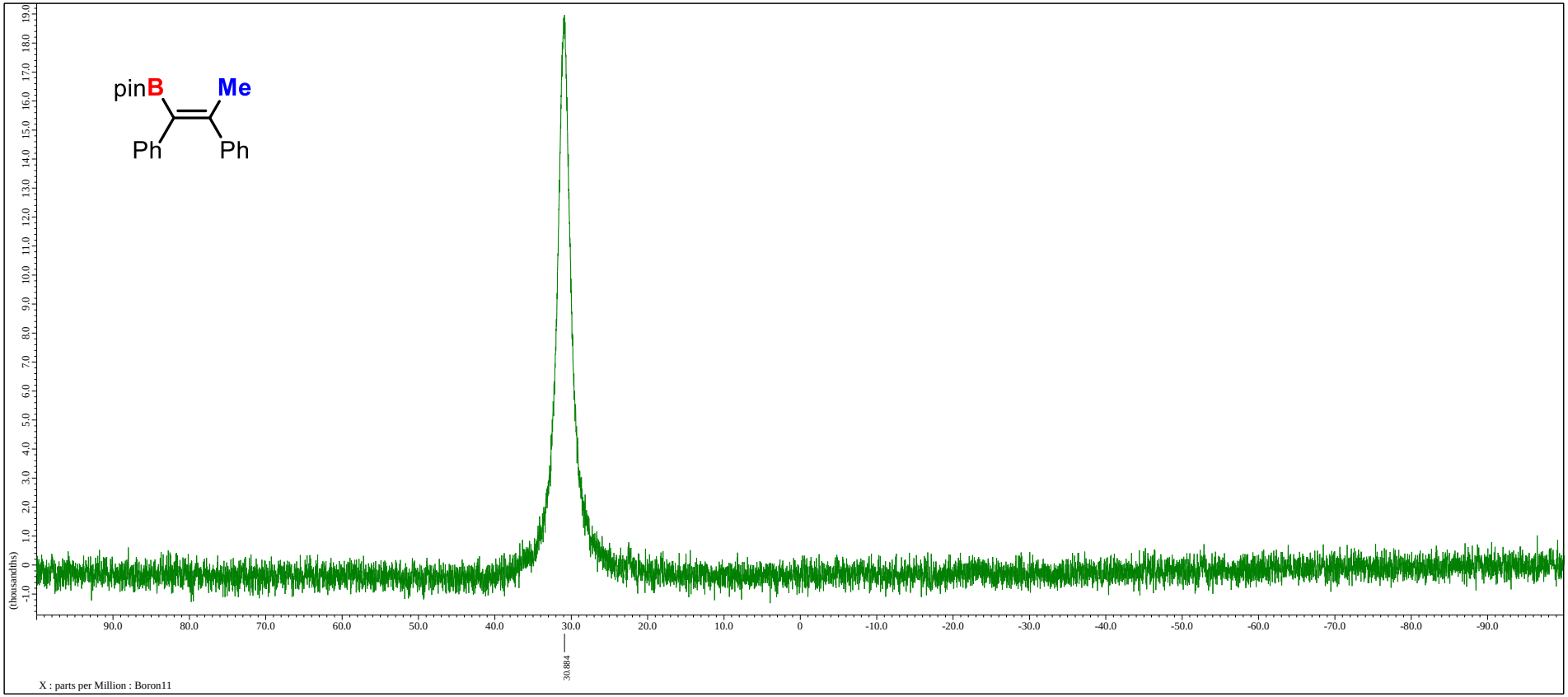

Figure S43. ^{11}B NMR (192 MHz, $CDCl_3$) spectrum of **2ae**.

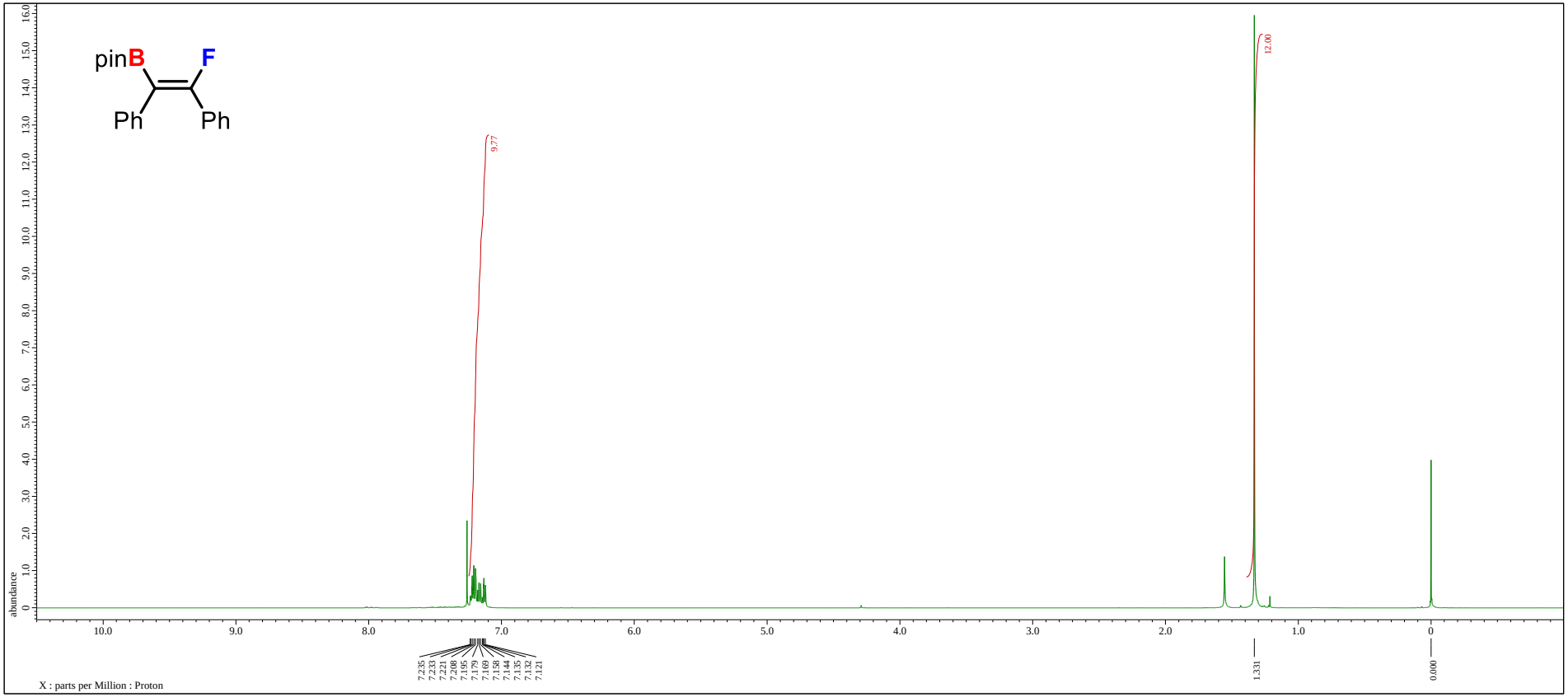

Figure S44. ^{1}H NMR (600 MHz, $CDCl_3$) spectrum of **2af**.

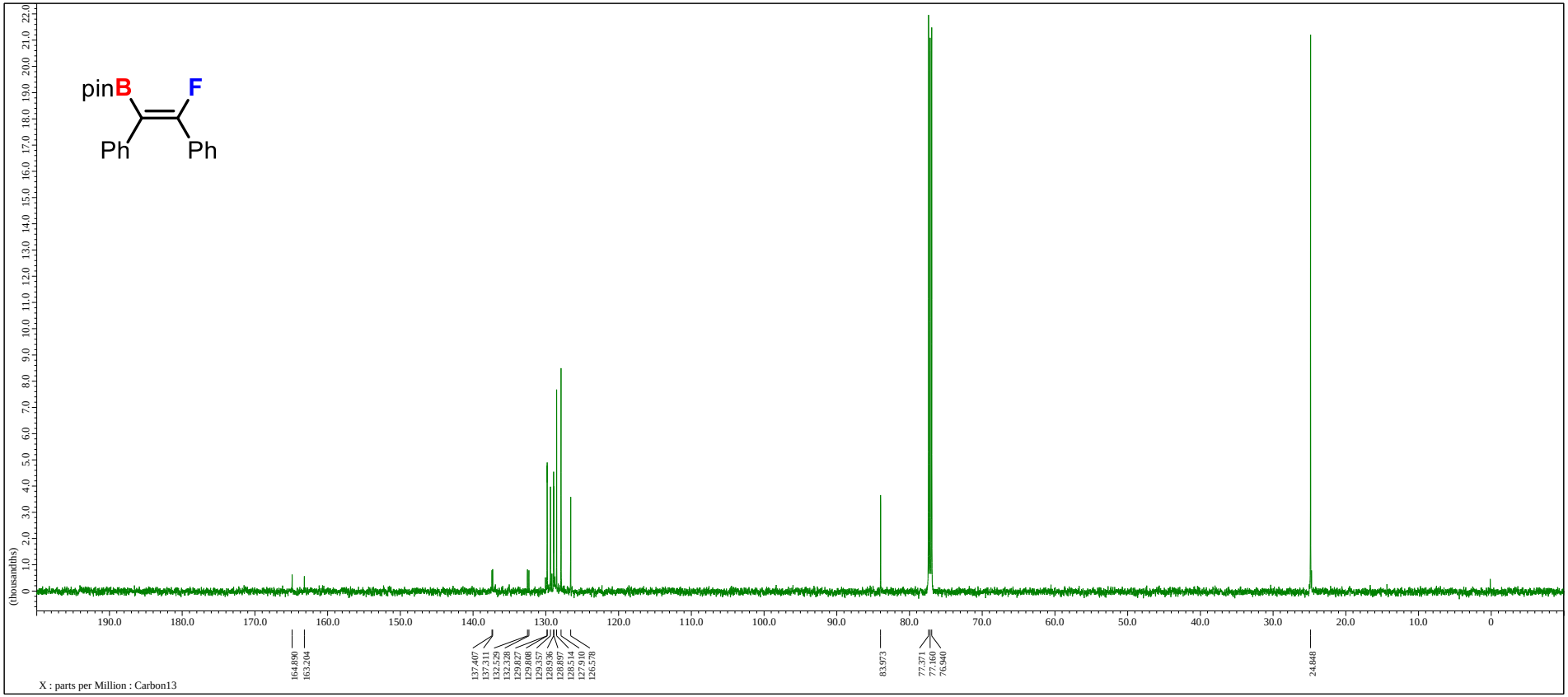

Figure S45. ^{13}C NMR (151 MHz, $CDCl_3$) spectrum of **2af**.

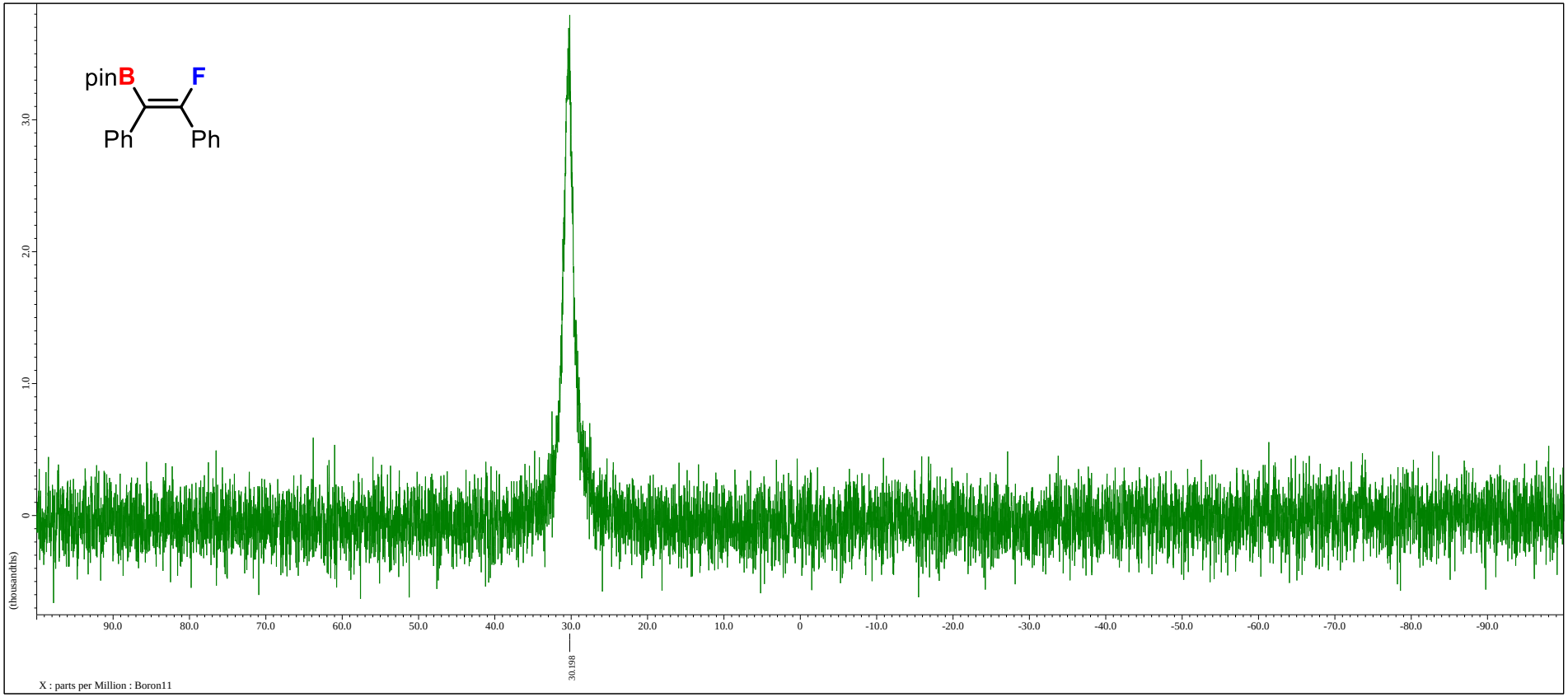

Figure S46. ^{11}B NMR (192 MHz, $CDCl_3$) spectrum of **2af**.

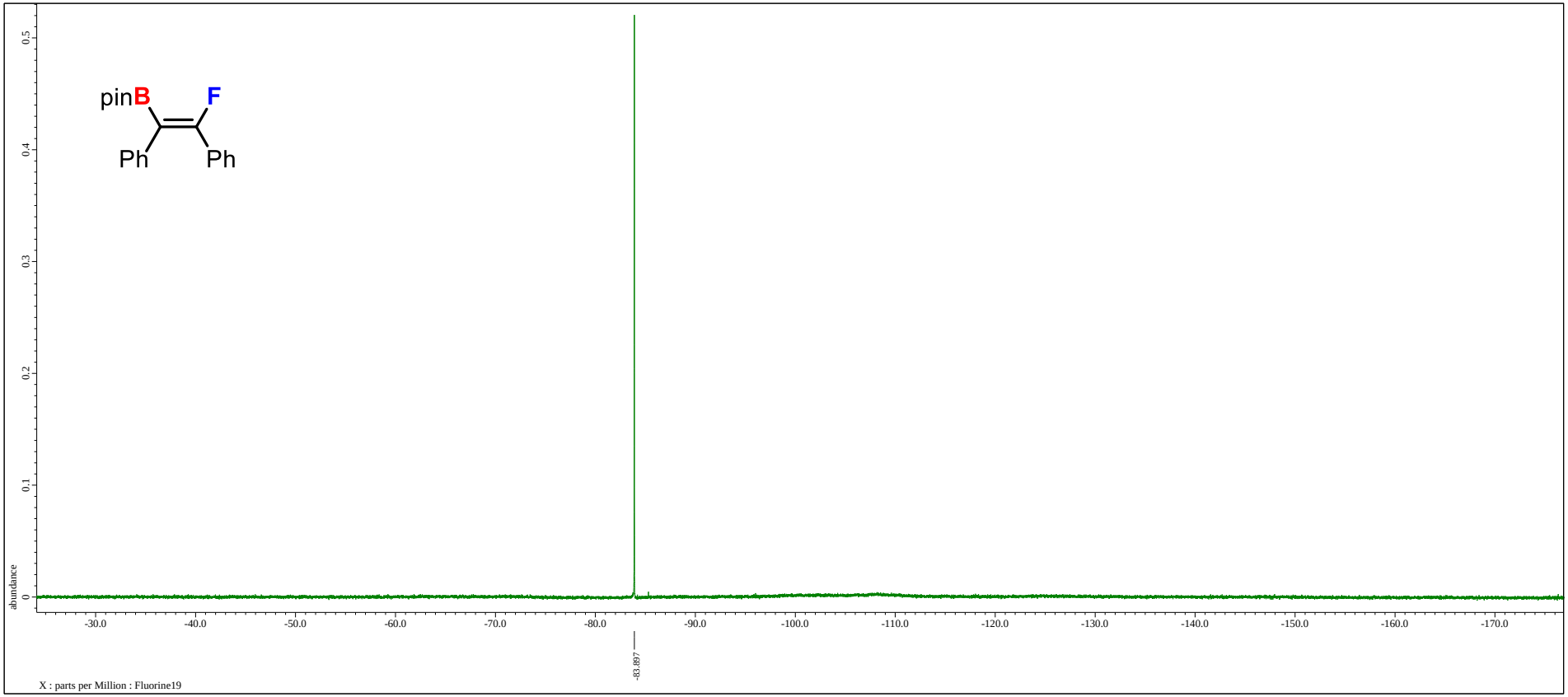

Figure S47. ^{19}F NMR (564 MHz, $CDCl_3$) spectrum of **2af**.

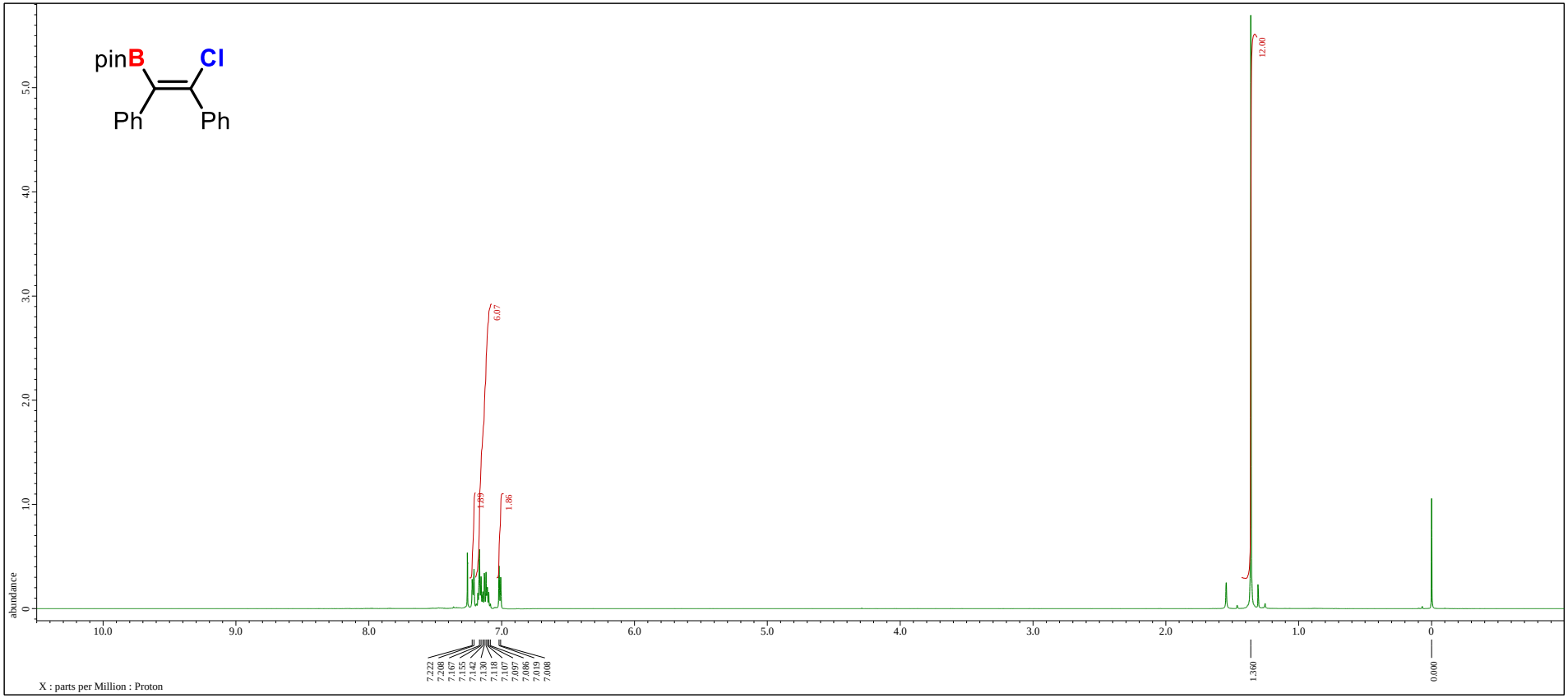

Figure S48. ^{1}H NMR (600 MHz, $CDCl_3$) spectrum of **2ag**.

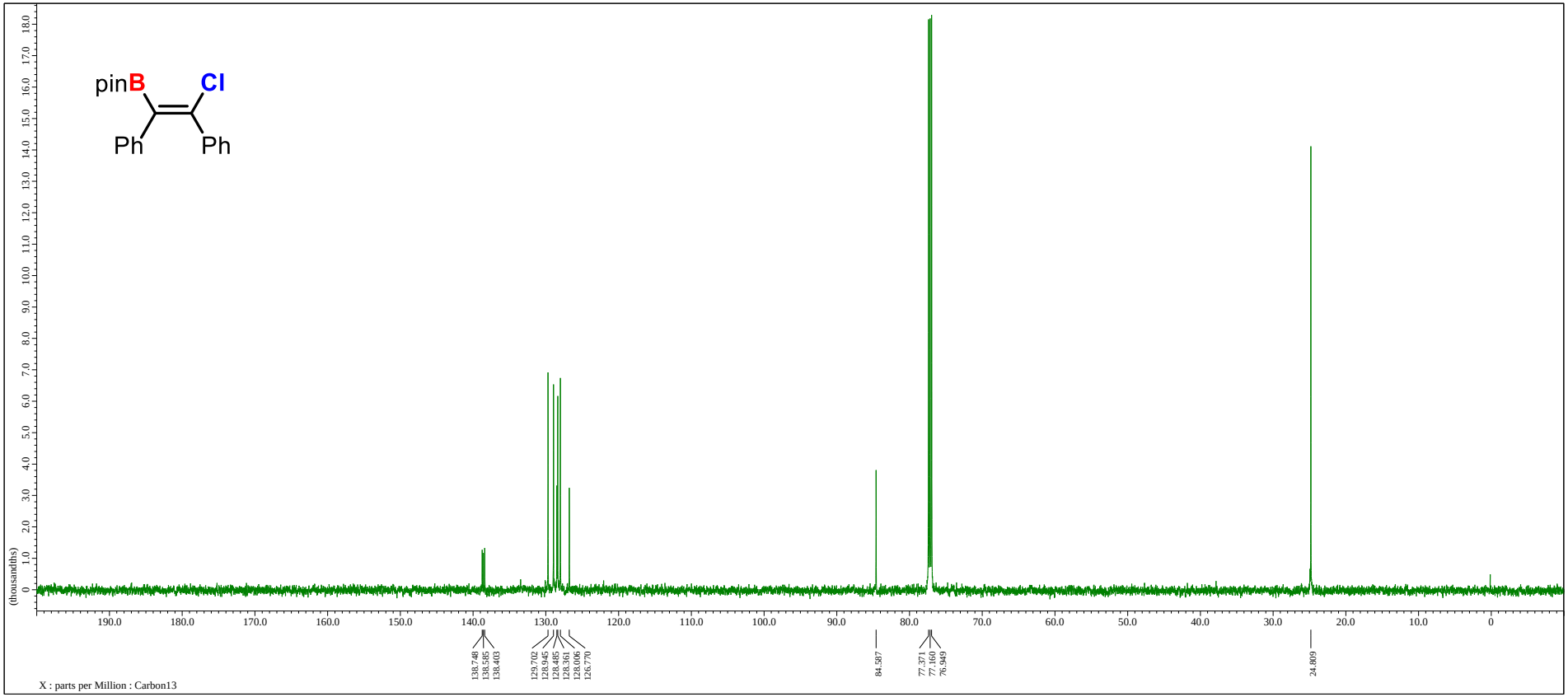

Figure S49. ^{13}C NMR (151 MHz, $CDCl_3$) spectrum of **2ag**.

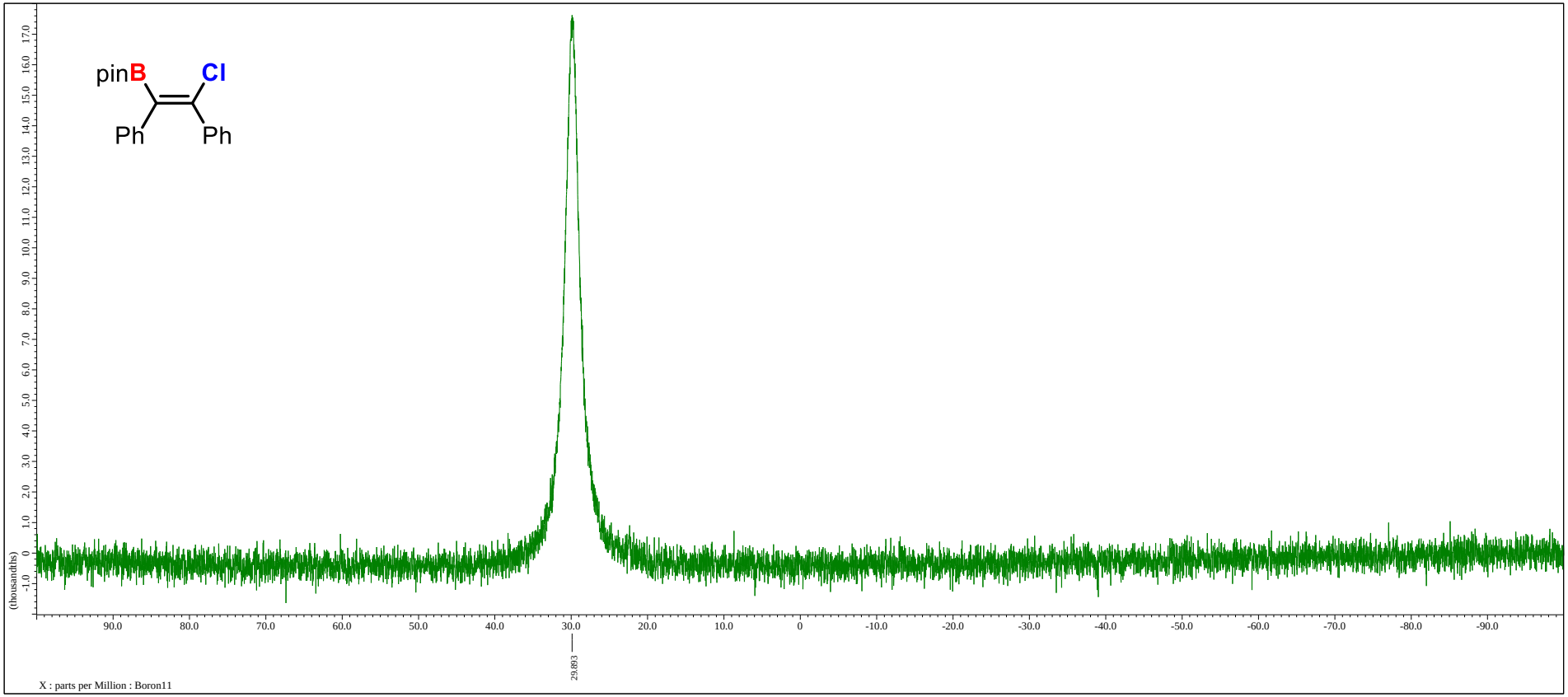

Figure S50. ^{11}B NMR (192 MHz, $CDCl_3$) spectrum of **2ag**.

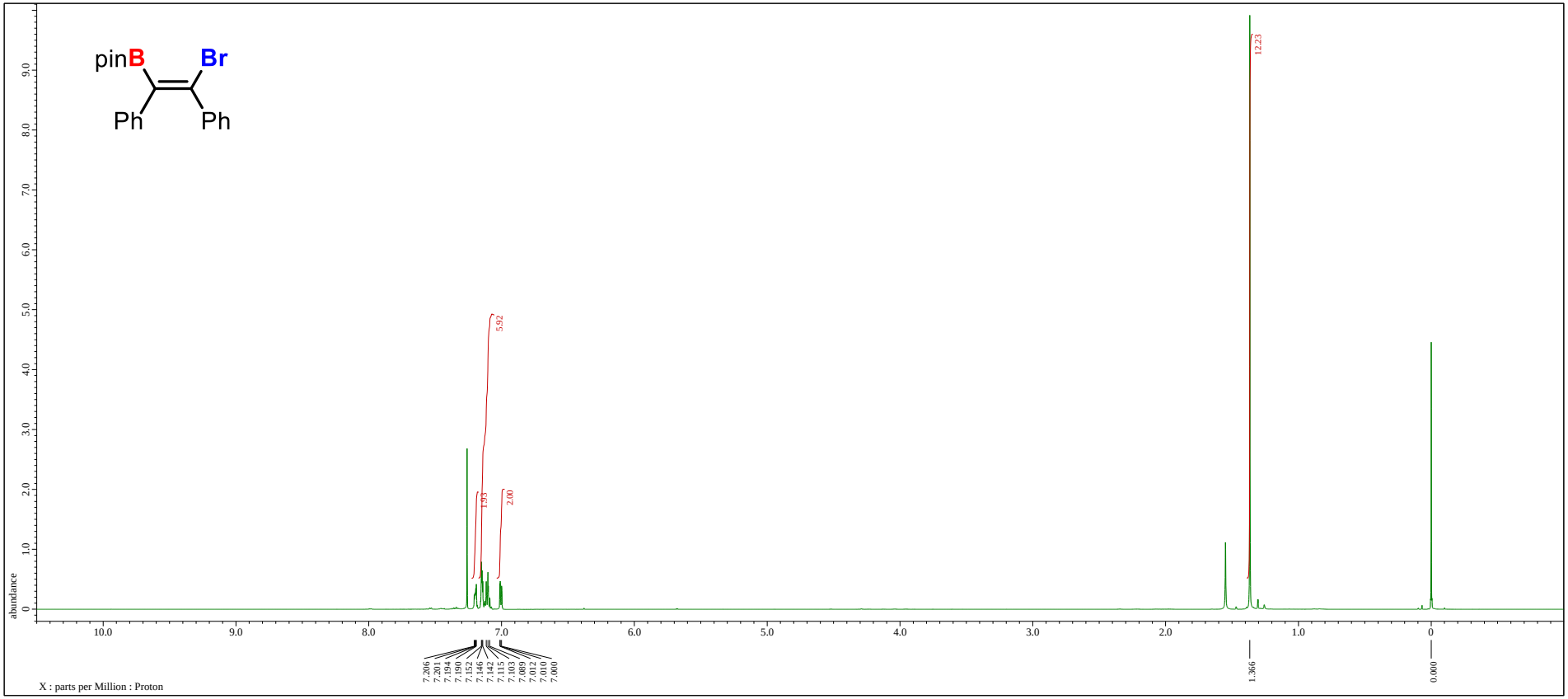

Figure S51. ^{1}H NMR (600 MHz, $CDCl_3$) spectrum of **2ah**.

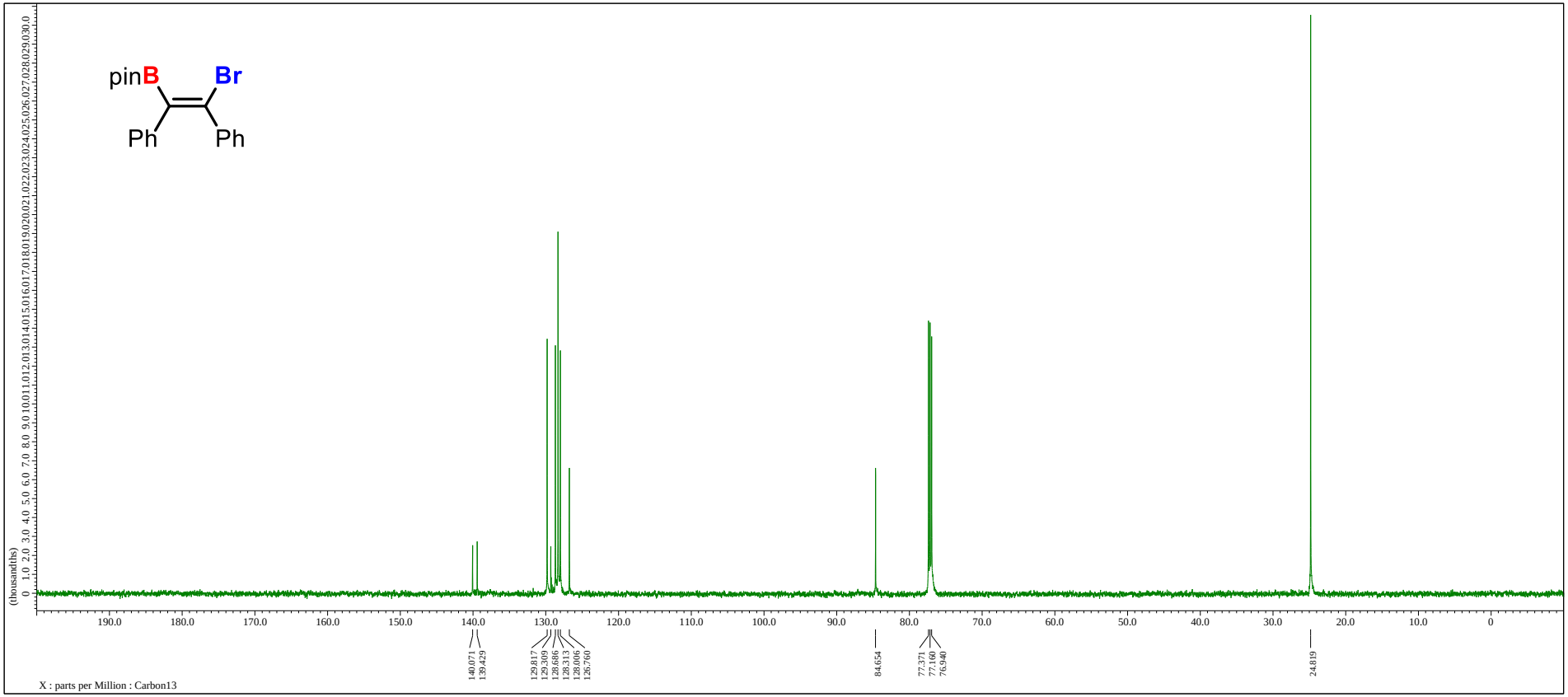

Figure S52. ^{13}C NMR (151 MHz, $CDCl_3$) spectrum of **2ah**.

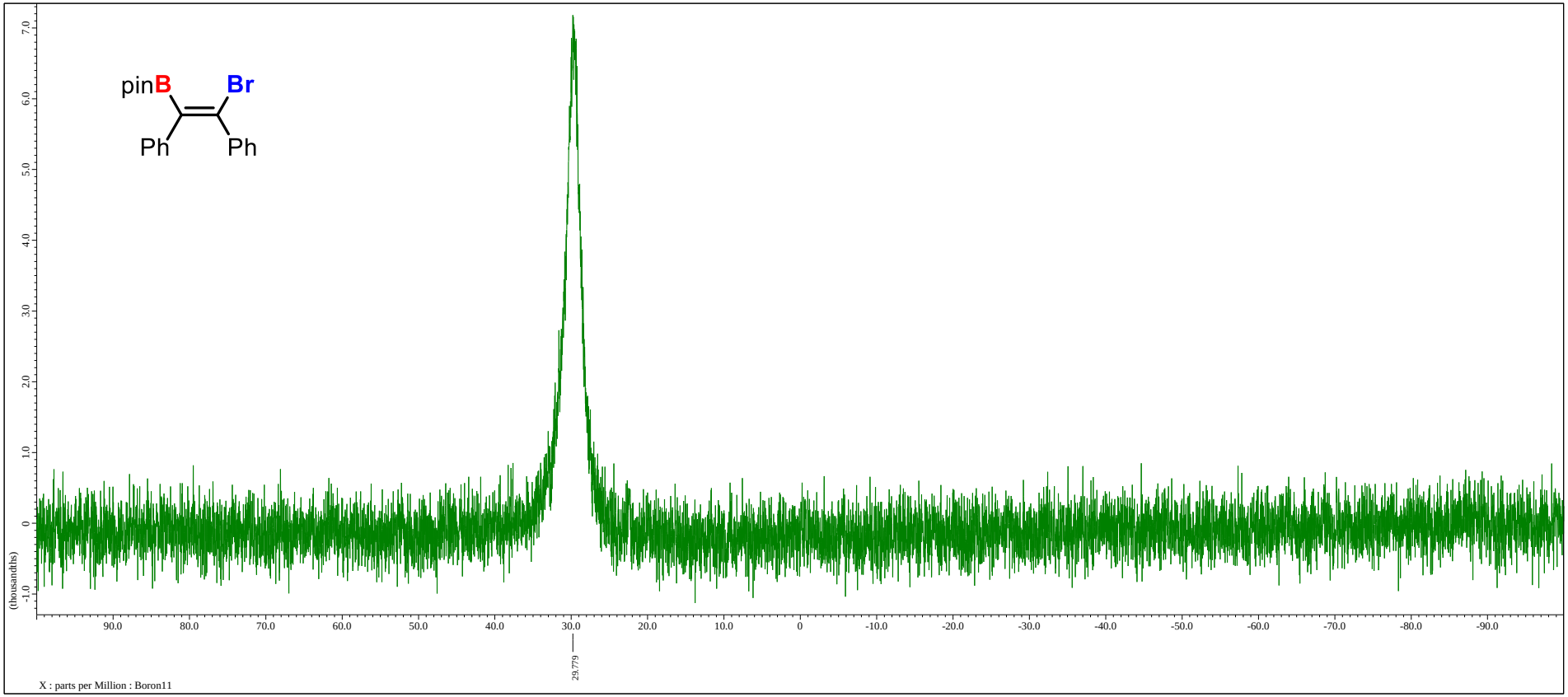

Figure S53. ^{11}B NMR (192 MHz, $CDCl_3$) spectrum of **2ah**.

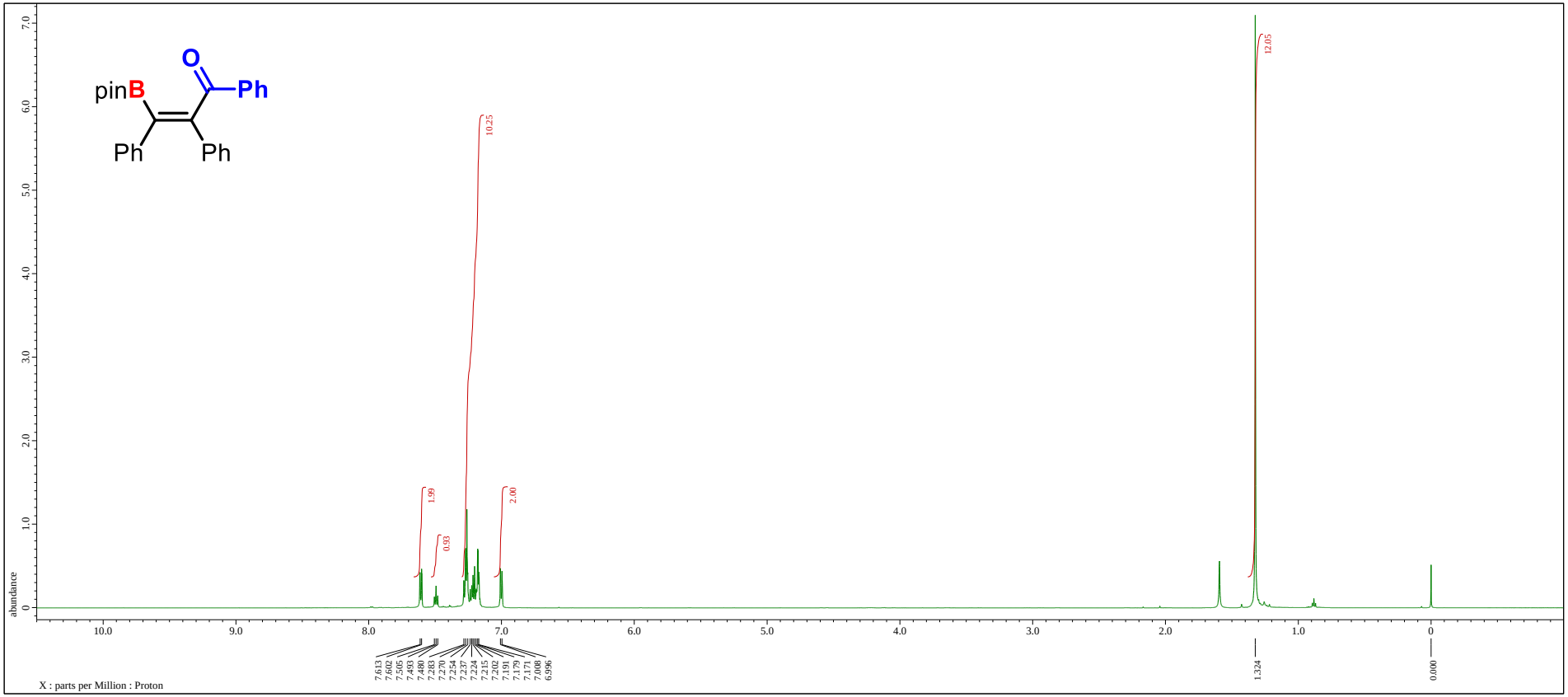

Figure S54. ^{1}H NMR (600 MHz, $CDCl_3$) spectrum of **2ai**.

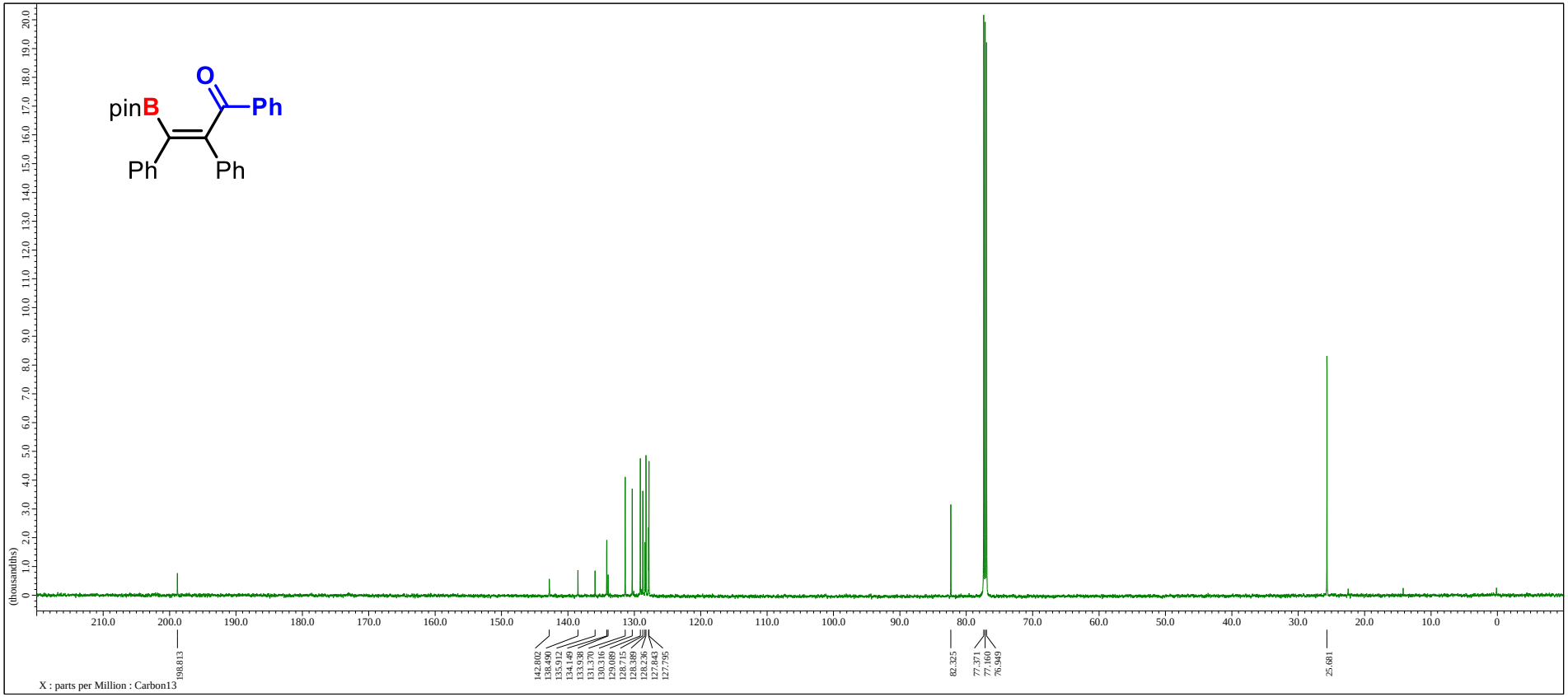

Figure S55. ^{13}C NMR (151 MHz, $CDCl_3$) spectrum of **2ai**.

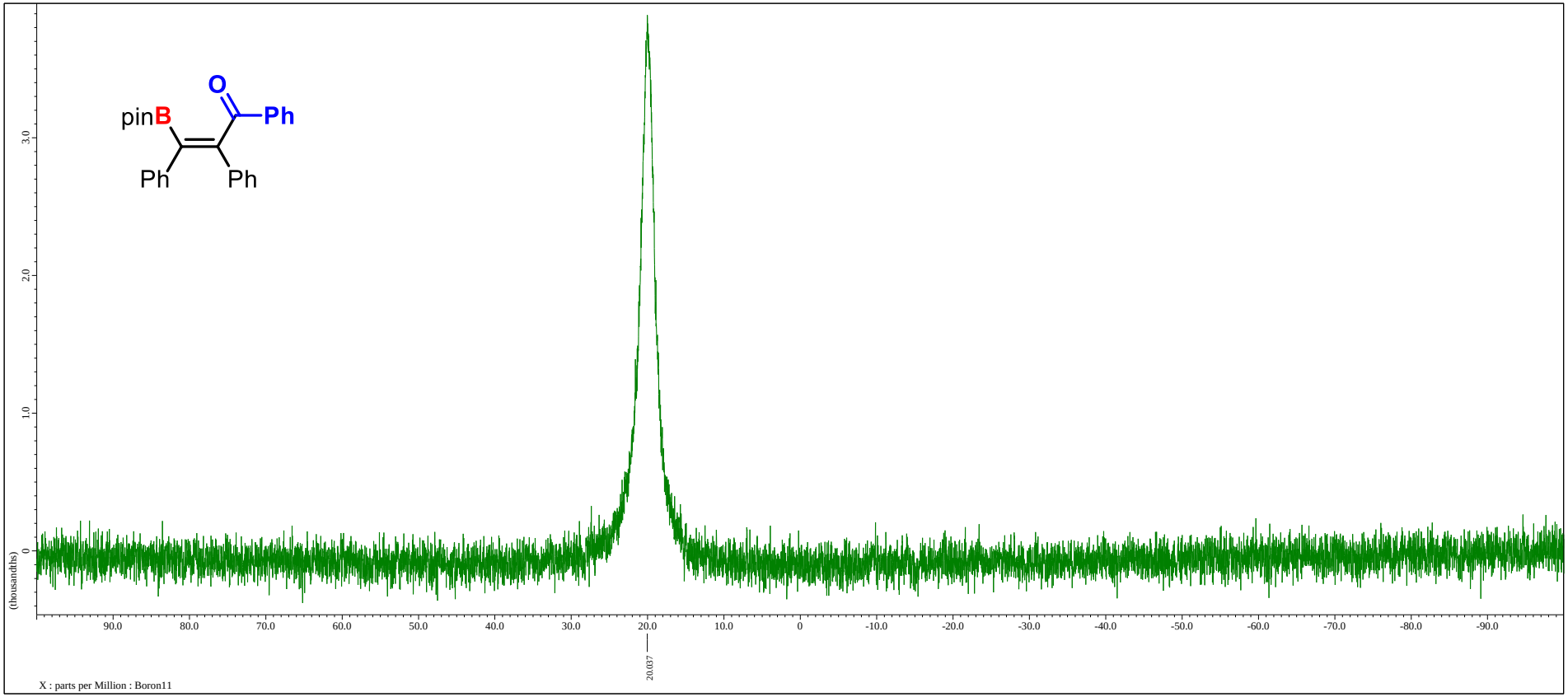

Figure S56. ^{11}B NMR (192 MHz, $CDCl_3$) spectrum of **2ai**.

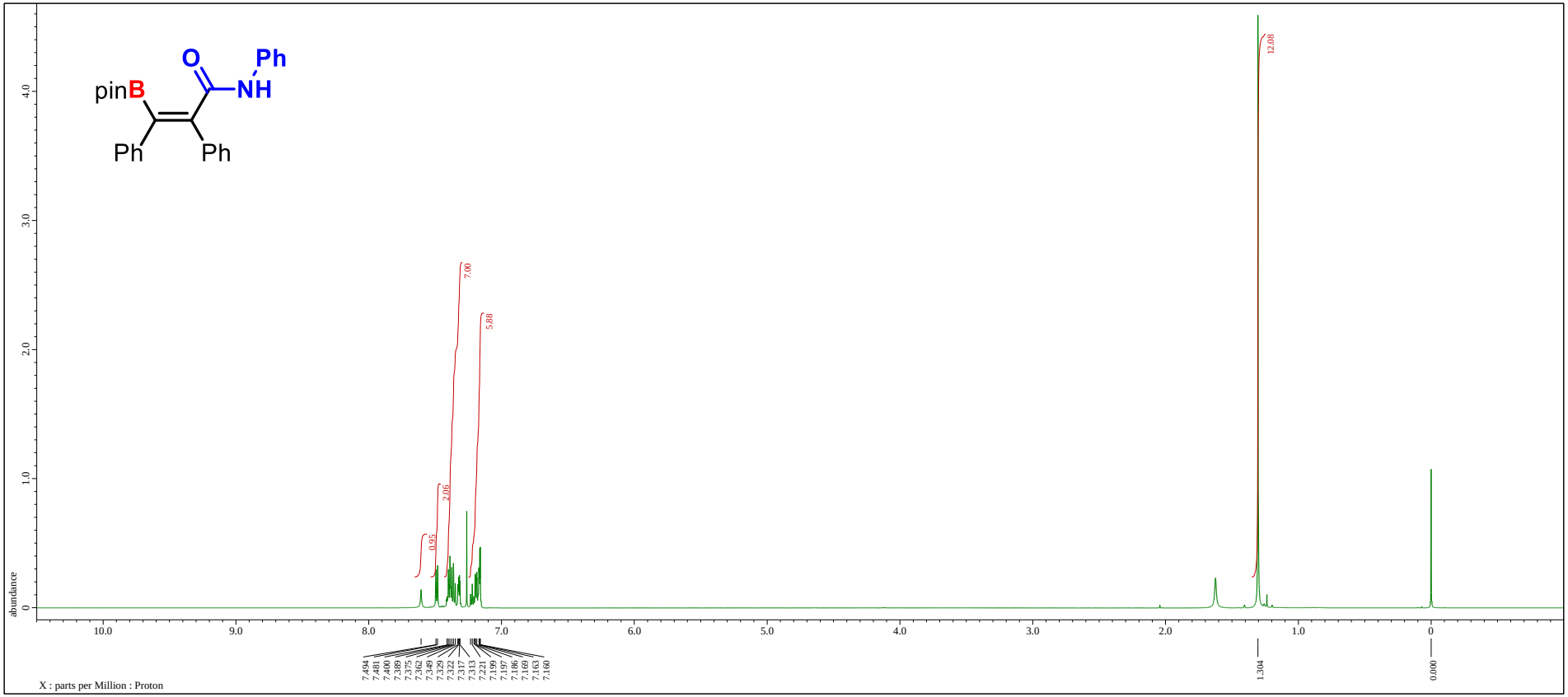

Figure S57. ^{1}H NMR (600 MHz, $CDCl_3$) spectrum of **2aj**.

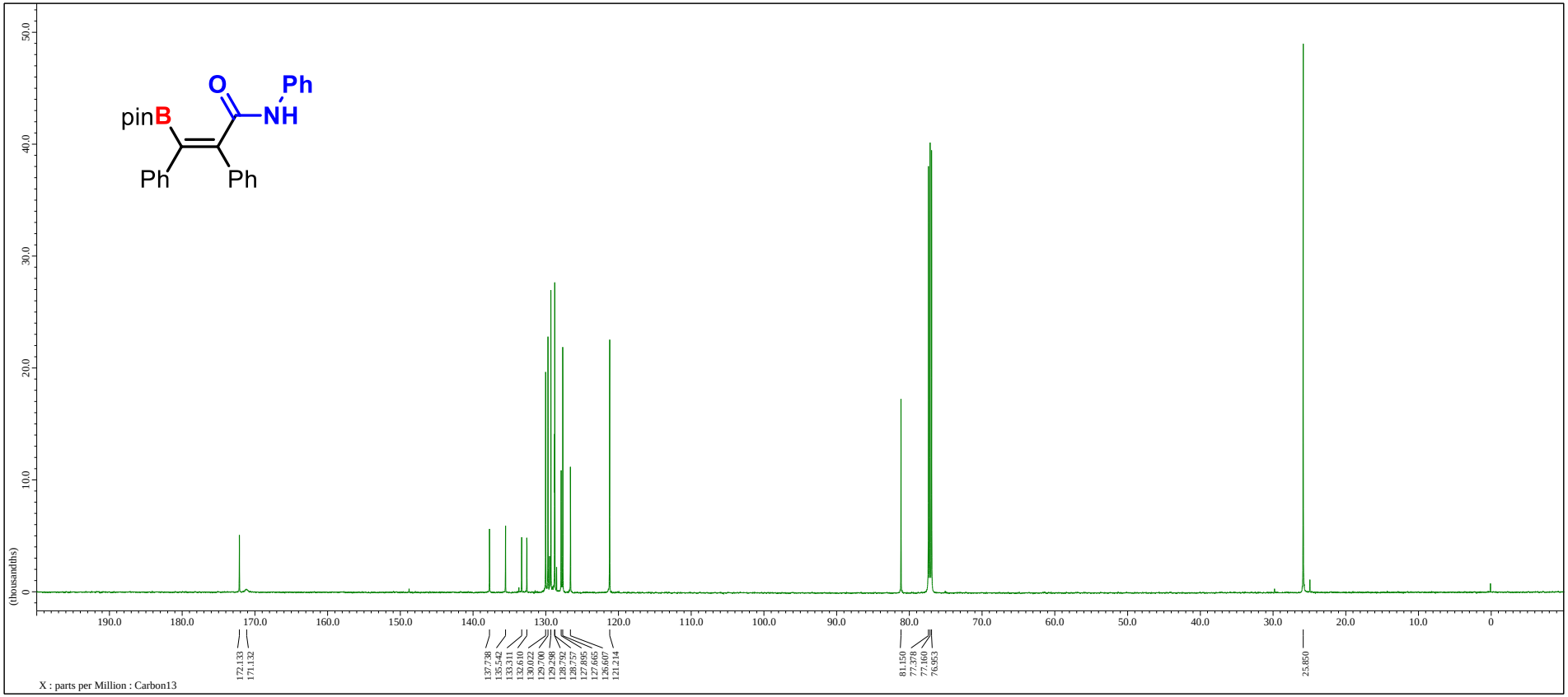

Figure S58. ^{13}C NMR (151 MHz, $CDCl_3$) spectrum of **2aj**.

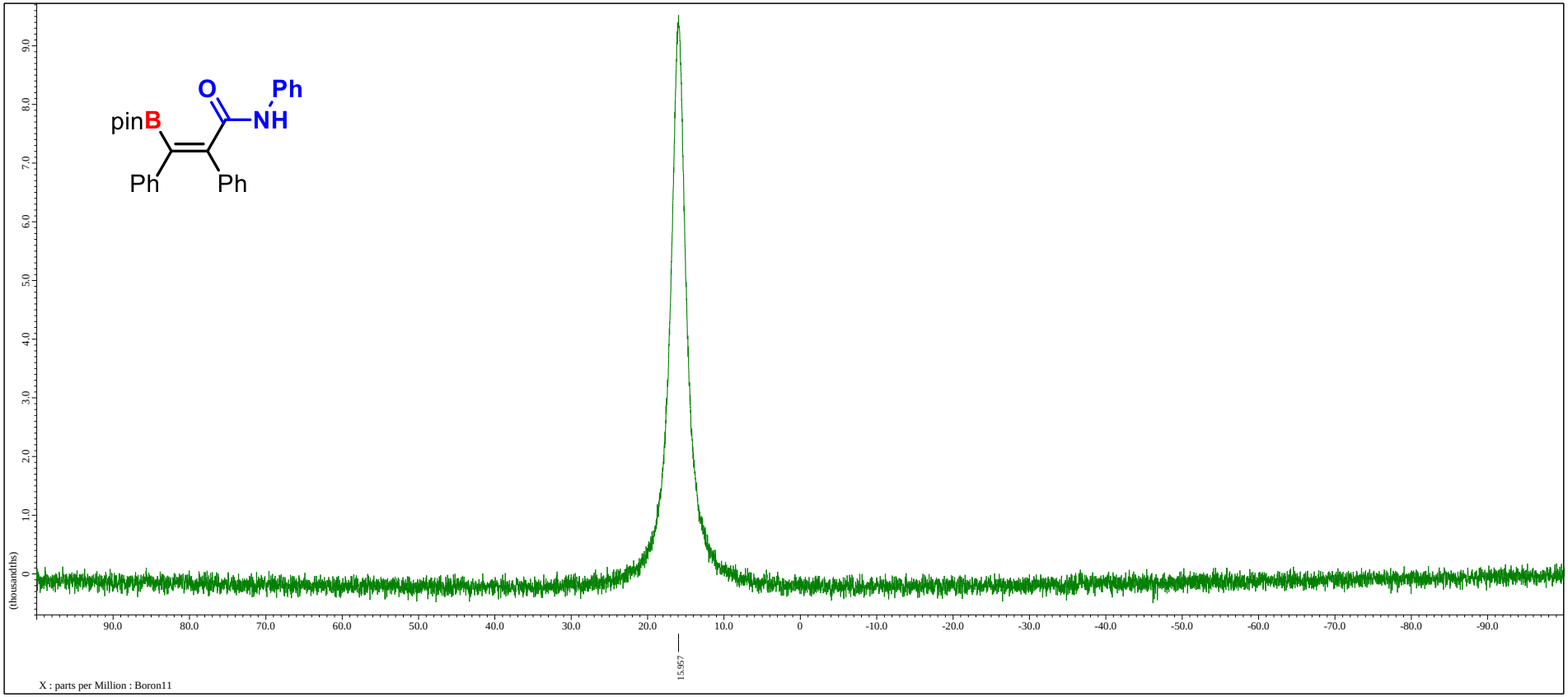

Figure S59. ^{11}B NMR (192 MHz, $CDCl_3$) spectrum of **2aj**.

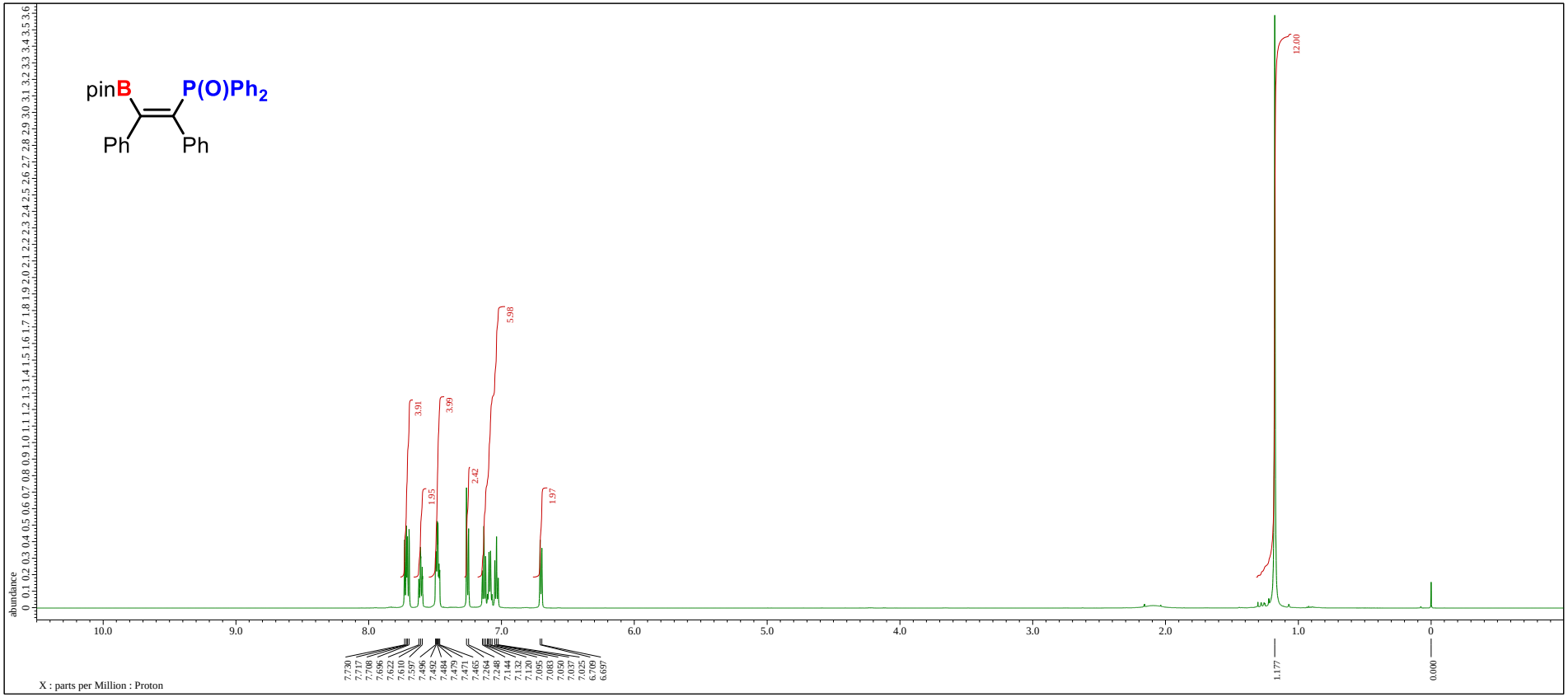

Figure S60. ^{1}H NMR (600 MHz, $CDCl_3$) spectrum of **2ak**.

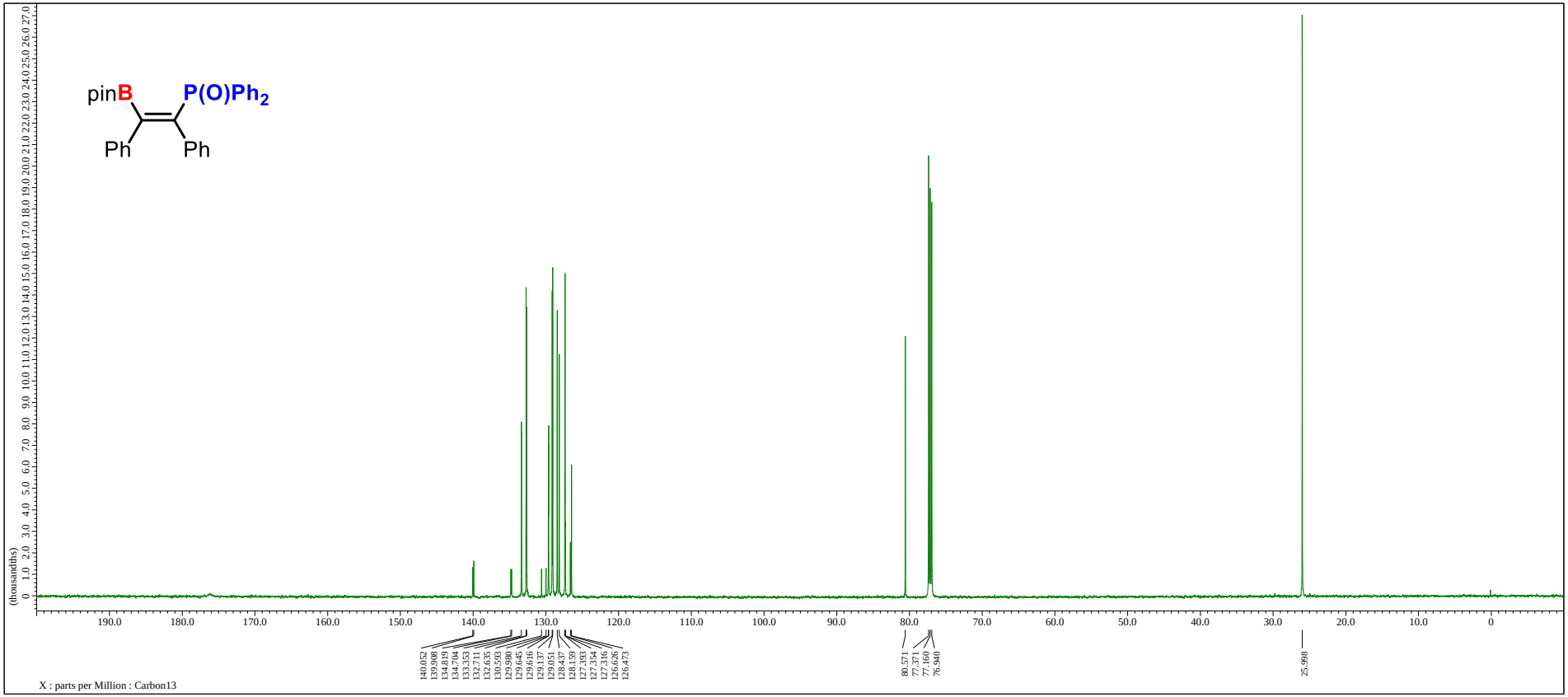

Figure S61. ^{13}C NMR (151 MHz, $CDCl_3$) spectrum of **2ak**.

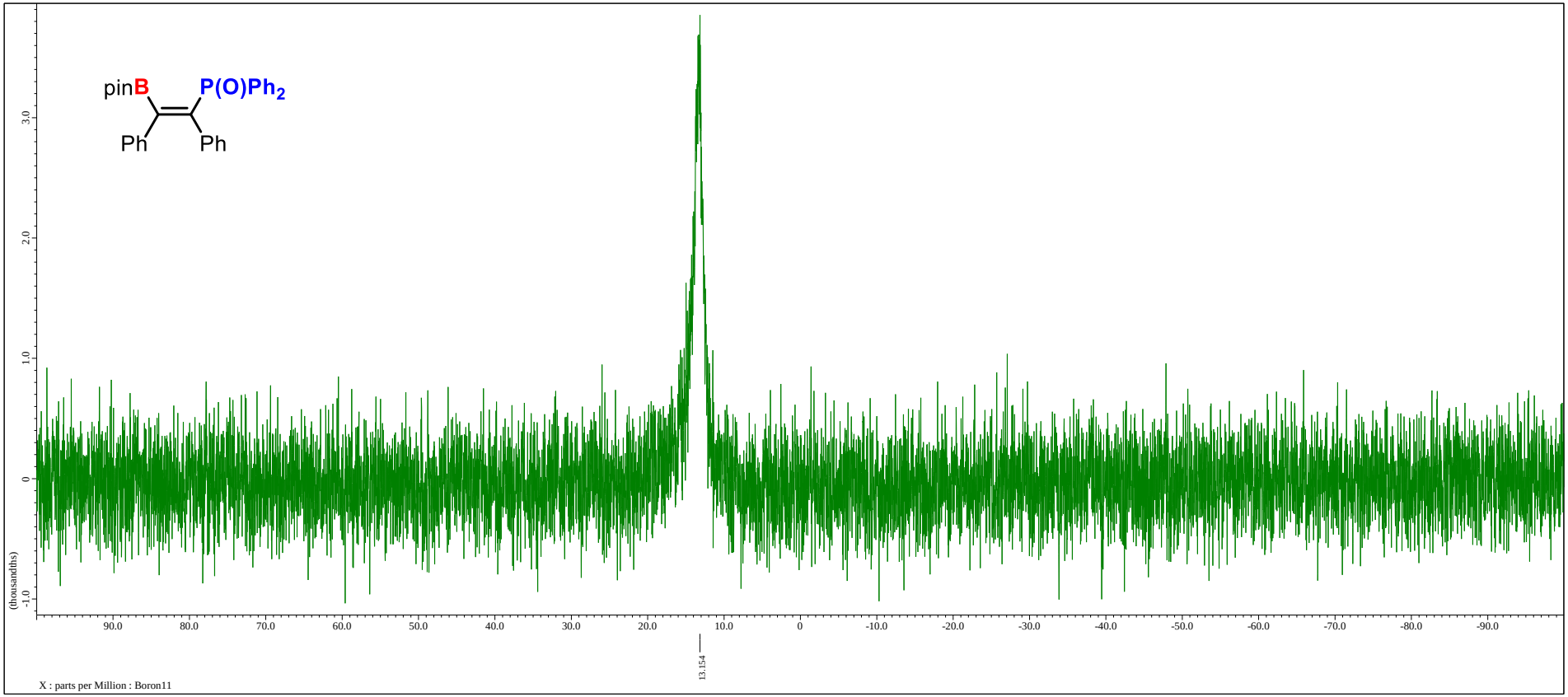

Figure S62. ^{11}B NMR (192 MHz, $CDCl_3$) spectrum of **2ak**.

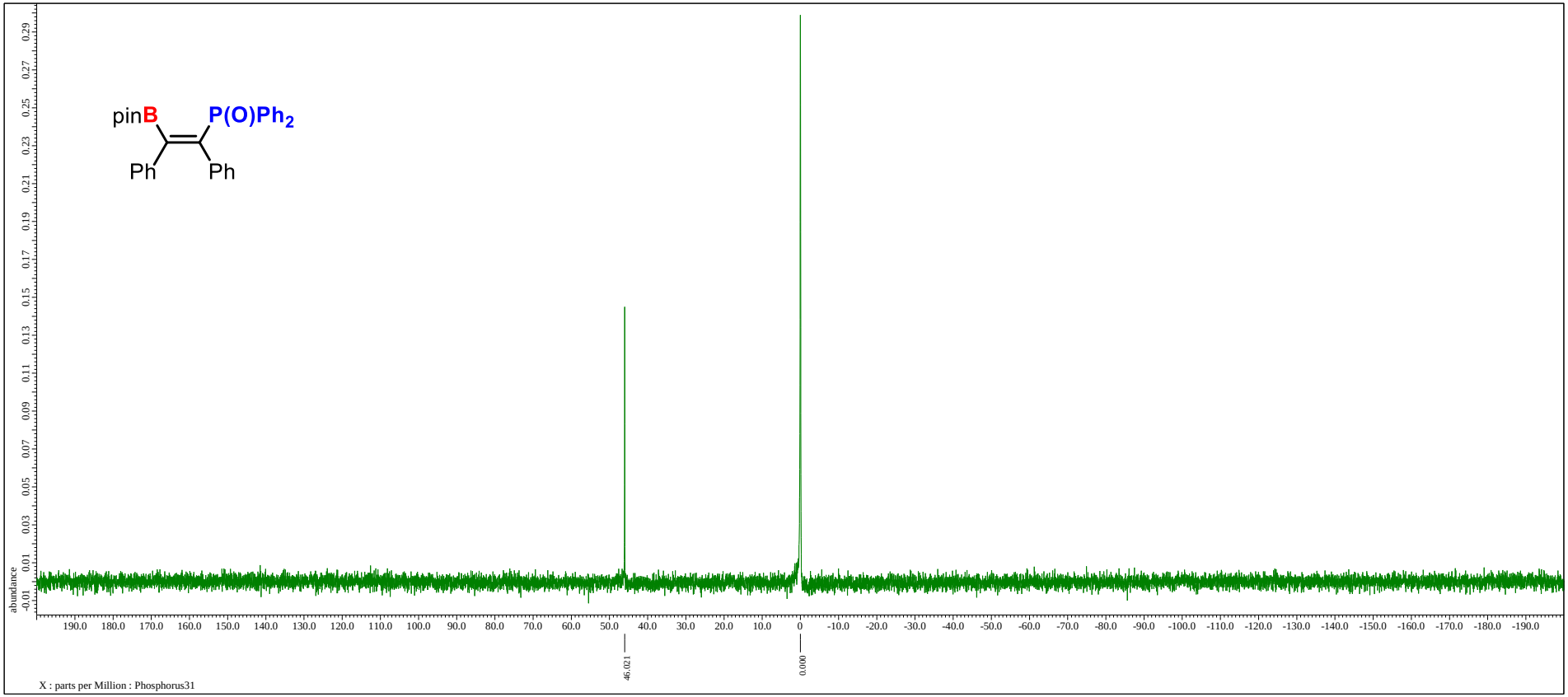

Figure S63. ^{31}P NMR (243 MHz, $CDCl_3$) spectrum of **2ak**.

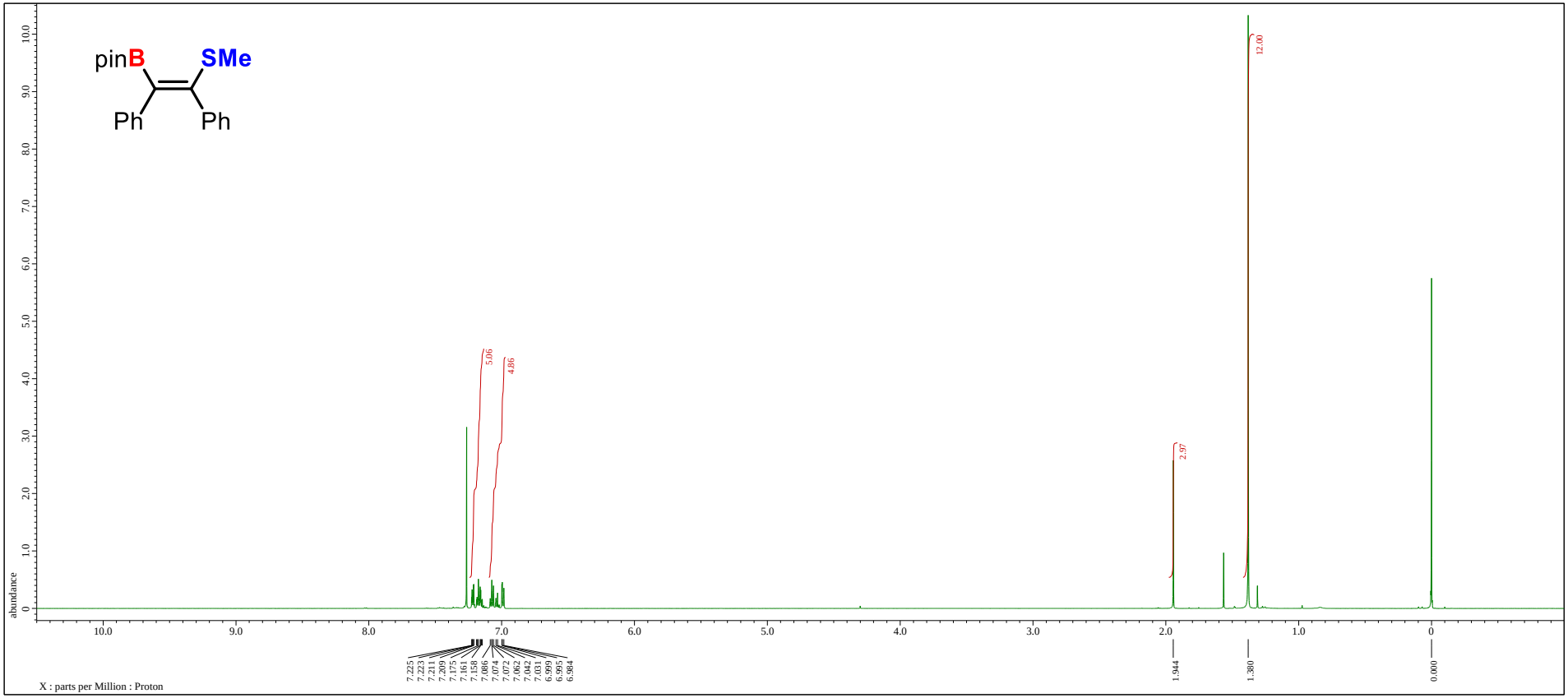

Figure S64. ^{1}H NMR (600 MHz, $CDCl_3$) spectrum of **2al**.

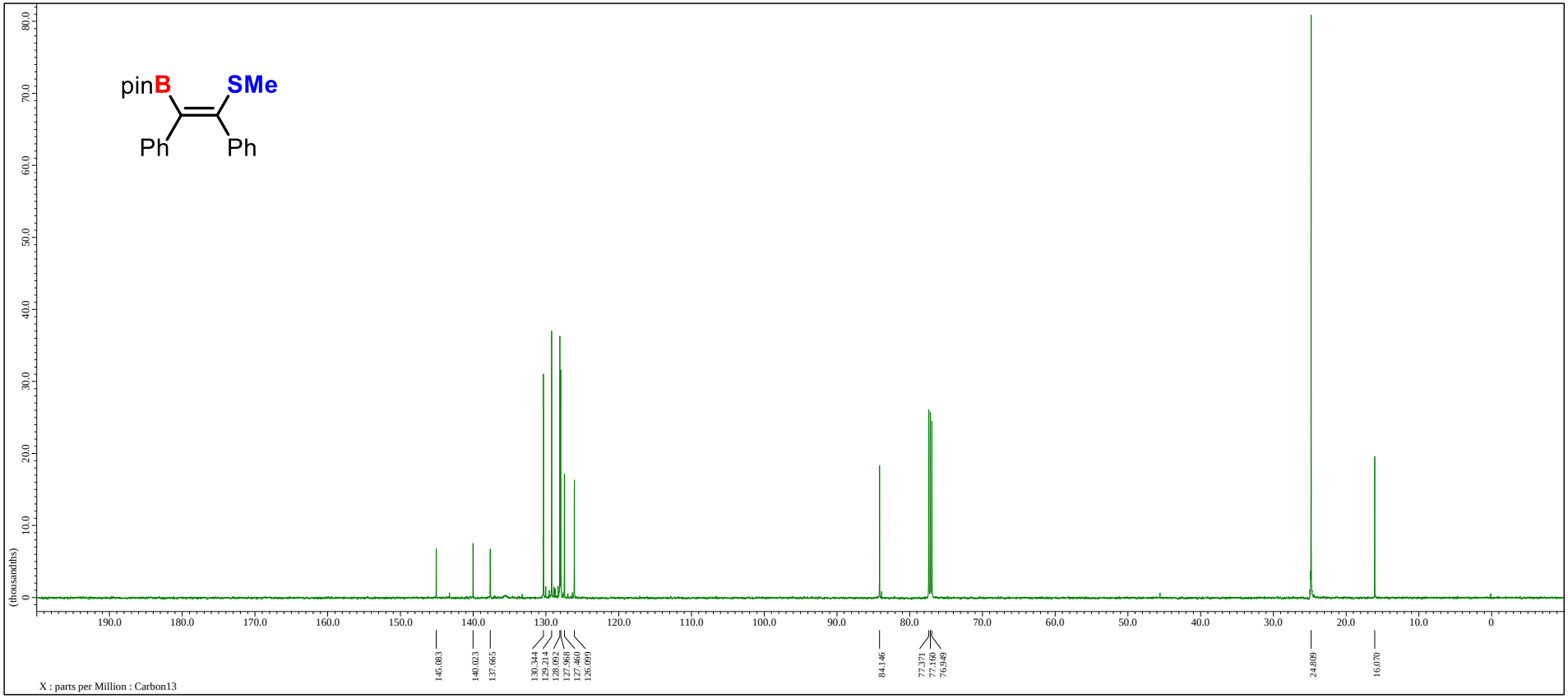

Figure S65. ^{13}C NMR (151 MHz, $CDCl_3$) spectrum of **2al**.

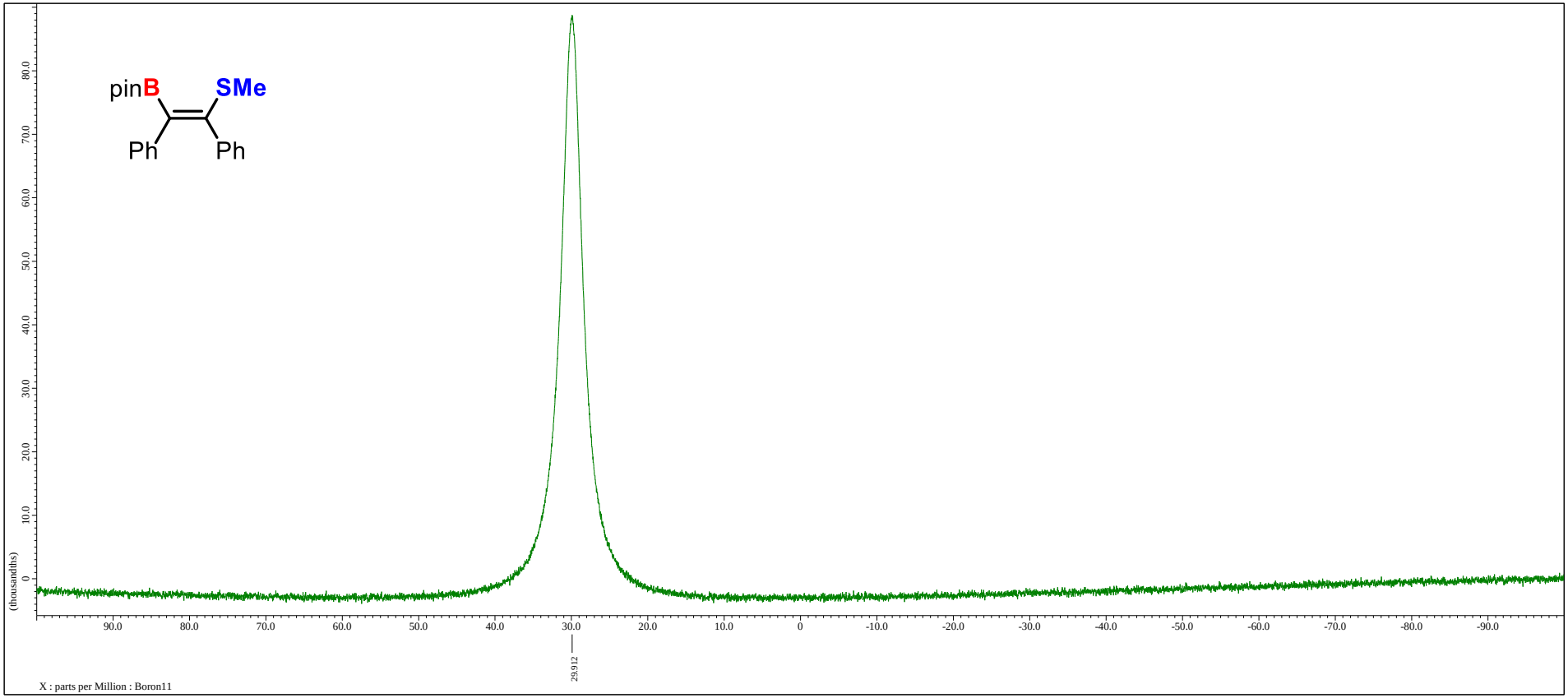

Figure S66. ^{11}B NMR (192 MHz, $CDCl_3$) spectrum of **2al**.

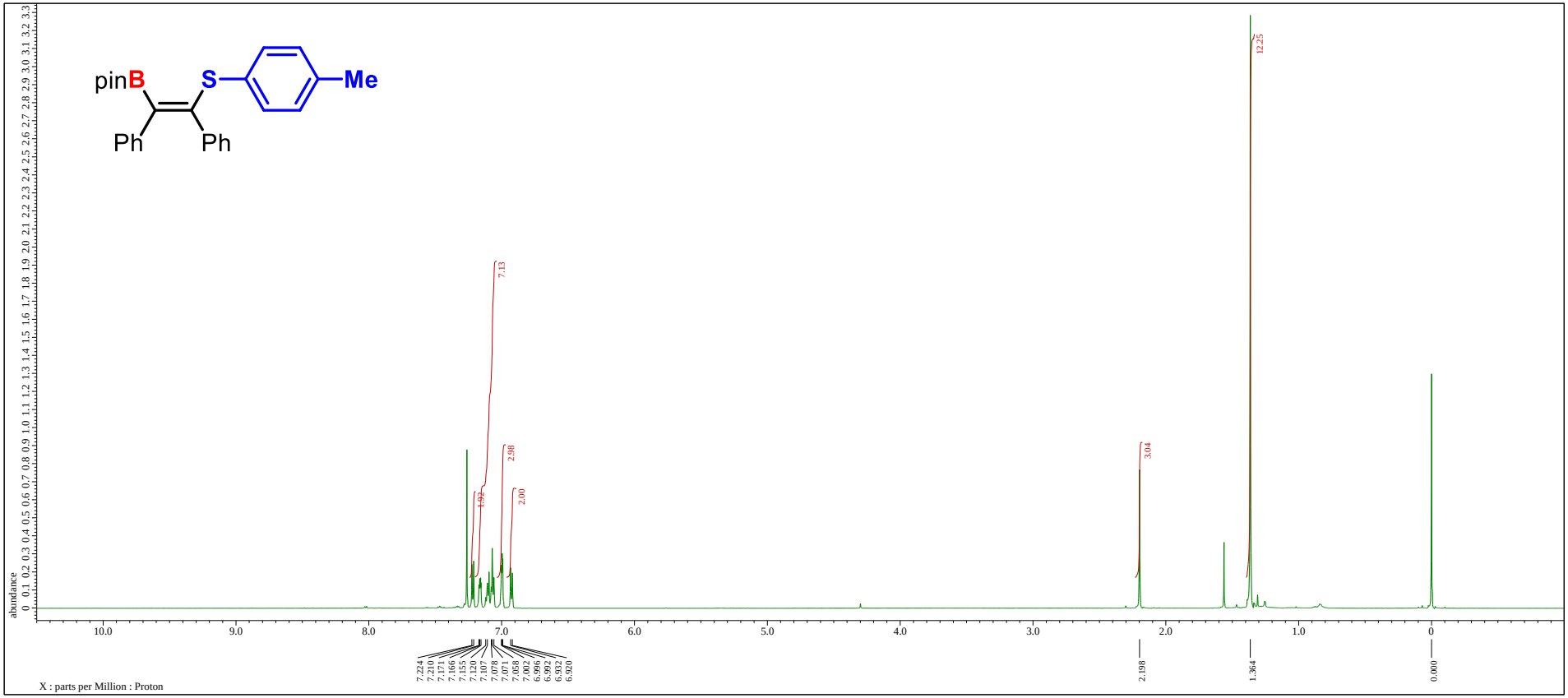

Figure S67. ^{1}H NMR (600 MHz, $CDCl_3$) spectrum of **2am**.

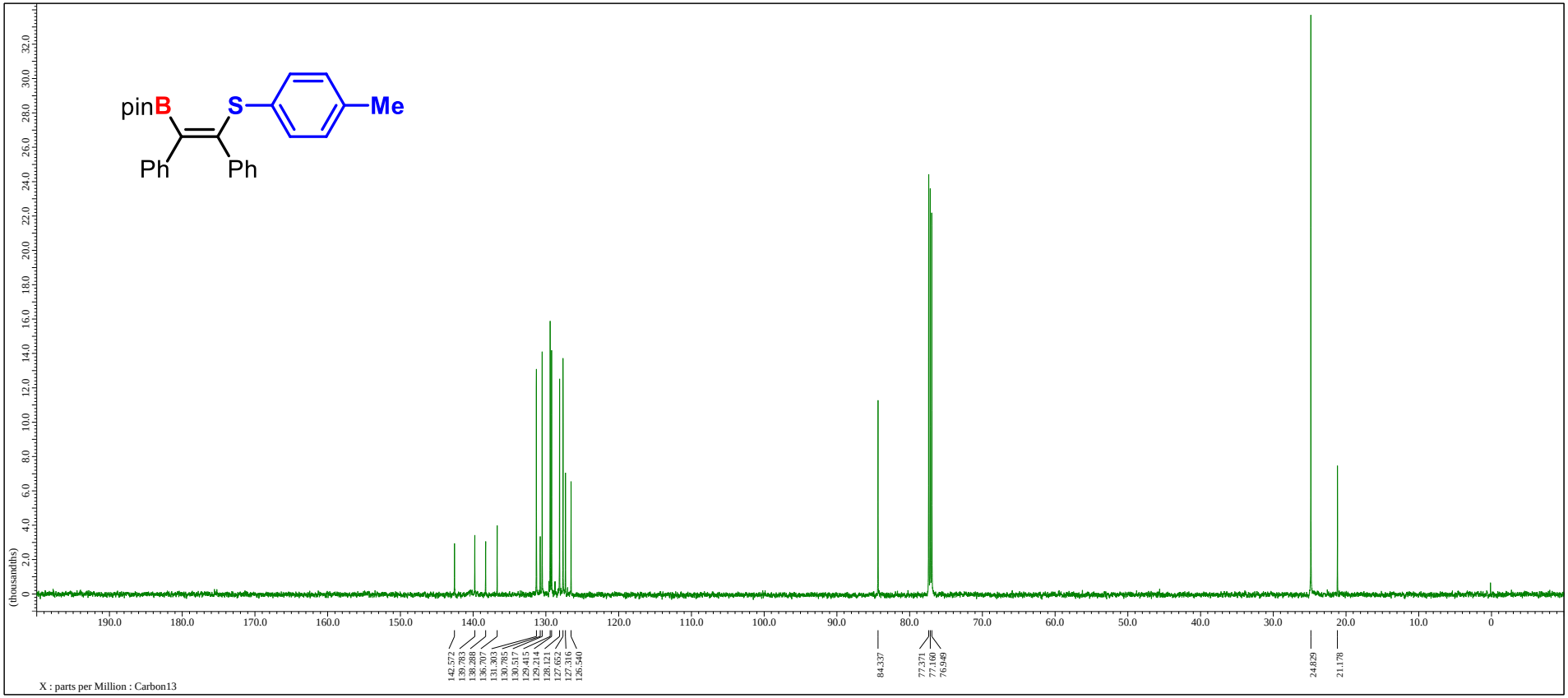

Figure S68. ^{13}C NMR (151 MHz, $CDCl_3$) spectrum of **2am.**

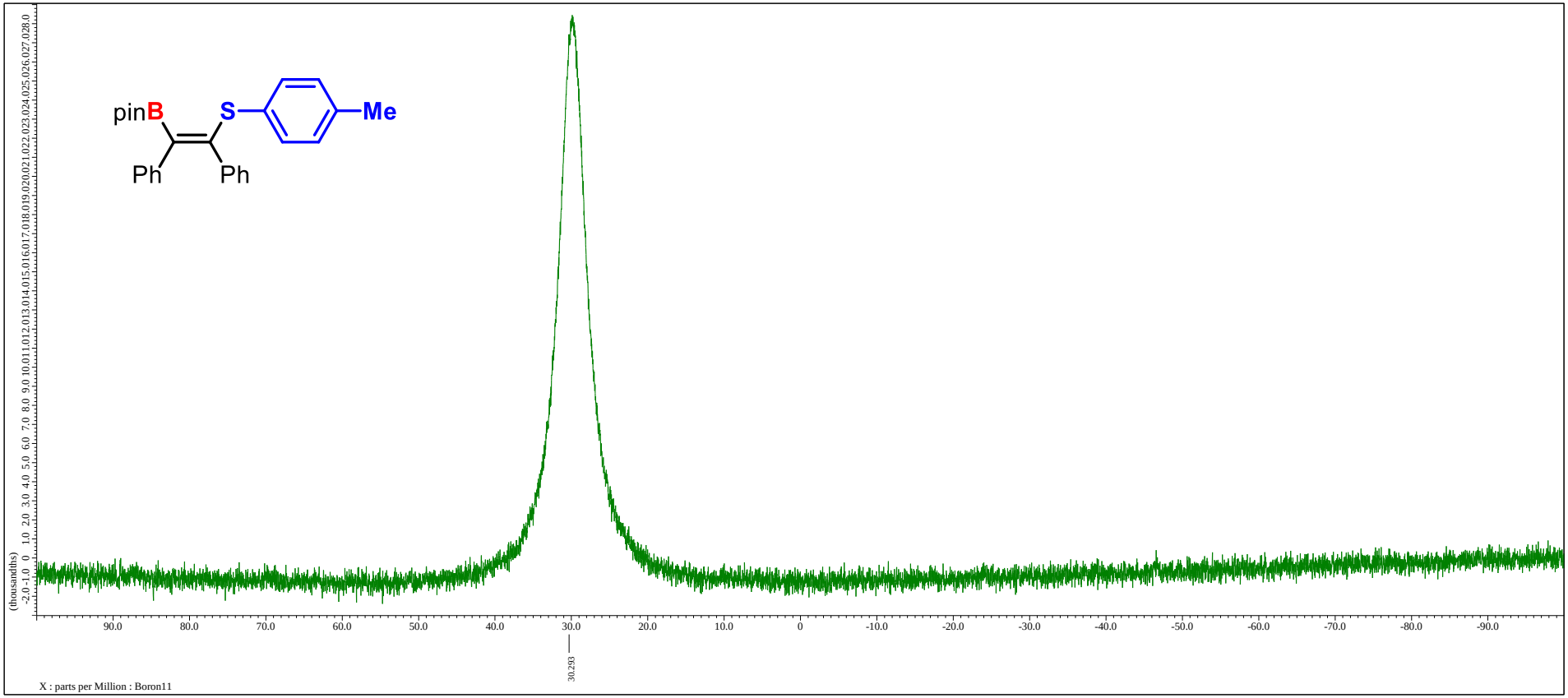

Figure S69. ^{11}B NMR (192 MHz, $CDCl_3$) spectrum of **2am**.

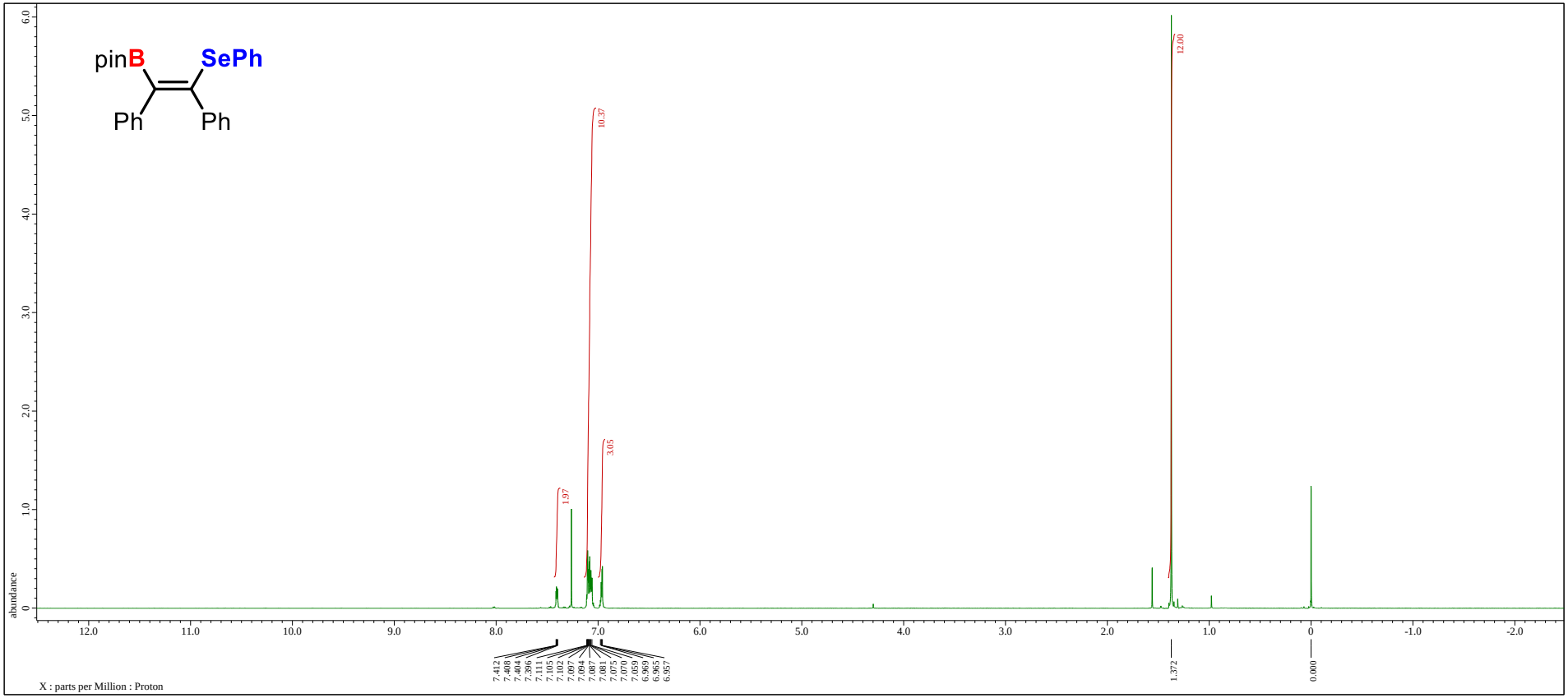

Figure S70. ^{1}H NMR (600 MHz, $CDCl_3$) spectrum of **2an**.

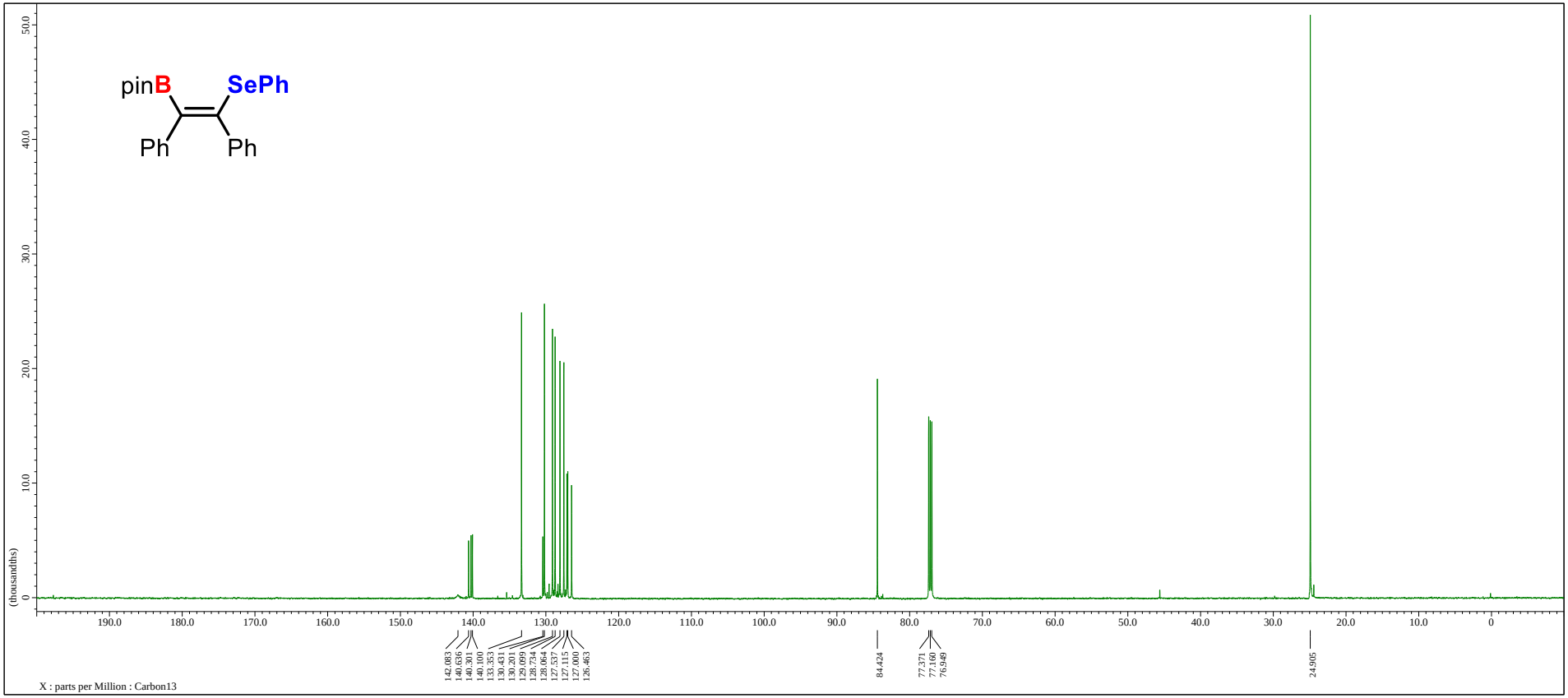

Figure S71. ^{13}C NMR (151 MHz, $CDCl_3$) spectrum of **2an**.

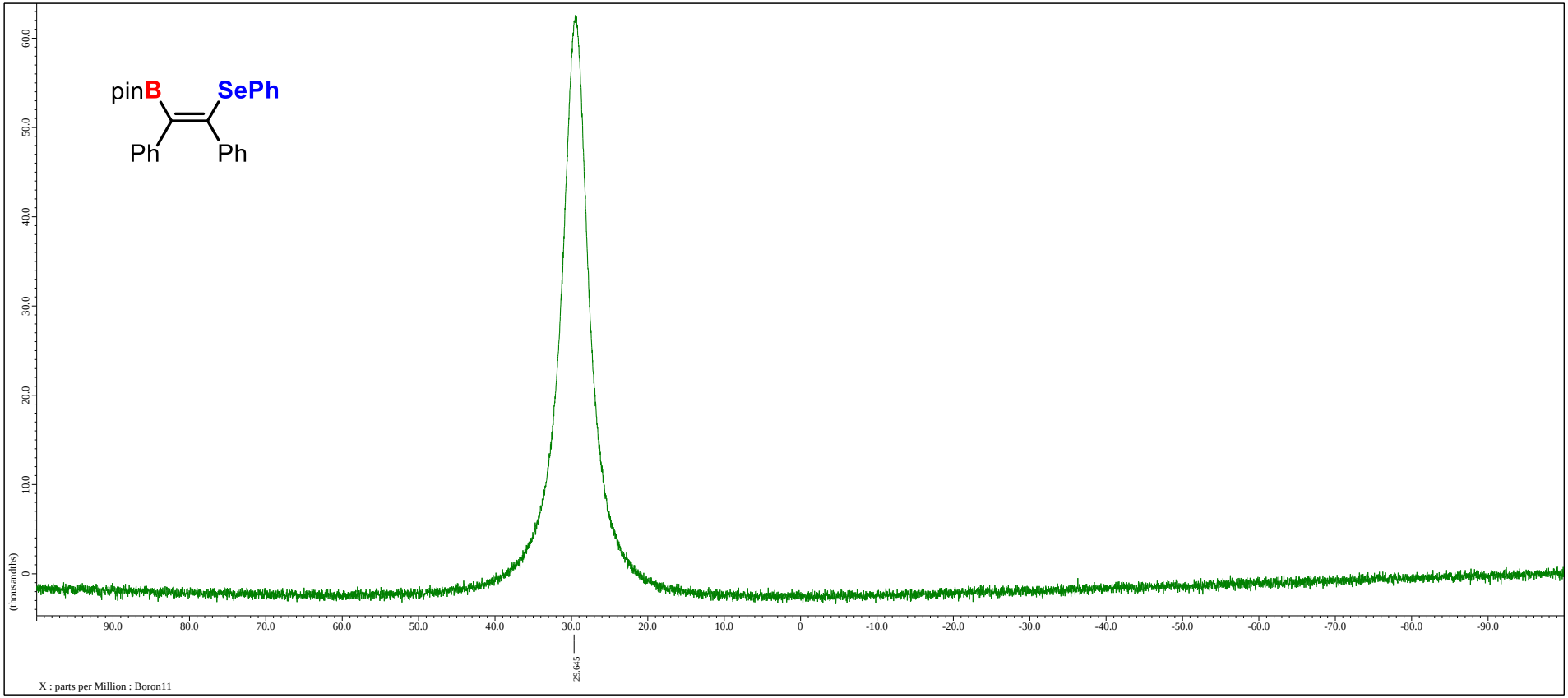

Figure S72. ^{11}B NMR (192 MHz, $CDCl_3$) spectrum of **2an**.

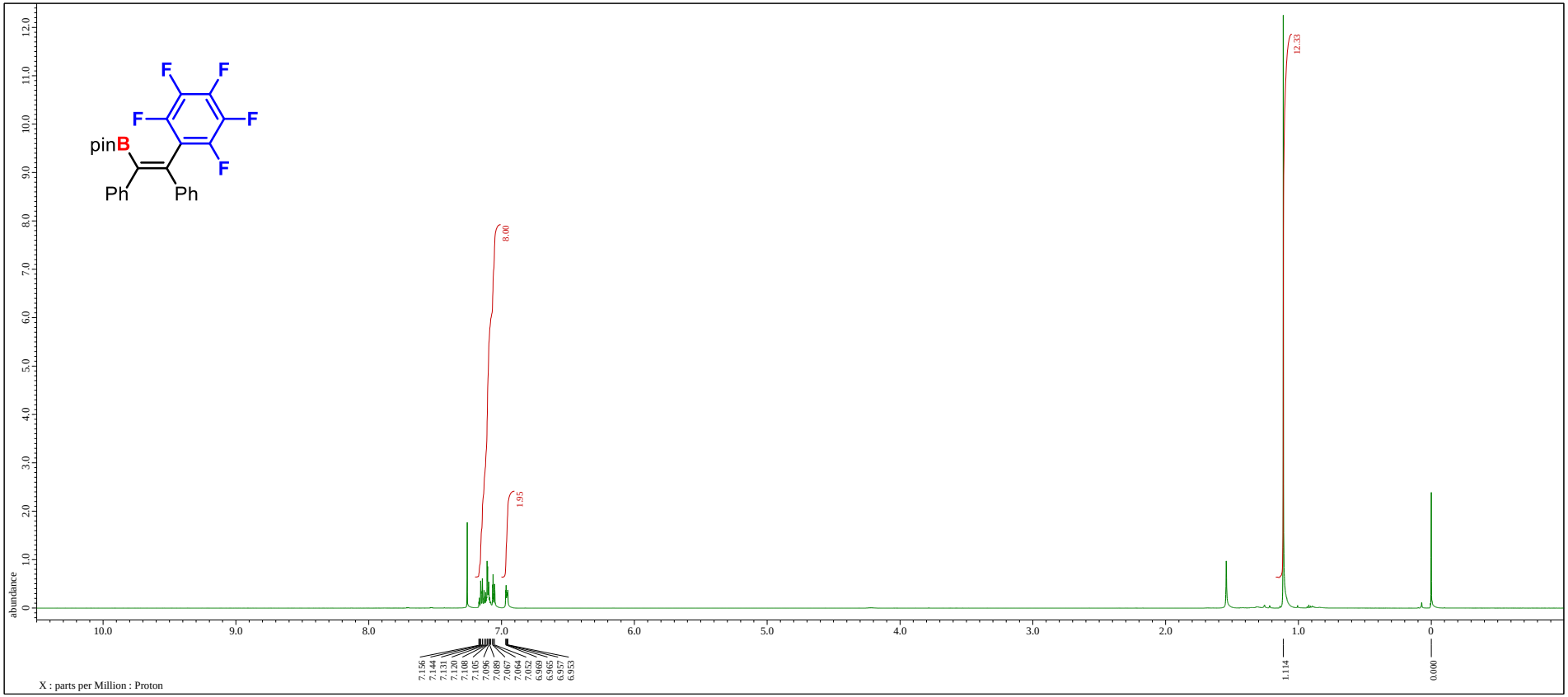

Figure S73. ^{1}H NMR (600 MHz, $CDCl_3$) spectrum of **2ao**.

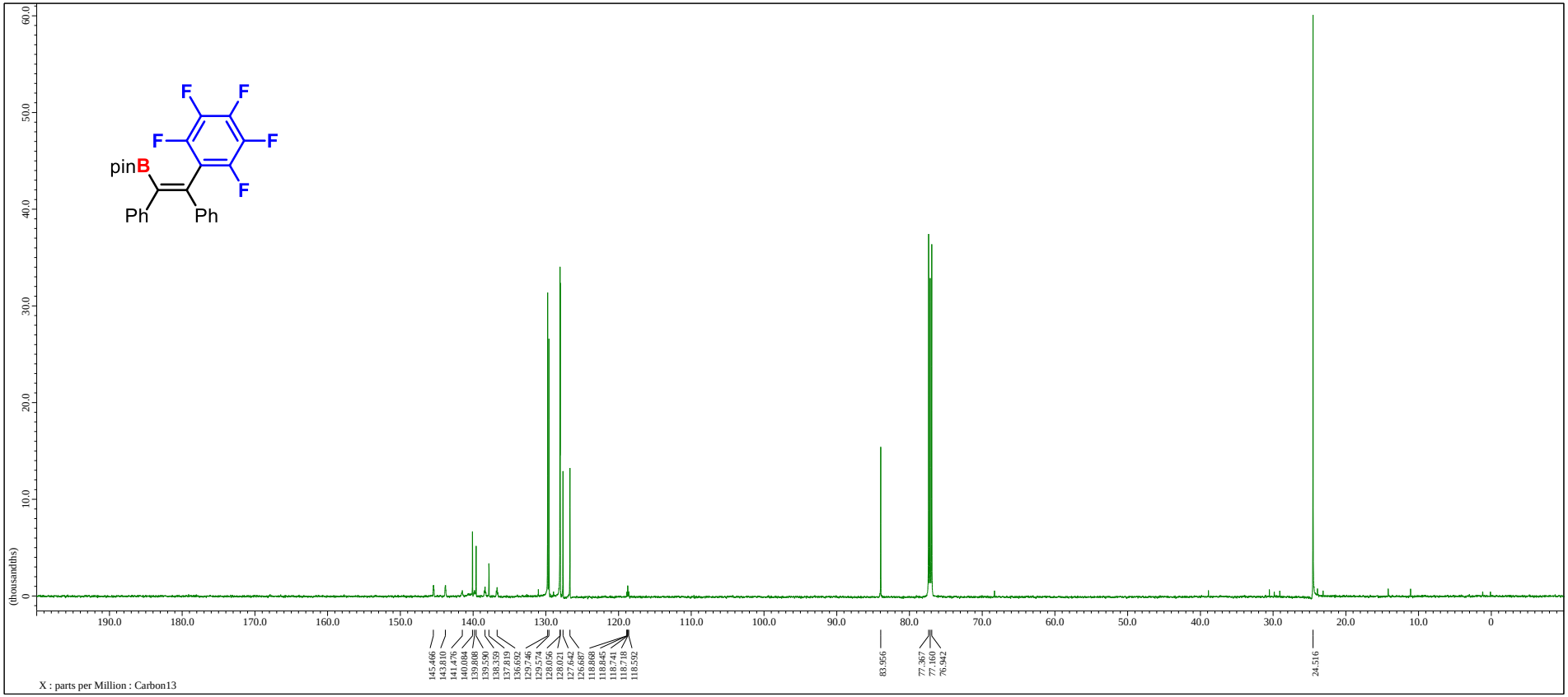

Figure S74. ^{13}C NMR (151 MHz, $CDCl_3$) spectrum of **2ao**.

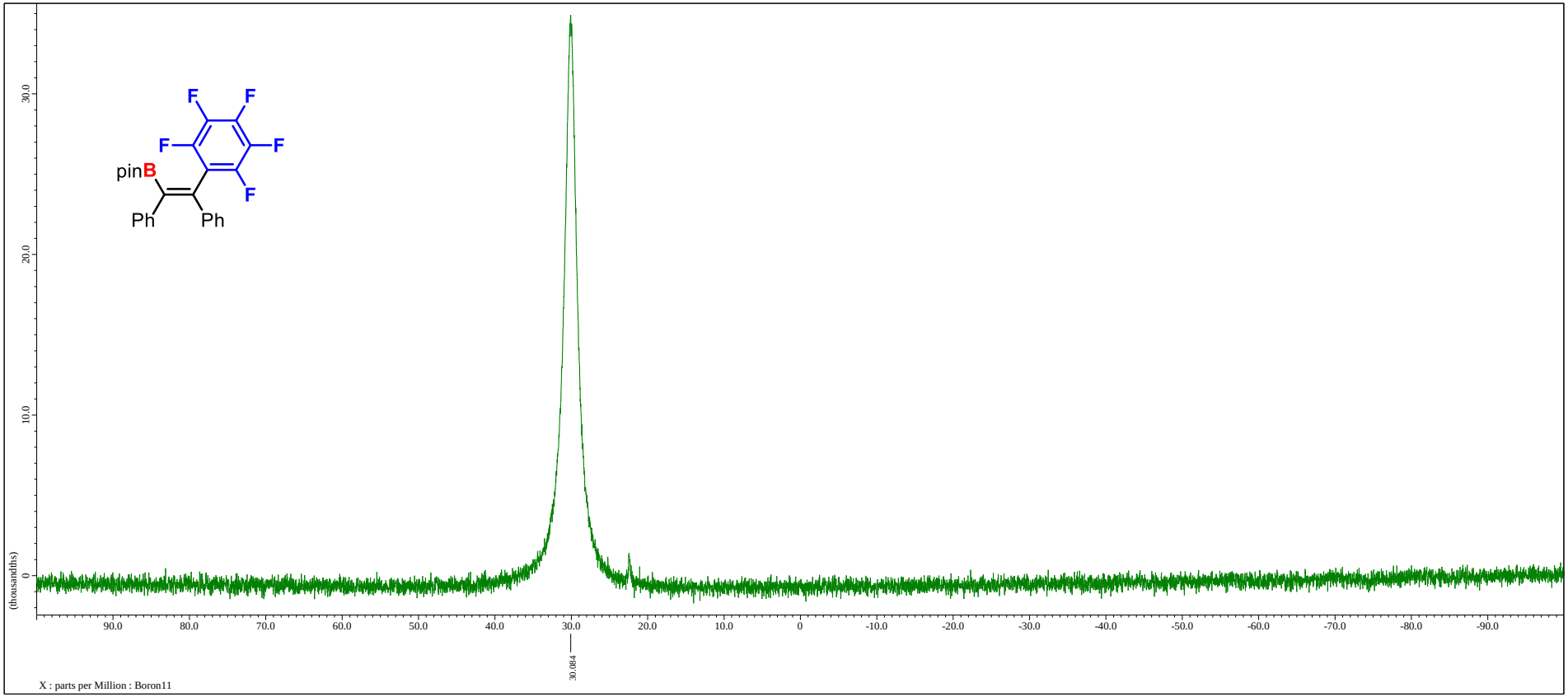

Figure S75. ^{11}B NMR (192 MHz, $CDCl_3$) spectrum of **2ao**.

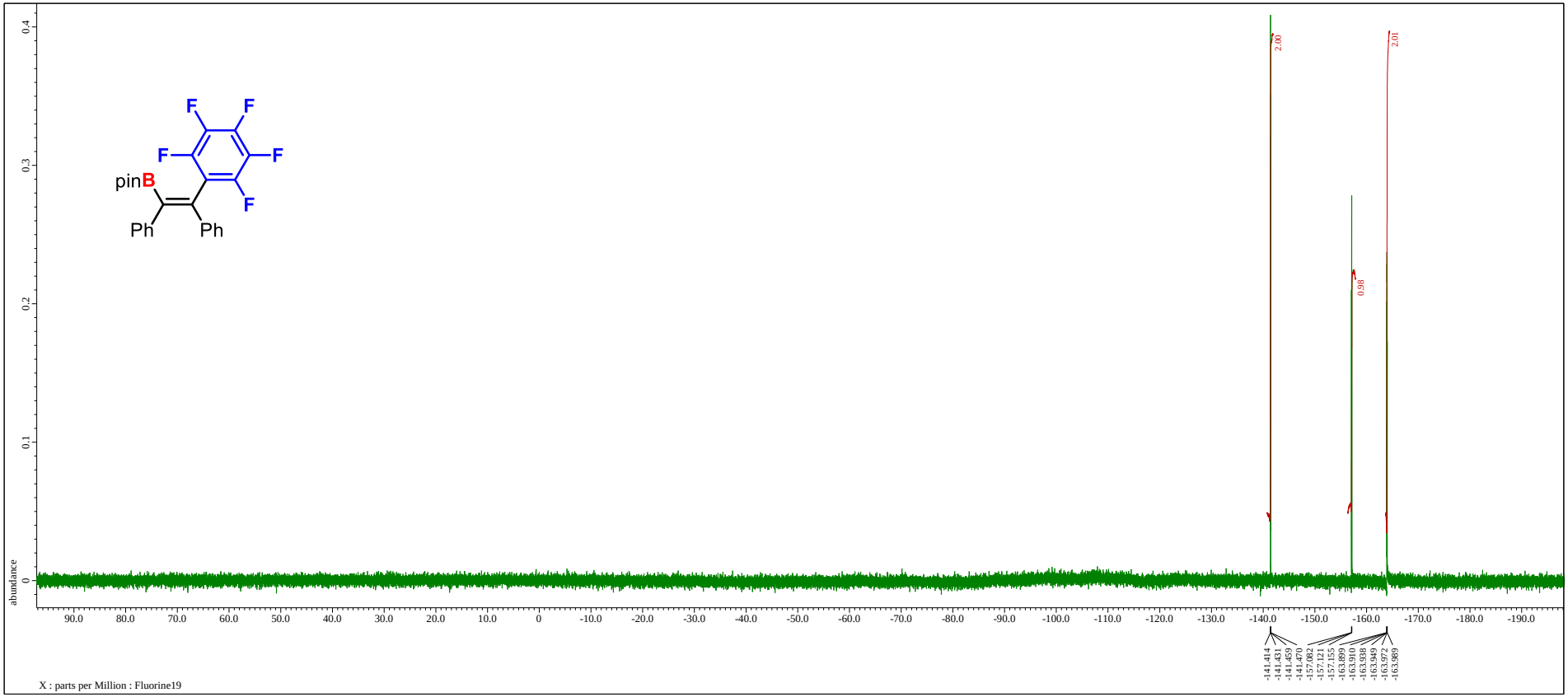

Figure S76. ^{19}F NMR (564 MHz, $CDCl_3$) spectrum of **2ao**.

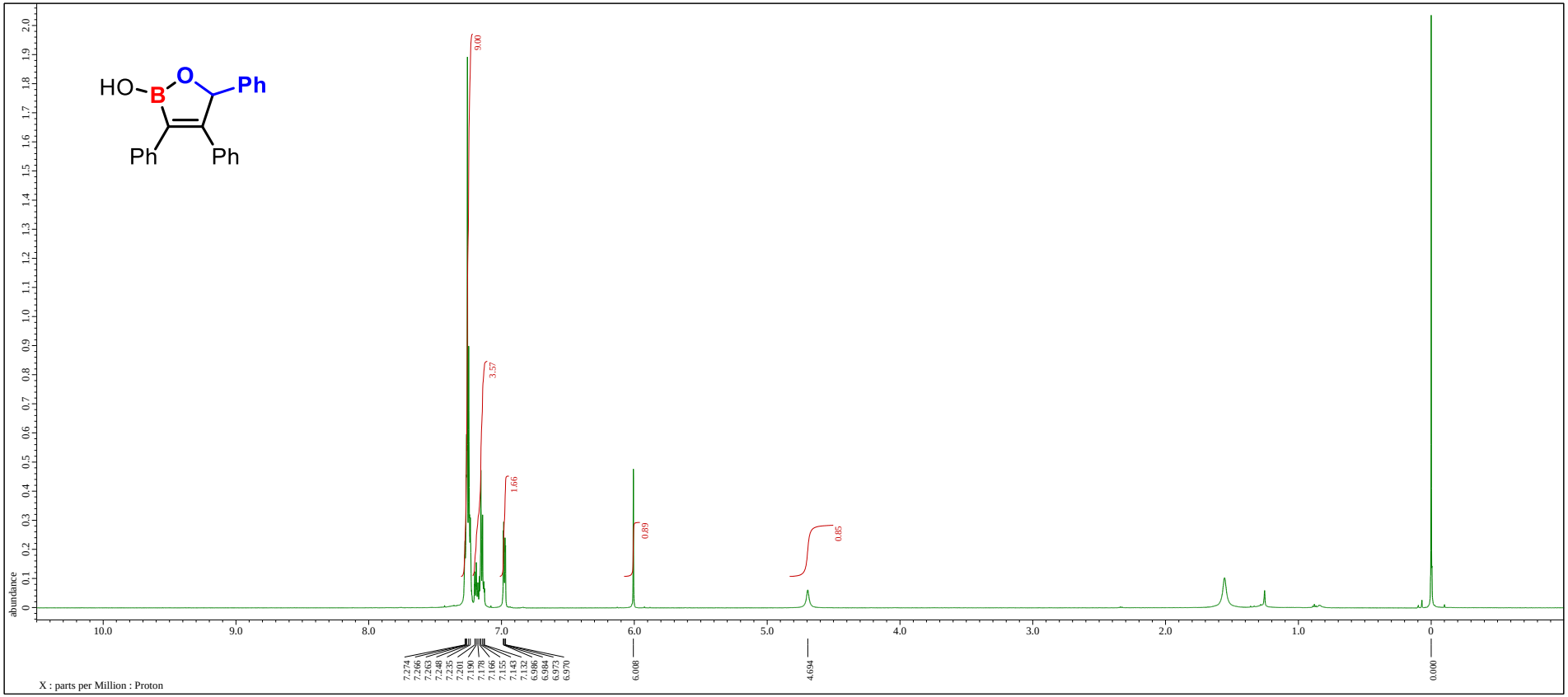

Figure S77. ^{1}H NMR (600 MHz, $CDCl_3$) spectrum of **2ap**.

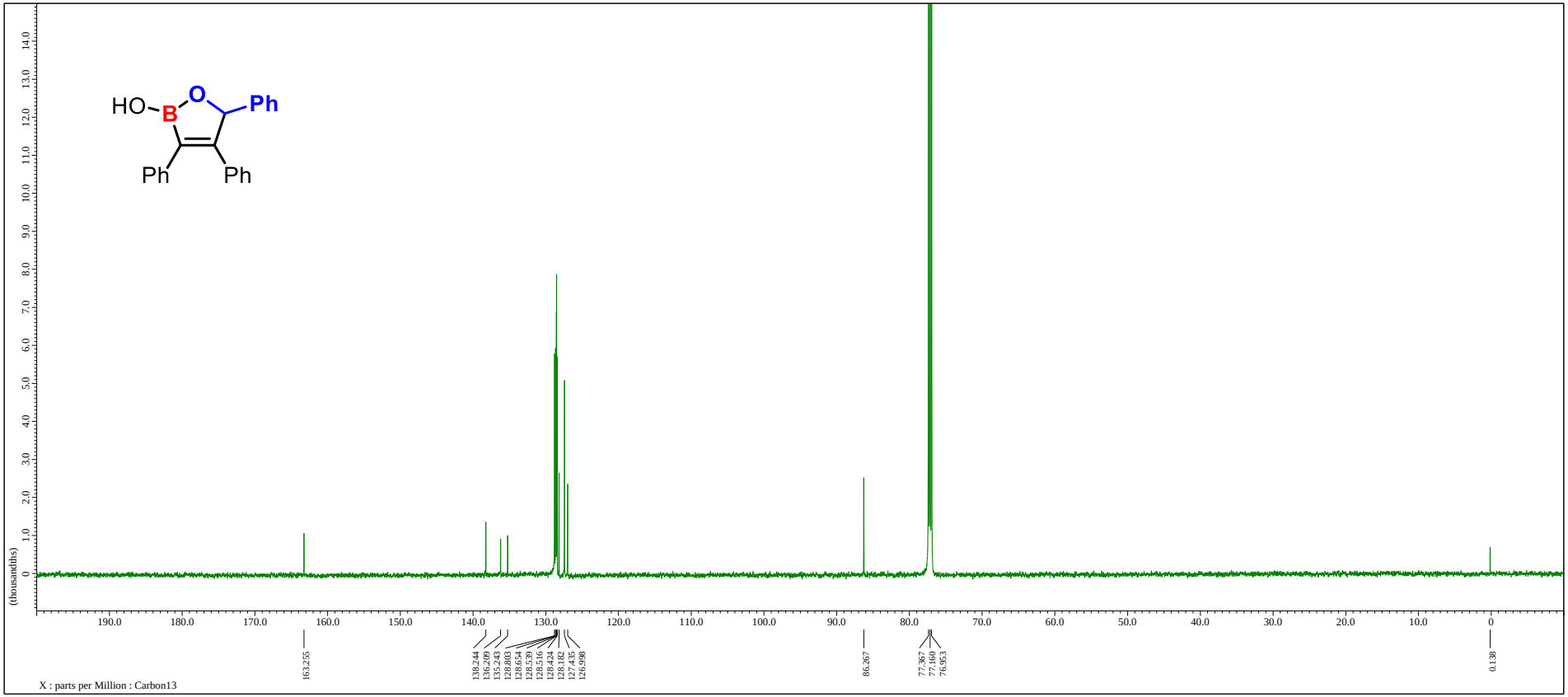

Figure S78. ^{13}C NMR (151 MHz, $CDCl_3$) spectrum of **2ap**.

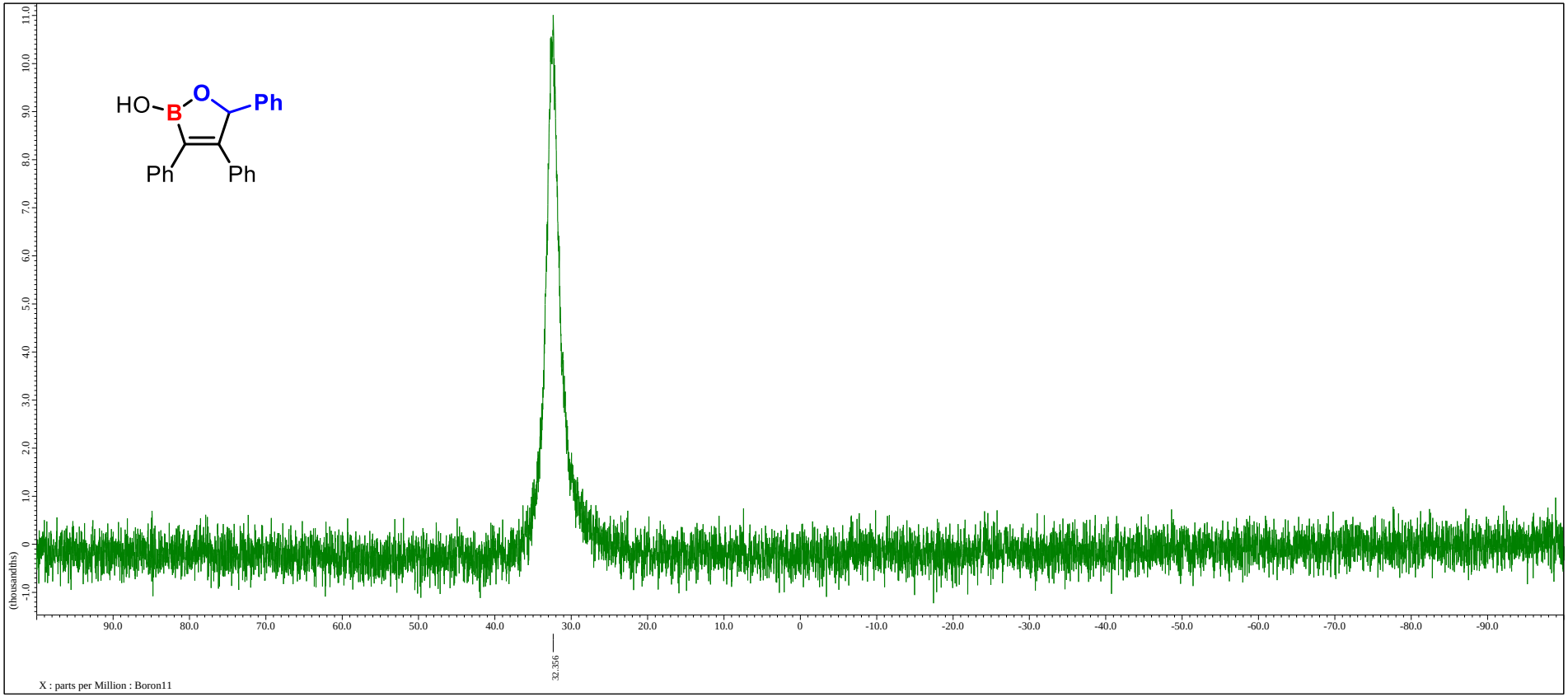

Figure S79. ^{11}B NMR (192 MHz, $CDCl_3$) spectrum of **2ap**.

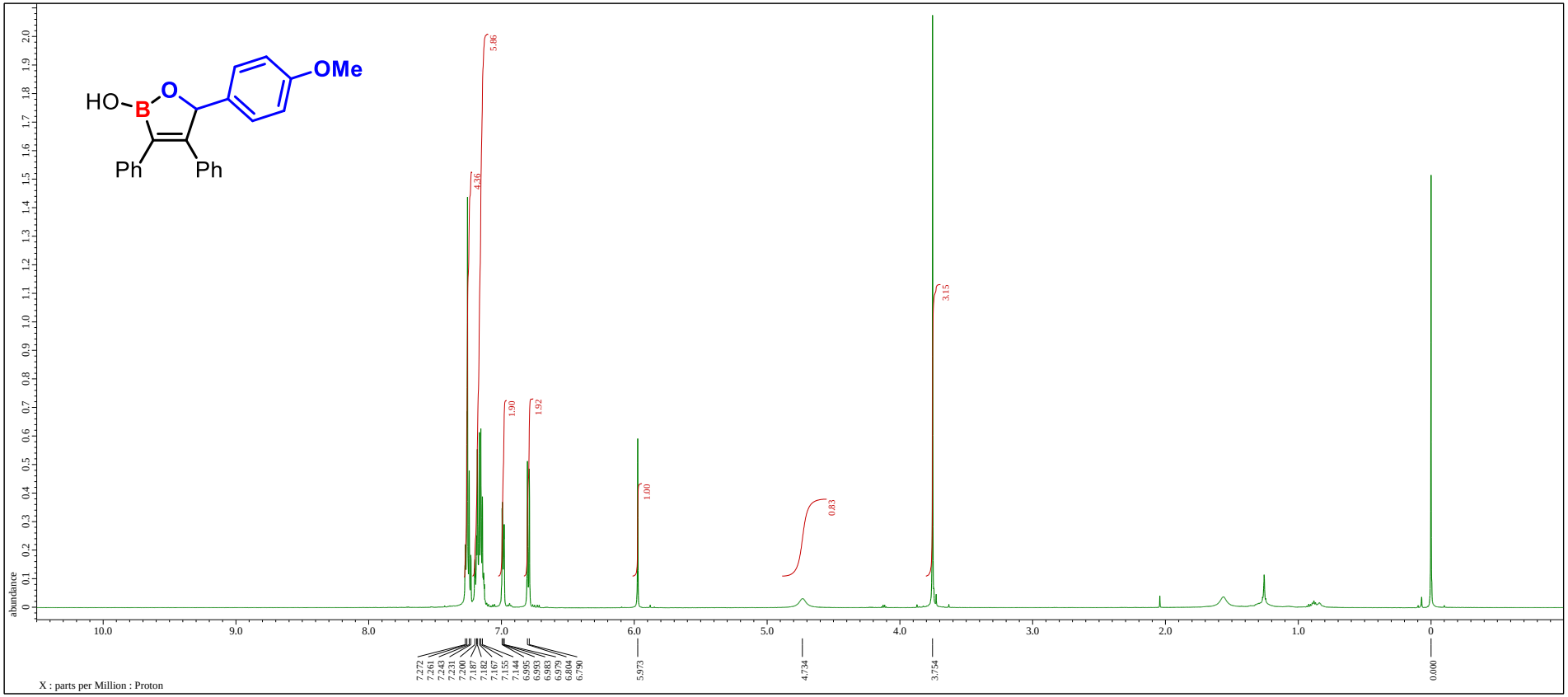

Figure S80. ^{1}H NMR (600 MHz, $CDCl_3$) spectrum of **2aq**.

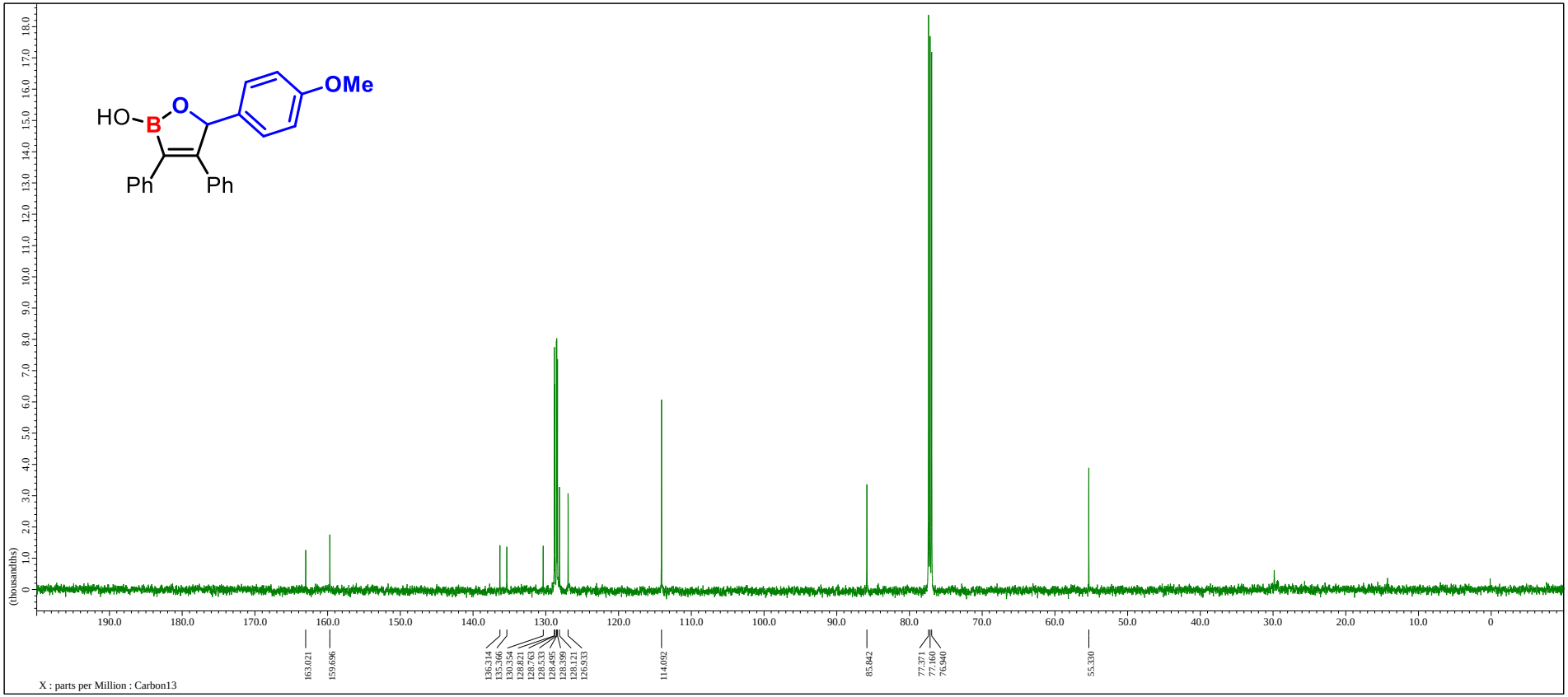

Figure S81. ^{13}C NMR (151 MHz, $CDCl_3$) spectrum of **2aq**.

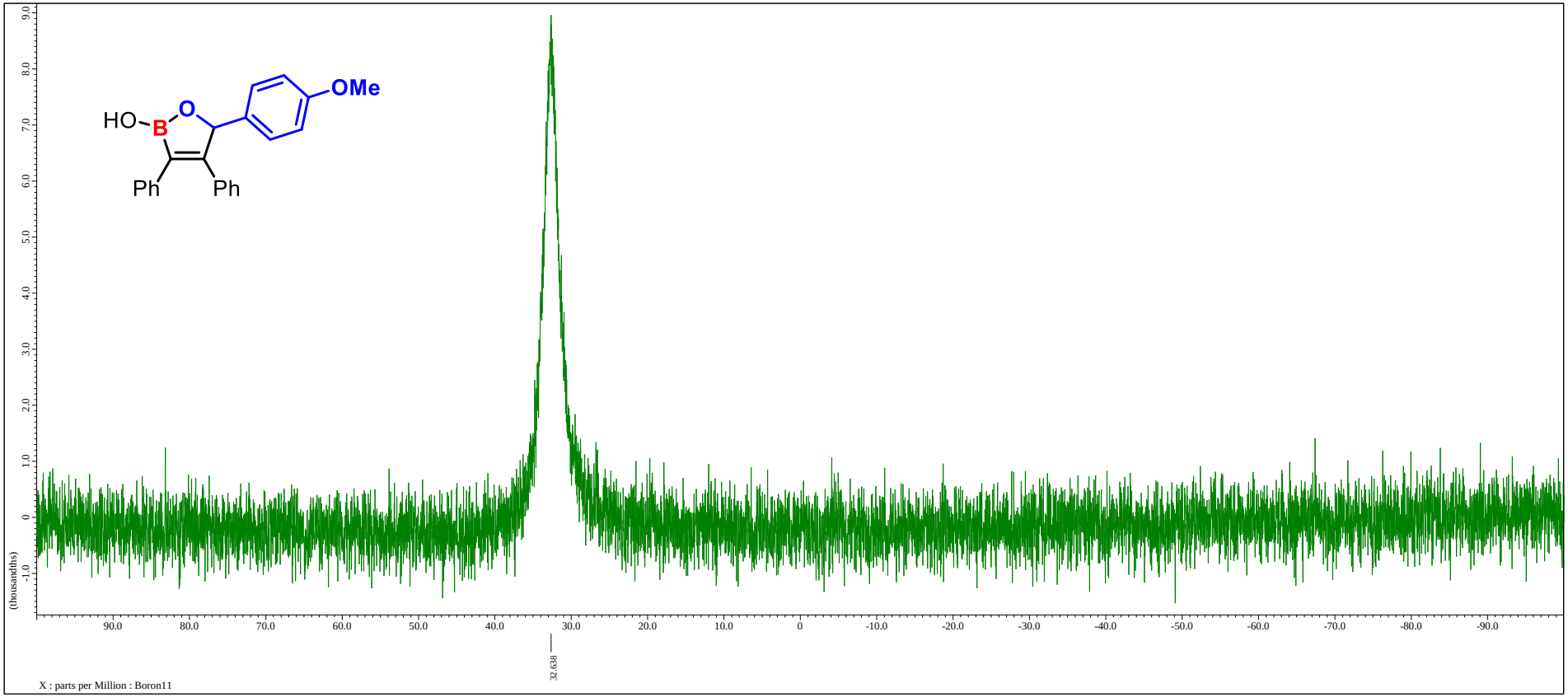

Figure S82. ^{11}B NMR (192 MHz, $CDCl_3$) spectrum of **2aq**.

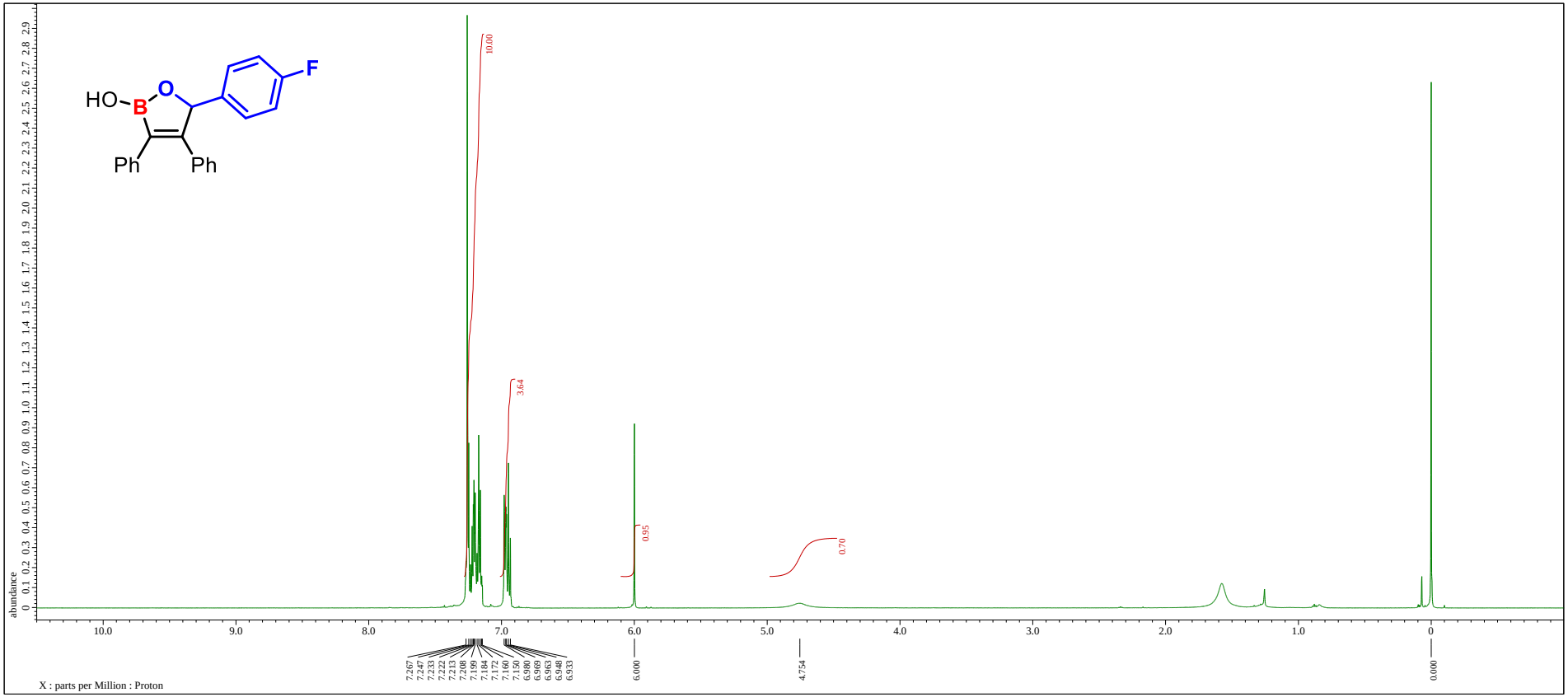

Figure S83. ^{1}H NMR (600 MHz, $CDCl_3$) spectrum of **2ar**.

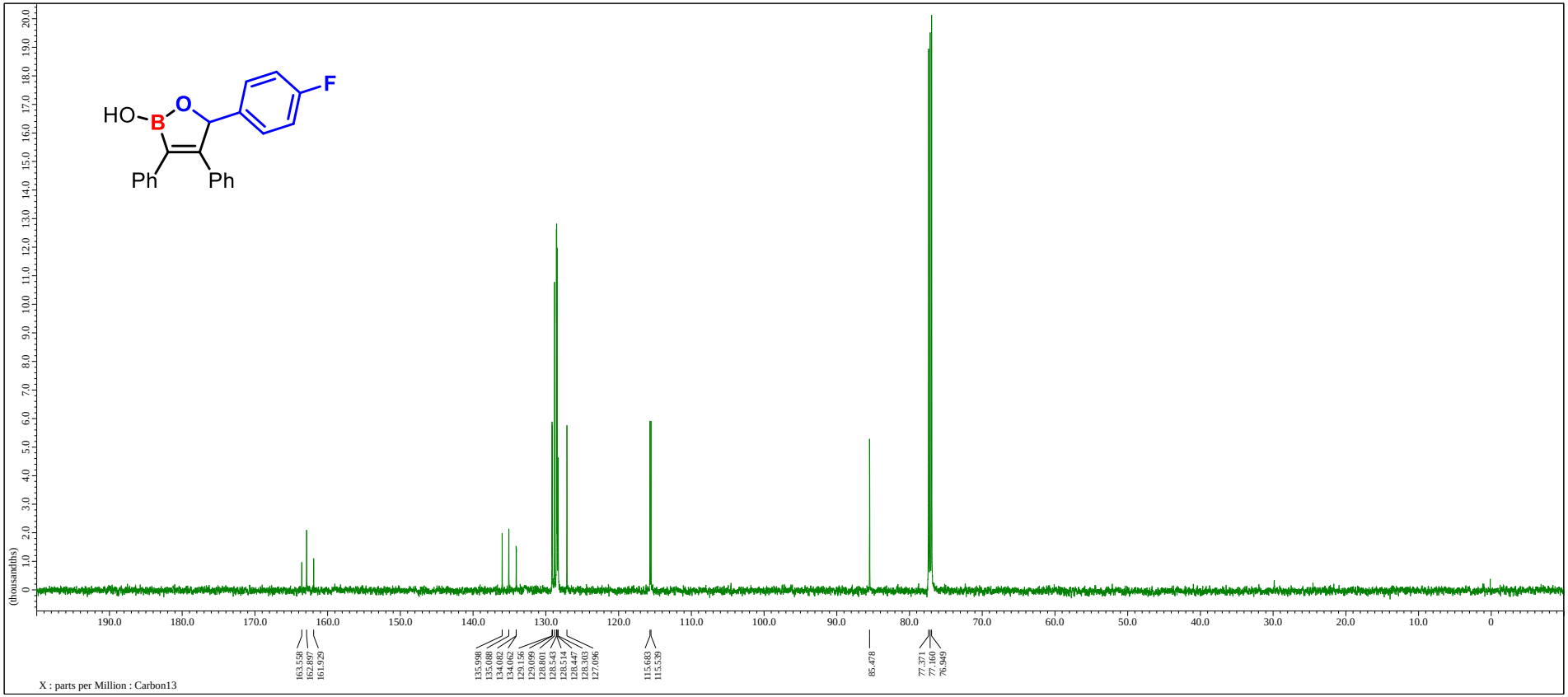

Figure S84. ^{13}C NMR (151 MHz, $CDCl_3$) spectrum of **2ar**.

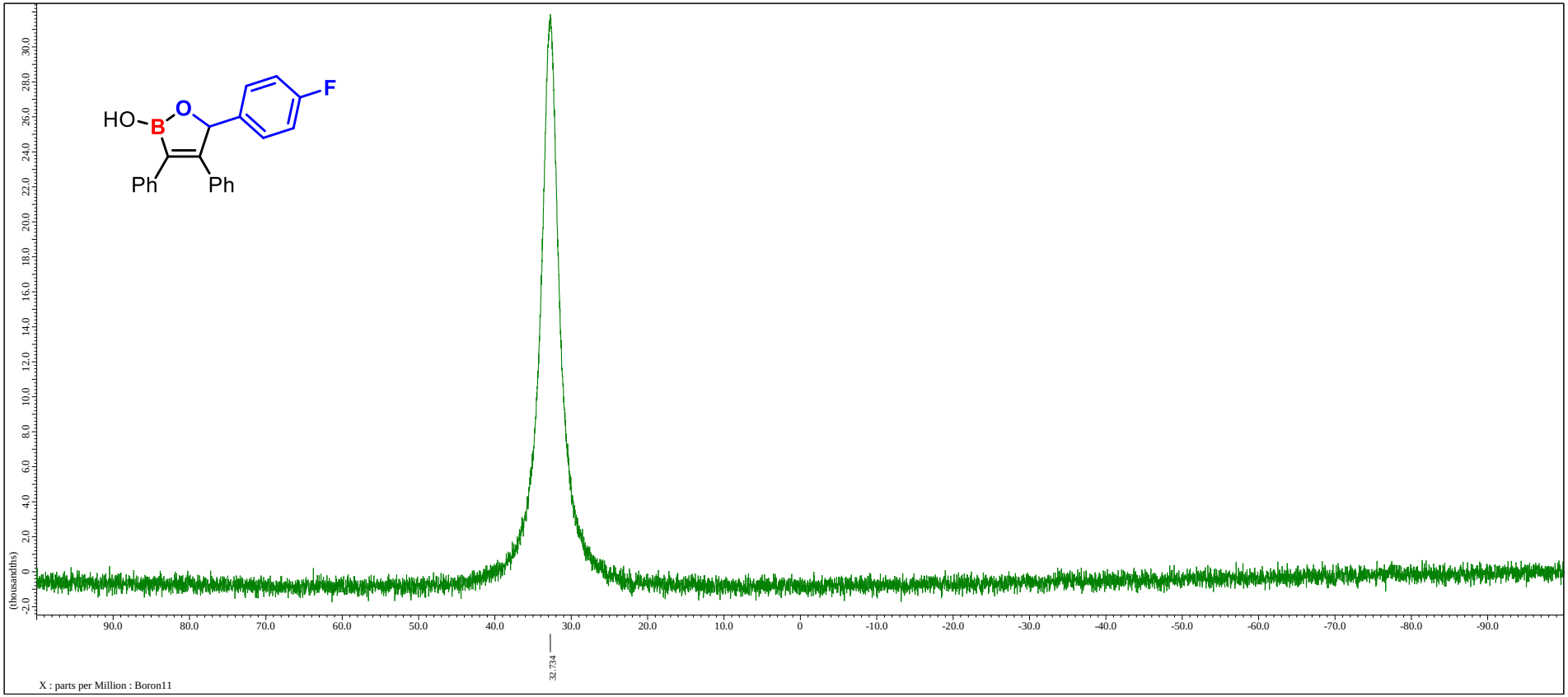

Figure S85. ^{11}B NMR (192 MHz, $CDCl_3$) spectrum of **2ar**.

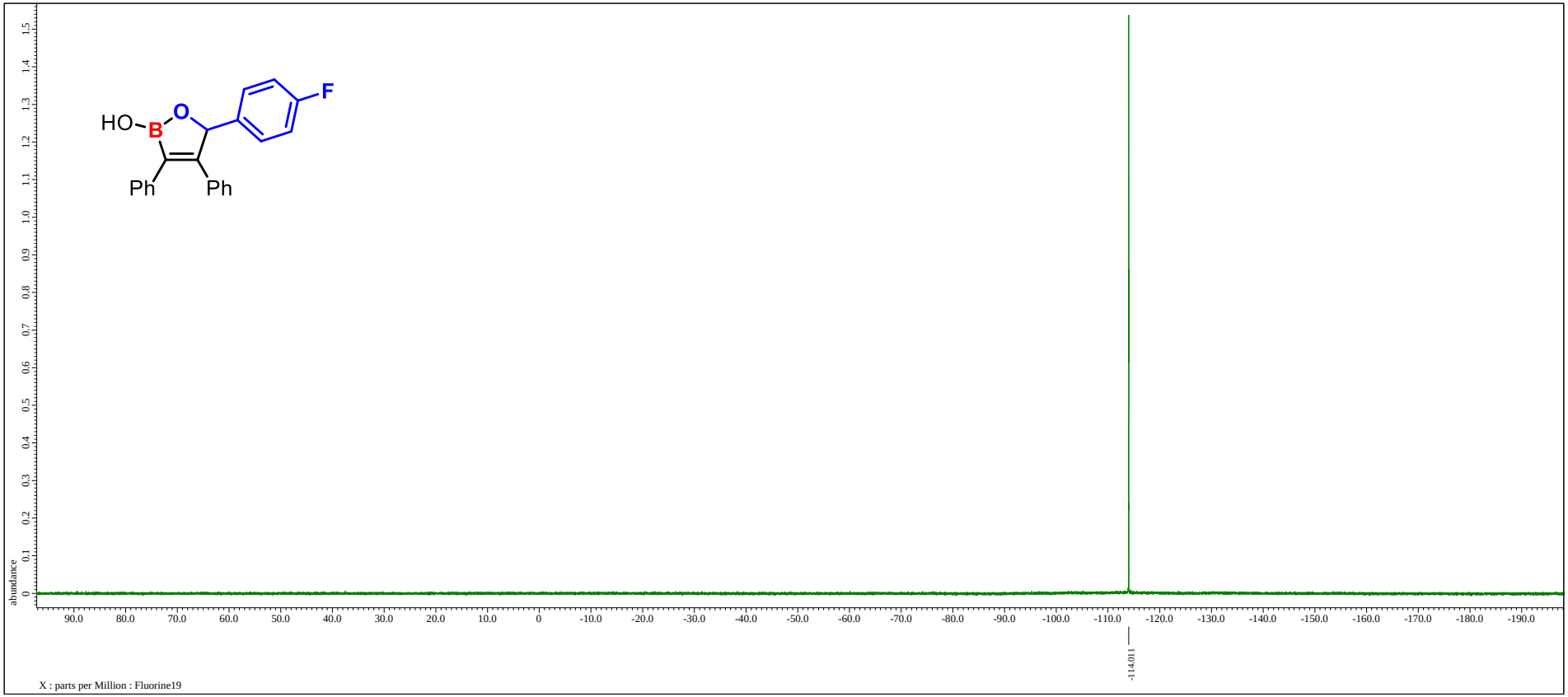

Figure S86. ^{19}F NMR (564 MHz, $CDCl_3$) spectrum of **2ar**.

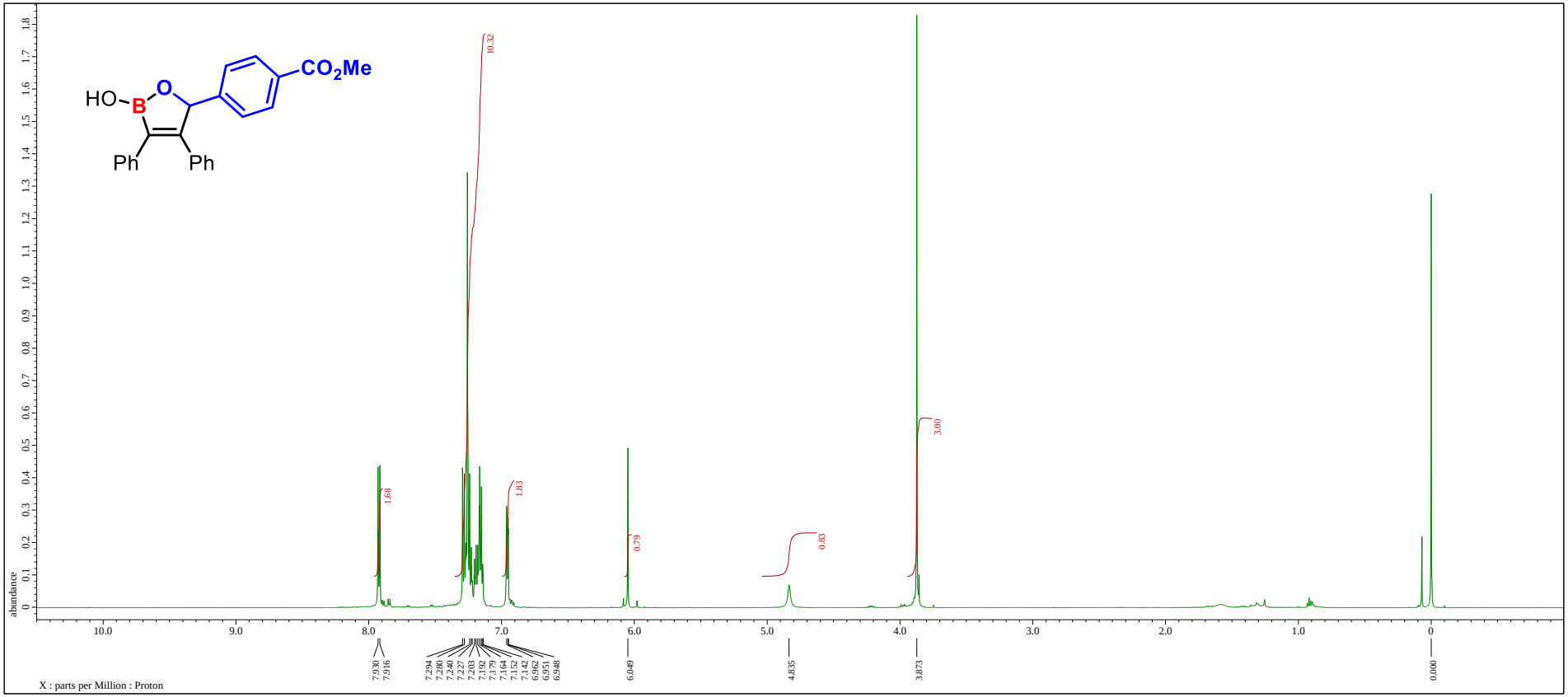

Figure S87. ^{1}H NMR (600 MHz, $CDCl_3$) spectrum of **2as**.

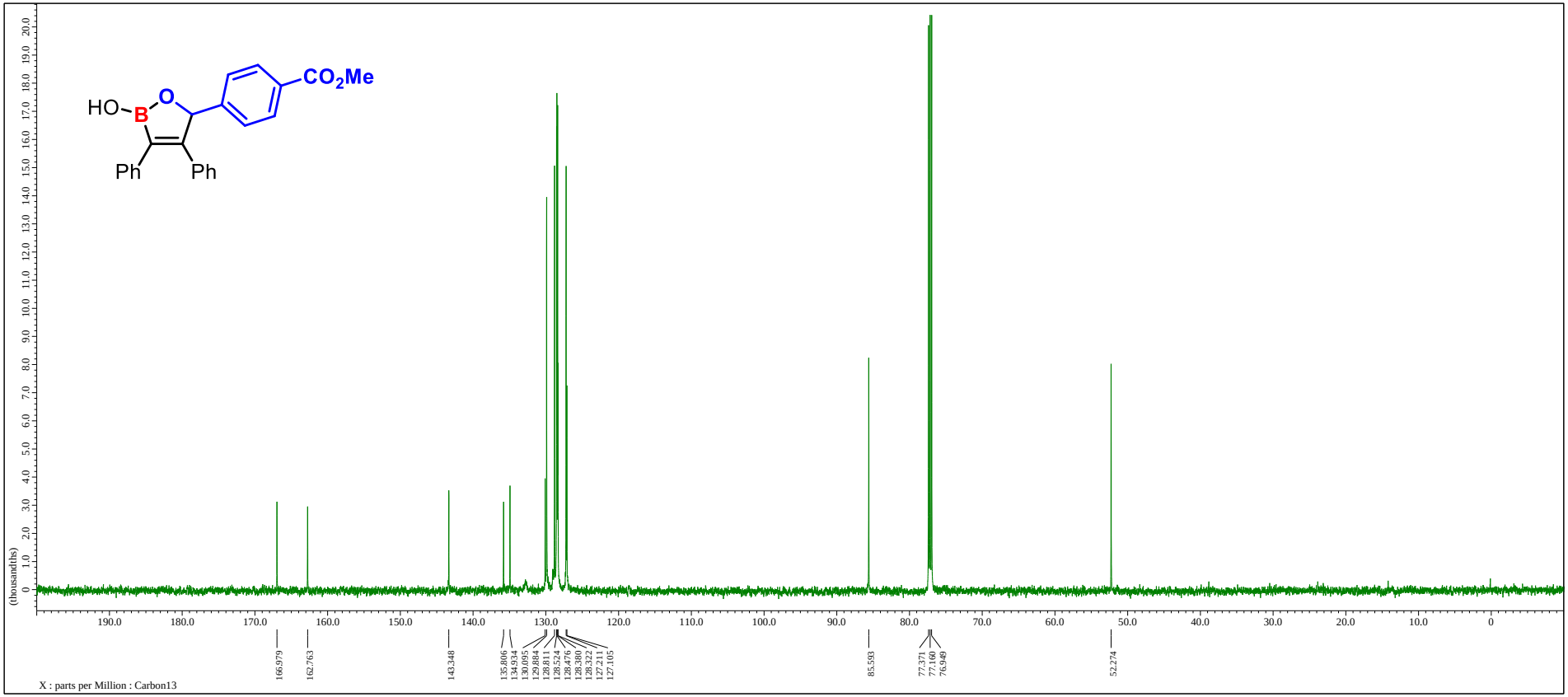

Figure S88. ^{13}C NMR (151 MHz, $CDCl_3$) spectrum of **2as**.

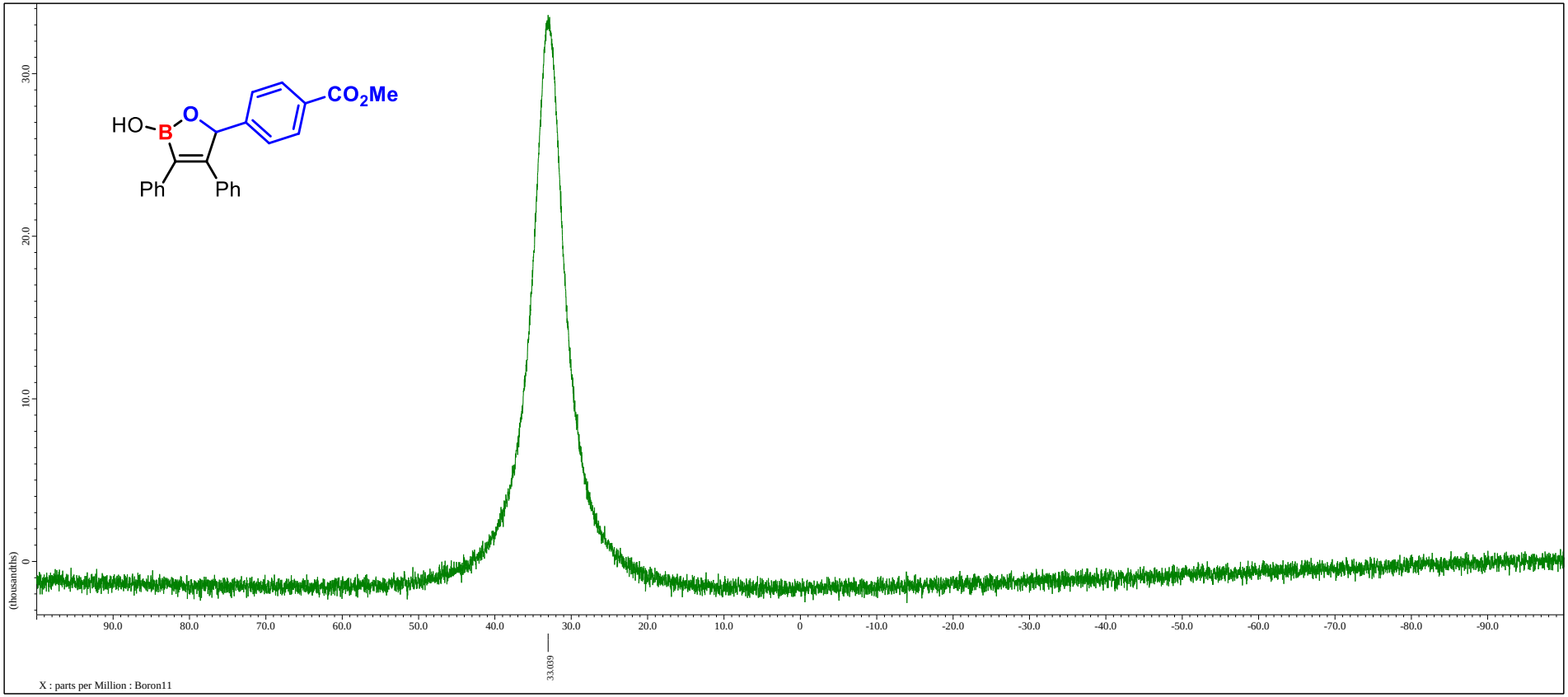

Figure S89. ^{11}B NMR (192 MHz, $CDCl_3$) spectrum of **2as**.

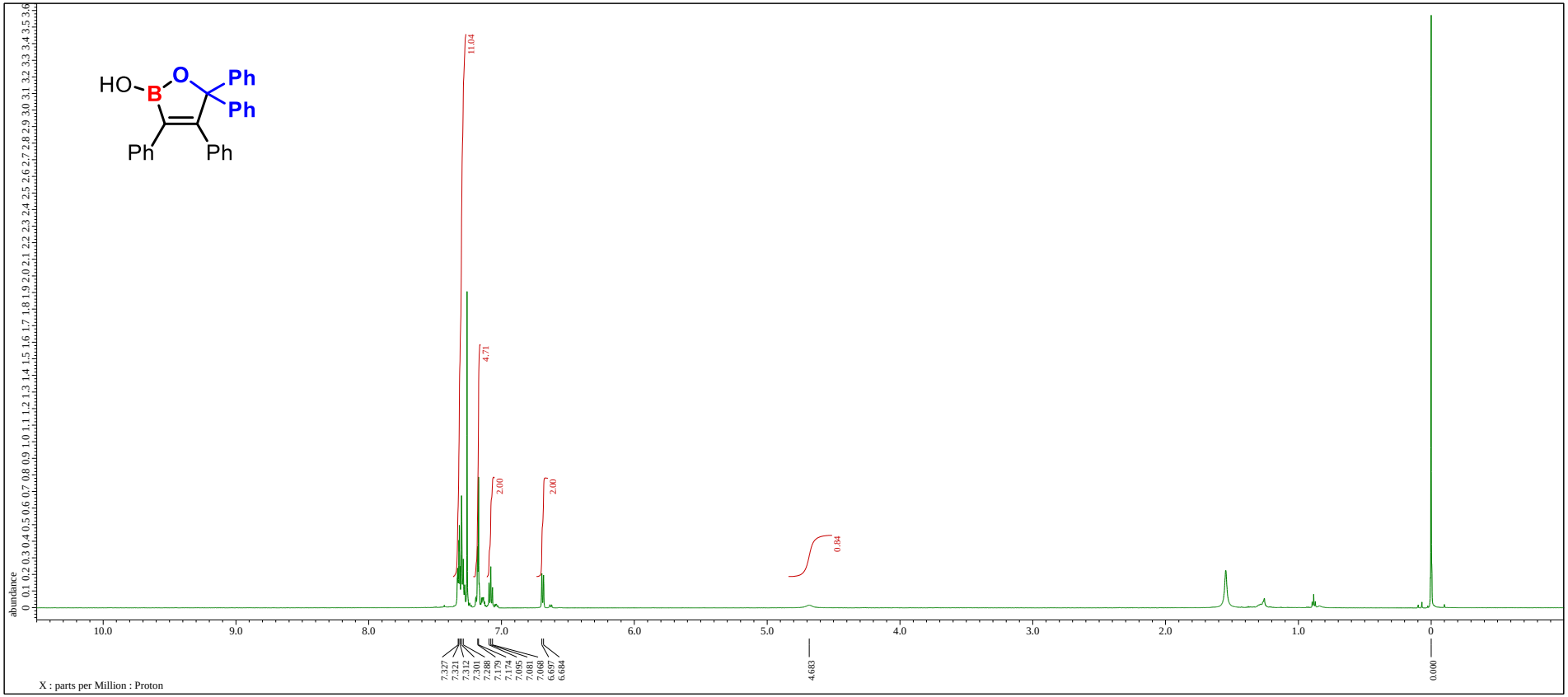

Figure S90. ^{1}H NMR (600 MHz, $CDCl_3$) spectrum of **2at**.

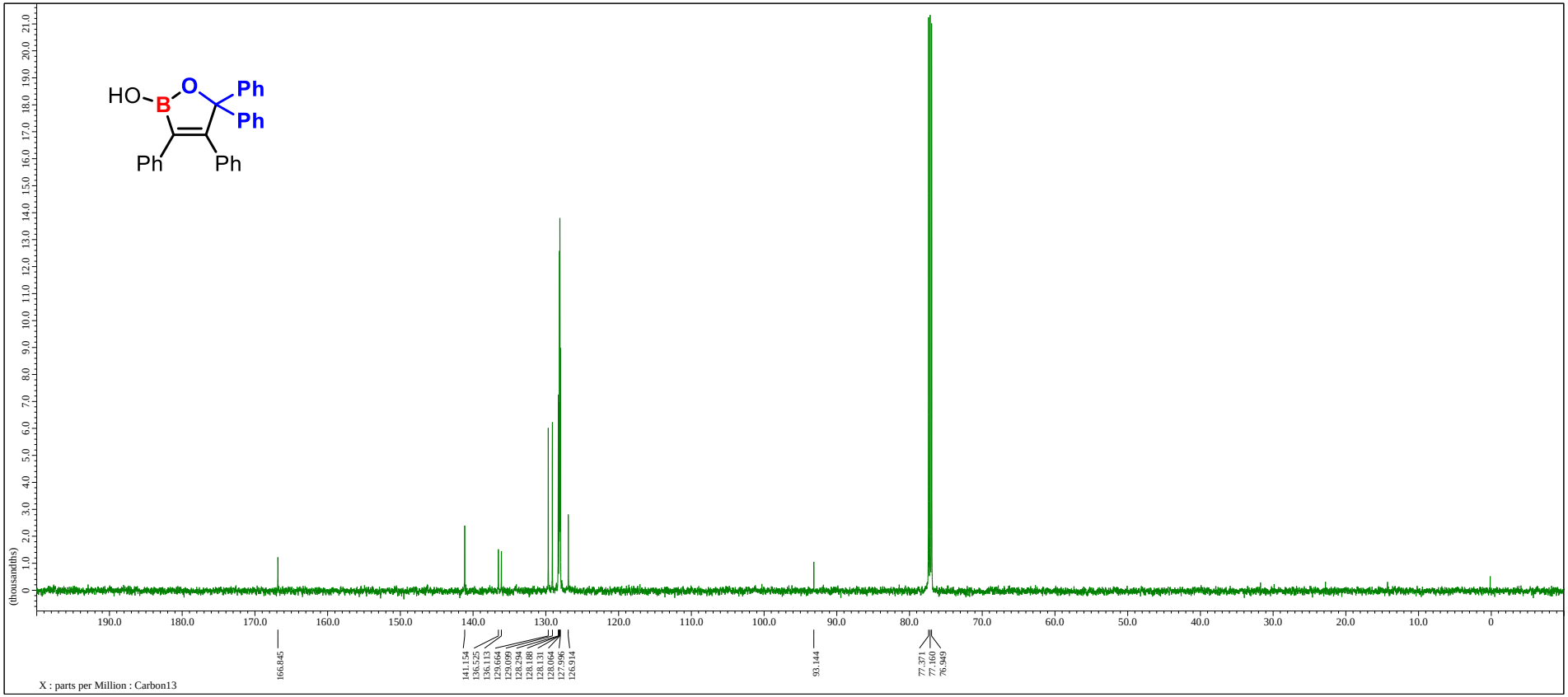

Figure S91. ^{13}C NMR (151 MHz, $CDCl_3$) spectrum of **2at**.

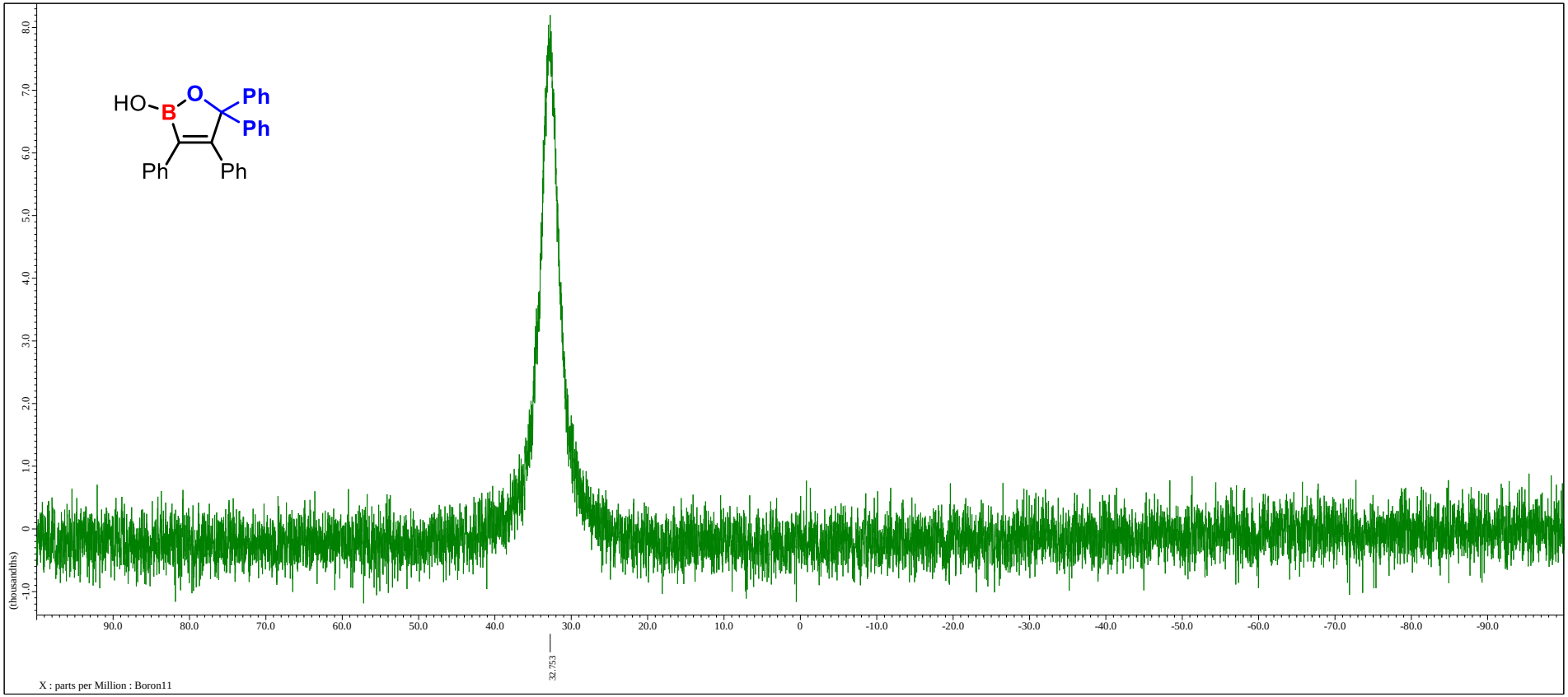

Figure S92. ^{11}B NMR (192 MHz, $CDCl_3$) spectrum of **2at**.

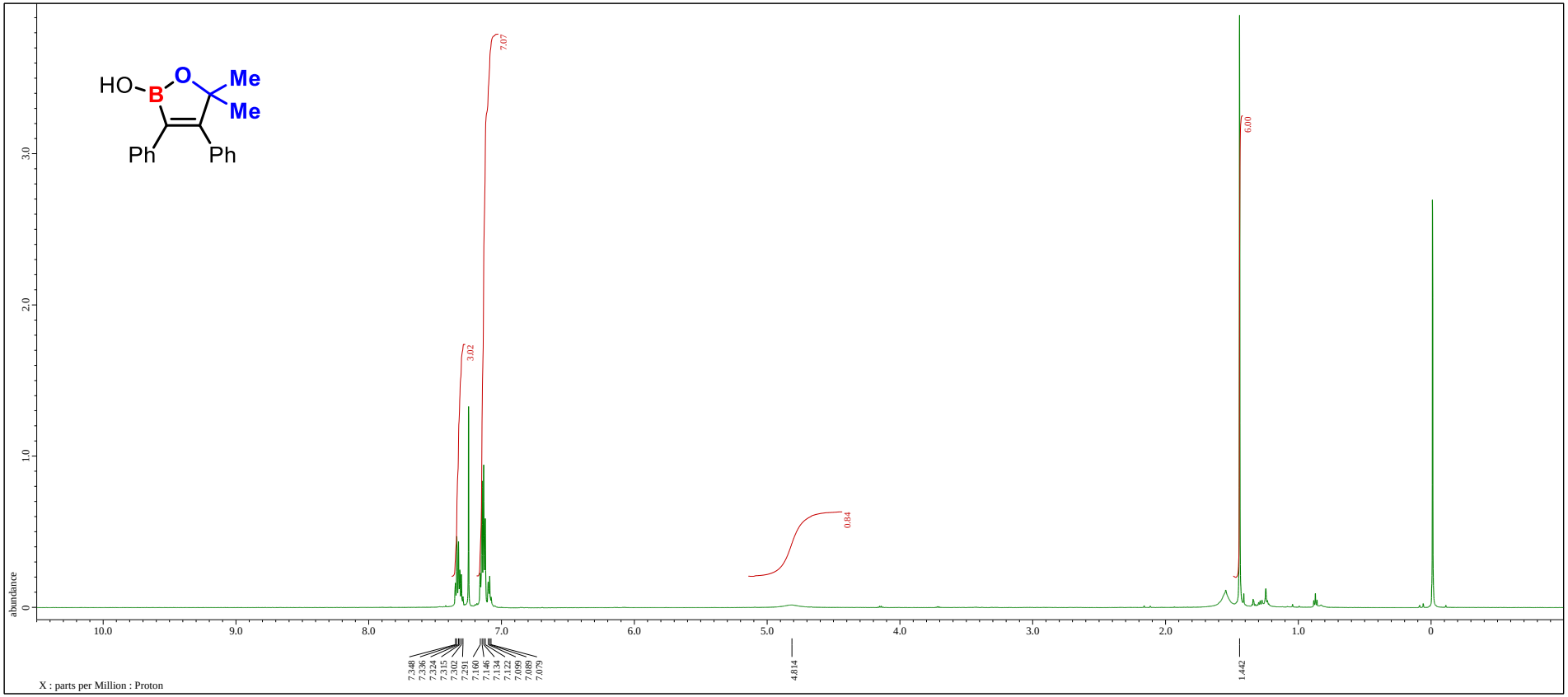

Figure S93. ^{1}H NMR (600 MHz, $CDCl_3$) spectrum of **2au**.

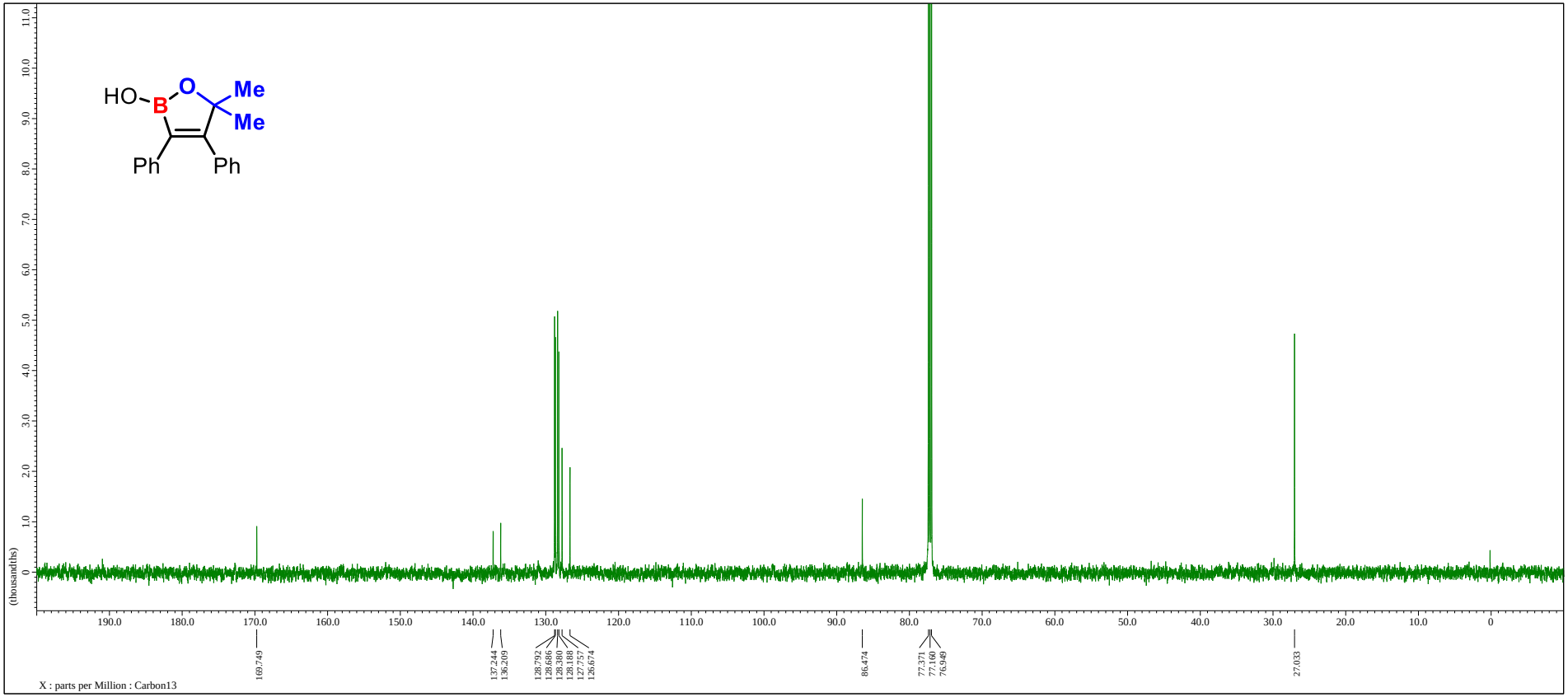

Figure S94. ^{13}C NMR (151 MHz, $CDCl_3$) spectrum of **2au**.

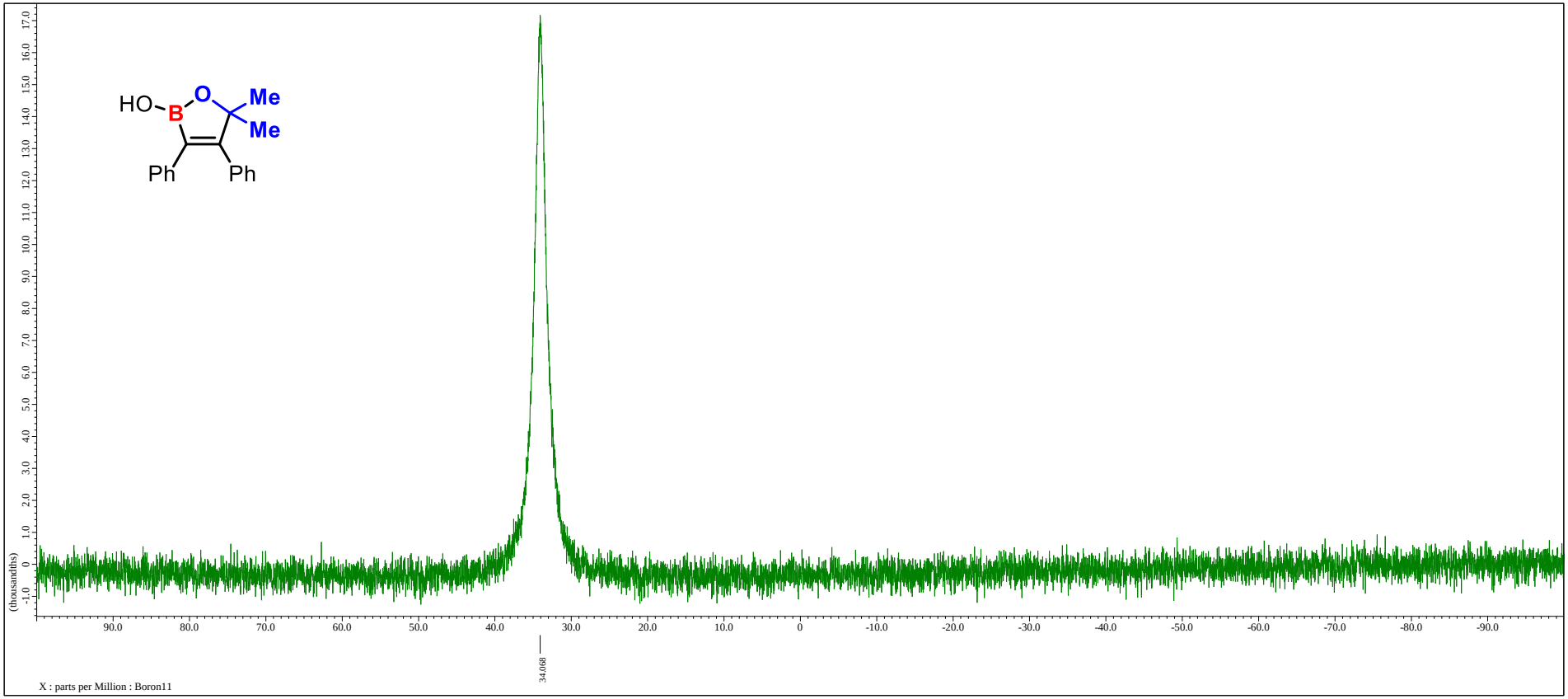

Figure S95. ^{11}B NMR (192 MHz, $CDCl_3$) spectrum of **2au**.

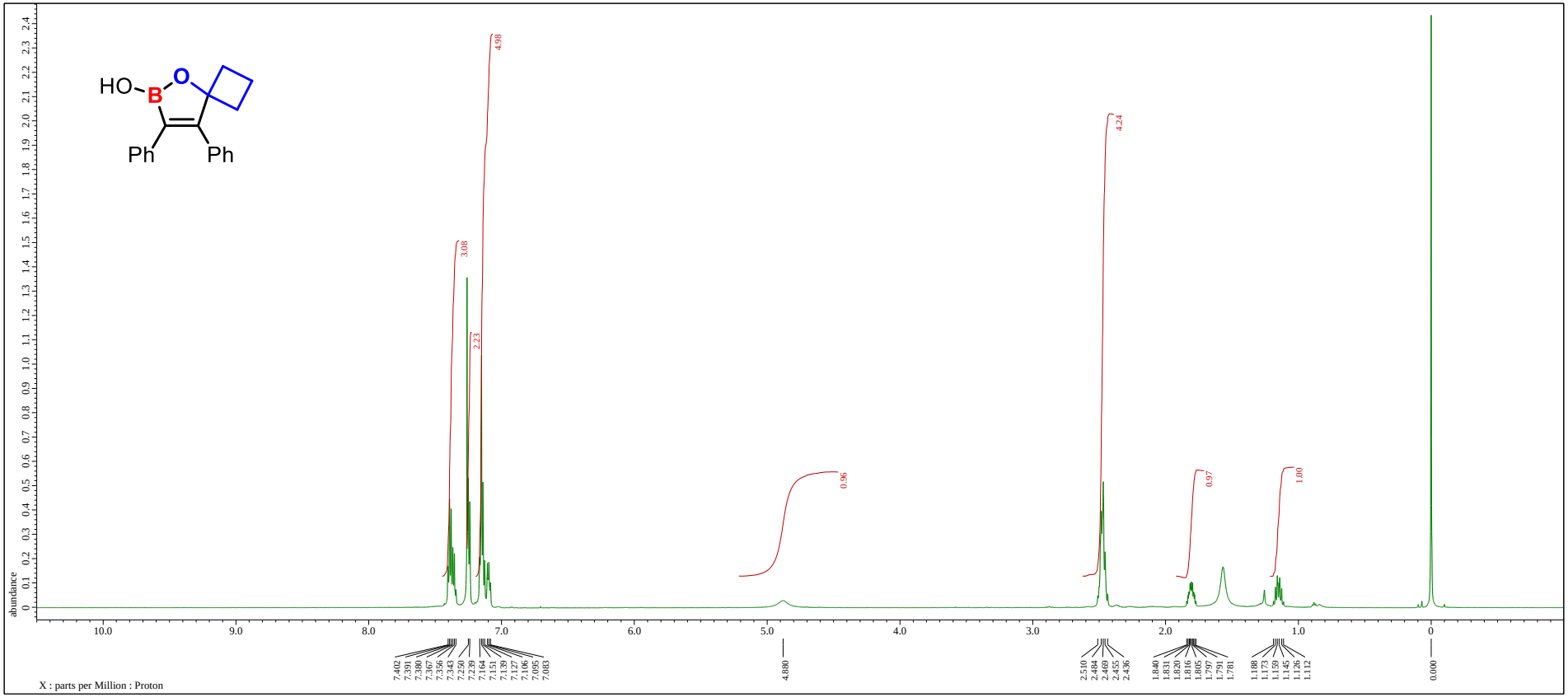

Figure S96. ^{1}H NMR (600 MHz, $CDCl_3$) spectrum of **2av**.

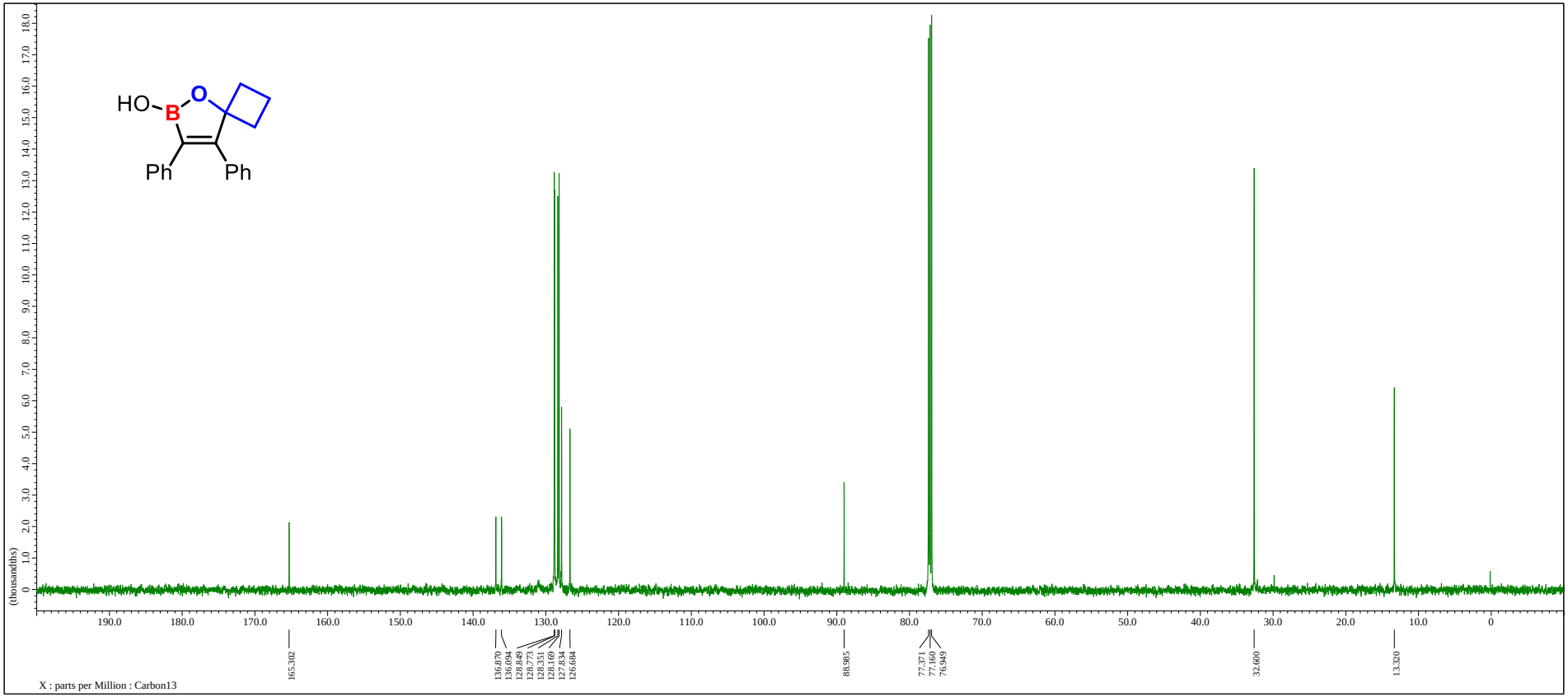

Figure S97. ^{13}C NMR (151 MHz, $CDCl_3$) spectrum of **2av**.

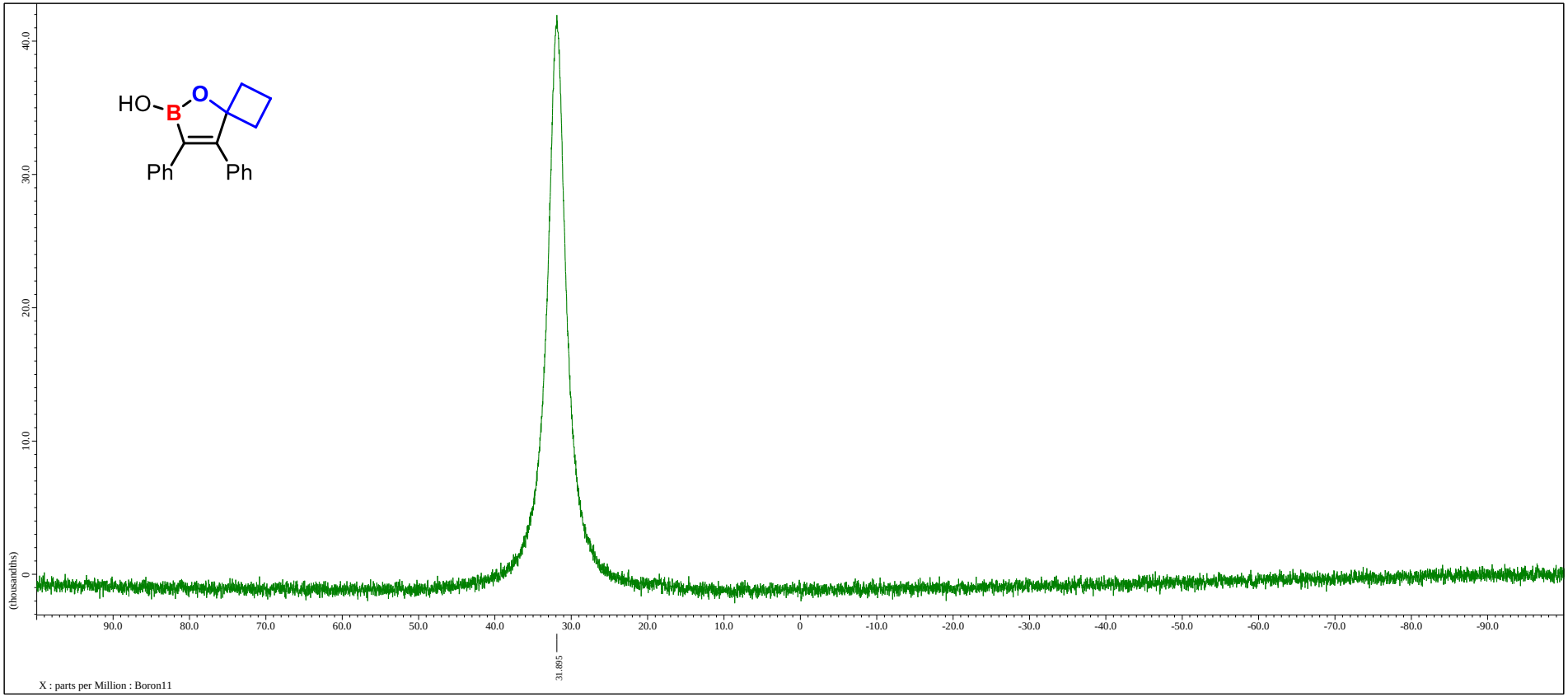

Figure S98. ^{11}B NMR (192 MHz, $CDCl_3$) spectrum of **2av**.

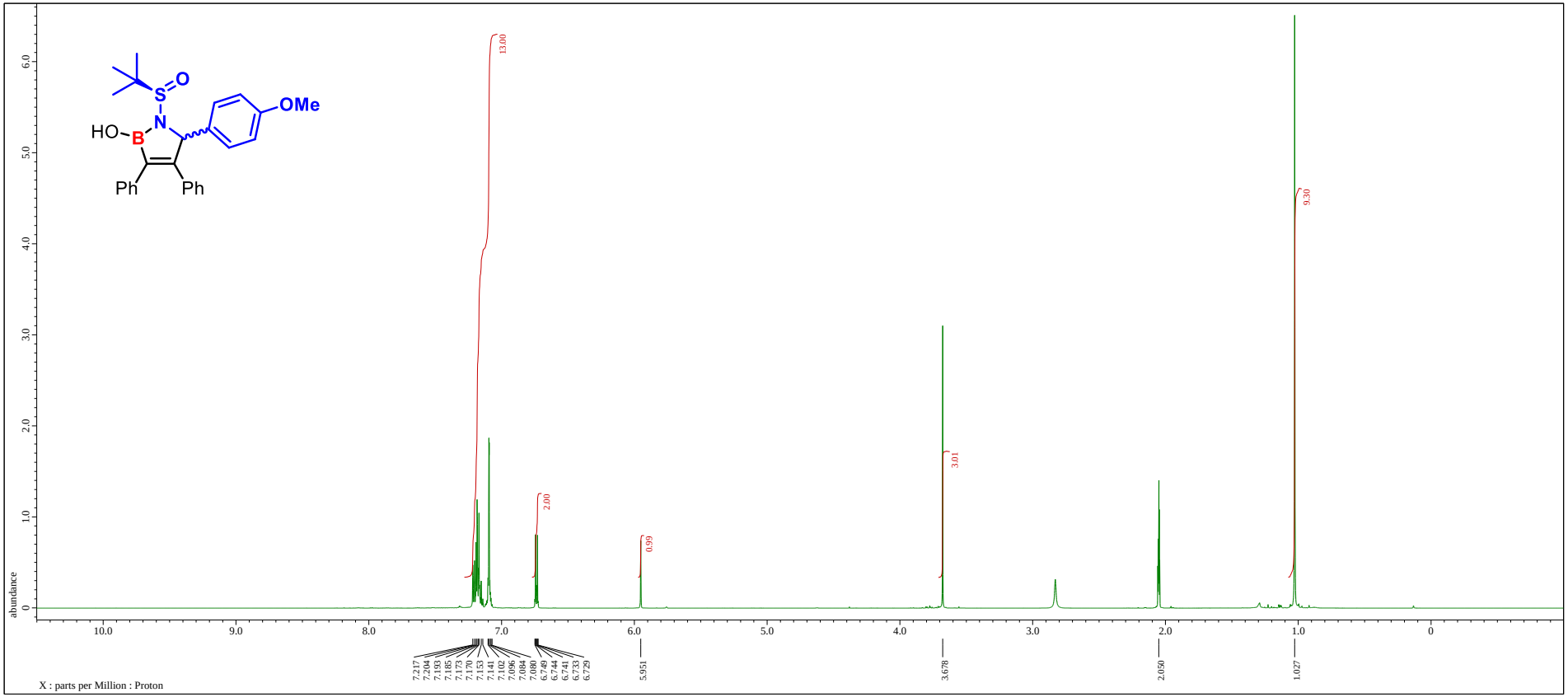

Figure S99. ^{1}H NMR (600 MHz, acetone-d_6) spectrum of **2aw**.

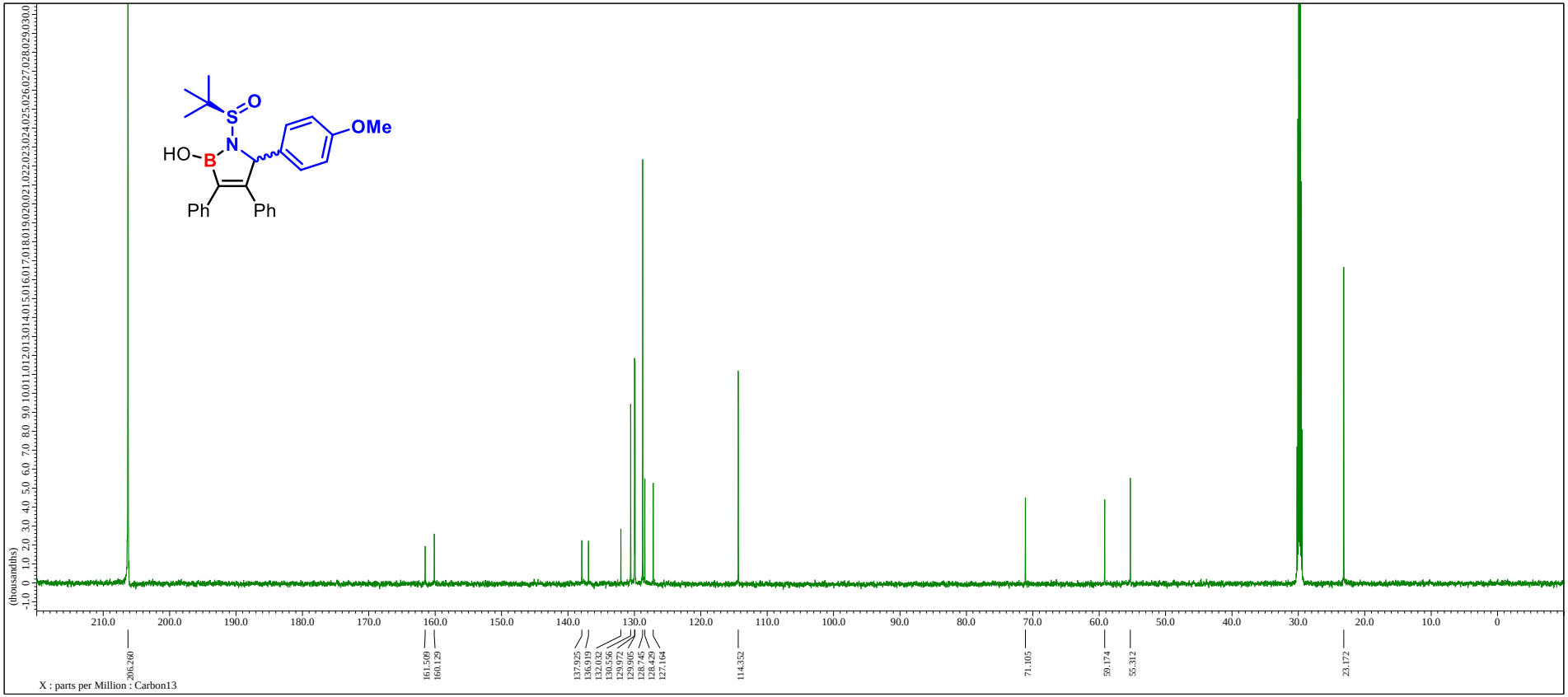

Figure S100. ^{13}C NMR (151 MHz, acetone-d_6) spectrum of **2aw**.

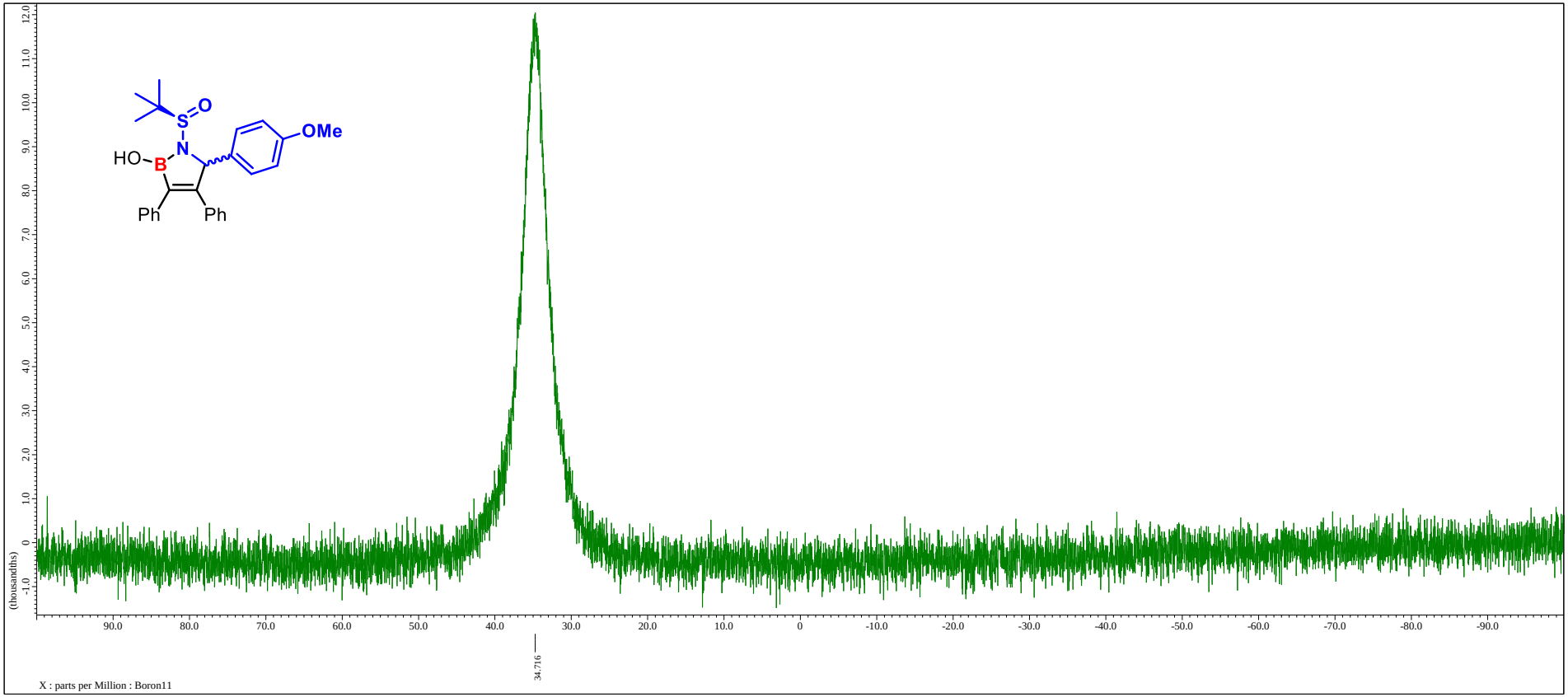

Figure S101. ^{11}B NMR (192 MHz, $CDCl_3$) spectrum of **2aw**.

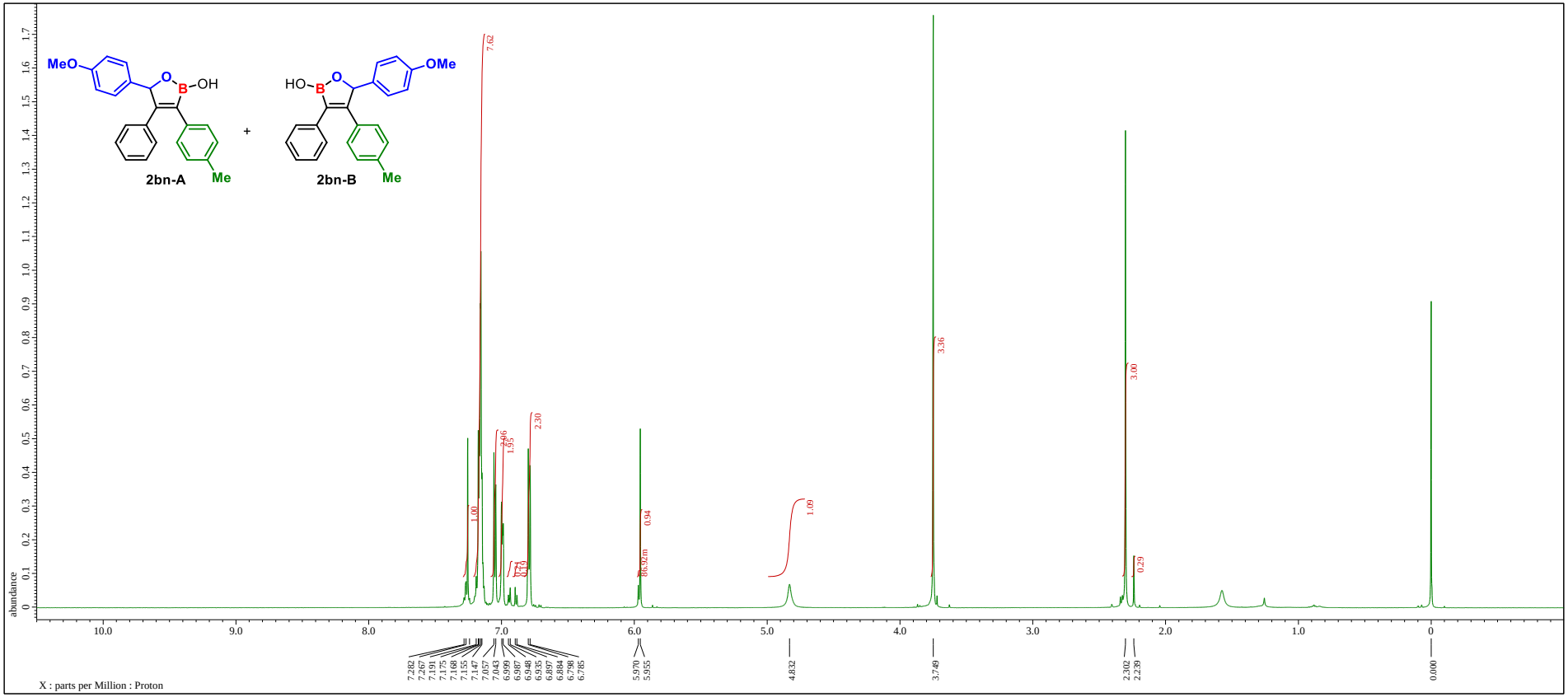

Figure S102. ^{1}H NMR (600 MHz, $CDCl_3$) spectrum of **2bn-A** and **2bn-B**.

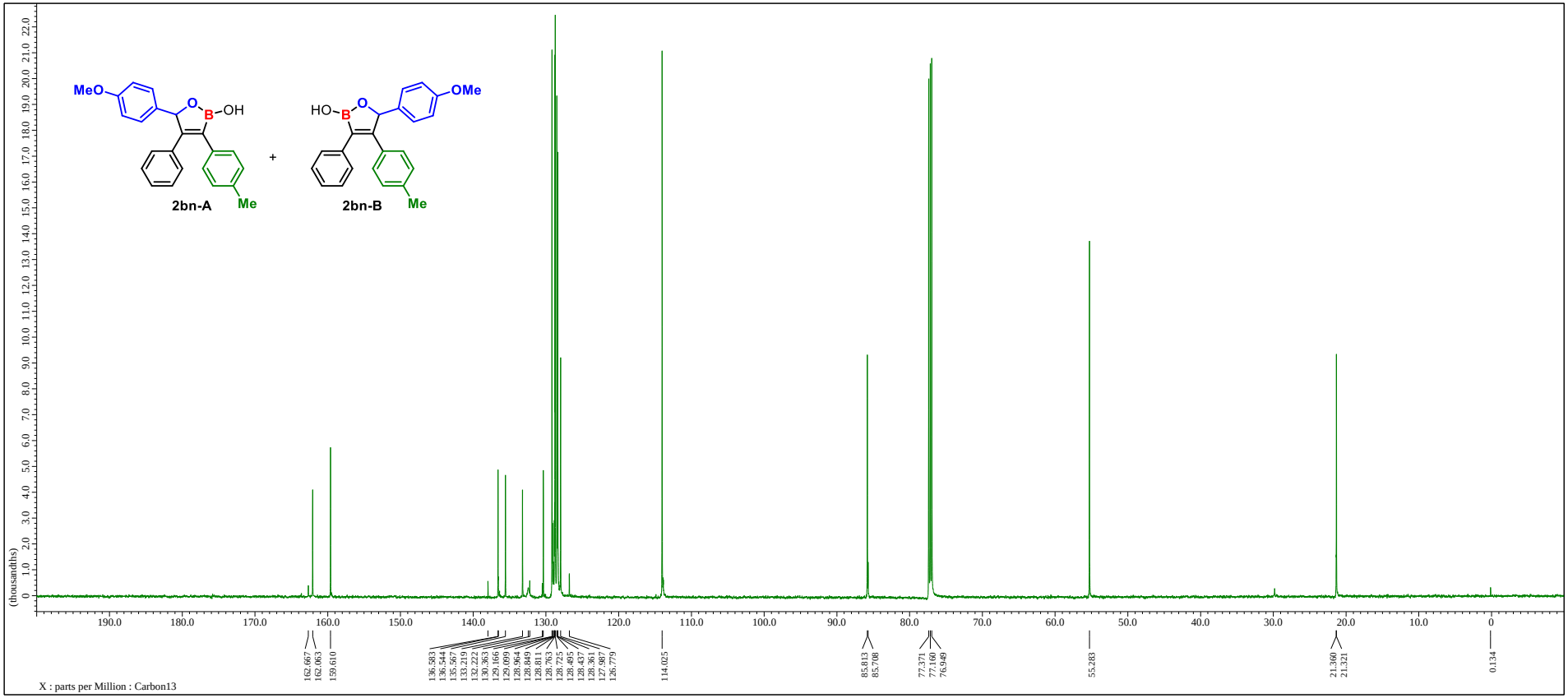

Figure S103. ^{13}C NMR (151 MHz, $CDCl_3$) spectrum of **2bn-A** and **2bn-B**.

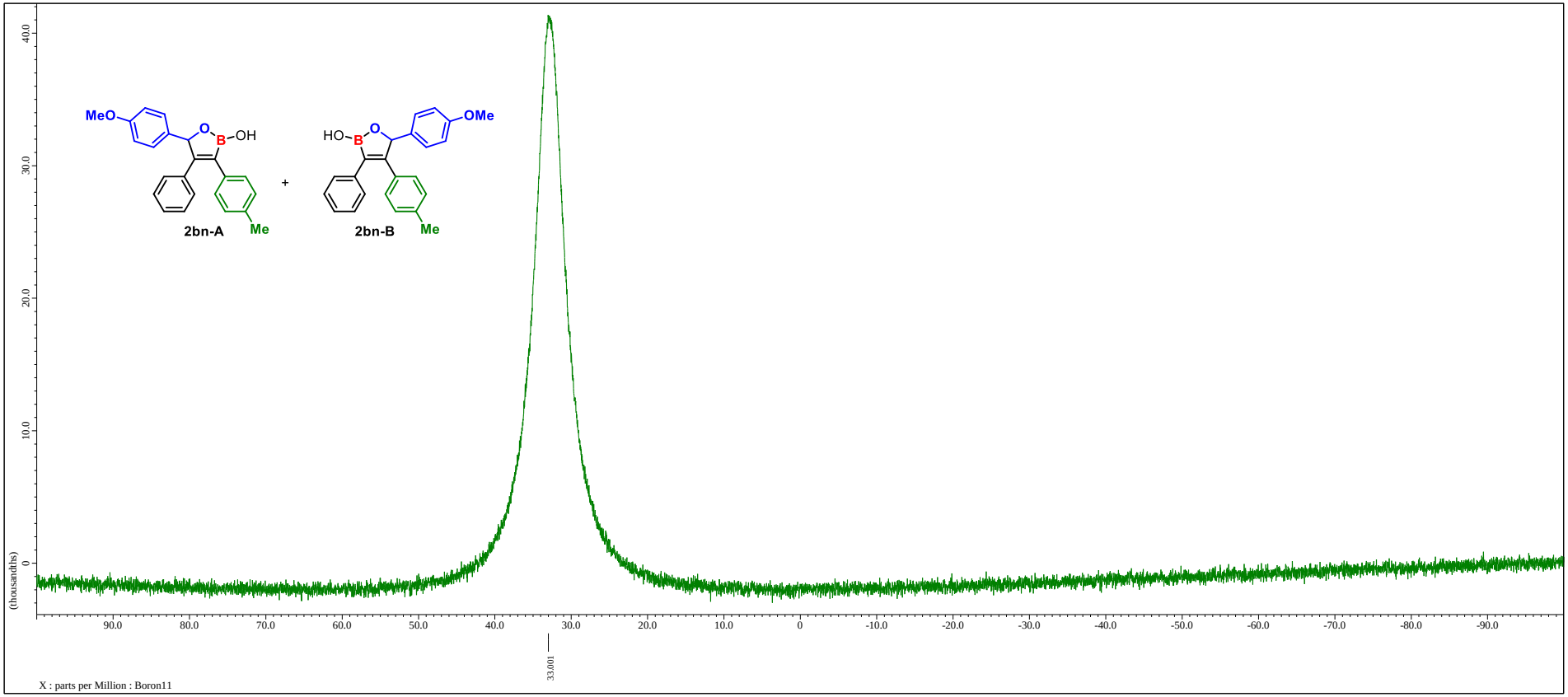

Figure S104. ^{11}B NMR (192 MHz, $CDCl_3$) spectrum of **2bn-A** and **2bn-B**.

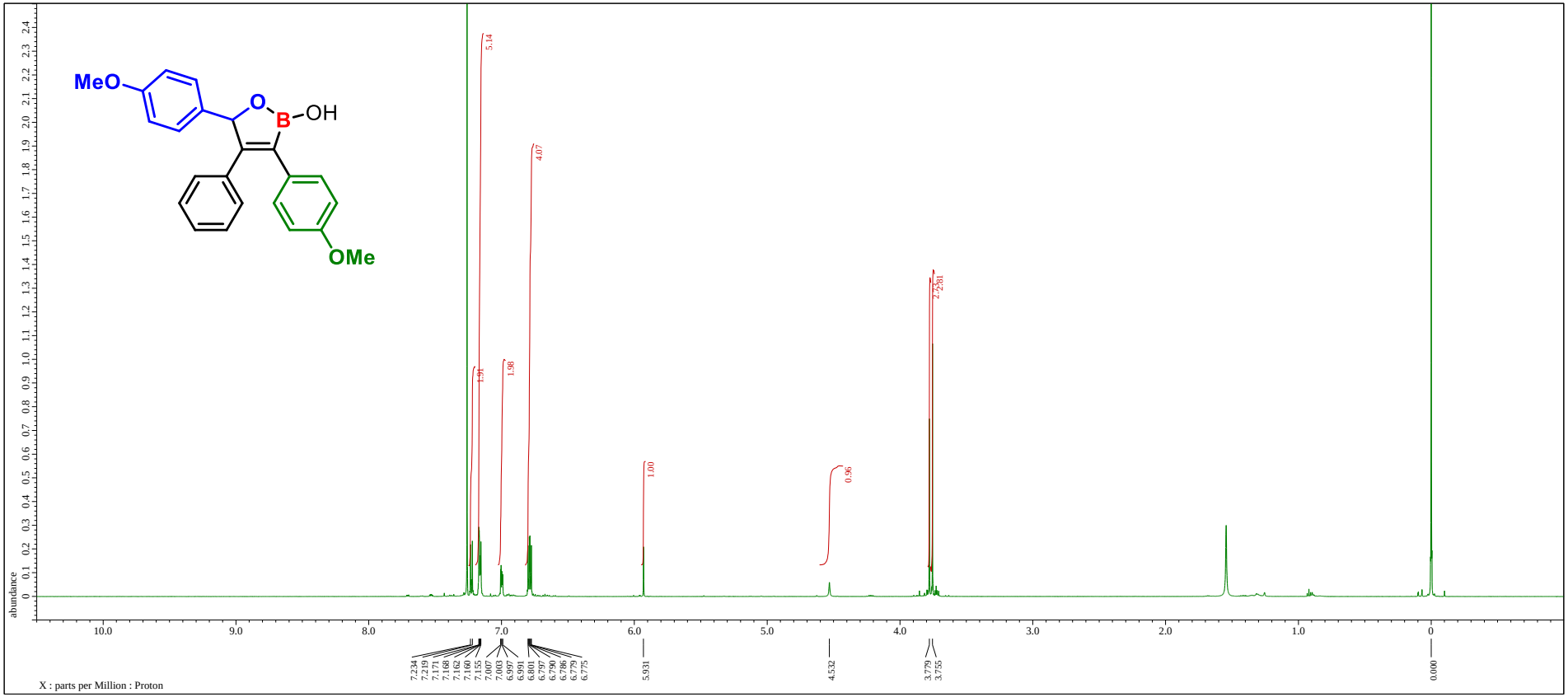

Figure S105. ^{1}H NMR (600 MHz, $CDCl_3$) spectrum of **2cn-A**.

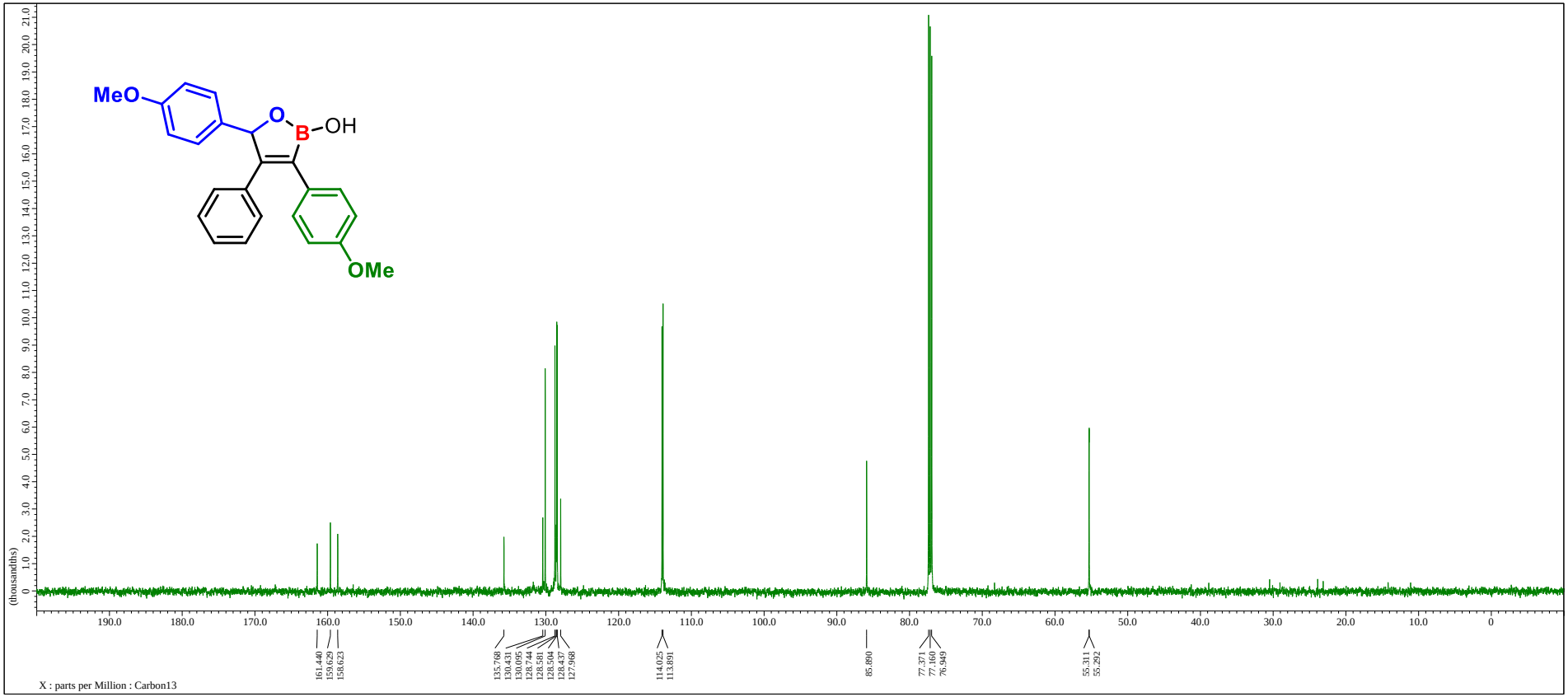

Figure S106. ^{13}C NMR (151 MHz, $CDCl_3$) spectrum of **2cn-A**.

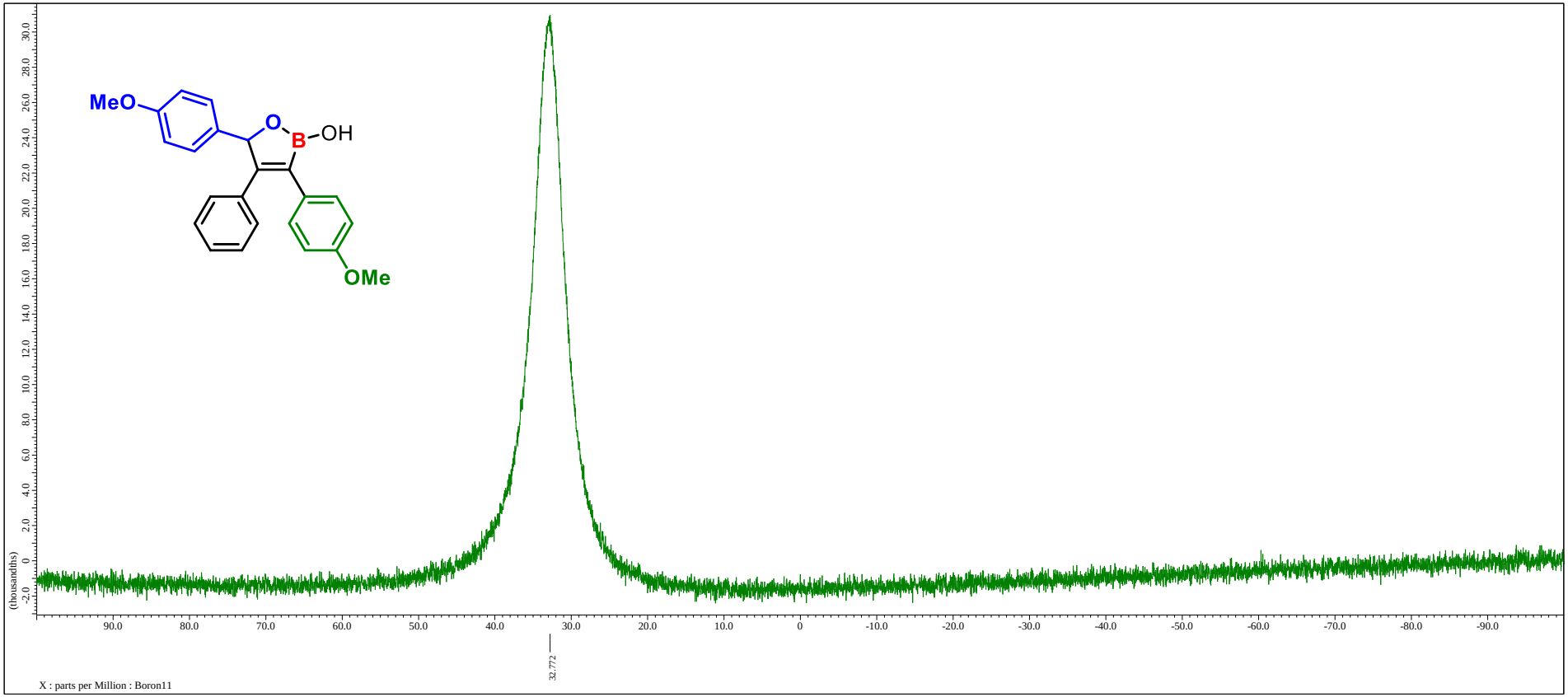

Figure S107. ^{11}B NMR (192 MHz, $CDCl_3$) spectrum of **2cn-A**.

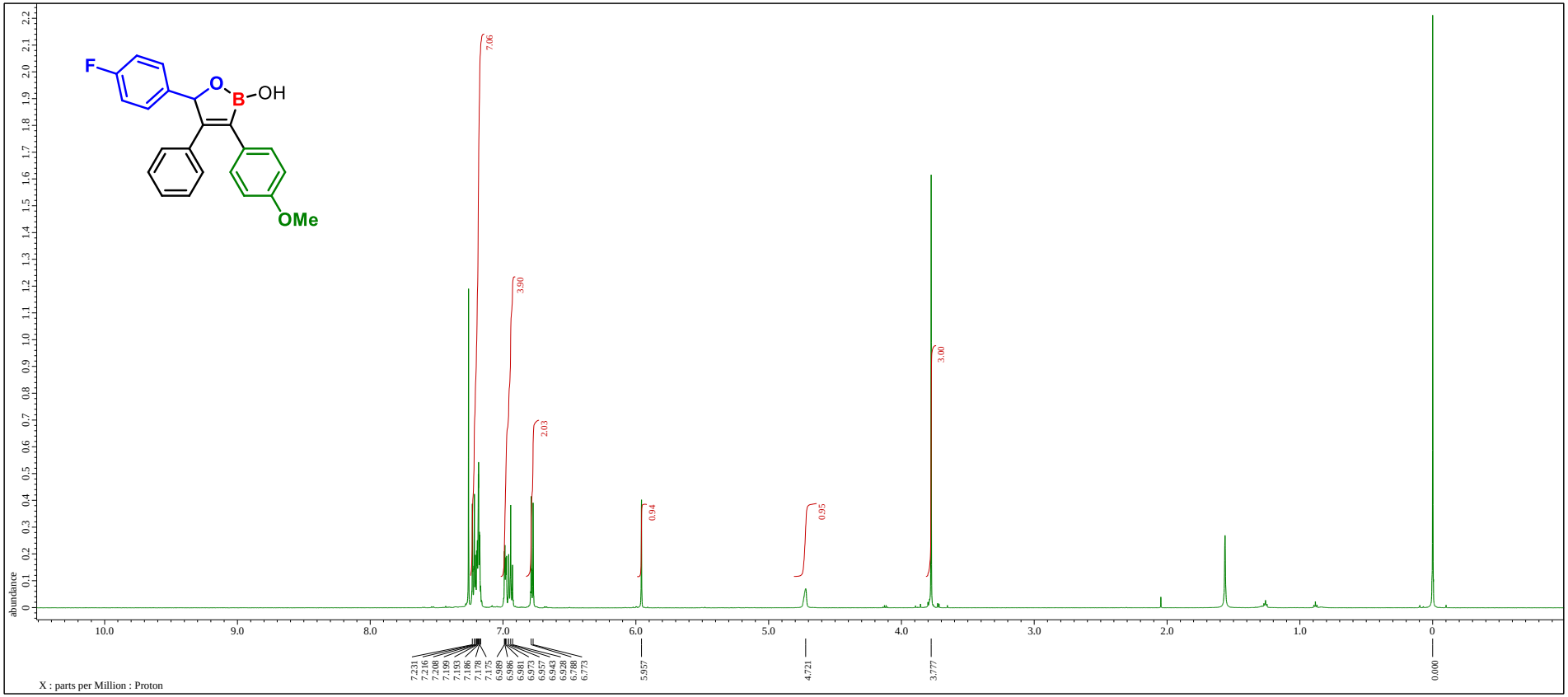

Figure S108. ^{1}H NMR (600 MHz, $CDCl_3$) spectrum of **2co-A**.

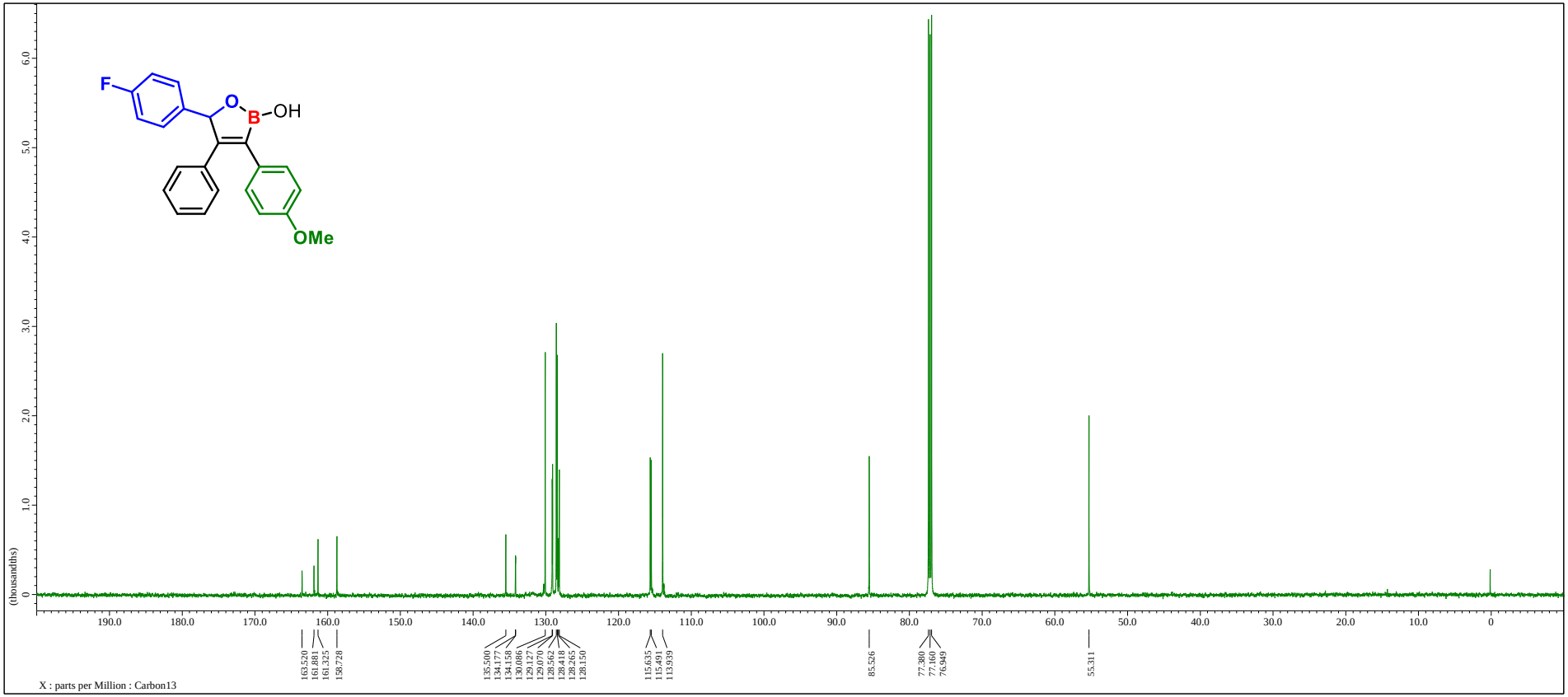

Figure S109. ^{13}C NMR (151 MHz, $CDCl_3$) spectrum of **2co-A**.

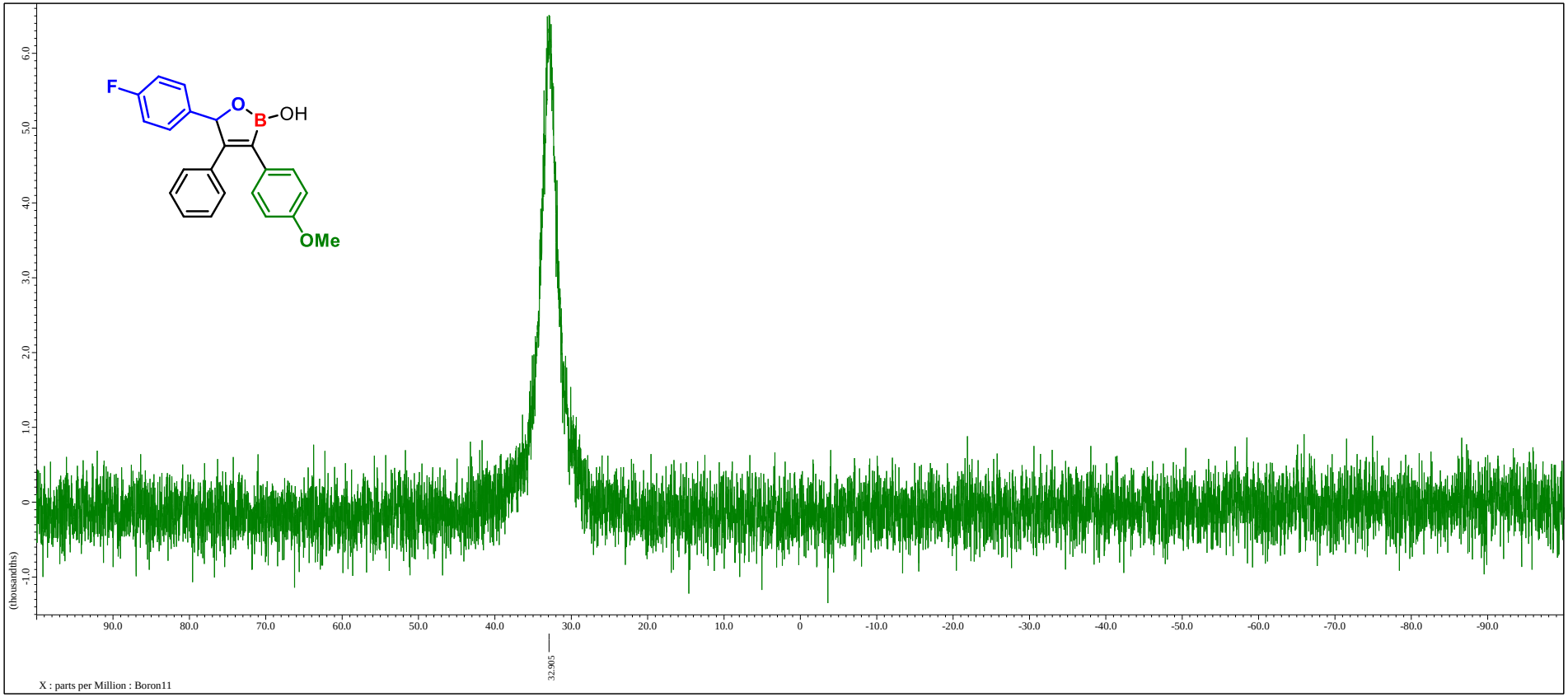

Figure S110. ^{11}B NMR (192 MHz, $CDCl_3$) spectrum of **2co-A**.

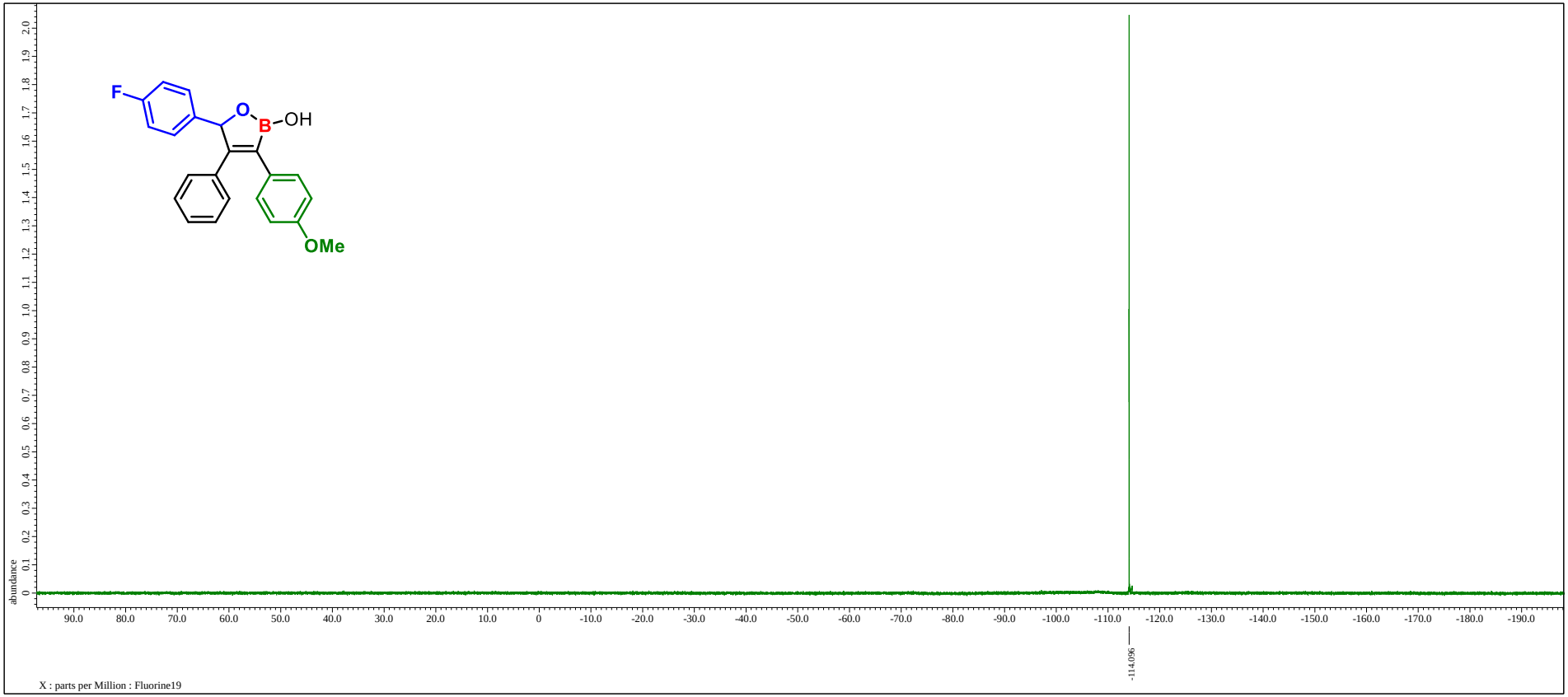

Figure S111. ^{19}F NMR (564 MHz, $CDCl_3$) spectrum of **2co-A**.

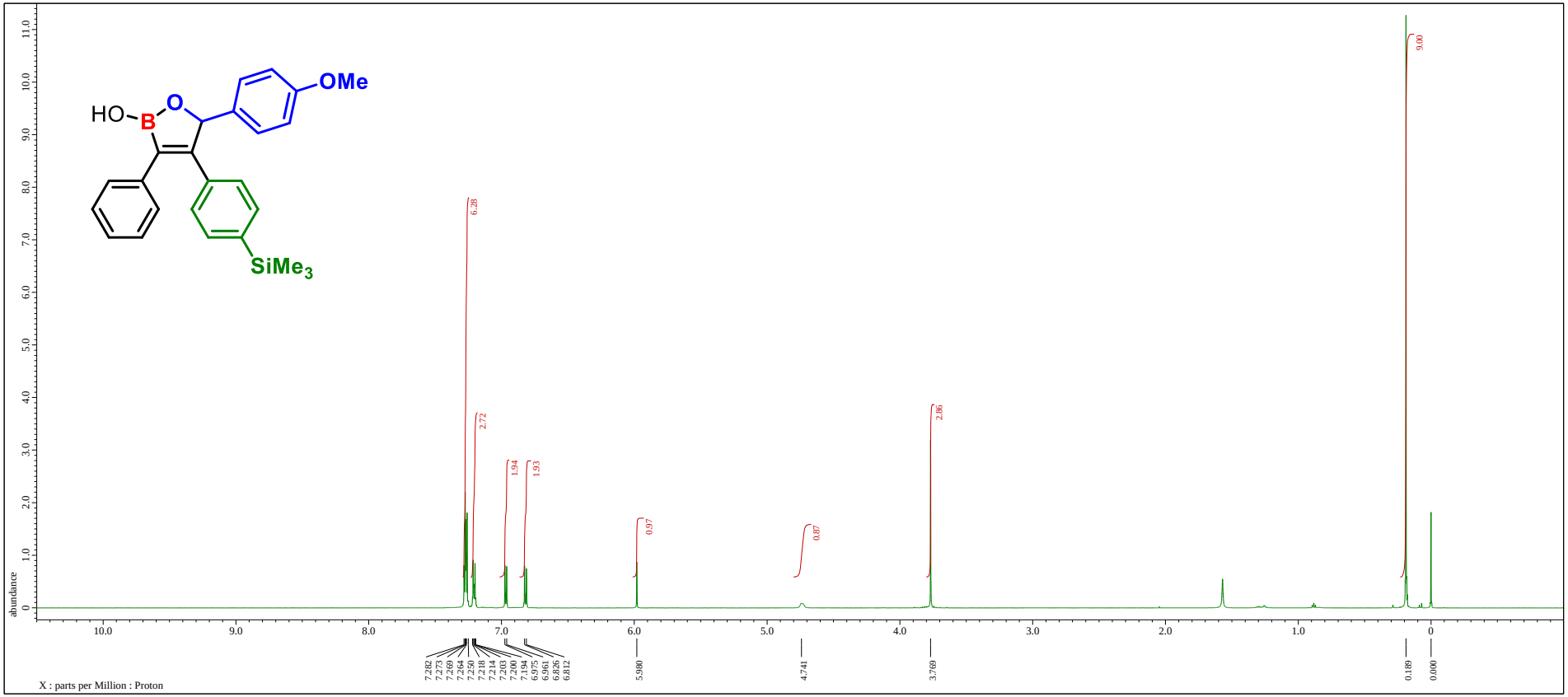

Figure S112. ^{1}H NMR (600 MHz,$CDCl_3$) spectrum of **2dn-B**.

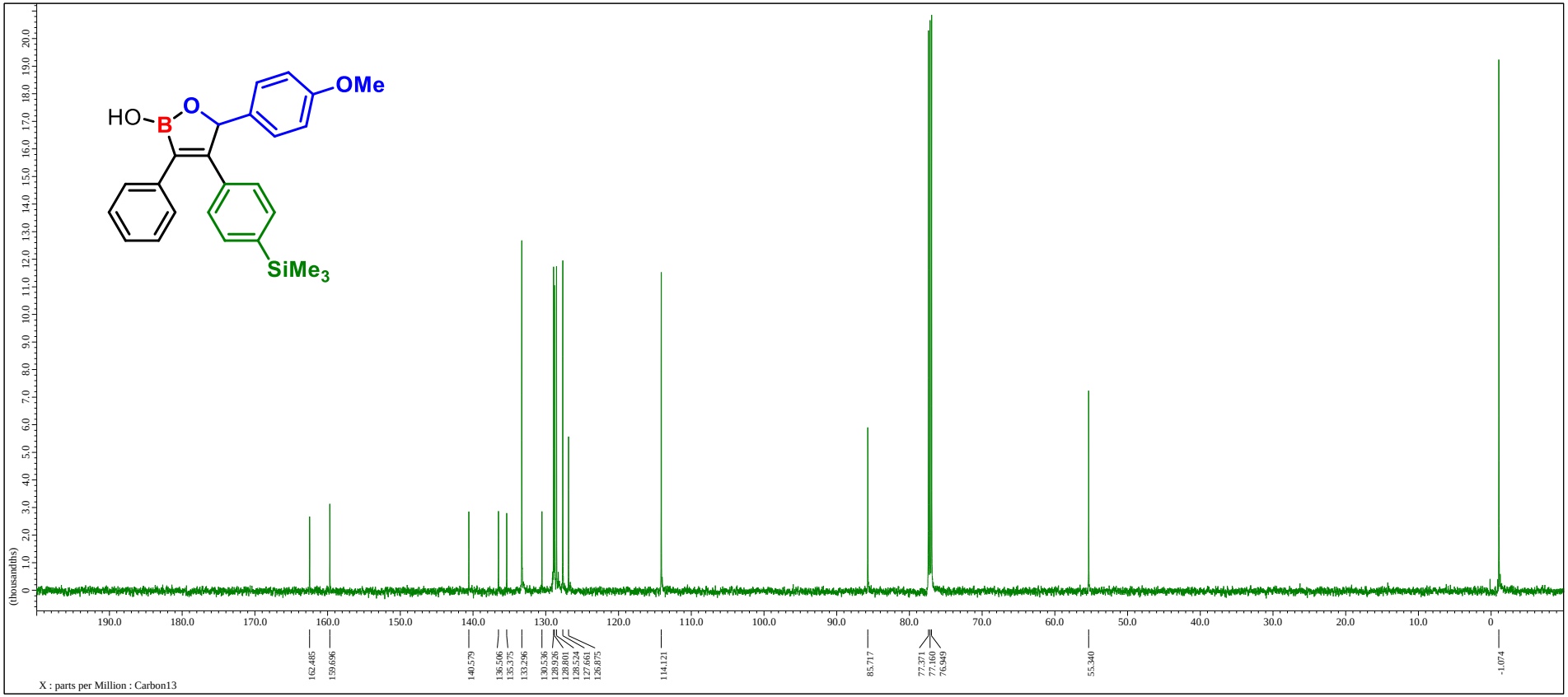

Figure S113. ^{13}C NMR (151 MHz, $CDCl_3$) spectrum of **2dn-B**.

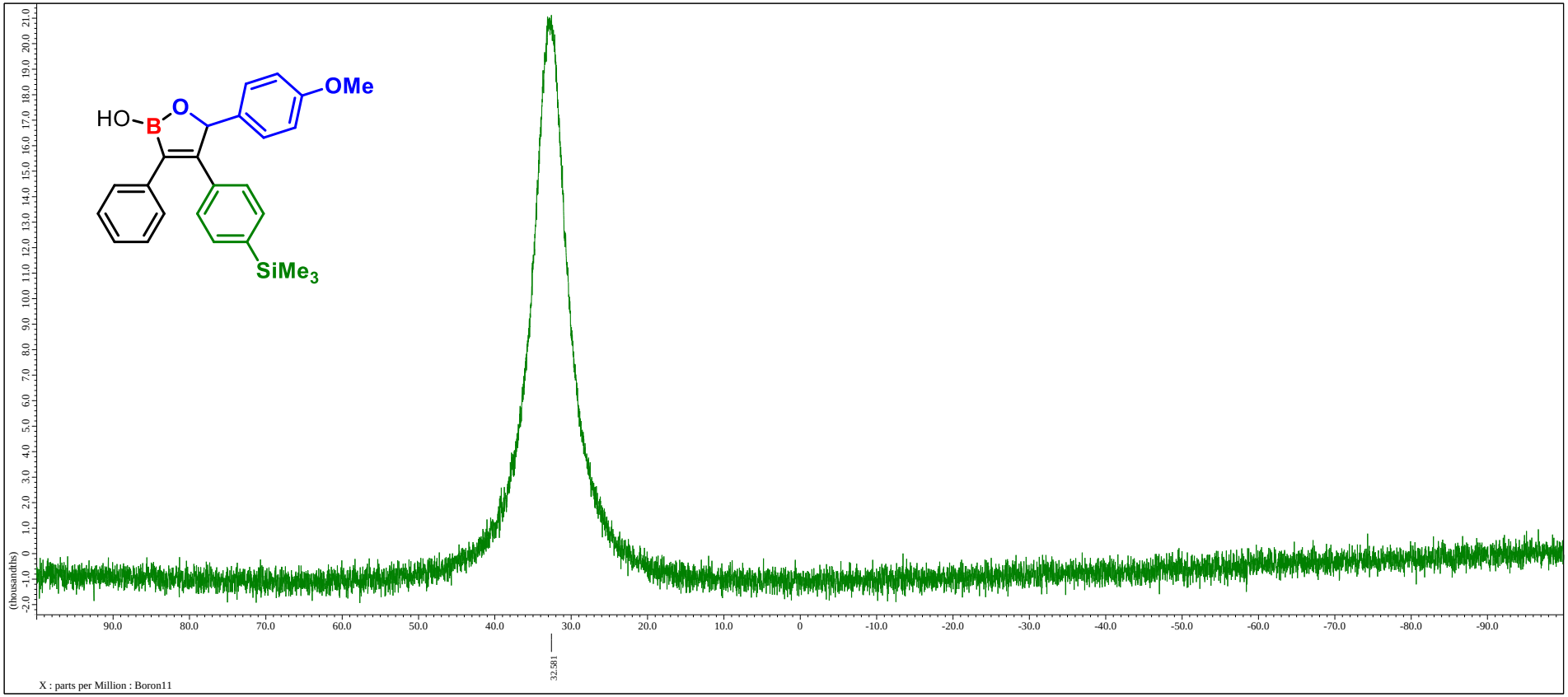

Figure S114. ^{11}B NMR (192 MHz, $CDCl_3$) spectrum of **2dn-B**.

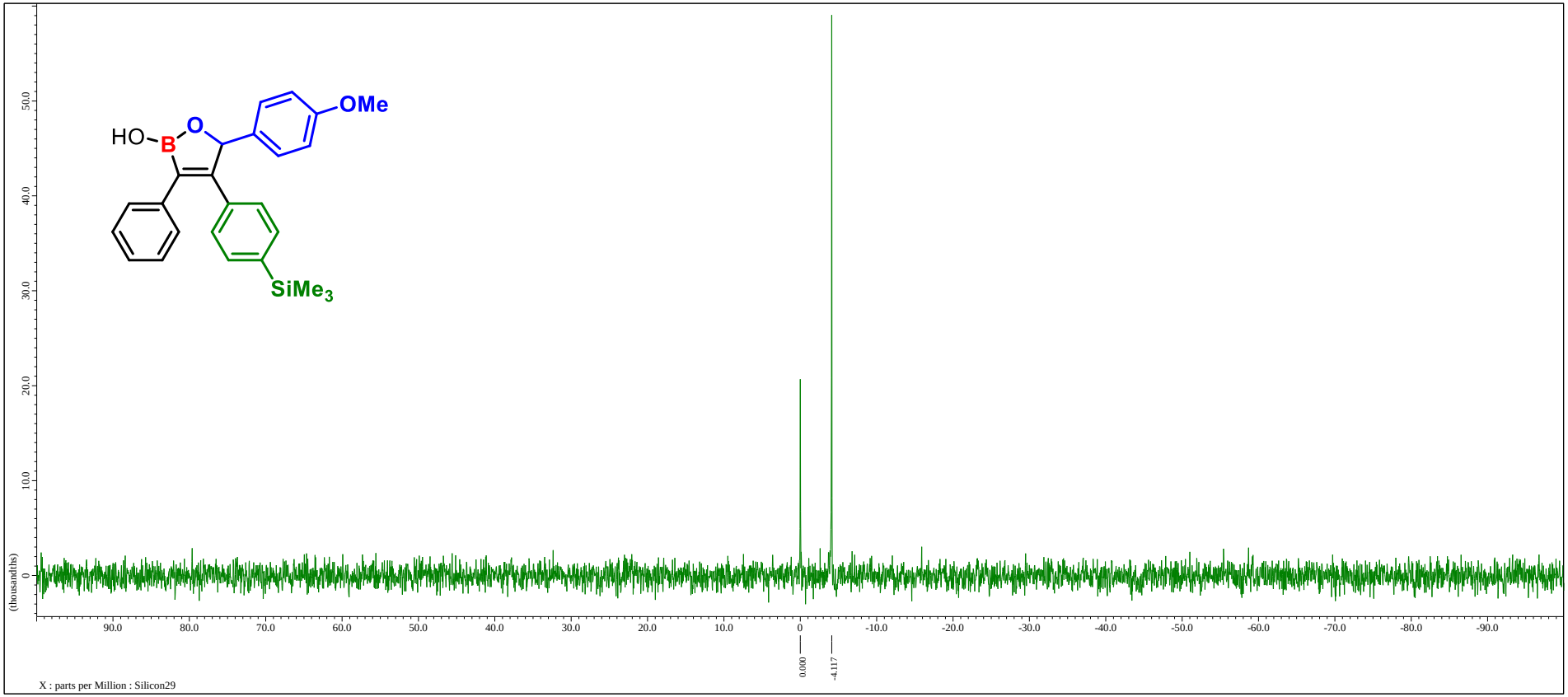

Figure S115. ^{29}Si NMR (119 MHz, $CDCl_3$) spectrum of **2dn-B**.

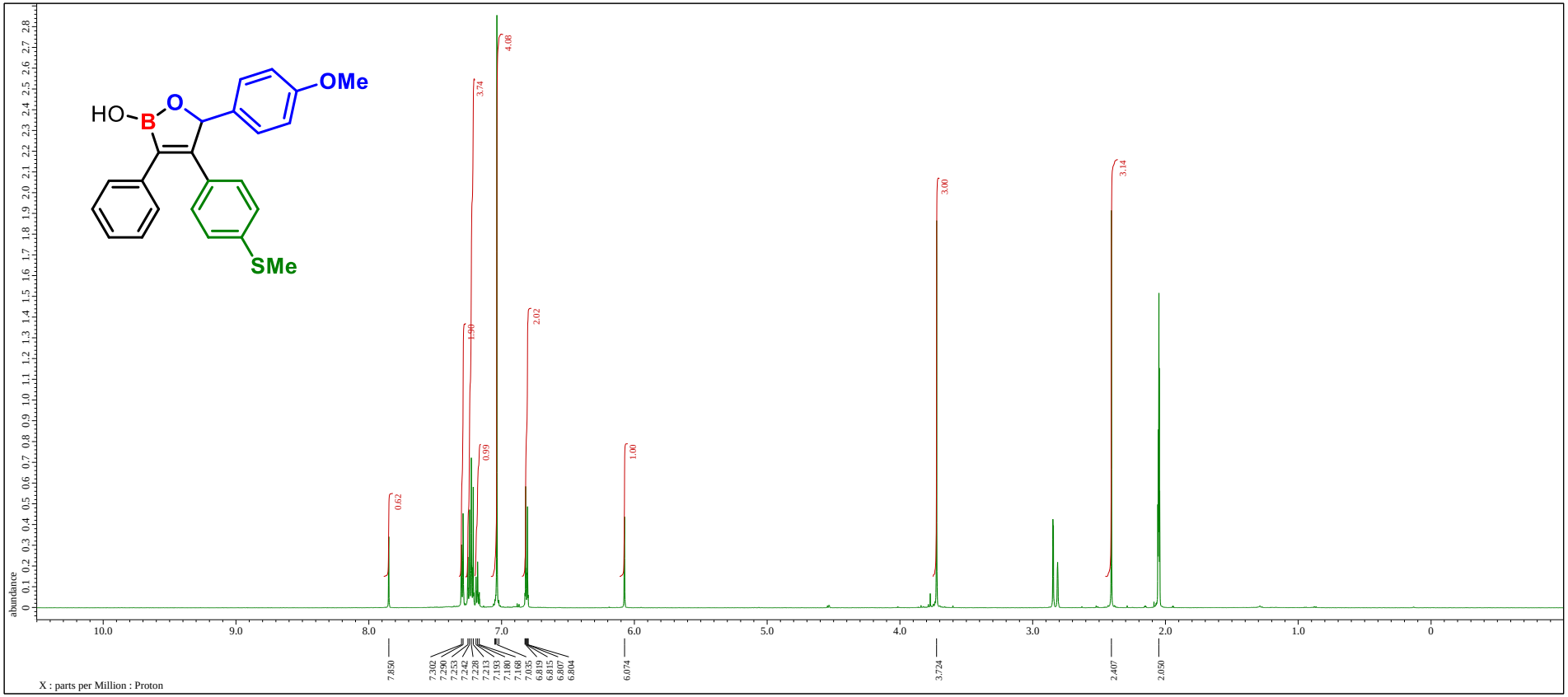

Figure S116. ^{1}H NMR (600 MHz, acetone-d_6) spectrum of **2en-B**.

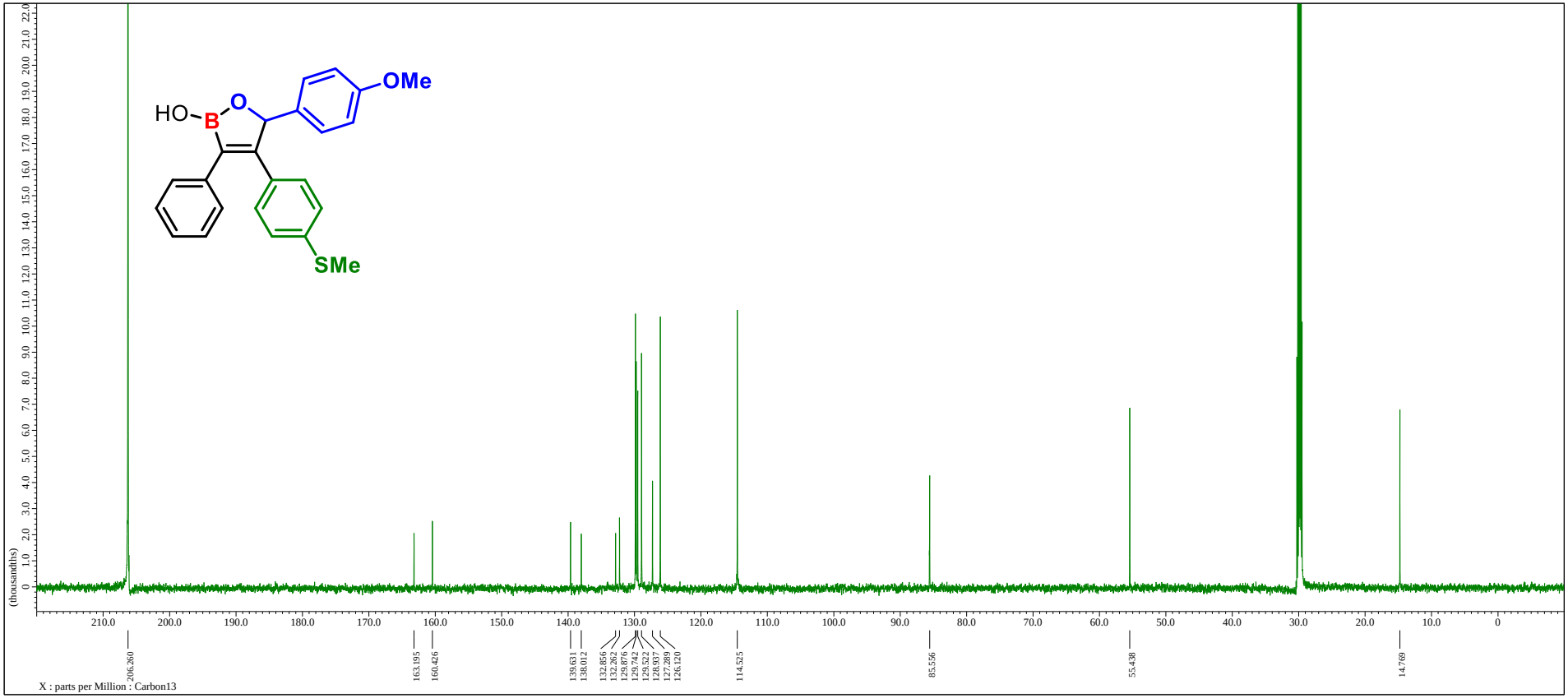

Figure S117. ^{13}C NMR (151 MHz, acetone-d_6) spectrum of **2en-B**.

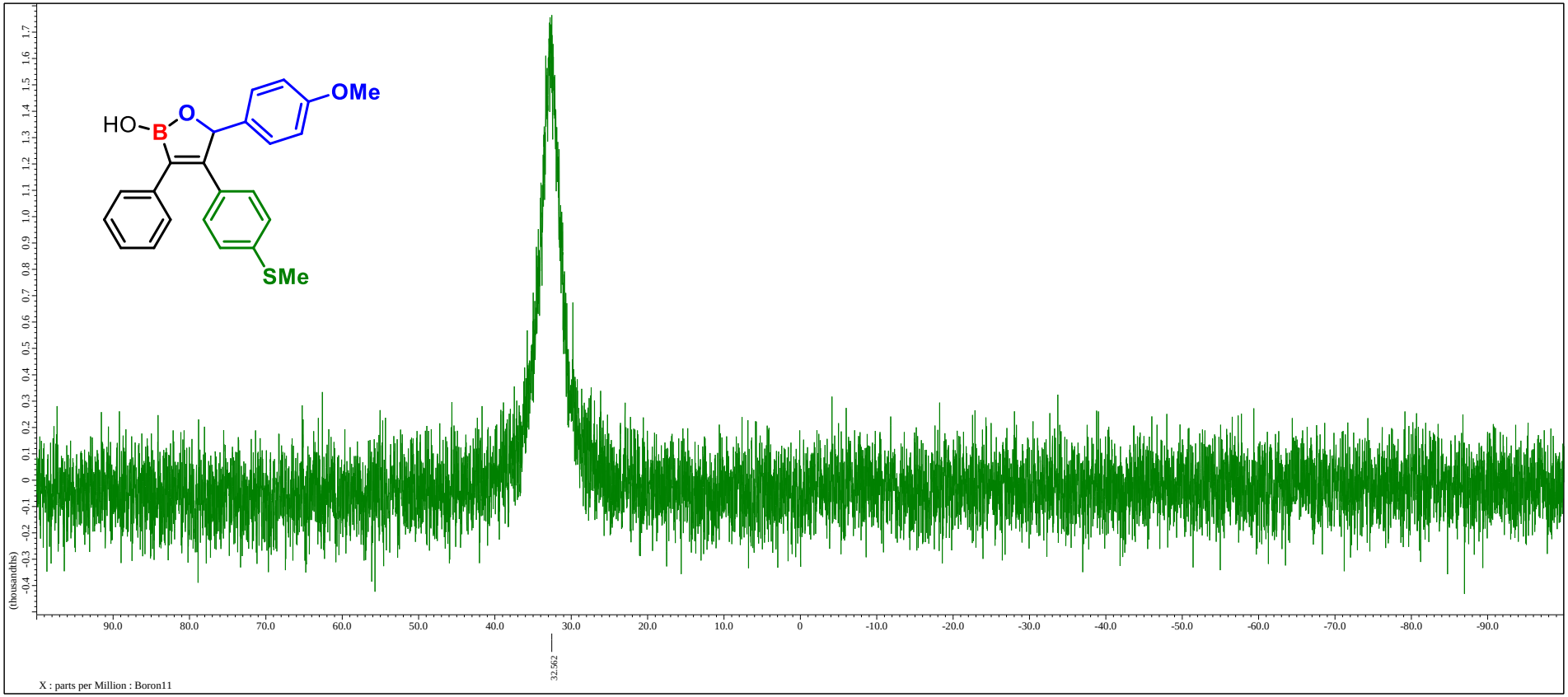

Figure S118. ^{11}B NMR (192 MHz, $CDCl_3$) spectrum of **2en-B**.

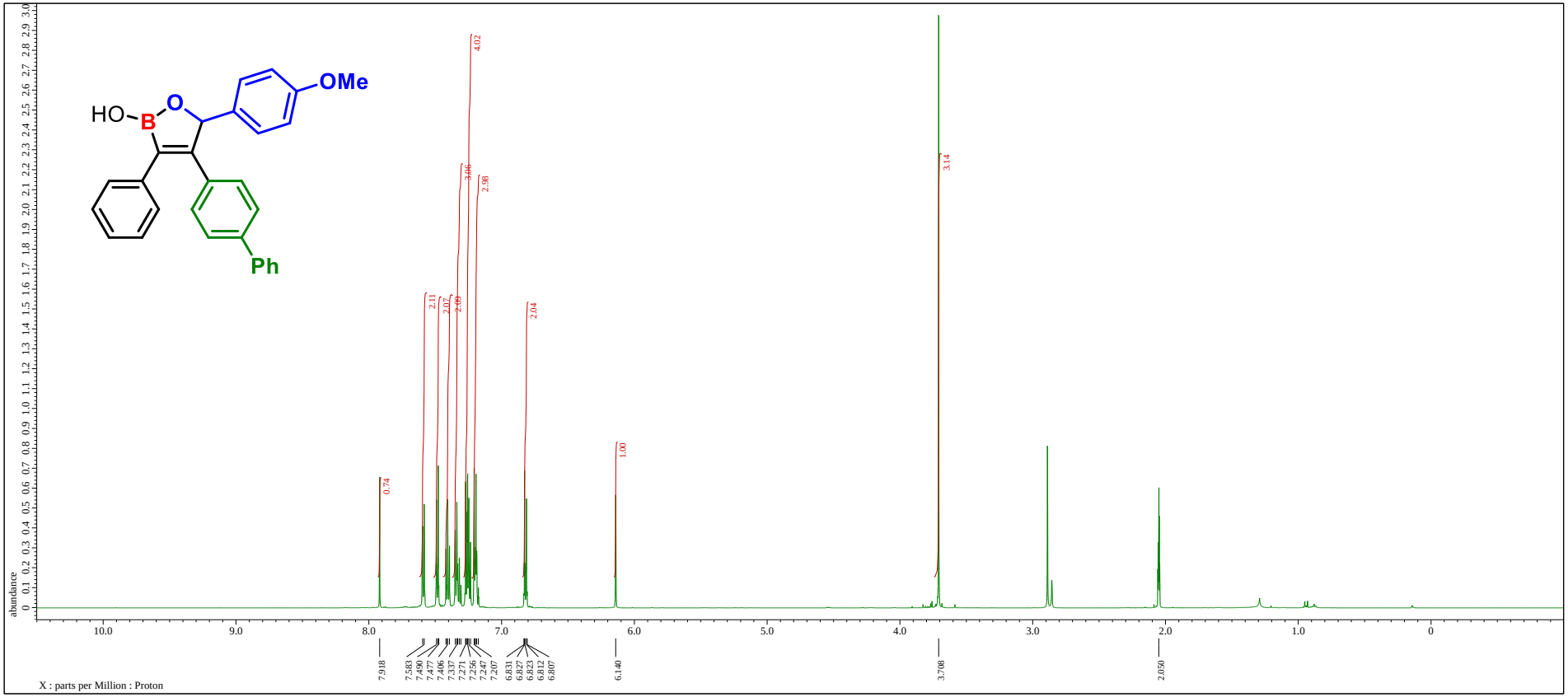

Figure S119. ^{1}H NMR (600 MHz, acetone-d_6) spectrum **2fn-B**.

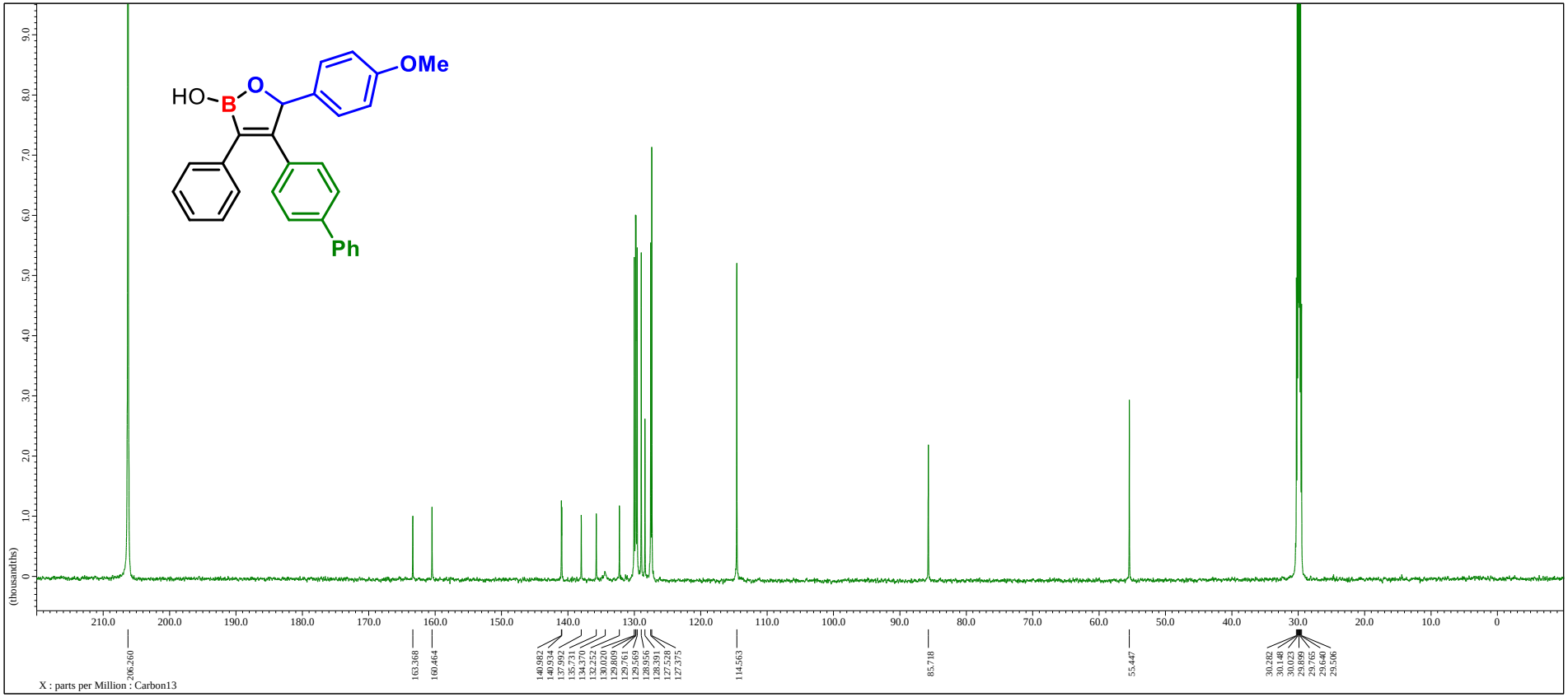

Figure S120. ^{13}C NMR (151 MHz, acetone-d_6) spectrum of **2fn-B**.

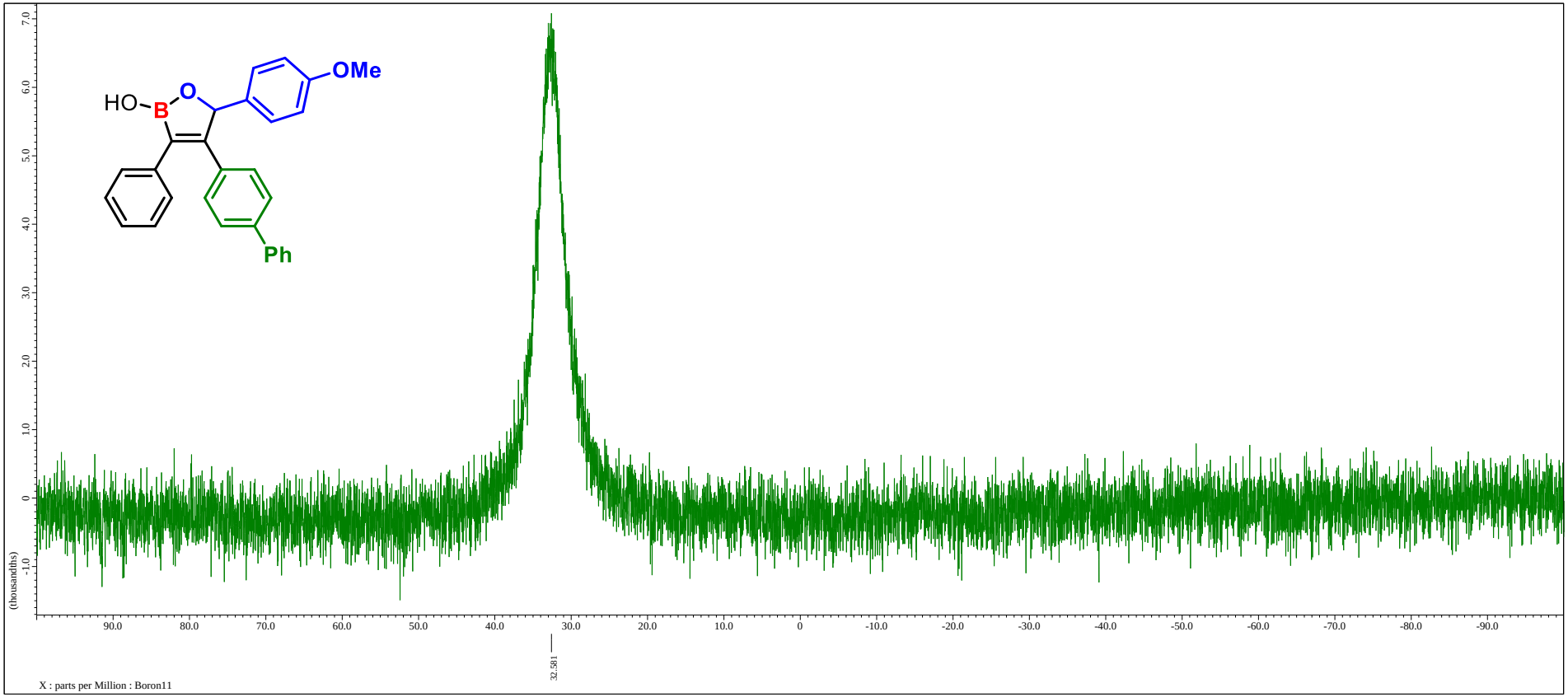

Figure S121. ^{11}B NMR (192 MHz, $CDCl_3$) spectrum of **2fn-B**.

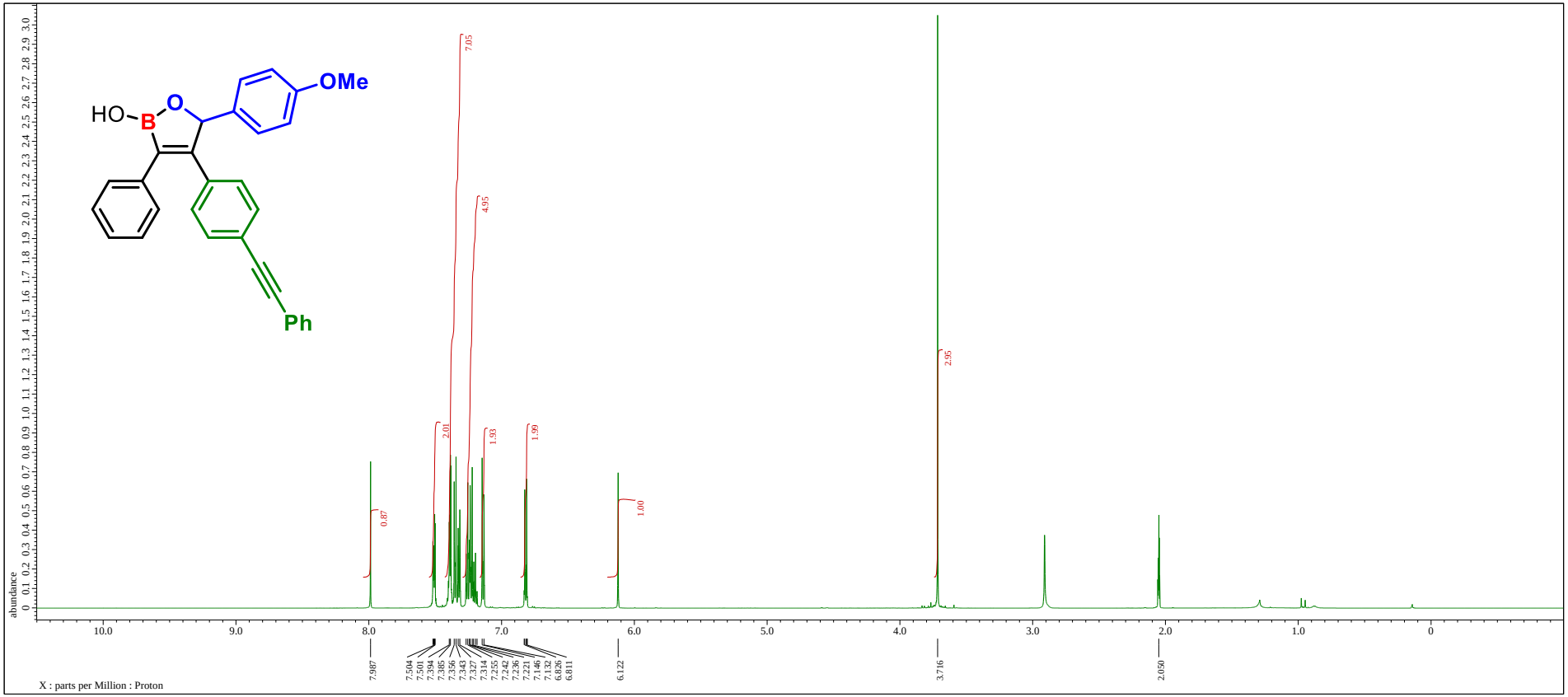

Figure S122. ^{1}H NMR (600 MHz, acetone-d_6) spectrum of **2gn-B**.

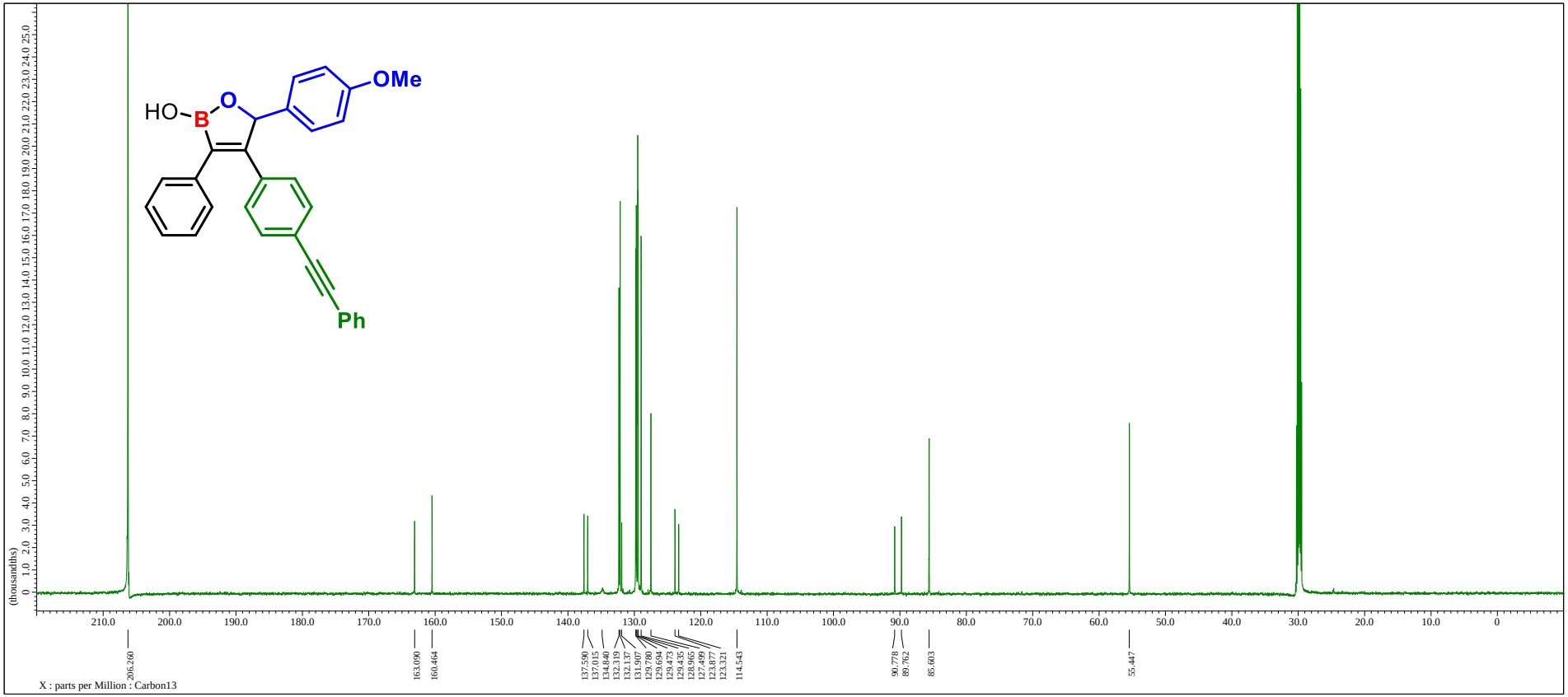

Figure S123. ^{13}C NMR (151 MHz, acetone-d_6) spectrum of **2gn-B**.

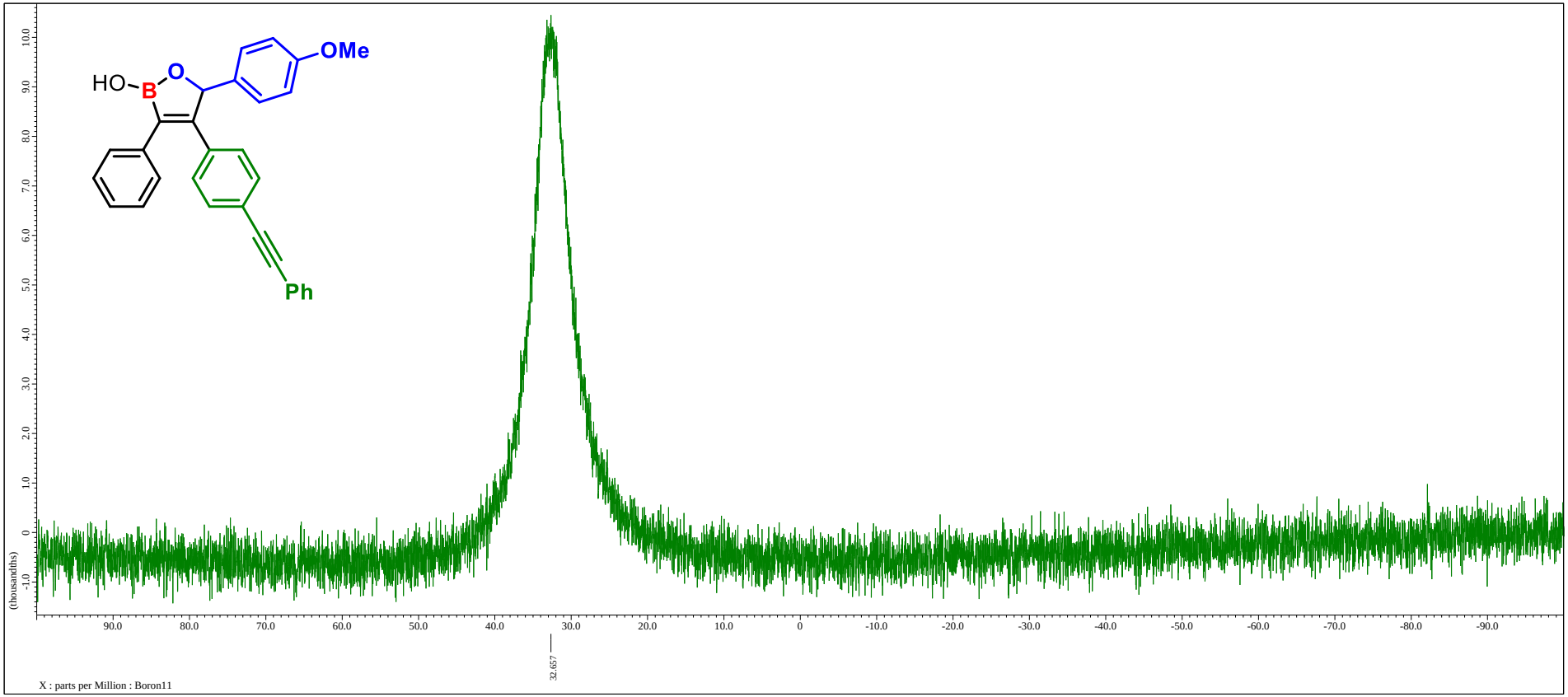

Figure S124. ^{11}B NMR (192 MHz, $CDCl_3$) spectrum of **2gn-B**.

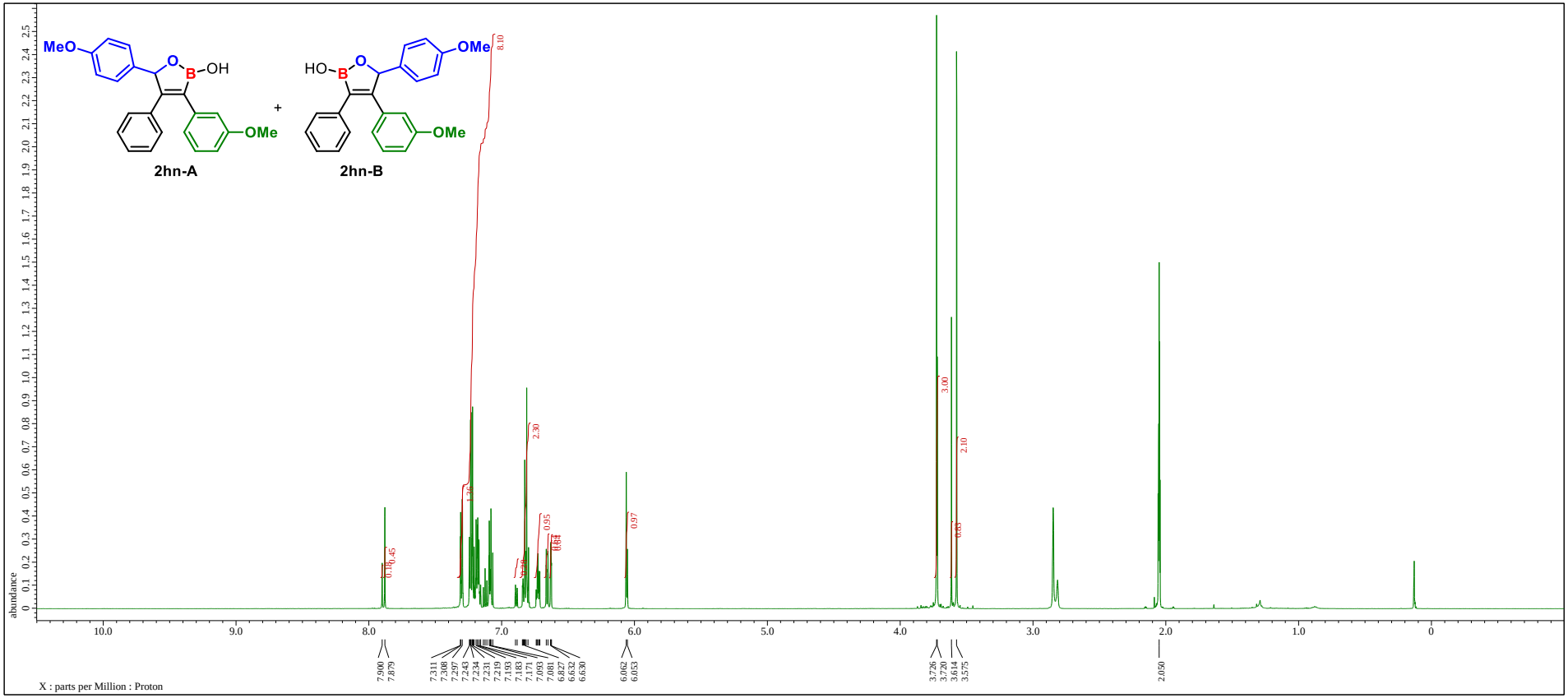

Figure S125. ^{1}H NMR (600 MHz, acetone-d_6) spectrum of **2hn-A** and **2hn-B**.

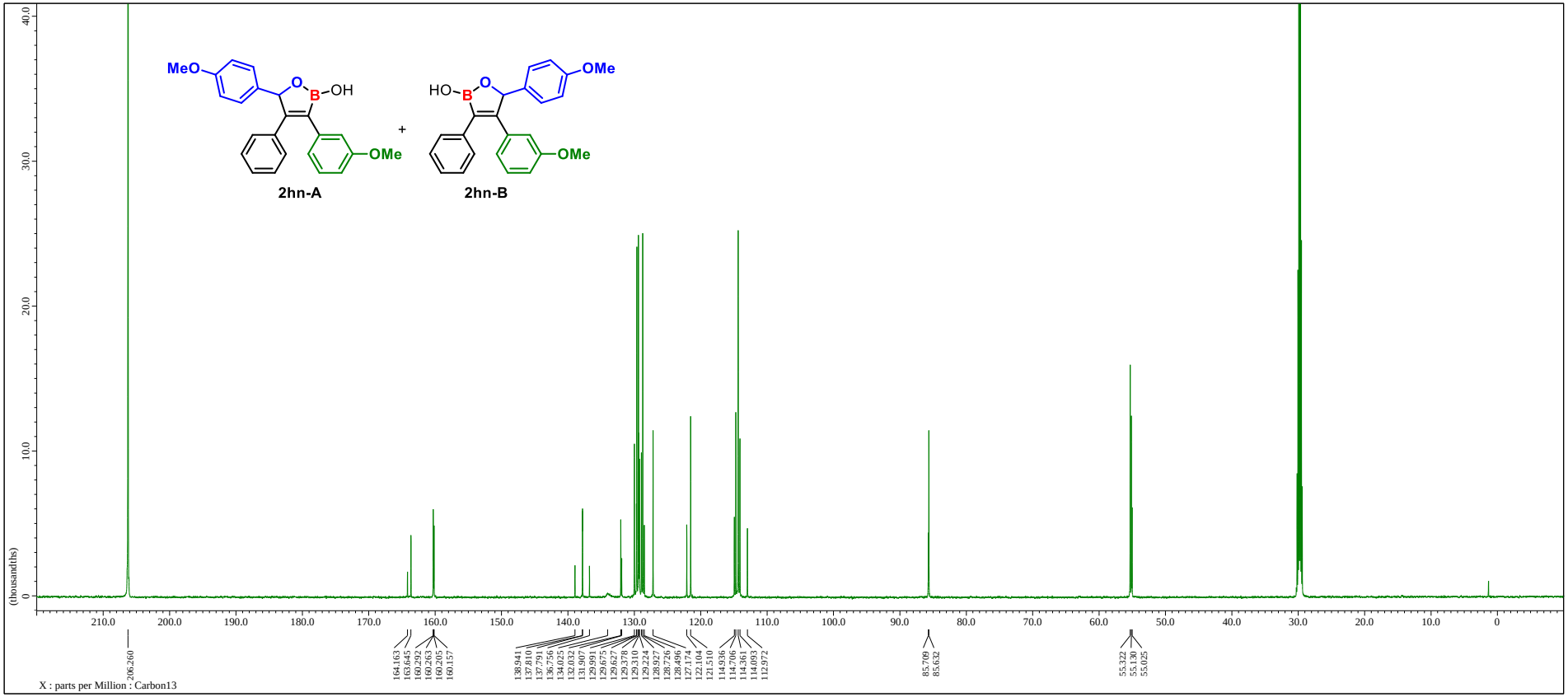

Figure S126. ^{13}C NMR (151 MHz, acetone-d_6) spectrum of **2hn-A** and **2hn-B**.

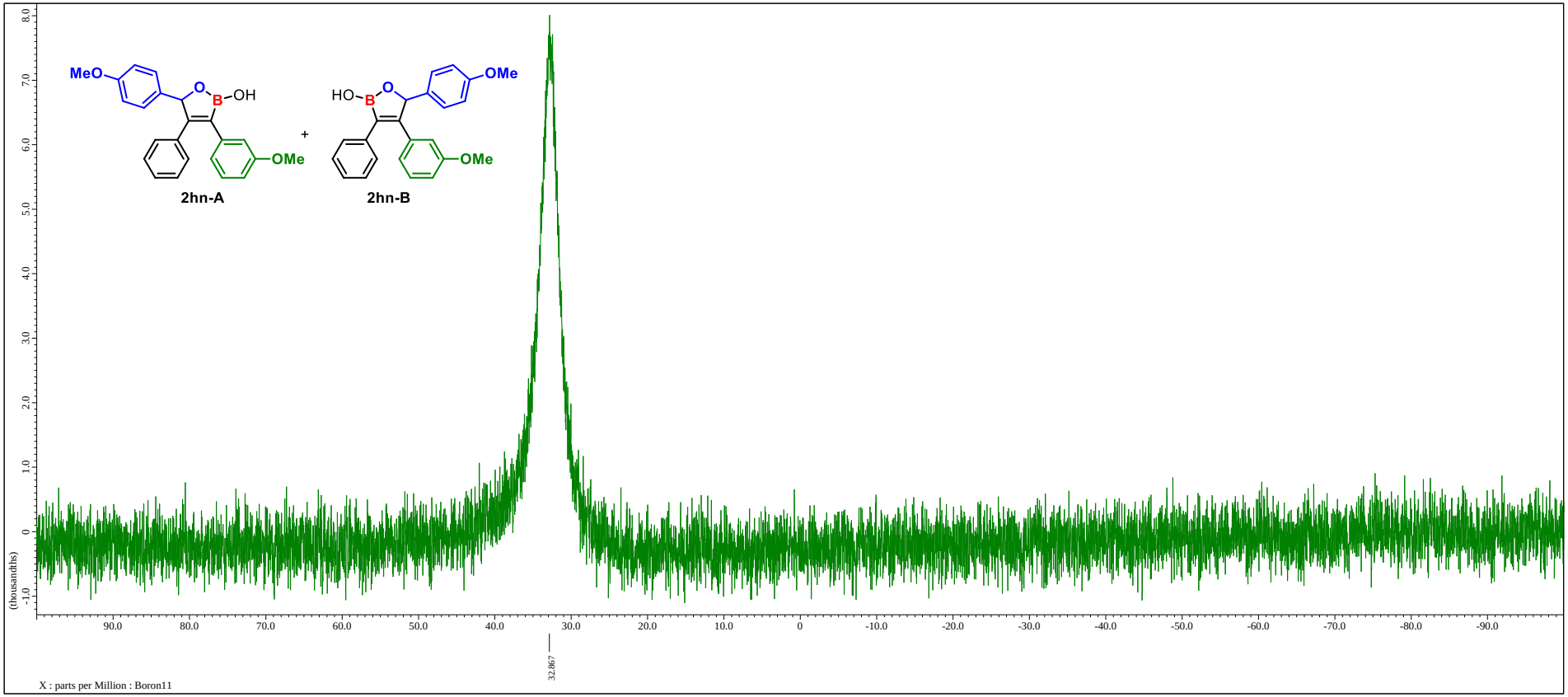

Figure S127. ^{11}B NMR (192 MHz, $CDCl_3$) spectrum of **2hn-A** and **2hn-B**.

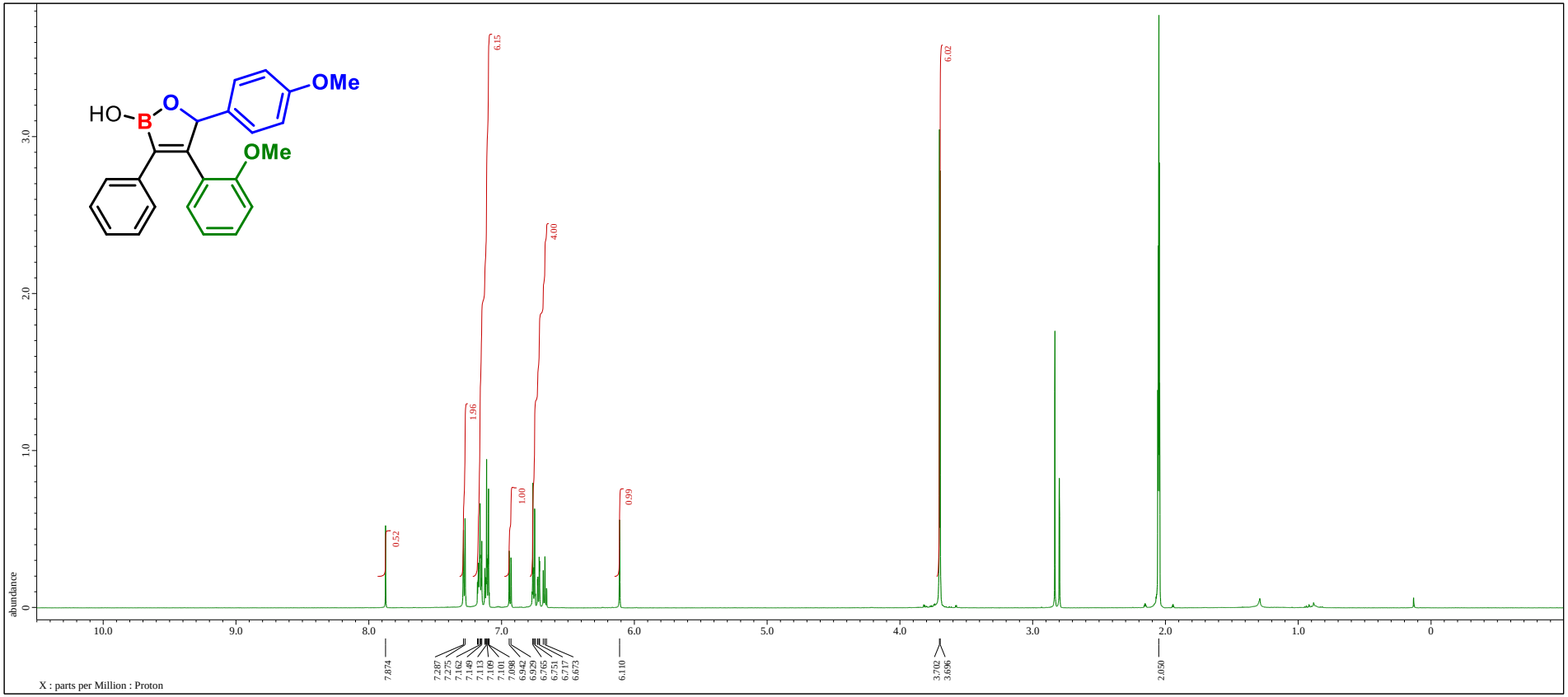

Figure S128. ^{1}H NMR (600 MHz, acetone-d_6) spectrum of **2in-B**.

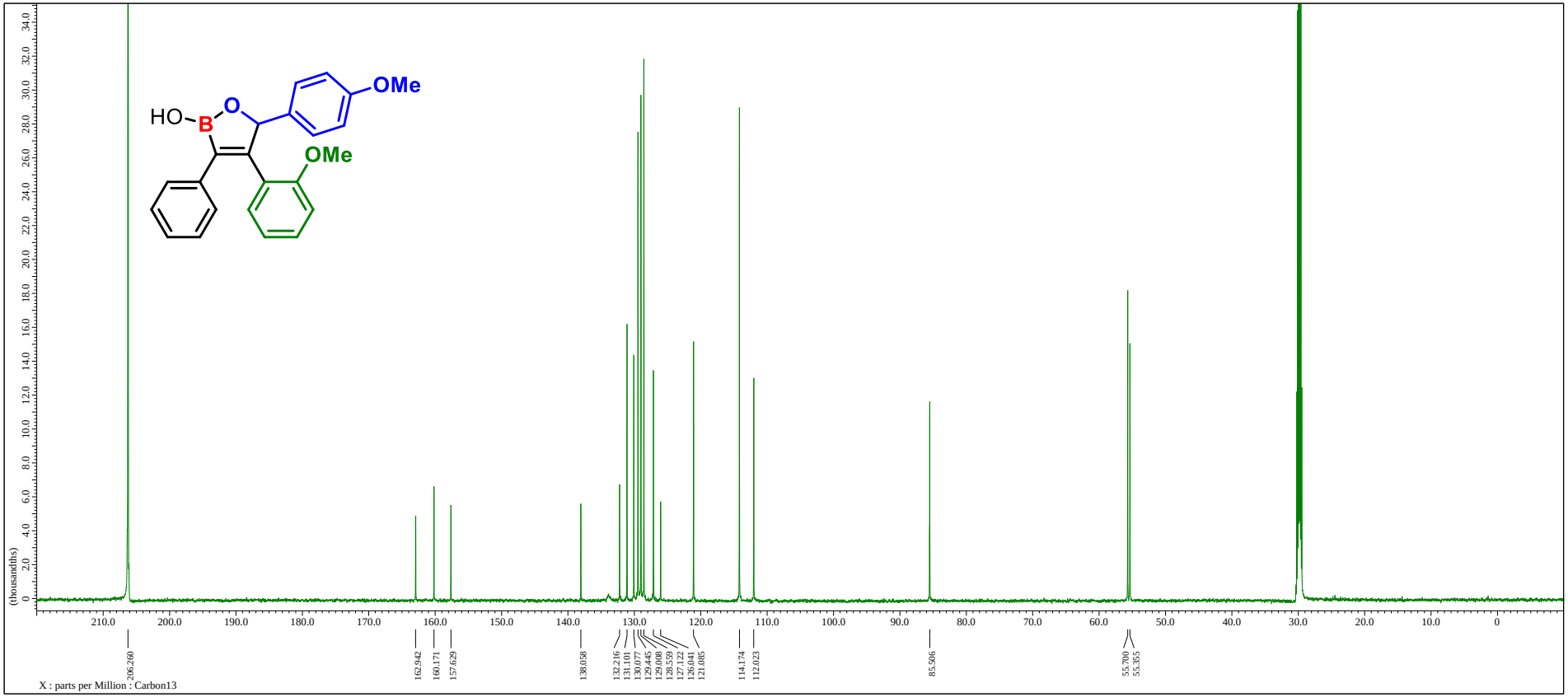

Figure S129. ^{13}C NMR (151 MHz, acetone-d_6) spectrum of **2in-B**.

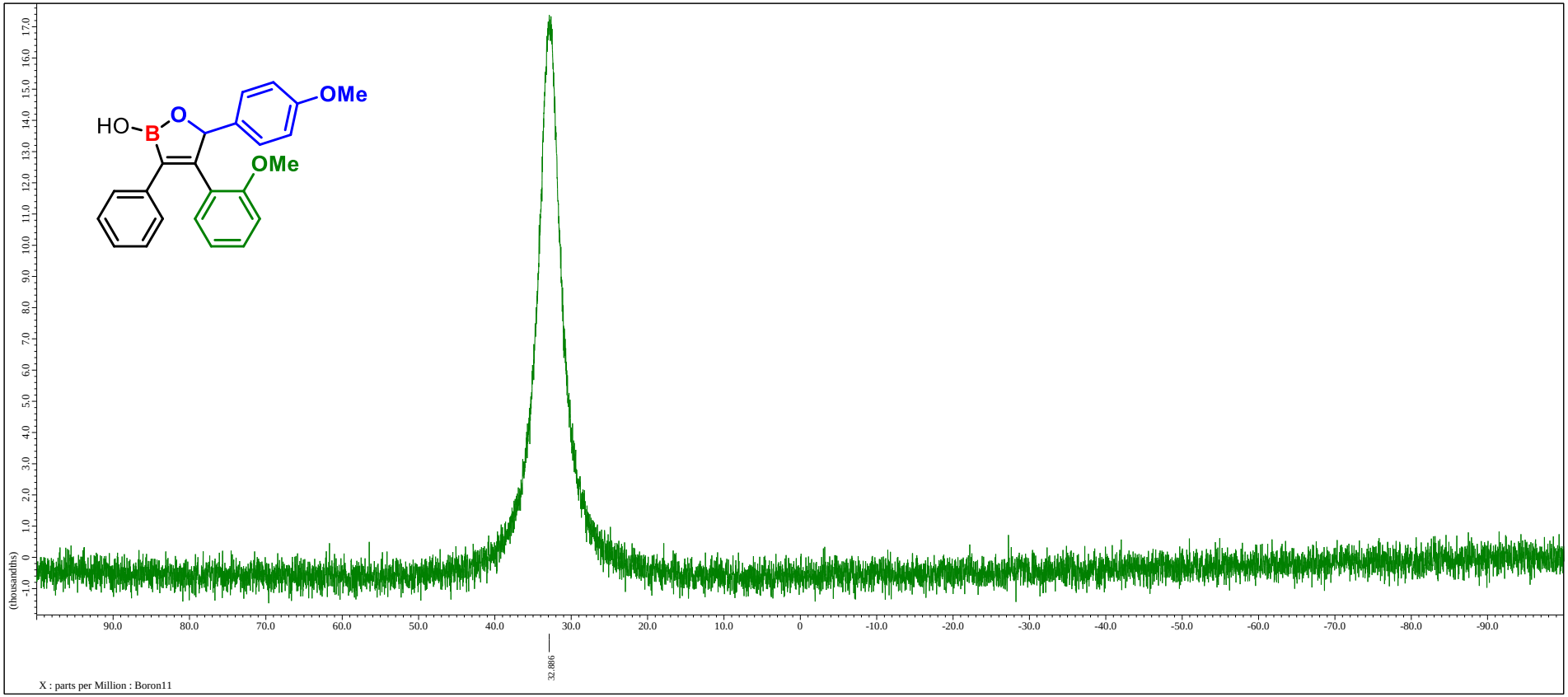

Figure S130. ^{11}B NMR (192 MHz, $CDCl_3$) spectrum of **2in-B**.

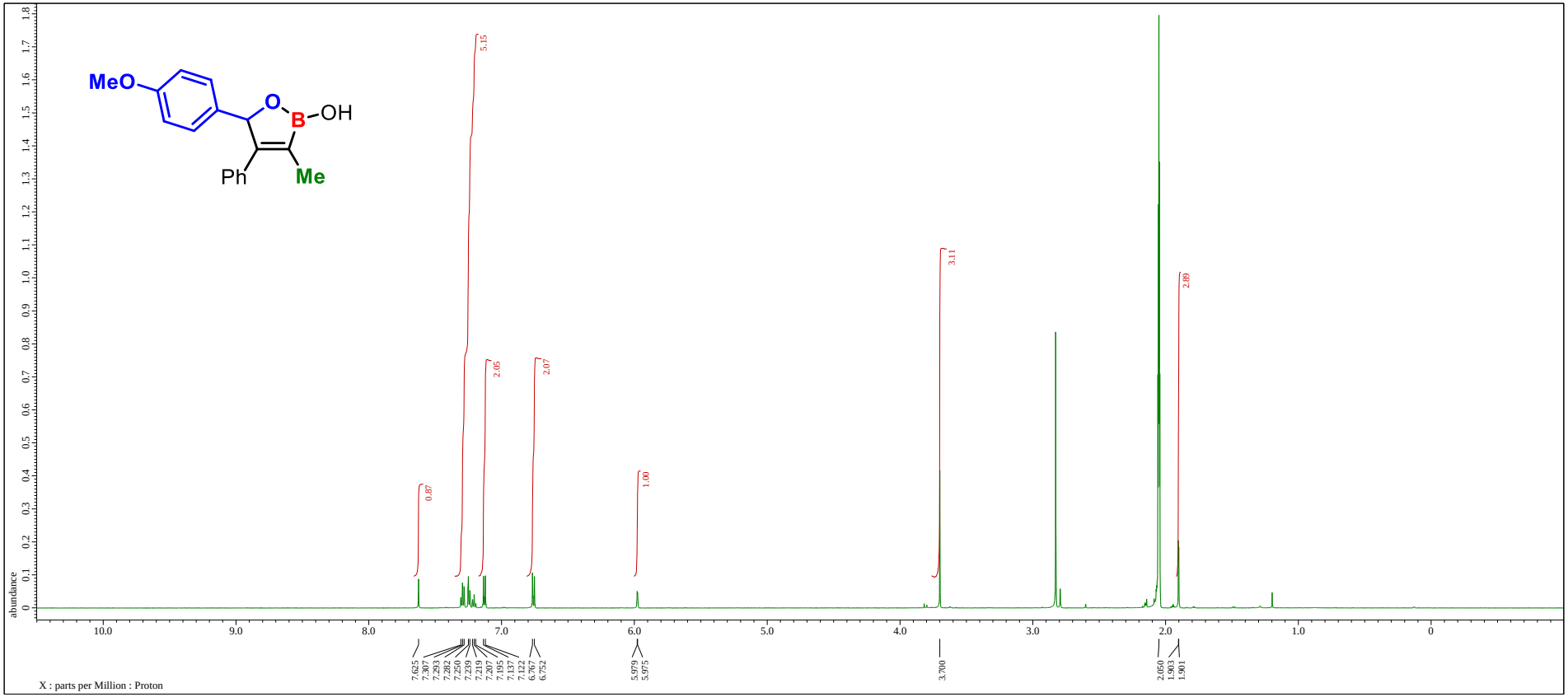

Figure S131. ^{1}H NMR (600 MHz, acetone-d_6) spectrum of **2jn-A**.

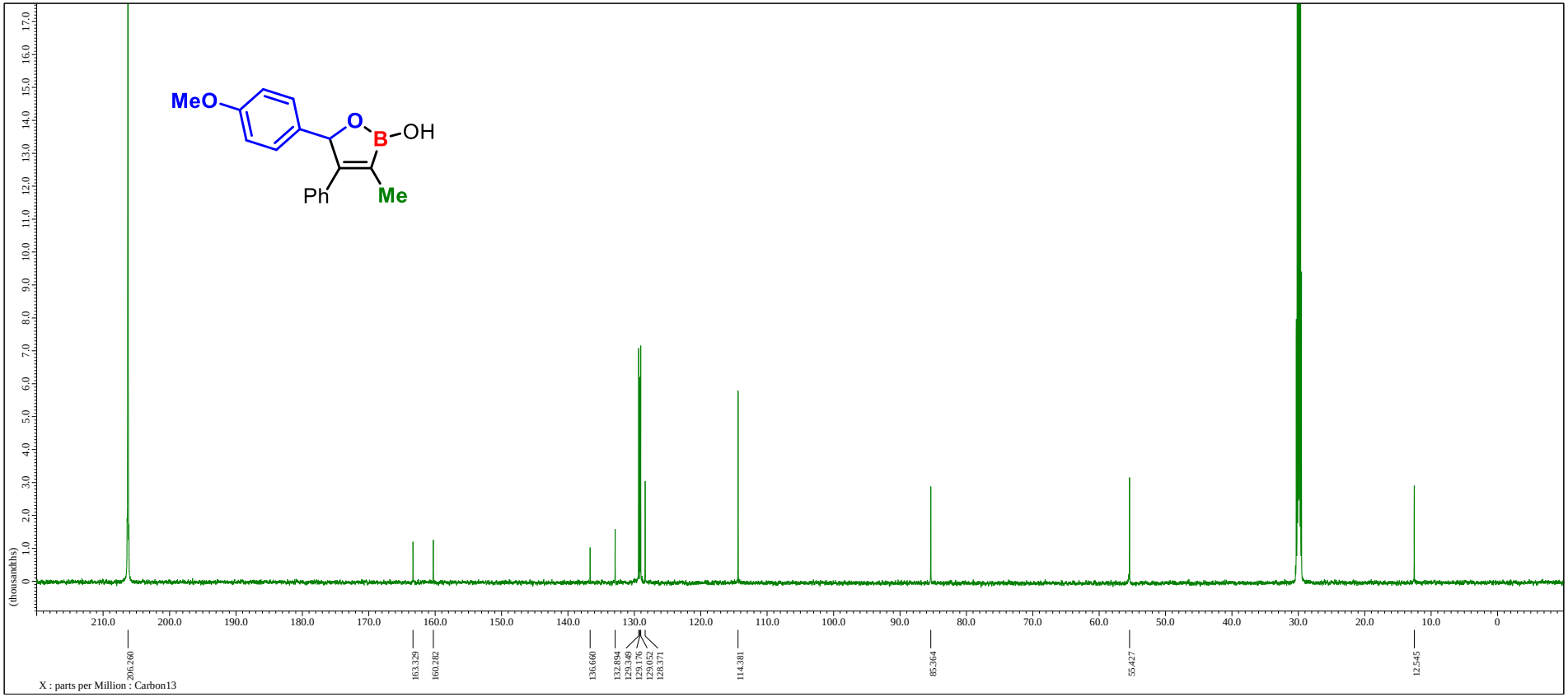

Figure S132. ^{13}C NMR (151 MHz, acetone-d_6) spectrum of **2jn-A**.

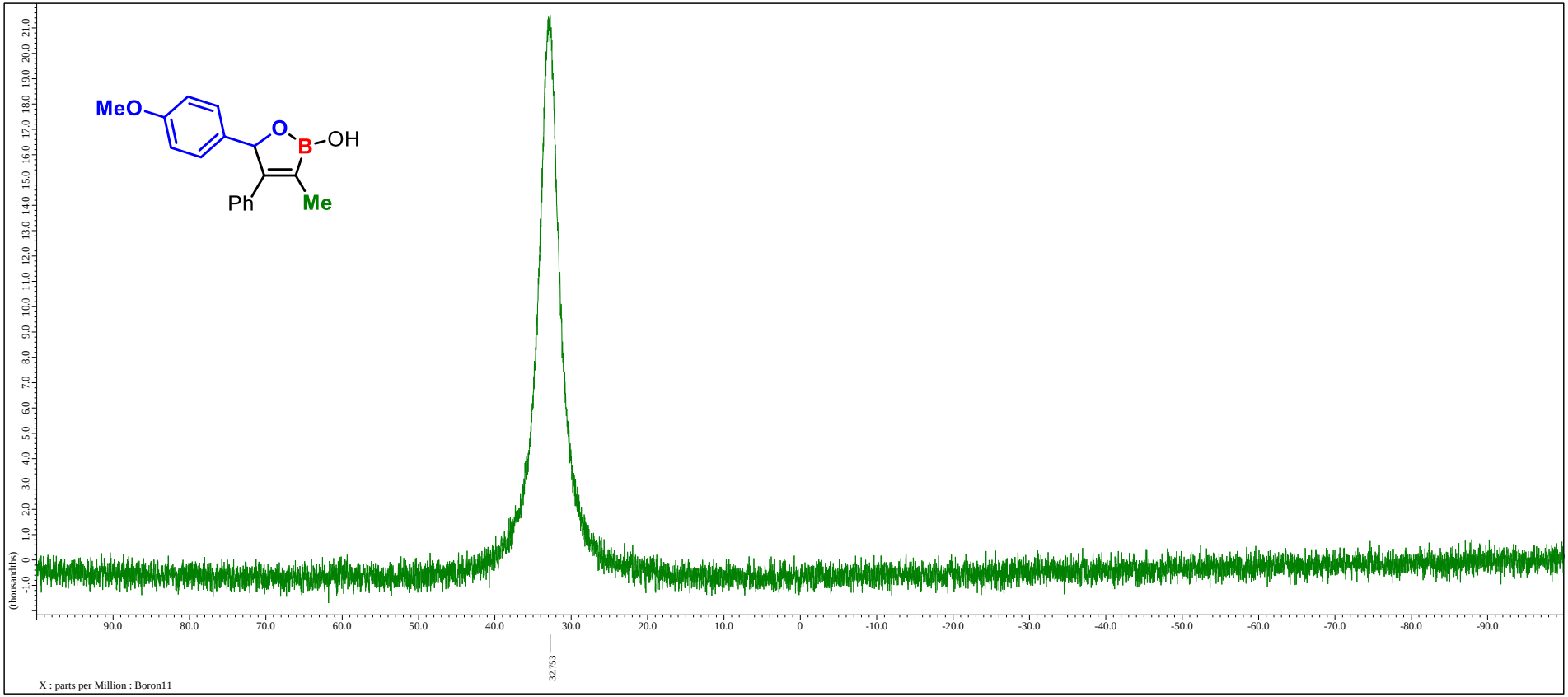

Figure S133. ^{11}B NMR (192 MHz, $CDCl_3$) spectrum of **2jn-A**.

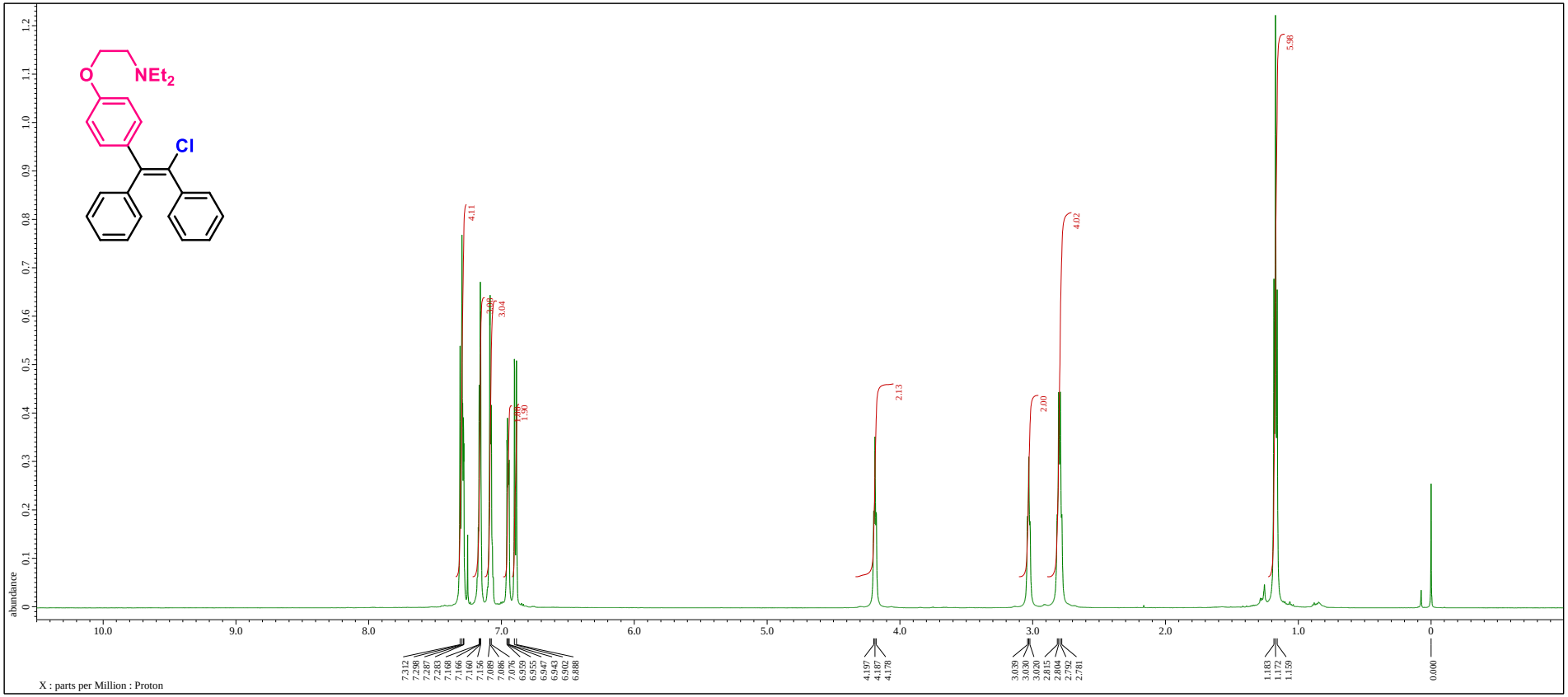

Figure S134. ^{1}H NMR (600 MHz, $CDCl_3$) spectrum of **5**.

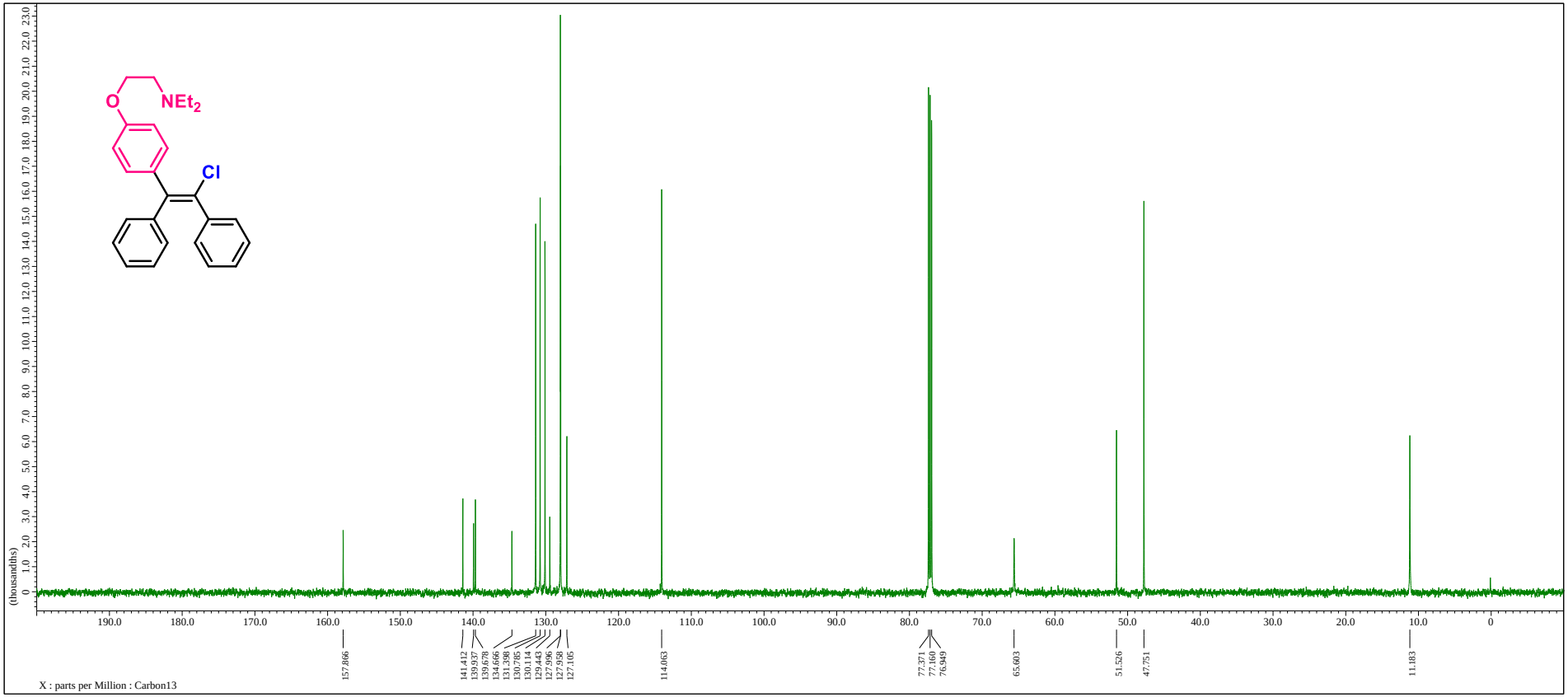

Figure S135. ^{13}C NMR (151 MHz, $CDCl_3$) spectrum of **5**.

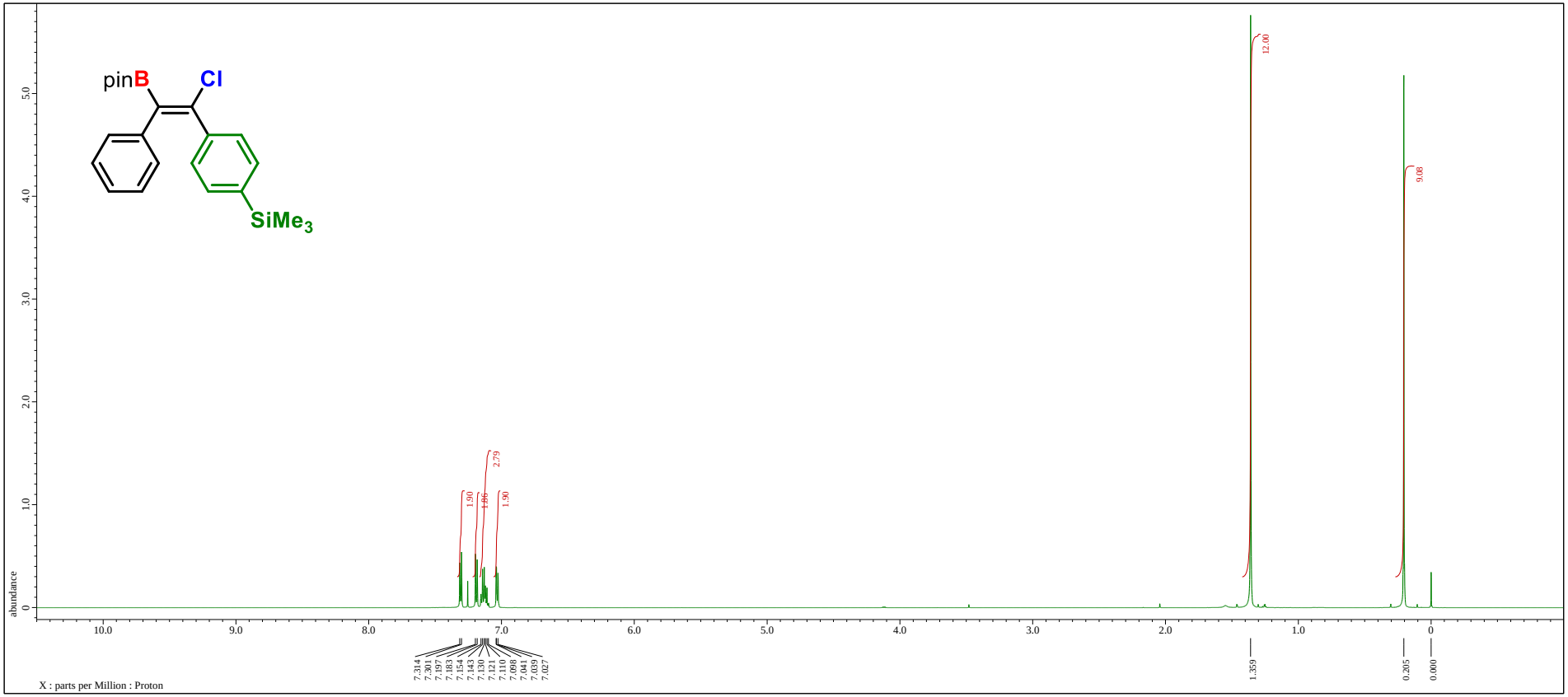

Figure S136. ^{1}H NMR (600 MHz, $CDCl_3$) spectrum of **2eg**.

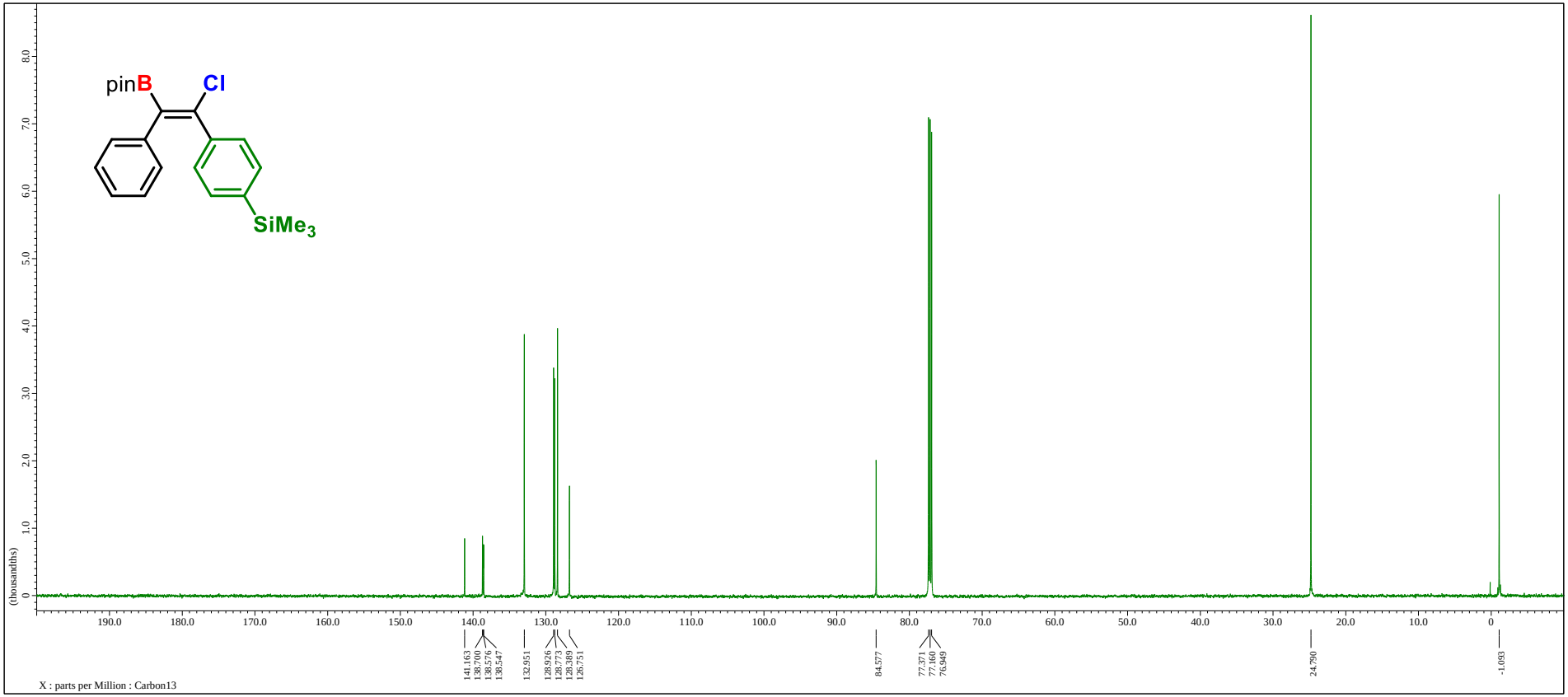

Figure S137. ^{13}C NMR (151 MHz, $CDCl_3$) spectrum of **2eg**.

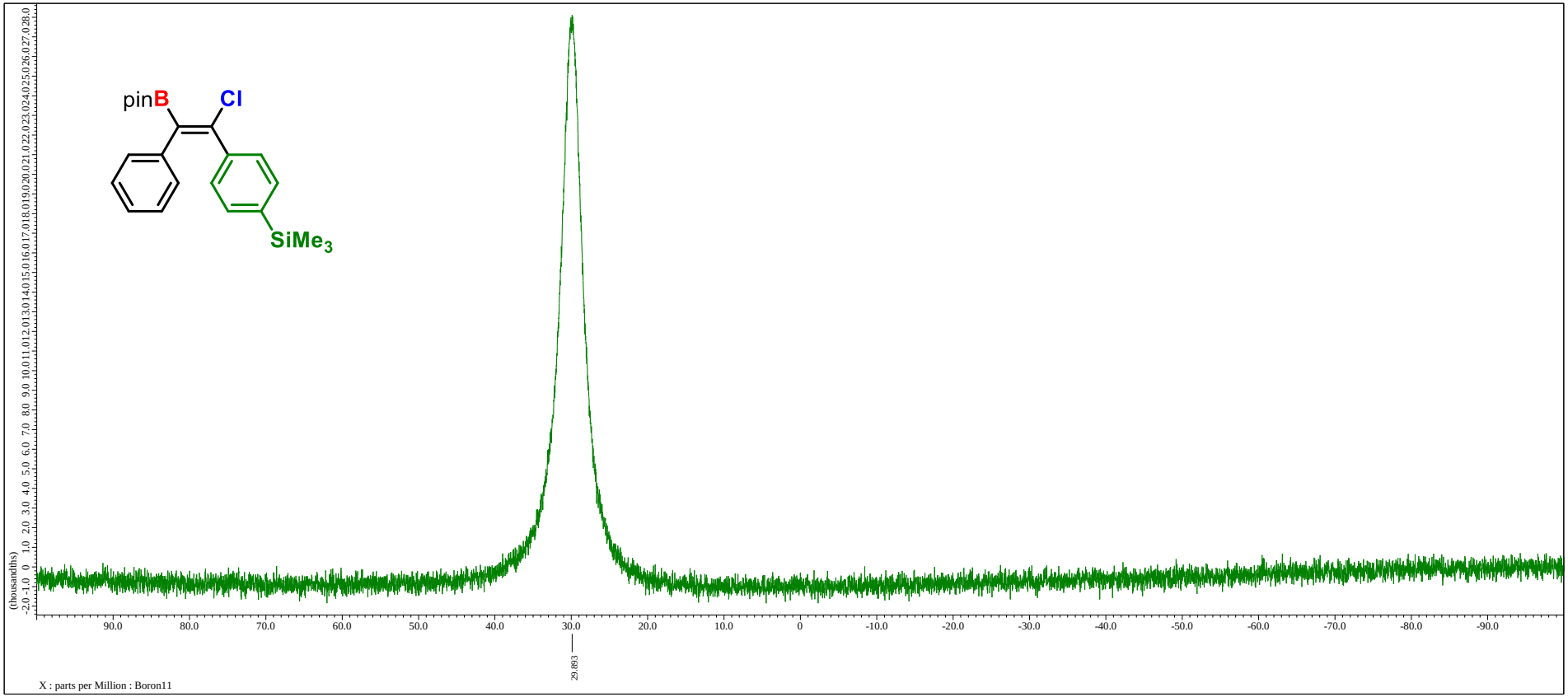

Figure S138. ^{11}B NMR (192 MHz, $CDCl_3$) spectrum of **2eg**.

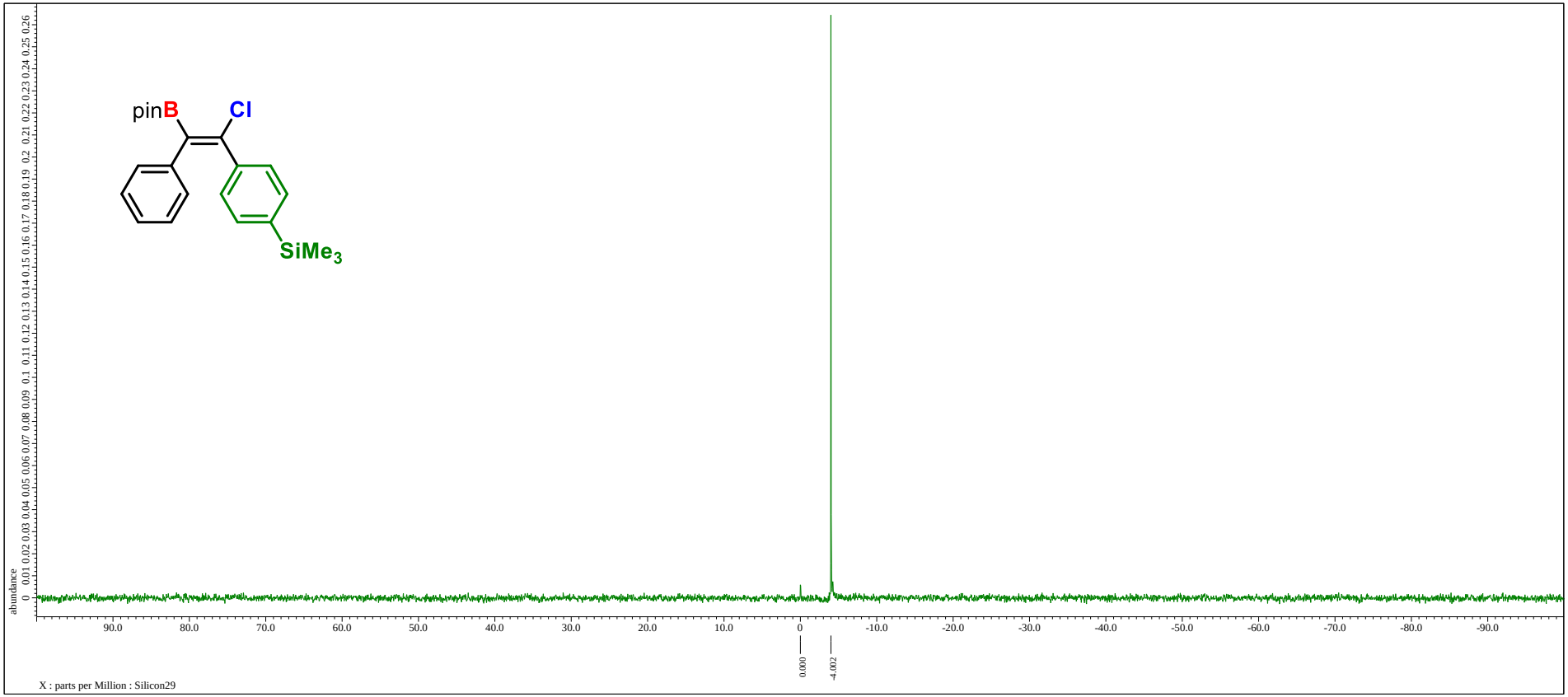

Figure S139. ^{29}Si NMR (119 MHz, $CDCl_3$) spectrum of **2eg**.

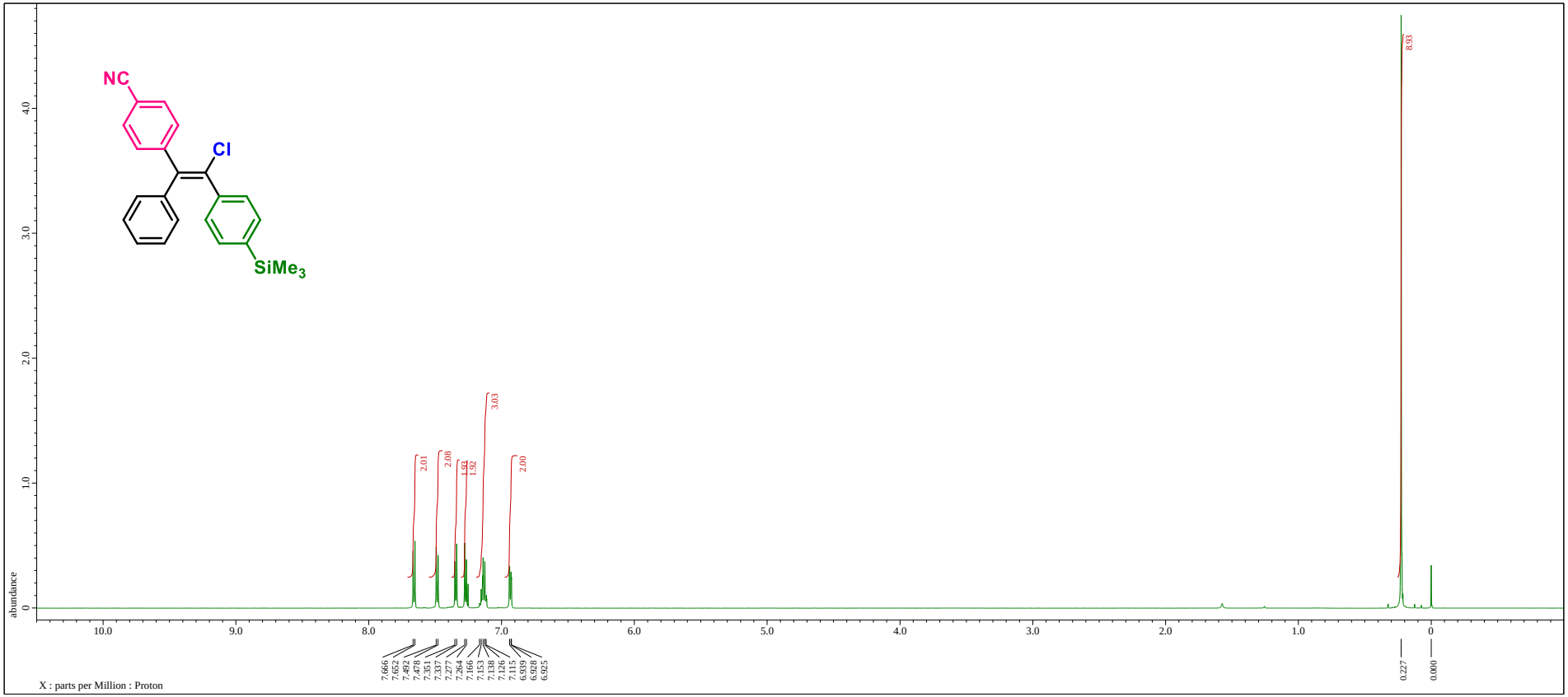

Figure S140. ^{1}H NMR (600 MHz, $CDCl_3$) spectrum of **6**.

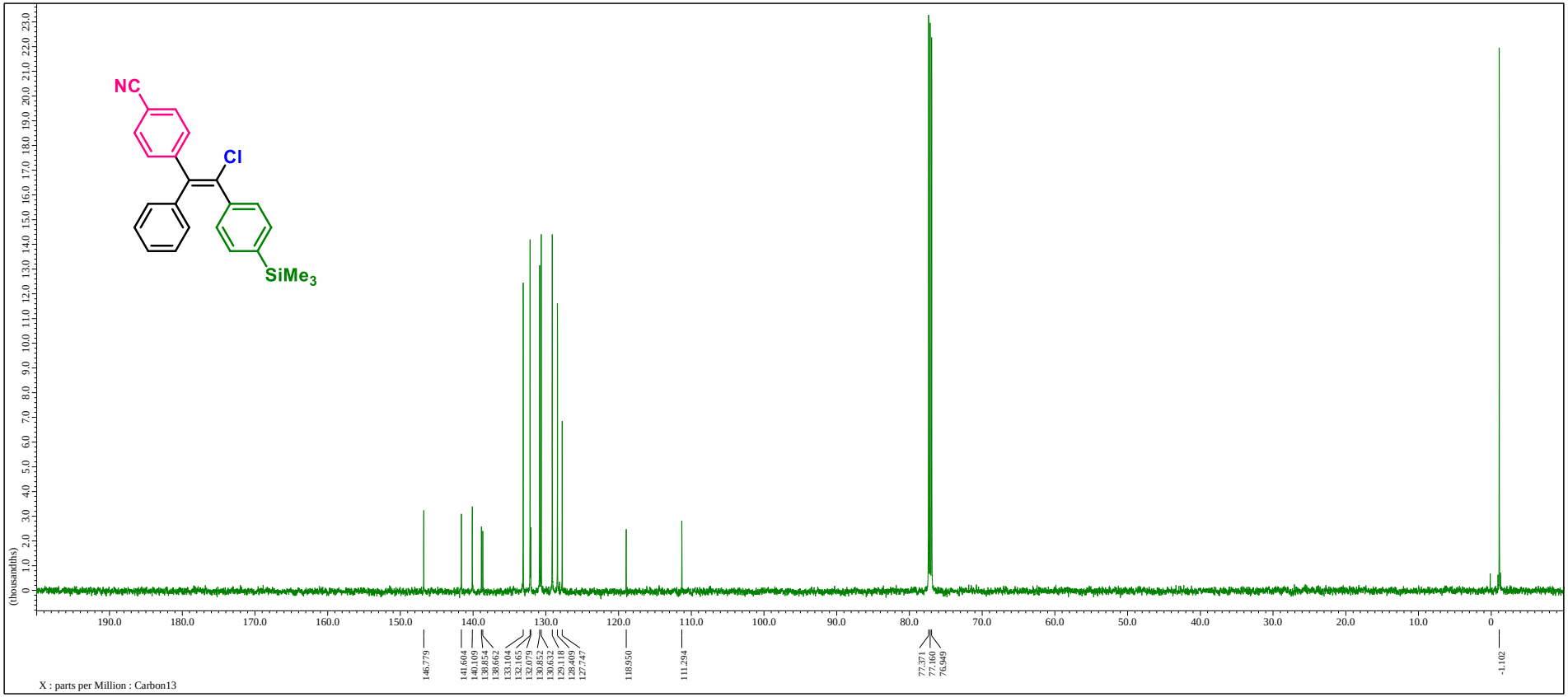

Figure S141. ^{13}C NMR (151 MHz, $CDCl_3$) spectrum of **6**.

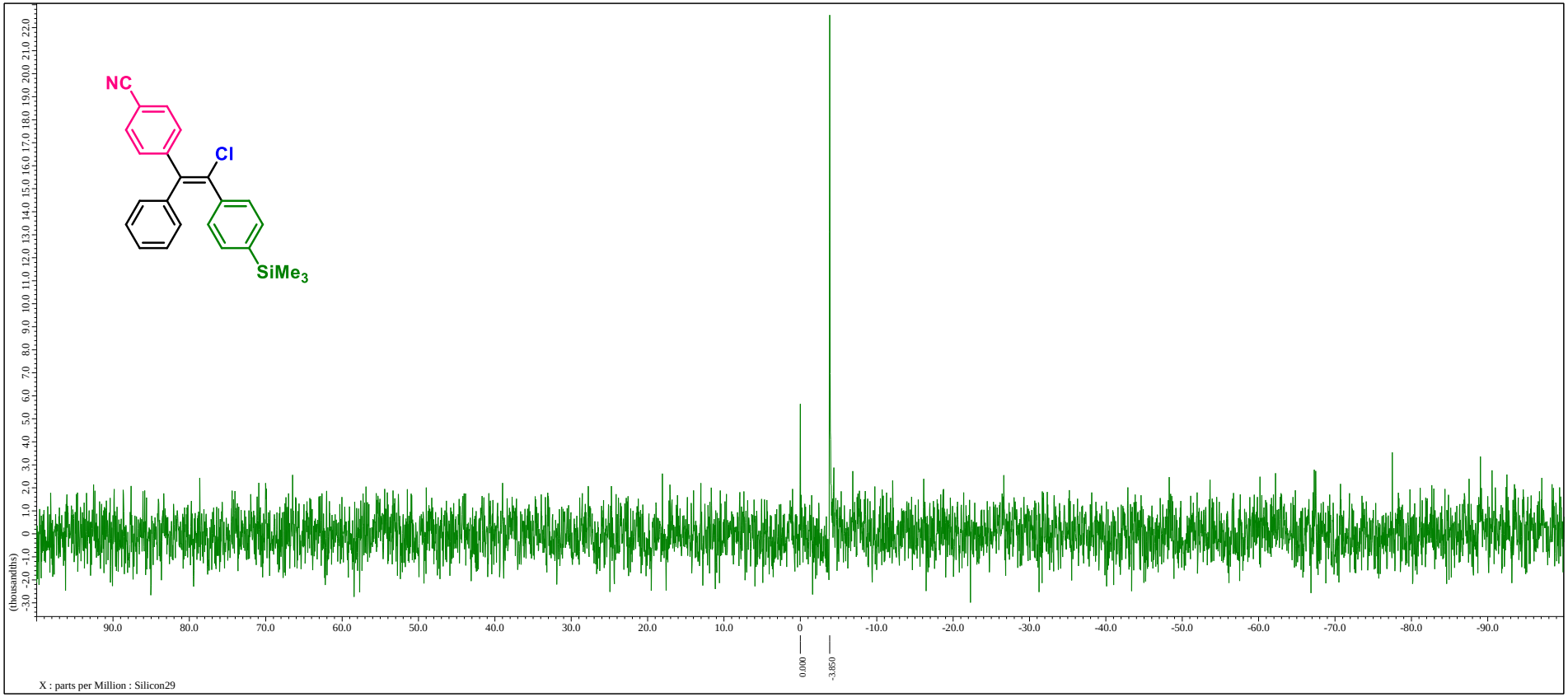

Figure S142. ^{29}Si NMR (119 MHz, $CDCl_3$) spectrum of **6**.

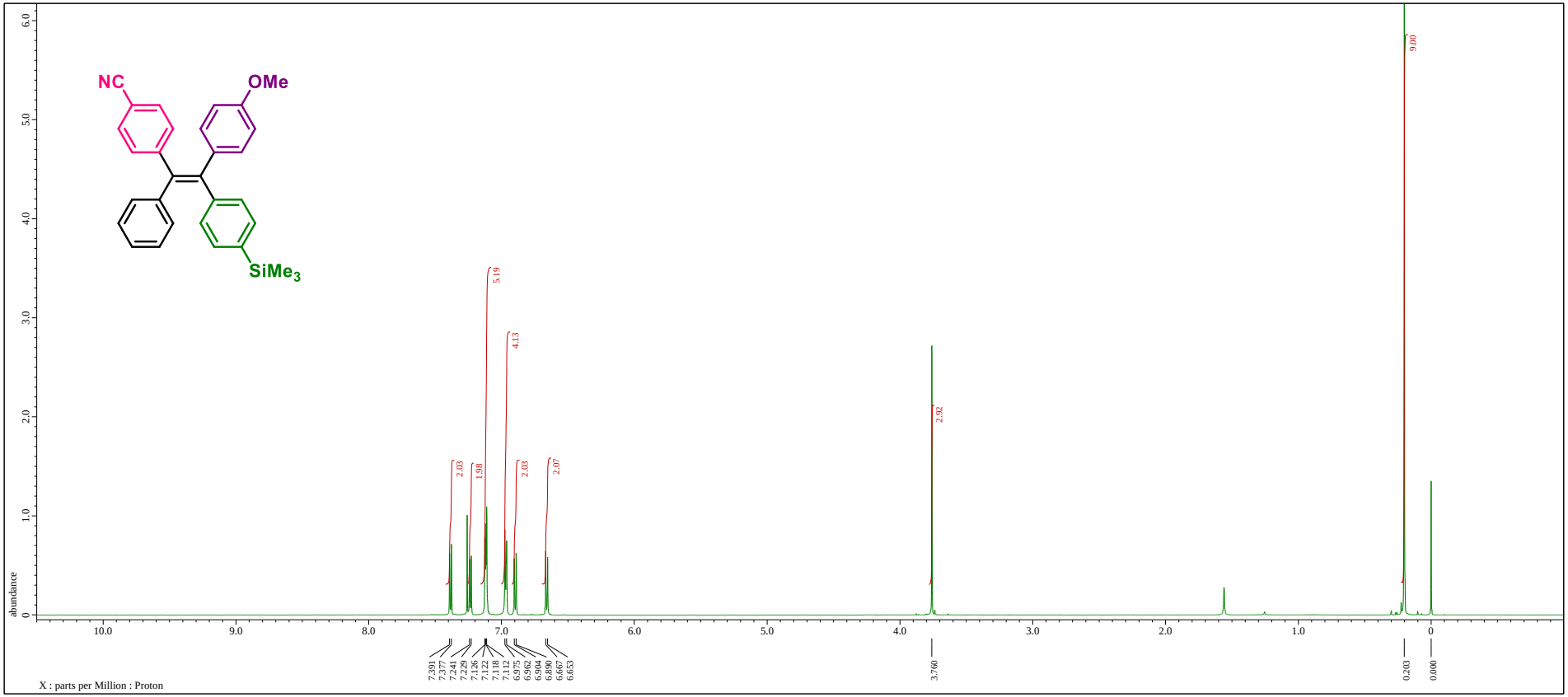

Figure S143. ^{1}H NMR (600 MHz, $CDCl_3$) spectrum of **7**.

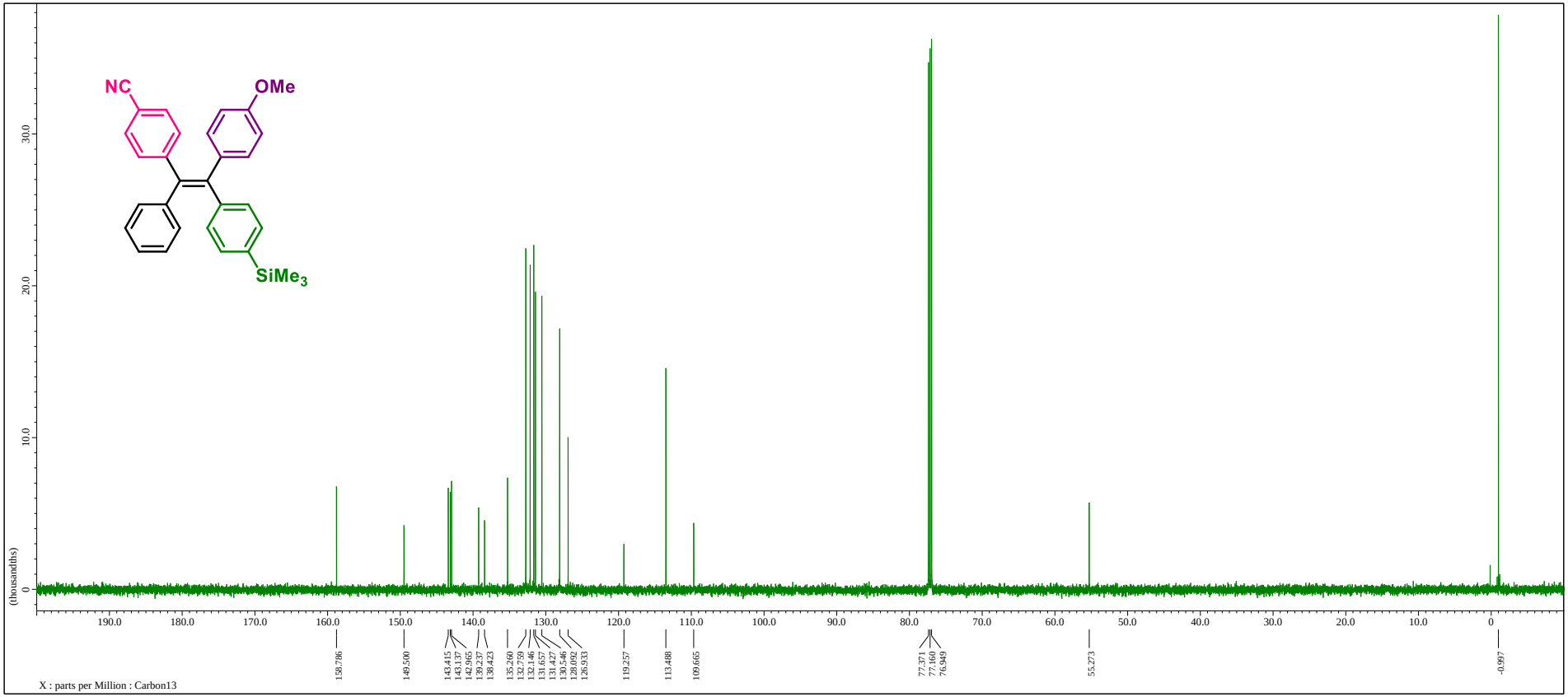

Figure S144. ^{13}C NMR (151 MHz, $CDCl_3$) spectrum of **7**.

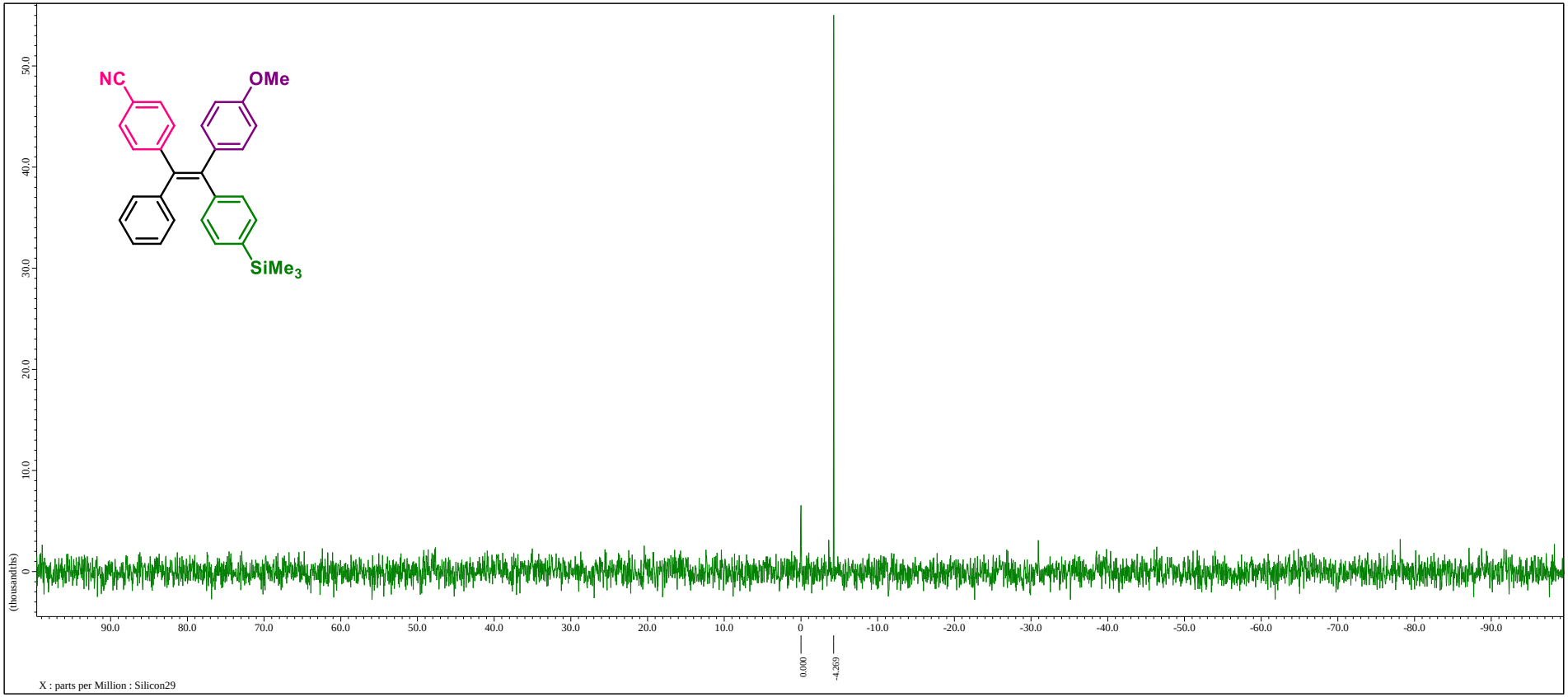

Figure S145. ^{29}Si NMR (119 MHz, $CDCl_3$) spectrum of **7**.

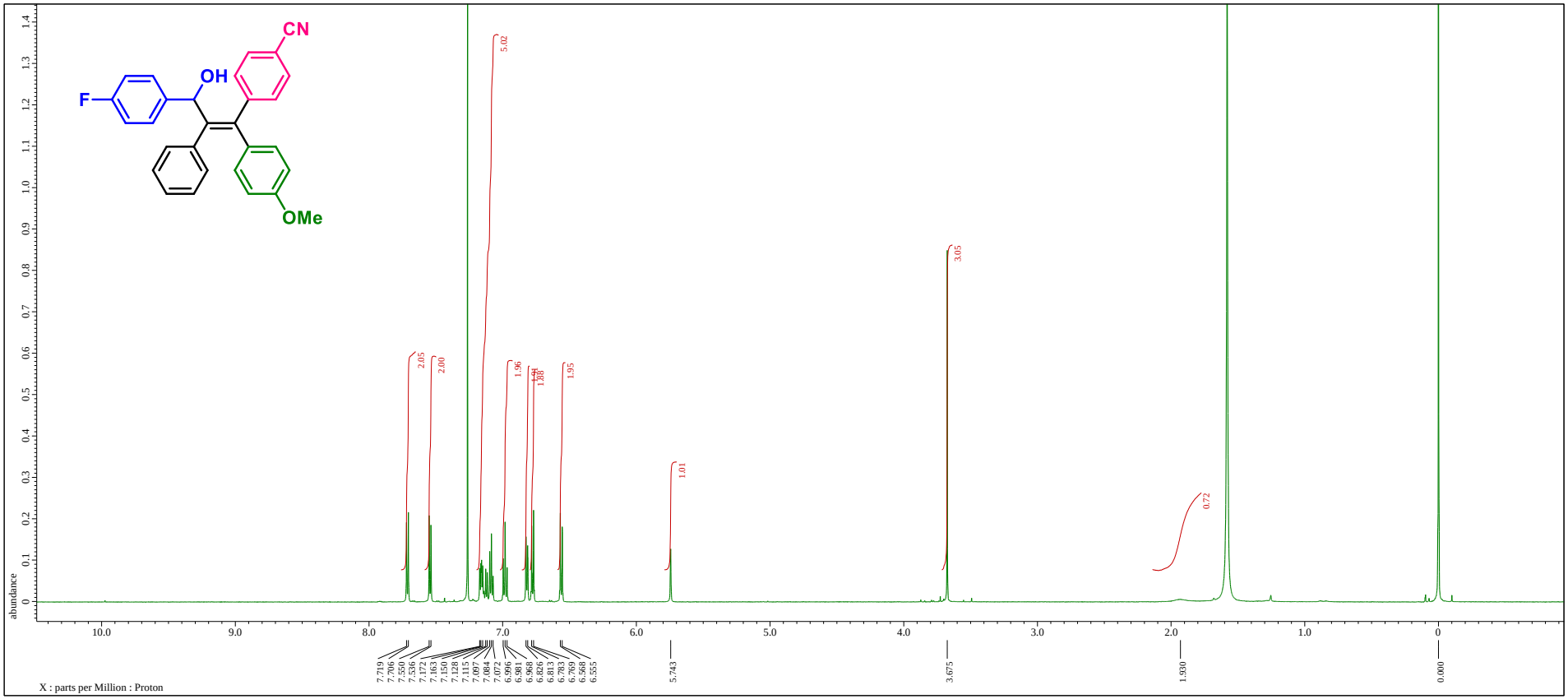

Figure S146. ^{1}H NMR (600 MHz, $CDCl_3$) spectrum of **8**.

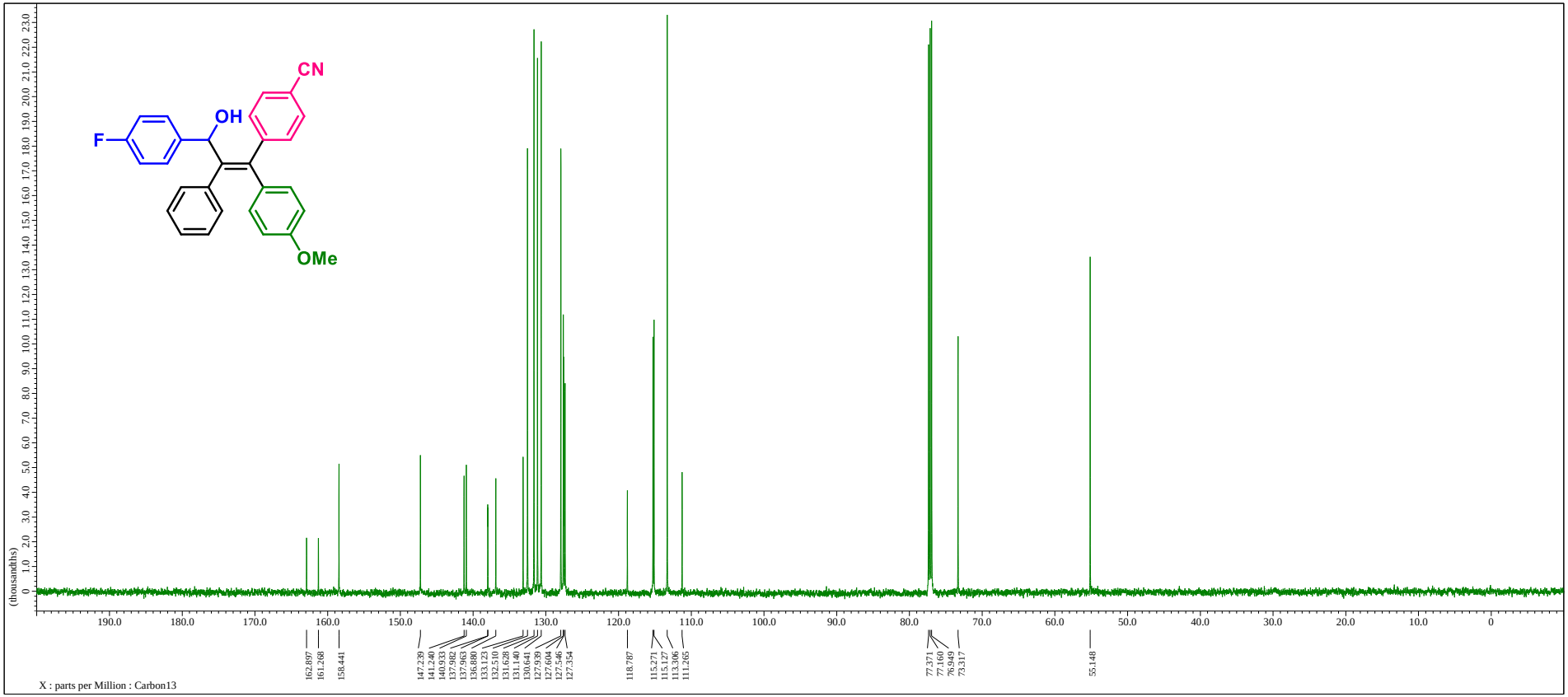

Figure S147. ^{13}C NMR (151 MHz, $CDCl_3$) spectrum of **8**.

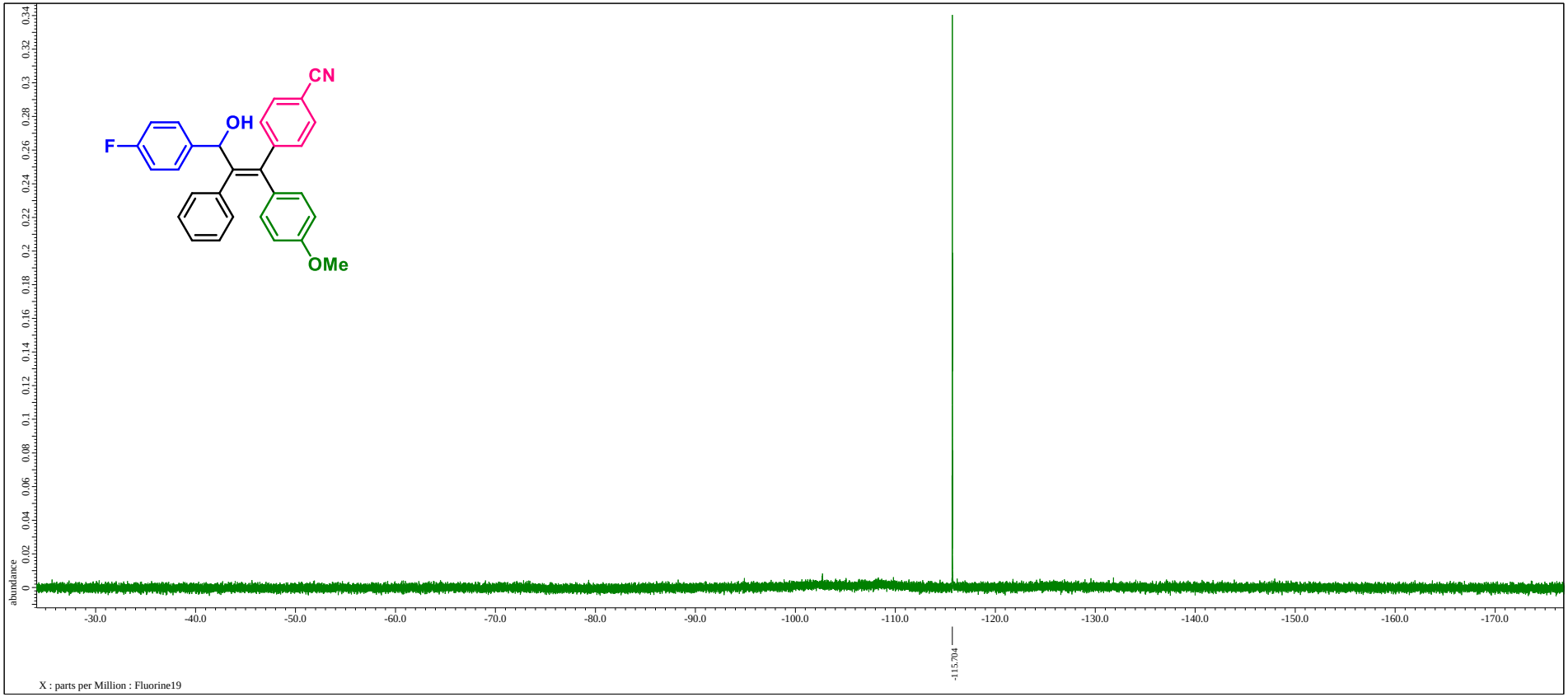

Figure S148. ^{19}F NMR (564 MHz, $CDCl_3$) spectrum of **8**.

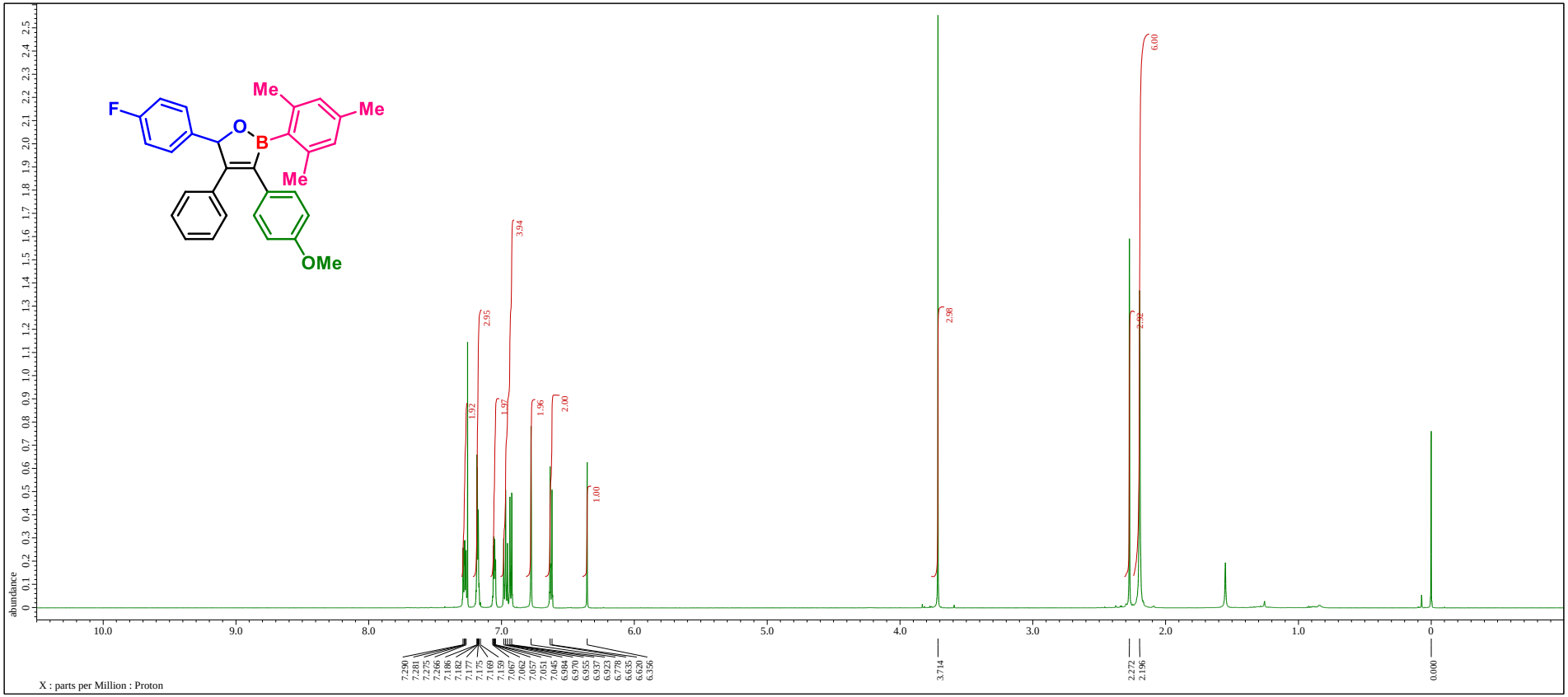

Figure S149. ^{1}H NMR (600 MHz, $CDCl_3$) spectrum of **9**.

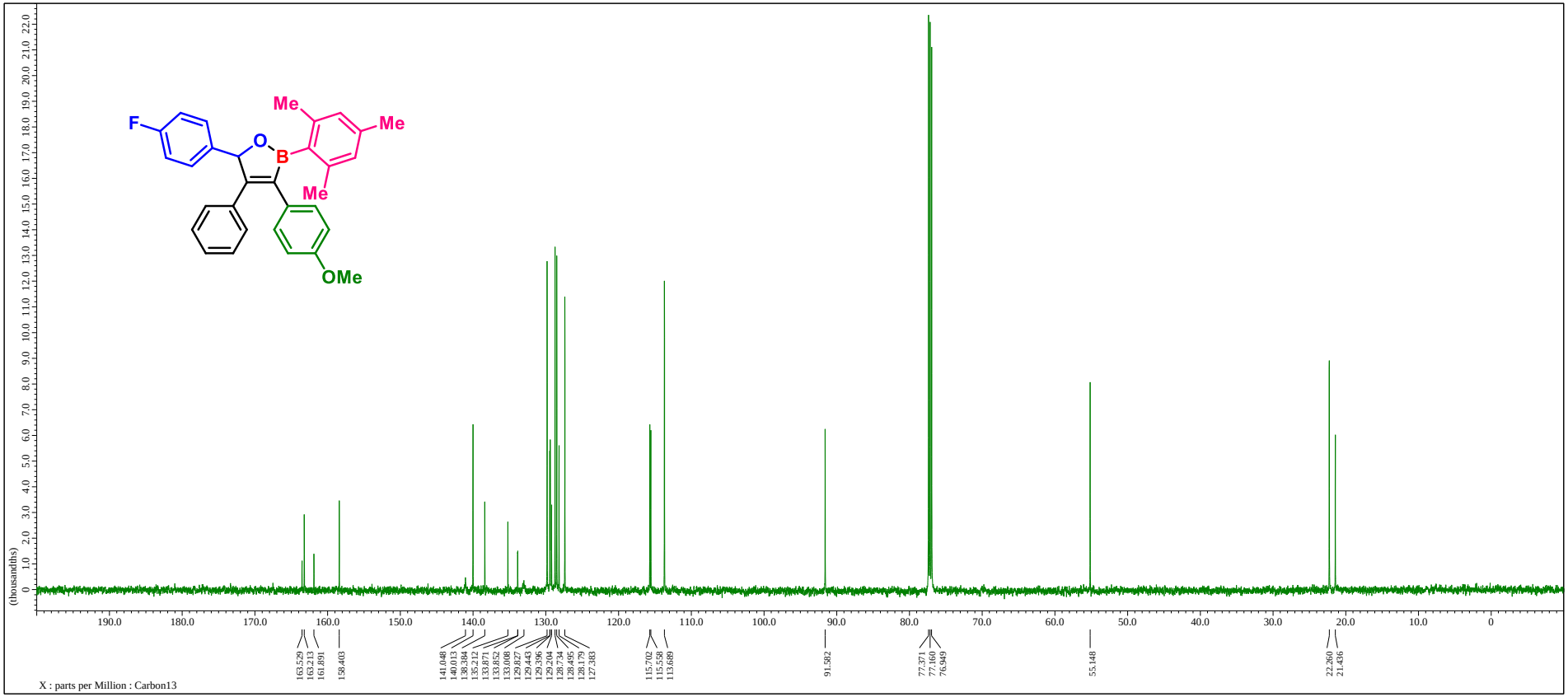

Figure S150. ^{13}C NMR (151 MHz, $CDCl_3$) spectrum of **9**.

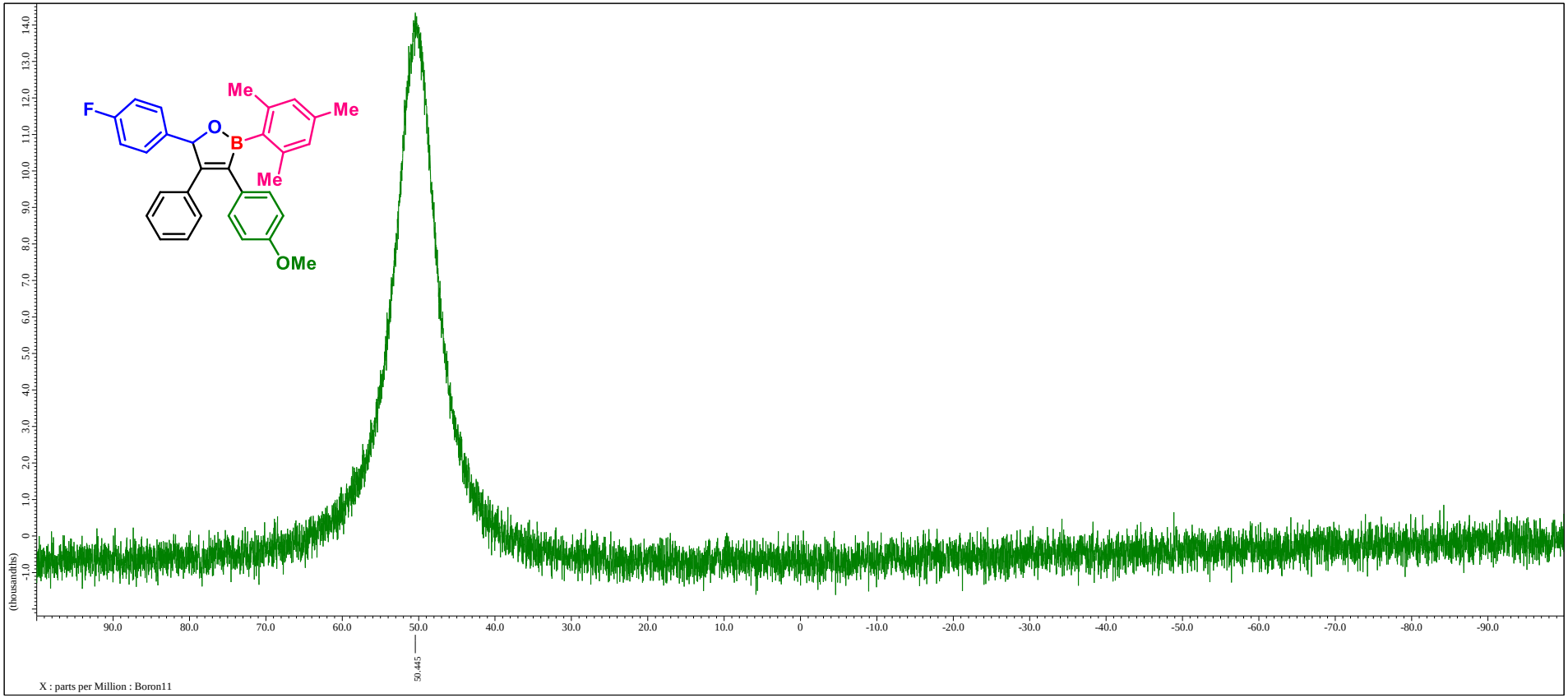

Figure S151. ^{11}B NMR (192 MHz, $CDCl_3$) spectrum of **9**.

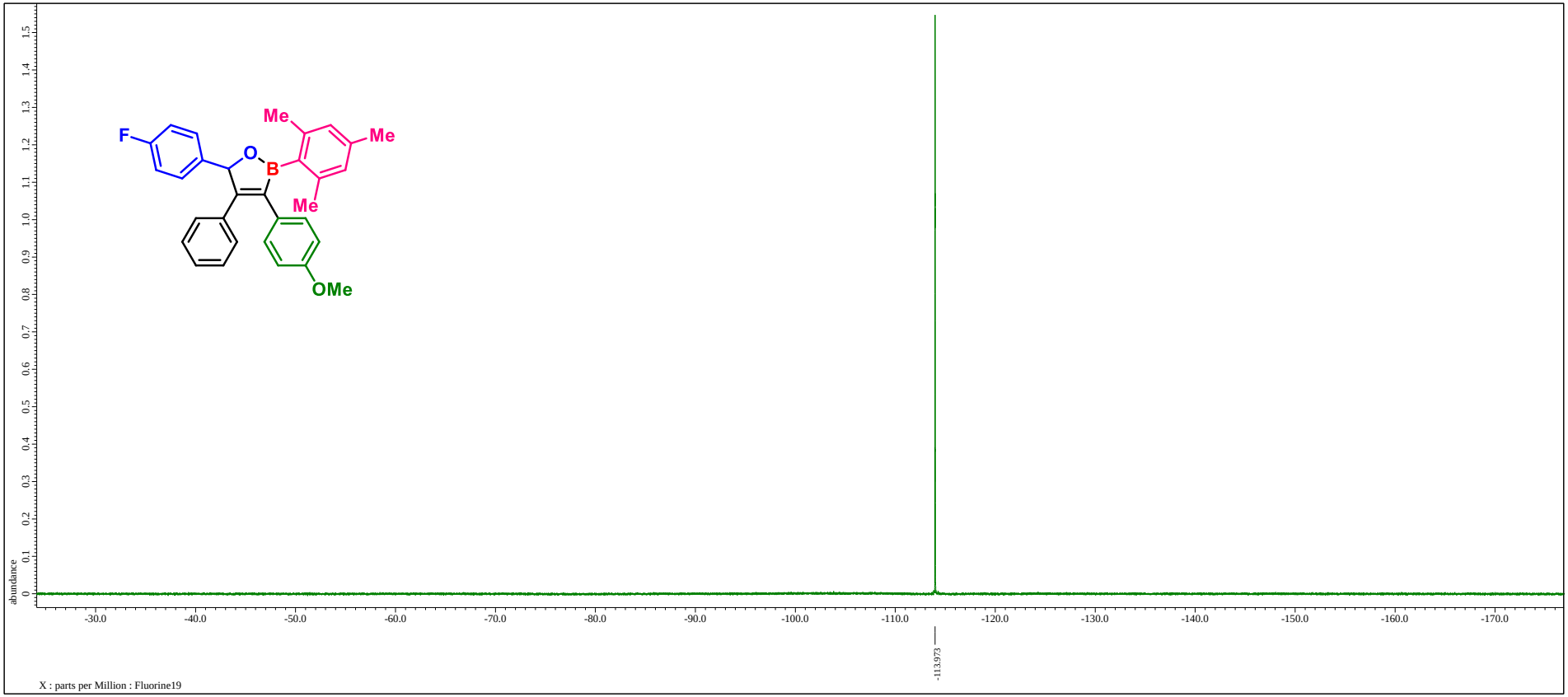

Figure S152. ^{19}F NMR (564 MHz, $CDCl_3$) spectrum of **9**.*J*